

1999

Distribution, swimming physiology, and swimming mechanics of brief squid *Lolliguncula brevis*

Ian K. Bartol

College of William and Mary - Virginia Institute of Marine Science

Follow this and additional works at: <https://scholarworks.wm.edu/etd>



Part of the [Marine Biology Commons](#), and the [Zoology Commons](#)

Recommended Citation

Bartol, Ian K., "Distribution, swimming physiology, and swimming mechanics of brief squid *Lolliguncula brevis*" (1999). *Dissertations, Theses, and Masters Projects*. Paper 1539616562.

<https://dx.doi.org/doi:10.25773/v5-6vw2-zd52>

This Dissertation is brought to you for free and open access by the Theses, Dissertations, & Master Projects at W&M ScholarWorks. It has been accepted for inclusion in Dissertations, Theses, and Masters Projects by an authorized administrator of W&M ScholarWorks. For more information, please contact scholarworks@wm.edu.

INFORMATION TO USERS

This manuscript has been reproduced from the microfilm master. UMI films the text directly from the original or copy submitted. Thus, some thesis and dissertation copies are in typewriter face, while others may be from any type of computer printer.

The quality of this reproduction is dependent upon the quality of the copy submitted. Broken or indistinct print, colored or poor quality illustrations and photographs, print bleedthrough, substandard margins, and improper alignment can adversely affect reproduction.

In the unlikely event that the author did not send UMI a complete manuscript and there are missing pages, these will be noted. Also, if unauthorized copyright material had to be removed, a note will indicate the deletion.

Oversize materials (e.g., maps, drawings, charts) are reproduced by sectioning the original, beginning at the upper left-hand corner and continuing from left to right in equal sections with small overlaps.

Photographs included in the original manuscript have been reproduced xerographically in this copy. Higher quality 6" x 9" black and white photographic prints are available for any photographs or illustrations appearing in this copy for an additional charge. Contact UMI directly to order.

**Bell & Howell Information and Learning
300 North Zeeb Road, Ann Arbor, MI 48106-1346 USA**

UMI[®]
800-521-0600

**DISTRIBUTION, SWIMMING PHYSIOLOGY, AND SWIMMING MECHANICS
OF BRIEF SQUID *LOLLIGUNCULA BREVIS***

A Dissertation

Presented to

The Faculty of the School of Marine Science

The College of William and Mary in Virginia

In Partial Fulfillment

Of the Requirements for the Degree of

Doctor of Philosophy

by

Ian K. Bartol

1999

UMI Number: 9961160

UMI[®]

UMI Microform 9961160

Copyright 2000 by Bell & Howell Information and Learning Company.

**All rights reserved. This microform edition is protected against
unauthorized copying under Title 17, United States Code.**

**Bell & Howell Information and Learning Company
300 North Zeeb Road
P.O. Box 1346
Ann Arbor, MI 48106-1346**

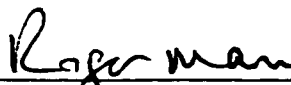
This dissertation is submitted in partial fulfillment of
the requirements for the degree of

Doctor of Philosophy



Jan Kurt Bartol

Approved November, 1999



Roger L. Mann, Ph.D.

Committee Co-Chairman/Advisor

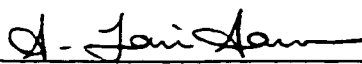


Mark R. Patterson, Ph.D.

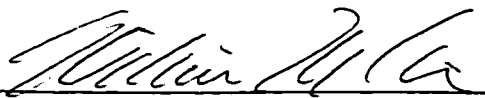
Committee Co-Chairman/Advisor



Mark W. Luckenbach, Ph.D.

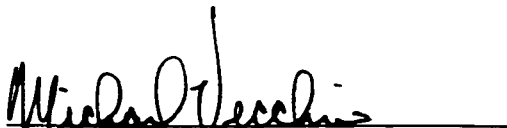


S. Laurie Sanderson, Ph.D.



William M. Kier, Ph.D.

University of North Carolina, Chapel Hill



Michael Vecchione, Ph.D.

National Museum of Natural History, Smithsonian Institution

Dedicated to my wife, Soraya, for her unconditional love, support, and unique blend of humor and wit.

TABLE OF CONTENTS

ACKNOWLEDGMENTS	vii
LIST OF TABLES	ix
LIST OF FIGURES.....	xi
ABSTRACT	xv
GENERAL INTRODUCTION.....	2
Evolution of locomotion in squids	3
<i>Lolliguncula brevis</i>	10
Chapter 1 overview.....	12
Chapter 2 overview.....	13
Chapter 3 overview.....	13
Chapter 4 overview.....	14
Literature cited	15
CHAPTER 1: DISTRIBUTION AND ABUNDANCE.....	19
Abstract.....	20
Introduction.....	22
Materials and Methods.....	25
Sampling design.....	25
Statistical analysis.....	29
Spatial maps.....	35
Results	36
Discussion	52
Literature cited	61
CHAPTER 2: RESPIRATORY COSTS OF SWIMMING	65
Abstract.....	66
Introduction.....	68

Materials and Methods	71
Experimental animals	71
Oxygen consumption measurements	72
Video analysis	74
Statistical procedures	75
Results	77
Swimming behavior	77
O₂ consumption	78
Discussion	86
Summary	99
Literature cited	100
CHAPTER 3: SWIMMING MECHANICS AND BEHAVIOR	105
Abstract	106
Introduction	109
Materials and Methods	113
Experimental animals	113
Flow tunnels	113
Critical and transition swimming speeds	114
Swimming kinematics	115
Flow visualization	117
Force measurements	119
Hydrodynamics	122
Results	127
Critical and transition swimming speeds	127
Kinematic measurements	127
Flow visualization	142
Force measurements	145
Hydrodynamics	147
Discussion	155
Literature cited	178

CHAPTER 4: ROLE OF CIRCULAR MUSCLE FIBERS IN SWIMMING.....	185
Abstract.....	186
Introduction.....	188
Materials and Methods.....	192
Experimental animals.....	192
Electromyogram recordings.....	193
Kinematic analysis.....	195
Results.....	197
Discussion.....	201
Literature Cited.....	205
SUMMARY AND CONCLUSIONS.....	208
VITA.....	215

ACKNOWLEDGMENTS

I wish to thank my co-advisors Roger Mann and Mark Patterson, who both played an integral role in my academic development. Roger provided a high level of intellectual input throughout the project, motivated me to think critically, and was always willing to offer a helping hand both in the lab and in the field (even when it meant going to Wachapreague on the hottest day of the year to help me with respiration experiments). Through his teaching and our discussions, Roger got me excited about physiology and intrigued about the functional design of molluscs. Most importantly, Roger encouraged my exploration of squid swimming mechanics, despite limited funding and the non-conventional subject matter. Mark (a.k.a Pig-Pen) introduced me to physical biology and biomechanics (and his bizarre and somewhat disturbing world of bathroom humor) and got me to think about biology from an entirely new and exciting perspective. Mark was a colossal intellectual resource and wonderful educator. He helped me develop many of the ideas in this dissertation and taught me enough electronics, computer programming, and fluid mechanics to get me through my experiments. Mark also spent countless hours, often late at night or on the weekend, helping me configure and construct equipment and encouraged me to take *every* piece of electronic equipment apart (no matter how expensive) to learn how it works.

This project could not have been accomplished without the generosity and input of my committee. Bill Kier offered valuable insight, provided thorough critiques of my work, and helped me write more concisely. Mark Luckenbach let me use a great deal of expensive equipment, continually provided field assistance at Wachapreague, and offered useful suggestions when my experimental equipment was not working properly. A large portion of this experiment could not have been accomplished without the tremendous generosity of Laurie Sanderson, who lent me pricey video equipment and gave me unlimited access to her motion analysis system and lab. Laurie taught me a great deal about videography and electromyography. Finally, I would like to thank Mike Vecchione, whom I credit with getting me excited about cephalopods. Mike was a tremendous resource throughout this project. He taught me much about cephalopod biology and ecology and provided prompt and insightful reviews of my work.

Richard Kraus graciously allowed me to piggyback along with him during his flounder trawling trips, participated in almost all of my own squid catching adventures, and incidentally, got me addicted to Yoo-Hoo and beef jerky in the field. Without Richard's assistance, this project simply could not have been completed. Dean Grubbs, Jim Gelsleichter, Dave "The Great Squidini" Carlini, Tripp MacDonald, Missy Southworth, Sarah Gaichas, and Mike Wagner also were extremely helpful during trawling trips. Ken "commonsense-wise" Walker also provided valuable trawling assistance and advice on swim tunnel construction. I gratefully acknowledge both Wayne Reisner and Reade Bonniwell, who performed considerable machine work free of charge and assisted me in the construction of swim tunnels and force beams.

I wish to thank Valerie Harmon, Kim Simmons, and Diana Bonniwell for caring for my squid when I was away and Francis O'Beirn, Al Curry, and Nancy Lewis for providing valuable field, laboratory, and administrative assistance when I was in Wachapreague. Pat Geer and the VIMS Trawl Survey were enormously helpful, often bringing back live squid from the field and collecting squid samples when I requested them. Moreover, the VIMS Trawl Survey collected some wonderful data on squid in the Chesapeake Bay, which were the basis of chapter 1 of this dissertation. I greatly acknowledge NASA Langley Research Center for providing access to a water tunnel and a dye injection system. Mike Walsh and Barry Lazos at NASA Langley were particularly helpful. I could not have conducted the electromyographic portion of this study (chapter 4) were it not for the generosity of Martin Lenhardt at MCV/VCU, who lent me his Nicolet Compass Portabook II for several consecutive months at a time.

I wish to thank Carol Tomlinson, Gail Reardon, Gloria Rowe, and Jane Lopez for helping me navigate through the worlds of funding, purchasing, and departmental protocol. I thank Pat Blake and Patrice Mason, who helped me with a shark denticle study that provided indirect funding for portions of my doctoral research. I also thank all of the members of the molluscan ecology group both past and present and all of my friends at VIMS for valuable support and advice.

I could not have completed this work without the encouragement, love, and support of both the Bartol and Moein families. Watson Bartol, in particular, was a much needed distraction and convinced me that there is more to life than squid (but not much more to life than Frisbees, long walks, and Milk-Bones). I especially thank my wife Soraya Moein Bartol for putting up with my incessant and at times incoherent squid babble, infusing humor into my life, and being an unconditional source of love and support.

This project was supported in part by the Lerner-Gray Fund for Marine Research, VIMS/SMS Minor Research Grants, the Eastern Shore Corporate Scholarship, NASA Langley Research Center, and Newport News Shipbuilding.

LIST OF TABLES

CHAPTER 1

Table

1. Factors, factor type, and categories considered initially in logistic regression model construction..... 31
2. Factors, factor type, and categories used in the final multivariate logistic regression model..... 40
3. Multivariate logistic regression of *Lolliguncula brevis* presence/absence in trawls conducted within the Chesapeake Bay 41

CHAPTER 2

Table

1. Linear regression results of O₂ consumption on swimming speed for eight *Lolliguncula brevis* that were uncooperative at low and sometimes high speeds during respirometry trials 79
2. Mean wet weights, O₂ consumption values, and aerobic swimming capacities for *Lolliguncula brevis* of various sizes..... 82

CHAPTER 3

Table

1. Mean critical swimming speeds (U_c), U_c ranges, mean transition speeds (U_t), and U_t ranges for four size classes of *Lolliguncula brevis* 128

2.	Summary of results of paired t-tests and linear regressions performed on kinematic data collected from <i>Lolliguncula brevis</i> swimming in tail-first and arms-first orientations over a range of speeds.....	139
3.	Froude propulsion efficiencies for <i>Lolliguncula brevis</i> swimming in both tail-first and arms-first orientations.....	143
4.	Mean resistive and propulsive forces computed for <i>Lolliguncula brevis</i> swimming in both tail-first and arms-first orientations over a range of speeds in a flume	149
5.	Local Reynolds numbers calculated for fins of four size classes of <i>Lolliguncula brevis</i> swimming over a range of speeds	161

LIST OF FIGURES

CHAPTER 1

Figure

1.	Map of Chesapeake Bay study site	26
2.	Number of <i>Lolliguncula brevis</i> captured in trawls from 1992–1997 in the Chesapeake Bay	37
3.	Length/frequency data of <i>Lolliguncula brevis</i> captured in spring, summer, and fall during the VIMS Trawl Surveys from 1992–1997.....	38
4.	Bathymetry of the Chesapeake Bay	43
5.	Probability of catching at least one squid in a trawl plotted as a function water temperature and salinity	44
6.	Mean monthly bottom water salinities of sampling sites considered during VIMS Trawl Surveys from 1992–1997	46
7.	Mean monthly bottom water temperatures of sampling sites considered during VIMS Trawl Surveys from 1992–1997	47
8.	Typical bottom water temperatures within the Chesapeake Bay in winter (January), spring (April), summer (July), and fall (October).....	49
9.	Typical bottom salinities within the Chesapeake Bay in winter (January), spring (April), summer (July), and fall (October).....	50
10.	Length/frequency data of <i>Lolliguncula brevis</i> collected during NMFS Groundfish Surveys (1992–1997) along the coastline of the U.S. from Delaware to Florida	58

CHAPTER 2

Figure

1. Schematic diagram of swim tunnel respirometer 73
2. O₂ consumption rates of *Lolliguncula brevis* plotted as a function of swimming velocity 80
3. Linear regressions of mean body angle of attack on swimming speed for six size classes of *Lolliguncula brevis* 83
4. Linear regressions of mean number of fin beats s⁻¹ on swimming speed for six size classes of *Lolliguncula brevis* 84
5. Mean standard deviation along the axis parallel to free stream flow plotted as a function of swimming speed 85
6. O₂ consumption rates of various cephalopods plotted against swimming speed 95
7. O₂ consumption rates of *Lolliguncula brevis* and various fishes plotted against swimming speed 97

CHAPTER 3

Figure

1. Mantle, arm, and funnel angles of attack for *Lolliguncula brevis* swimming at various speeds 129
2. Video frames of a 4.4 cm DML *Lolliguncula brevis* swimming tail-first at 3 and 24 cm s⁻¹ and arms-first at 3 and 12 cm s⁻¹ 130
3. Arm and mantle angles of attack, vertical fin motion, mantle diameter, changes in linear velocity, and acceleration for a 4.4 cm DML *Lolliguncula brevis* swimming tail-first at 6 cm s⁻¹ against a current in a flume 132

4.	Number of mantle contractions s^{-1} and fin beats s^{-1} for <i>Lolliguncula brevis</i> swimming against a steady current in a flume over a range of speeds in both tail-first and arms-first orientations	134
5.	Mantle diameter, funnel diameter, and vertical fin motion of <i>Lolliguncula brevis</i> swimming tail-first and arms-first at 9 cm s^{-1} against a steady flow in a flume	136
6.	Mantle expansion and vertical fin motion of <i>Lolliguncula brevis</i> , swimming over a range of speeds in both tail-first and arms-first orientations	138
7.	Hypothetical and actual toroidal vortex formation in brief squid.....	144
8.	Polar diagrams of drag and lift coefficients calculated from squid models oriented tail-first and arms-first and at various angles of attack	146
9.	Added mass coefficients calculated from squid models oriented tail-first and arms-first and at various angles of attack	148
10.	Vertical and horizontal forces acting on a 4.4 cm <i>Lolliguncula brevis</i> swimming tail-first at 6 cm s^{-1}	151
11.	Vertical and horizontal forces acting on a 4.4 cm <i>Lolliguncula brevis</i> swimming tail-first at 15 cm s^{-1}	152
12.	Lift, parasite/profile, and total power requirements for three size classes of <i>Lolliguncula brevis</i> swimming over a range of speeds	154
13.	Aerobic efficiency versus mantle length for <i>Lolliguncula brevis</i>	169
14.	Diagram of vortex formation around biofoils at various angles of attack	175

CHAPTER 4

Figure

1. **EMG recordings from electrodes embedded in both peripheral aerobic circular muscle and central anaerobic circular muscle of a brief squid while swimming at 6, 15, and 24 cm s⁻¹ 198**
2. **EMG recordings from electrodes embedded in central anaerobic circular muscle of a brief squid while swimming at 6, 15, and 24 cm s⁻¹ 200**

ABSTRACT

Squids are thought to have physiological and locomotive deficiencies that put them at a competitive disadvantage to fishes and exclude them from inshore, highly variable environments that are rich in nektonic fauna. However, brief squid *Lolliguncula brevis*, which is morphologically, physiologically, and ecologically distinct from squid considered previously in fish/squid metabolic comparisons, may be a notable exception. To determine how extensively *L. brevis* uses the Chesapeake Bay, a diverse, temporally variable environment densely populated with fishes but devoid of other cephalopods, and how distribution changes with selected abiotic factors for which squid typically have limited tolerance, a trawl survey of the Chesapeake Bay was conducted. Furthermore, three studies were performed to assess locomotion in brief squid: (1) respiratory costs of swimming were measured in swim tunnel respirometers; (2) swimming behavior and mechanics were examined by analyzing video footage of locomotion in flumes, performing flow visualization experiments, and collecting force measurements from squid models; and (3) the role of circular muscle fibers during swimming were examined using electromyography.

Trawl surveys indicate that brief squid, particularly juveniles < 6 cm dorsal mantle length (DML), are abundant in the Chesapeake Bay, especially when salinity and water temperature are high, and tolerate a wide range of water temperatures (8.1–29.6°C), salinities (17.9–35.0‰), dissolved oxygen levels (1.9–14.6 mg O₂/l), and depths (1.8–29.9 m) relative to other cephalopods. *L. brevis* is also different from other cephalopods examined previously because its pattern of O₂ consumption as a function of velocity was parabolic and thus similar to aerial flight, and its swimming costs were competitive with ecologically equivalent fishes. As was the case with O₂ consumption curves, power-speed curves derived from kinematic measurements of swimming squid and hydrodynamic force calculations were parabolic in shape, with high costs both at low and high speeds because of power requirements for lift generation and overcoming drag, respectively. *L. brevis* employed various behaviors to increase swimming efficiency and compensate for negative buoyancy, such as swimming in various orientations (e.g., arms-first and tail-first), altering angles of attack of the mantle, arms, and funnel, and using fin activity. Fin motion, which could not be classified exclusively as drag- or lift-based propulsion, was used over 50–95% of the sustained speed range and provided as much as 78% of the vertical and 55% of the horizontal thrust. Small squid (< 3.0 cm DML) used different swimming strategies than larger squid possibly to maximize the benefits of toroidal induction, and aerobic efficiency curves revealed that squid 3–5 cm DML are most efficient. Brief squid also may take advantage of unsteady phenomena, such as attached vortices, for added lift and thrust. Furthermore, *L. brevis* used different circular muscle fibers at various speeds and thus, like fish, have muscular “gears”, suggesting that there is specialization and efficient use of locomotive muscle in some cephalopods.

The presumption that squids are inescapably constrained by a second-rate propulsive system and physiological deficiencies is not applicable to *L. brevis*. This species has adapted well to the variable, highly populated, inshore waters of the Chesapeake Bay, has swimming costs that are reasonably competitive with ecologically relevant fishes, and compensates for the inefficiencies associated with jet propulsion by using complex behaviors and functionally distinct muscle fibers.

DISTRIBUTION, SWIMMING PHYSIOLOGY, AND SWIMMING MECHANICS
OF BRIEF SQUID *LOLLIGUNCULA BREVIS*

GENERAL INTRODUCTION

Evolution of Locomotion in Squids

The earliest unequivocally recognizable cephalopod, known as *Plectronoceras*, arose in the late Cambrian (Teichert, 1989; Wells and O'Dor, 1991). This organism, which likely resembled today's *Nautilus*, had a siphuncle and was capable of retracting its head and body within an extensive chambered shell, which was its primary means of protection from predation (Chamberlain, 1990). Coincidentally, this behavior resulted in the displacement of fluid from the mantle cavity and the generation of a backward directed water jet. This directed stream of fluid coupled with neutral buoyancy (made possible by gas and fluid retention within various chambers of the shell) allowed 3-dimensional movement and greatly enhanced mobility. Moreover, the water jet freed the molluscan foot from its locomotive duties and allowed it to either extend as flaps that could be overlapped to form a jet-directing funnel or to extend as a series of grasping tentacles (Wells and O'Dor, 1991).

Increased mobility provided by jet propulsion and neutral buoyancy was highly advantageous during the late Cambrian/early Paleozoic because it allowed the early nautiloid and later ammonoid cephalopods to move off the seafloor and vertically into the water column when threatened by benthic predators and to view and attack potential prey from a higher vantage point, capabilities other aquatic organisms did not have at the time (Wells and O'Dor, 1991; Wells, 1994). Not surprisingly, early cephalopods with their unique locomotory system and their imposing beaks and tentacles were highly

successful pelagic animals and underwent a rapid and extensive evolution (Packard, 1972). At the end of the Paleozoic, however, fishes with their inherently more efficient means of undulatory/oscillatory locomotion began to outcompete the cephalopods, forcing them out of their niches and into more peripheral environments (Denton, 1974).

The large external shell (relative to total body size) present in the early cephalopods limited high speed locomotion and allowed fishes to overtake cephalopods as masters of the pelagic world. The large shell not only elevated drag but also restricted mantle cavity volume. Both factors reduce the locomotive efficiency of jetters. Thrust in jet-propelled organisms is generated by making fluid move rearward faster than the organism is moving forward, and it is equal to the product of the mass (M) per unit time and the velocity (V) of the fluid driven backwards. Jetters generally use two strategies for thrust generation: (1) impart a small increase in rearward speed to a large amount of fluid or (2) move a small amount of fluid backwards very rapidly. Although either strategy generates thrust, it is preferable to implement the former because the energetic cost associated with generating jet thrust increases with the square of the velocity of expelled water ($E = 1/2MV^2$) (Vogel, 1994a, 1994b). Therefore, ejecting a large volume of water at a velocity only slightly higher than the animal's speed—something that wasn't possible for early cephalopods because of volume constraints associated with the external shell—is most efficient, provided added mass and drag associated with increasing volume do not dominate jet costs.

In response to the pressure of competition from faster and more energetically efficient vertebrates, some cephalopods (coleoids and to some extent the ammonites) progressively reduced portions of the shell that limited volume; others (nautiloids and many ammonites) retained the external shell and a jet system with limitations in mantle volume. Those lineages that persisted with the external shell enjoyed protection from predation because of external armor, neutral buoyancy as a result of gas retention within cavities of the shell, and the ability to travel both vertically and horizontally economically using rhythmic beating of funnel wings. This form of propulsion involved elaborate peristaltic movement of the funnel wings that forced water forward, down the gills, and out through the funnel in a continuous fashion (Wells and Wells, 1985; Wells, 1987). Rhythmic beating of the funnel wings probably was fueled by aerobic metabolism since the funnel wings likely were composed mostly of aerobic muscle fibers as is the case with today's *Nautilus*, while jet propulsion, generated by retraction of the head, was probably periodic and fueled by anaerobic metabolism (Baldwin, 1987). The rhythmic beating presumably served to ventilate the gills and allowed for propulsion on the order of a few centimeters per second; at these speeds cephalopods probably had a lower cost of transport than fish, whose respiratory and locomotor systems were not so closely coupled (Wells and O'Dor, 1991). The trade-off was confinement to a slow-paced life of low swimming velocities.

Shell reduction to achieve greater locomotive efficiency at high speeds in the coleoids contributed to measurable increases in expellable water mass and greater mantle

musculature. *Nautilus* of today can only eject water that is 15% of its total body mass, whereas coleoids such as *Sepia* and *Loligo* have increased this value to 25% and 50%, respectively (Wells, 1990; Chamberlain, 1990; O'Dor and Webber, 1991). Shell reduction likely required the simultaneous progressive development of the musculature and connective tissue lattice of the mantle, initially to prevent it from bulging outwards when the head was drawn down during jetting, but soon to take on the role of contracting to force the water out through the funnel (Wells, 1990; Wells and O'Dor, 1991). As the mantle muscle became an integral part of the locomotive engine, many coleoids (generally squids) evolved increased muscle mass and power production. The mass of the mantle wall musculature accounts for 9% of body mass in *Nautilus*, whereas the mantle wall in *Loligo* and *Illex* accounts for 35% and 40% of body mass, respectively (Wells, 1990; Chamberlain, 1987; O'Dor and Webber, 1991). Increases in mantle muscle mass and expelled water mass increased power output and speed substantially. *Illex illecebrosus* reaches sustained speeds of nearly 1.0 m s^{-1} with a power output of 6.0 W kg^{-1} , whereas *Nautilus* reaches maximum speeds of only 30 cm s^{-1} with a power output of 0.1 W kg^{-1} (O'Dor, 1988c; O'Dor et al., 1990; O'Dor and Webber, 1991).

Reductions in the shell reduced bulk and improved streamlining, made swimming at higher speeds attainable, and allowed for the evolution of lateral fins that provided a complementary propulsion system and increased maneuverability. Shell reduction, however, exposed the vulnerable exterior and made maintenance of neutral buoyancy by trapping gas within the exterior shell more difficult. Some coleoid cephalopods like *Sepia*

and *Spirula* are still capable of trapping gas within the inner shell to maintain neutral buoyancy, but most coleoids lost the ability to remain neutrally buoyant and must expend considerable energy to maintain their position in the water column (Wells, 1990).

Selection for efficient jet propulsion resulted in several paradoxes for the shell-reducing coleoids. As Wells (1990) and Wells and O'Dor (1991) point out, efficient jet propulsion, where expelled water volume is maximized, is incompatible with efficient oxygen uptake, where a minimum amount of water passes through the gills so that a high proportion of the available oxygen can be extracted. Thus, within the shell-reducing coleoids, two groups emerged: (1) those that specialize in jet propulsion (i.e., squid) and (2) those that specialize in efficient oxygen uptake (i.e., octopus and cuttlefish). The squids have large, elongated mantle volumes, are generally streamlined, and remove 5-10% of the available oxygen from the ventilatory stream, while octopus and cuttlefish have small rounded bodies, which minimize the length of the flow path and acceleration that must be given to the ventilatory stream, and routinely remove 40-50% of the available oxygen (Wells 1990). There also was (and still is) a trade-off for squids between the need for mantle muscle for forcible ejection of water and the need for increased mantle volume to elevate the efficiency of jet propulsion. Maximizing both compromises swimming efficiency since negative buoyancy and overall drag increase. This trade-off was not a factor in the evolution of fish because the body could be packed with power-generating muscle without requiring space for fluid entry and expulsion.

Although squids, which specialized in jet propulsion, were far more capable of high acceleration and speed than the nautiloids, ammonoids, and coleoids that maximize the efficiency of oxygen uptake, their jet propulsion was presumably inferior to undulatory locomotion of many fish. As mentioned earlier, thrust, whether generated by beating a tail or ejecting water in a jet stream, is equal to the product of the mass per unit time and velocity of the fluid driven rearward, and consequently it is selectively advantageous to increase the mass term to minimize energetic cost for a given level of thrust. Fishes could undoubtedly push a greater mass of water back with each tail or body movement than squids could expel from their relatively limited mantle cavities with each mantle contraction. Therefore, to keep pace with fishes, squids expelled small (relative to fish) masses of water at high speeds, which was energetically costly.

To compensate for a relatively inefficient propulsion system, many squids evolved a number of adaptations to compete ecologically with aquatic vertebrates. Squids have adopted a life cycle where an emphasis is placed on short life spans (1-3 years), rapid growth, and *semelparous* reproduction (O'Dor and Webber, 1986a). This is in contrast to many fishes, which are long-lived and *iteroparous*. Just as fishes evolved fins to aid in locomotion, squids evolved fins on the sides of the mantle that contribute to thrust and maneuverability and provide an alternative to the inefficient jet system. Generating thrust by fin movement is presumably more efficient than jet propulsion because fins can move a larger mass of water than can be expelled from the jet. In addition, they produce forward momentum at all times, which is not possible with a

pulsating jet (Hoar et al., 1994). Fins in squids range in shape from large with a low aspect ratio, as in *Thysanoteuthis rhombus* and *Loligo forbesi*, to small with a high aspect ratio, as in *Ommastrephes bartrami* and *Illex illecebrosus* (Hoar et al., 1994; Wells, 1994). The exact role each type of fin plays in swimming mechanics is unclear.

Other adaptations to elevate swimming performance and help overcome the inherent inefficiency of jet propulsion include: retaining light ions, such as ammonium, in fluid compartments within tissues to elevate buoyancy (Clarke et al., 1985; Lipinski and Turboyski, 1983); the presence of specialized muscle fibers that are thought to work either anaerobically during burst activity or aerobically for cruising and ventilation (Bone, 1978; Gosline et al., 1983); the use of different gaits to increase the efficiency of jet propulsion at various speeds (O'Dor, 1988b); the presence of an efficient, high output heart (Wells, 1983; Shadwick and Gosline, 1983); the capacity for oxygen absorption via the skin (Wells et al., 1988; Pörtner, 1994); high conversion efficiencies and a metabolism geared towards the immediate use of carbohydrates but capable of operating efficiently on protein reserves (Boyle, 1983); high gill diffusive capacity and increased gill area (Wells, 1992), the presence of sophisticated eyes, equilibrium sensors, and water movement detectors (Budelman, 1980; Budelman and Bleckman, 1988); and a highly developed brain capable of fine tuning funnel aperture area, fin movement, and mantle contraction and controlling color patterning for predator avoidance (Wells and Wells, 1972; Young, 1977).

Despite these adaptations, recent biochemical and metabolic research suggests that when compared with fishes, squids have inferior osmoregulatory, endocrine, digestive,

and respiratory systems, and are still less capable swimmers (O'Dor and Webber, 1986a; O'Dor and Webber, 1991). In fact, cost of transport (COT) values of squids, such as *Illex illecebrosus* and *Loligo opalescens* are five to seven times higher than those of the average fish, such as *Salmo* (O'Dor, 1982; Webber and O'Dor, 1985, O'Dor and Webber, 1986b, 1991). As a result of these shortcomings, O'Dor and Webber (1986a) suggest that despite functional similarities between fishes and squids (Packard, 1972), the latter are actually no longer competing with fish as they once did during the Paleozoic, but are now trying to "stay out of their way".

Lolliguncula brevis

The assumption that all squids are not competitive with fishes may be overly simplistic. Squids, like fishes, are diverse, have evolved a multitude of behavioral and physiological mechanisms, and live in a range of environments. One species, the brief squid *Lolliguncula brevis*, is particularly distinctive from the squids *Loligo* and *Illex* considered in fish/squid comparisons. *Lolliguncula brevis* is common in nearshore waters of the Gulf of Mexico and along the western Atlantic coast from Delaware to Brazil (Vecchione et al., 1989). It has a small rounded body, relatively large rounded fins, and third (III) ventrolateral arms with extensive keels. Conversely, *Loligo* and *Illex* are typically larger, more elongate, and live in deeper, more pelagic regions (Hixon, 1980; 1983; O'Dor, 1983; Hanlon and Messenger, 1996). *Lolliguncula brevis* swims at low speeds, at which the energetic costs of jet propulsion are lower, and uses substantial fin

movement, which lacks the volume limitations of jet propulsion (Wells et al., 1988; Finke et al., 1996). *Loligo* and *Illex* swim at moderate/high speeds and use their fins primarily for steering and maneuvering (O'Dor, 1982; O'Dor, 1988b; Hoar et al., 1994).

Lolliguncula brevis is the only species of cephalopod known to inhabit low salinity estuaries (Hendrix et al., 1981; Vecchione 1991a, b) and withstand low dissolved oxygen levels ($< 3 \text{ mg O}_2/\text{l}$) (Vecchione, 1991a; Wells et al., 1988). Furthermore, *L. brevis*, which is a small squid that rarely reaches sizes $> 10\text{-}12 \text{ cm DML}$ (Hixon, 1980; Vecchione et al., 1989), has adapted to live in temperate waters. This is unusual since larger species of squid are generally the ones that have had most success radiating from tropical and subtropical waters (O'Dor, 1988c, 1992).

Despite apparent morphological, ecological, and physiological differences that distinguish brief squid from many cephalopods, especially those considered in present squid/fish comparison work, little is known about the distribution and abundance of brief squid in inshore, euryhaline environments rich in nektonic fauna but devoid of other cephalopods, or about the locomotive habits and abilities of this unusual cephalopod. Brief squid may well be a unique example of a cephalopod that is highly successful in physically and biologically hostile inshore environments, despite having presumed physiological and locomotive deficiencies. Moreover, slow-swimming brief squid that rely on fin activity may prove to be more proficient swimmers relative to biologically relevant fishes (their potential competitors and predators) than cephalopods examined previously. Therefore, four studies, which are presented in the chapters that follow and

described briefly below, were performed to evaluate the ecological success of brief squid within the Chesapeake Bay ecosystem and to assess its locomotive capabilities.

Chapter 1. Distribution and Abundance of the Euryhaline Squid Lolliguncula brevis in the Chesapeake Bay: Effects of Selected Abiotic Factors

Little is known about the distribution and abundance of brief squid *Lolliguncula brevis* along the eastern U.S. Coast, especially within the Chesapeake Bay, which is surprising given that brief squid are unique in their ability to tolerate low salinities and the Chesapeake Bay is one of the largest and most diverse estuaries in the world, with tributaries and rivers within the system constituting a shoreline several thousand kilometers long. Since abiotic factors, such as salinity and water temperature, are highly variable throughout the year within the Chesapeake Bay, it is of interest to determine how the abundance and distribution of brief squid, which generally are presumed to have physiological deficiencies, change in relation to these conditions. A survey was conducted, therefore, in the Virginia portion of the Chesapeake Bay from 1992–1997 using an outer trawl and is described in Chapter 1. The primary objectives of the study were: (1) determine what and how selected abiotic factors affect brief squid presence within the Chesapeake Bay, (2) assess how extensively brief squid use the Chesapeake Bay relative to other nekton, and (3) document size ranges of brief squid in the Chesapeake Bay.

Chapter 2. Respiratory Costs of Swimming in the Negatively Buoyant Brief Squid: An Analogue to Aerial Flight

Because *Lolliguncula brevis* differs from the cephalopods considered in previous squid/fish energetic comparisons yet little is known about its swimming costs, I performed a swimming respiratory study on *L. brevis*, which is presented in Chapter 2. In this study, oxygen consumption rates of *L. brevis* of various sizes (2-9 cm dorsal mantle length (DML) swimming over a range of speeds (3–30 cm s⁻¹) in swim tunnel respirometers were measured in conjunction with video footage to characterize patterns of oxygen consumption as a function of speed and to determine where brief squid rank metabolically in relation to other mobile nekton.

Chapter 3. Swimming Mechanics and Behavior of Brief Squid

Although squids are among the most versatile swimmers and rely on a unique locomotive system, involving a jet, fins, and arms, many aspects of squid locomotion remain unexplored, including how swimming mechanics and behavior change with size, how slow-swimming squids locomote, or what role unsteady phenomena, swimming orientation, fin activity, arm motion, and other behaviors play in locomotion over a range of speeds. Knowledge of these areas is fundamental to understanding squid locomotion and to assessing swimming efficiency in *Lolliguncula brevis*. In Chapter 3, I describe a comprehensive study of squid swimming behavior and mechanics. In this study, kinematic data of *Lolliguncula brevis* ranging in size from 1.8–8.9 cm DML swimming in

flumes were collected and used in hydrodynamic calculations. Flow visualization and force measurement experiments using live squid and/or models also were performed to investigate particular aspects of swimming, such as characteristics of the jet wake and magnitude of lift and drag forces.

Chapter 4. Role of Aerobic and Anaerobic Circular Mantle Muscle Fibers in Swimming

Squid: Electromyography

Circular mantle muscle, which is the muscle responsible for mantle contraction and the consequent ejection of water out of the funnel, consists of distinct zones of aerobic and anaerobic muscle fibers that are thought to have functional roles analogous to red and white muscle in fishes. If brief squid do have red and white muscle analogues and possess functional low and high “gears”, then there is specialization and efficient use of locomotive muscle, which may help compensate for inherent jet inefficiency. To test predictions of the functional role of the circular muscle zones, an electromyographic (EMG) study was performed and is presented in Chapter 4. In this study EMGs from the circular muscle layers in conjunction with video footage were recorded from brief squid *Lolliguncula brevis* swimming in a flume at speeds of 3–27 cm s⁻¹, and the speeds at which aerobic and anaerobic muscle are recruited were determined.

LITERATURE CITED

- Baldwin, J. 1987. Energy metabolism of *Nautilus* swimming muscles. In *Nautilus: the Biology and Paleobiology of a Living Fossil* (ed. W. B. Saunders and N. H. Landman), pp. 325-330. New York: Plenum Press.
- Bone, Q. 1978. Locomotor muscle. In *Fish Physiology*, vol. 7 (ed. W. S. Hoar and D. J. Randall), pp. 361-424. London: Academic Press.
- Boyle, P. R. (ed.). 1983. *Cephalopod life cycles*, vol. 2. London: Academic Press.
- Budelman, B. U. 1980. Equilibrium and orientation in cephalopods. *Oceanus* 23: 34-43.
- Budelman, B. U. and H. Bleckman. 1988. A lateral line analogue in cephalopods: water waves generate microphonic potentials in the epidermal head lines of *Sepia* and *Lolliguncula*. *J. Comp. Physiol. A* 164: 1-5.
- Chamberlain, J. A., Jr. 1987. Locomotion of *Nautilus*. In *Nautilus, the Biology and Palaeobiology of a Living Fossil* (ed. W. B. Saunders and N. H. Landman), pp. 489-525. New York: Plenum Press.
- Chamberlain, J. A., Jr. 1990. Jet propulsion of *Nautilus*: a surviving example of early Paleozoic cephalopod locomotor design. *Can. J. Zool.* 68: 806-814.
- Clarke, A., M. R. Clarke, L. J. Holmes, and T. D. Waters. 1985. Calorific values and elemental analysis of eleven species of oceanic squids (Mollusca: Cephalopoda). *J. Mar. Biol. Assoc. U. K.* 62: 983-986.
- Denton, E. J. 1974. On buoyancy and the lives of modern and fossil cephalopods. *Proc. Roy. Soc. Lond. (B)* 185: 273-299.
- Finke, E., H. O. Pörtner, P. G. Lee, and D. M. Webber. 1996. Squid (*Lolliguncula brevis*) life in shallow waters: oxygen limitation of metabolism and swimming performance. *J. Exp. Biol.* 199: 911-921.

- Gosline, J.M., J. D. Steeves, A. D. Harman, and M. E. DeMont. 1983. Patterns of circular and radial mantle activity in respiration and jetting in the squid *Loligo opalescens*. *J. Exp. Biol.* 104: 97-109.
- Hanlon, R. T. and J. B. Messenger. 1996. *Cephalopod Behaviour*. Cambridge: Cambridge University Press.
- Hendrix, J. P., Jr., W. H. Hulet, and M. J. Greenberg. 1981. Salinity tolerances and the responses to hypoosmotic stress of the bay squid *Lolliguncula brevis*, a euryhaline cephalopod mollusc. *J. Comp. Biochem. Physiol.* 69A: 641-648.
- Hixon, R. F. 1980. Growth, reproductive biology, distribution and abundance of three species of loliginid squid (Myopsida, Cephalopoda) in the northwest Gulf of Mexico. Ph.D. dissertation, University of Miami, Miami, FL, 182 p.
- Hoar, J. A., E. Sim, D. M. Webber, and R. K. O'Dor. 1994. The role of fins in the competition between squid and fish. In *Mechanics and Physiology of Animal Swimming* (ed. L. Maddock, Q. Bone, and J. M. V. Rayner), pp. 27-43. Cambridge: Cambridge University Press.
- Lipinski, M., and K. Turoboyski. 1983. The ammonium content in the tissues of selected species of squid (Cephalopoda: Teuthoidea). *J. Exp. Mar. Biol. Ecol.* 69: 145-150.
- Mangum, C. P. 1991. Salt sensitivity of the hemocyanin of eury- and stenohaline squids. *Comp. Biochem. Physiol.* 19A: 159-161.
- O'Dor, R. K. 1982. Respiratory metabolism and swimming performance of the squid, *Loligo opalescens*. *Can. J. Fish. Aquat. Sci.* 39: 580-587.
- O'Dor, R. K. 1983. *Illex illecebrosus*. In *Cephalopod Life Cycles. Vol. 1: Species Accounts* (ed. P. R. Boyle), pp. 95-114. New York: Academic Press.
- O'Dor, R. K. 1988a. Limitations on locomotor performance in squid. *J. Appl. Physiol.* 64: 128-134.
- O'Dor, R. K. 1988b. Forces acting on swimming squid. *J. Exp. Biol.* 137: 421-442.
- O'Dor, R. K. 1988c. The energetic limits of squid distributions. *Malacologia* 29: 113-119.
- O'Dor, R. K. 1992. Big squid in big currents. *S. Afr. J. Mar. Sci.* 12: 225-235.

- O'Dor, R. K. and D. M. Webber. 1986a. The constraints on cephalopods: why squid aren't fish. *Can. J. Zool.* 64: 1591-1605.
- O'Dor, R. K. and D. M. Webber. 1986b. Monitoring the metabolic rate and activity of free-swimming squid with telemetered jet pressure. *J. Exp. Biol.* 126: 205- 224.
- O'Dor, R. K. and D. M. Webber. 1991. Invertebrate athletes: trade-offs between transport efficiency and power density in cephalopod evolution. *J. Exp. Biol.* 160: 93-112.
- O'Dor, R. K., J. Wells, and M. J. Wells. 1990. Speed, jet pressure and oxygen consumption relationships in free-swimming *Nautilus*. *J. Exp. Biol.* 154: 383-396.
- Packard, A. 1972. Cephalopods and fish: limits of convergence. *Biol. Rev.* 47: 241-307.
- Pörtner, H. O. 1994. Coordination of metabolism, acid-base regulation and haemocyanin function in cephalopods. *Mar. Fresh. Behav. Physiol.* 25: 131-148.
- Shadwick, R. E. and J. M. Gosline. 1983. Molecular biomechanics of protein rubbers in molluscs. In *The Mollusca*, vol. 1 (ed. P. W. Hochachka), pp. 399-467. London: Academic Press.
- Teichert, C. 1989. Les principales caractéristiques de l'évolution des Cephalopodes. In *Cephalopodes. Traites de Zoologie*, vol. 5 (ed. P. P. Grasse), pp. 715-781. Paris: Masson.
- Vecchione, M. 1991a. Dissolved oxygen and the distribution of the euryhaline squid *Lolliguncula brevis*. *Bull. Mar. Sci.* 49: 668-669.
- Vecchione, M. 1991b. Observations on the paralarval ecology of a euryhaline squid *Lolliguncula brevis* (Cephalopoda: Loliginidae). *Fish. Bull.* 89: 515-521.
- Vecchione, M., C. F. Roper, and M. J. Sweeney. 1989. Marine Flora and Fauna of the Eastern United States Mollusca: Cephalopoda. NOAA Technical Report NMFS 73, 23p.
- Vogel, S. 1994a. *Life in moving fluids*, 2nd ed. Princeton: Princeton University Press.

- Vogel, S. 1994b. Second-rate squirts. *Discover* 15: 71-76.
- Webber, D. M. and R. K. O'Dor. 1985. Respiration and swimming performance of short-finned squid (*Illex illecebrosus*). *Scientific Council Studies Northw. Atl. Fish. Org.* 9: 133-138.
- Wells, M. J. 1983. Circulation in cephalopods. In *The Mollusca*, vol. 5. (ed. A. S. M. Saleuddin and K. M. Wilbur), pp. 239-290. London: Academic Press.
- Wells, M. J. 1987. Oxygen uptake and the effect of feeding in *Nautilus*. *Veliger* 30: 69-75.
- Wells, M. J. 1990. Oxygen extraction and jet propulsion in cephalopods. *Can. J. Zool.* 68: 815-824.
- Wells, M.J. 1992. The evolution of the circulatory system. *Comp. Physiol.* 11: 5-14.
- Wells, M. J. 1994. The evolution of a racing snail. *Mar. Fresh. Behav. Physiol.*, 25: 1-12.
- Wells, M.J., R. T. Hanlon, P. G. Lee, and F. P. Dimarco. 1988. Respiratory and cardiac performance in *Lolliguncula brevis* (Cephalopoda, Myopsida): the effects of activity, temperature, and hypoxia. *J. Exp. Biol.* 138: 17-36.
- Wells, M. J. and R. K. O'Dor. 1991. Jet propulsion and the evolution of the cephalopods. *Bull. Mar. Sci.* 49: 419-432.
- Wells, M. J. and J. Wells. 1972. Sexual displays and mating of *Octopus vulgaris* Cuvier and *O. cyanea* Gray and attempts to alter performance by manipulating the glandular condition of the animals. *Anim. Behav.* 20: 293-308.
- Wells, M. J. and J. Wells. 1985. Ventilation and oxygen uptake by *Nautilus*. *J. Exp. Biol.* 118: 297-312.
- Young, R. E. 1977. Ventral bioluminescent countershading in midwater cephalopods. *Symp. Zool. Soc. Lond.* 38: 161-190.

CHAPTER 1

**DISTRIBUTION AND ABUNDANCE OF THE EURYHALINE SQUID
LOLLIGUNCULA BREVIS IN THE CHESAPEAKE BAY: EFFECTS OF
SELECTED ABIOTIC FACTORS**

ABSTRACT

The majority of cephalopods are thought to have limitations due to physiology and locomotion that exclude them from shallow, highly variable, euryhaline environments. The brief squid, *Lolliguncula brevis*, may be a notable exception because it tolerates low salinities, withstands a wide range of environmental conditions, and swims readily in shallow water. Little is known about the distribution and abundance of *L. brevis* in the Chesapeake Bay, a diverse and highly variable estuary. A survey of *L. brevis*, therefore, was conducted in the Virginia portion of the Chesapeake Bay from 1992–1997 using a 9.1 m otter trawl, and the effects of selected factors on squid presence were assessed using logistic regression analysis. During spring through fall, *L. brevis* was collected over a wide range of bottom temperatures (8.1–29.6 °C), bottom salinities (17.9–35.0 ‰), dissolved oxygen levels (1.9–14.6 mg O₂/l), and depths (1.8–29.9 m), but *L. brevis* was not present in trawls conducted during winter in the Chesapeake Bay. *Lolliguncula brevis*, especially juveniles < 60 mm dorsal mantle length (DML), were abundant, frequently ranking in the upper 10% of overall annual nektonic trawl catches and during the fall of some years ranking second behind anchovies. The probability of catching a squid increased in the Chesapeake Bay at higher salinities and water temperatures, and these variables had a profound influence on both monthly and annual variability in distribution. Salinity had the largest influence on squid distribution, with squid being completely absent from the Bay when salinity was < 17.9‰ and most

abundant in the fall when salinity was highest (despite declines in water temperature). Squid were most prevalent at depths between 10 and 15 m. The results of this study suggest that *L. brevis* is an important component of the Chesapeake Bay ecosystem when salinities and water temperatures are within tolerance limits, and unlike other squids, *L. brevis* may be well-equipped for inshore, euryhaline existence.

INTRODUCTION

Squids are widely distributed in seas throughout the world despite being at a competitive disadvantage relative to fishes, their potential competitors and predators. Squids rely on jet propulsion, which is inherently less efficient than undulatory modes of aquatic locomotion used by most nekton (Alexander, 1977; O'Dor and Webber, 1986; Vogel, 1994). The energetic costs of transporting a unit mass of organism over a unit distance at optimum speeds (i.e., the minima of cost of transport curves) are 5–7 times higher for jetting squids, such as *Illex* and *Loligo*, compared to fishes, such as *Salmo* (O'Dor, 1982; Webber and O'Dor, 1985; O'Dor and Webber, 1991). Furthermore, the respiratory pigment of squids, hemocyanin, has less than half the oxygen binding capacity of hemoglobin, the respiratory pigment of fishes (Mangum, 1981; Wells, 1994). Compared to fishes, squids have less complex endocrine systems (O'Dor and Webber, 1986), possess limited potential for energy storage (Takahashi, 1960; Mommsen and Hochachka, 1981; Ballantyne et al., 1981), and have limited capacity for anaerobic metabolism (O'Dor and Webber, 1986; Pörtner et al. 1991, 1993; Finke et al., 1996). Moreover, most squids are unable to osmoregulate (Hendrix et al., 1981; Mangum, 1991) and are generally incapable of tolerating low salinity conditions, preventing the vast majority of squids from invading fresh or estuarine waters—two significant aquatic habitats where cephalopods are poorly represented.

The brief squid, *Lolliguncula brevis*, is the only species of cephalopod known typically to inhabit low-salinity estuaries (Vecchione, 1991a). Using physiological mechanisms we do not yet fully understand, *L. brevis* is capable of tolerating salinities as low as 17.5‰ under laboratory conditions (Hendrix et al., 1981; Mangum, 1991) and withstands low dissolved oxygen levels ($< 3 \text{ mg O}_2/\text{l}$) (Vecchione, 1991b; Wells et al., 1988). This species is smaller than most loliginids, seldom reaching sizes greater than 110 mm in dorsal mantle length (DML) (Hixon 1980). *Lolliguncula brevis* has rounded, wide fins and appears to swim at low velocities (Finke et al., 1996). These traits are beneficial for maneuvering in inshore bays and estuaries where *L. brevis* is commonly found (Gunter, 1950; Voss, 1956; Dragovich and Kelly, 1967; Laughlin and Livingston, 1982; Hixon, 1980).

Although *L. brevis* is common in nearshore waters of the Gulf of Mexico and along the western Atlantic Coast from Delaware to Brazil (Vecchione et al., 1989), surprisingly little is known about the distribution of this unique squid along the eastern U.S. Coast. Most of the distributional data on *L. brevis* have been collected in the coastal waters of Texas (Gunter, 1950; Hixon, 1980), Louisiana (Vecchione, 1991a, b), and Florida (Dragovich and Kelly, 1967; Livingston et al., 1975; Laughlin and Livingston, 1982). Only Haefner (1959), who examined brief squid in Delaware Bay, reported *L. brevis* distribution along the eastern U.S. Coast. No distribution or abundance data have been published on *L. brevis* within the Chesapeake Bay. This is surprising given that brief squid are unique in their ability to tolerate low salinities and the Chesapeake Bay is one of the largest and most diverse estuaries in the world, with tributaries and rivers within the system constituting a shoreline a few thousand kilometers long. Since abiotic

factors, such as salinity and water temperature, are highly variable throughout the year within the Chesapeake Bay, it is of great interest to determine how the abundance and distribution of brief squid, which are thought to have substantial physiological limitations, changes in relation to these conditions.

To learn more about the distribution and abundance of brief squid in the highly variable, euryhaline waters of the Chesapeake Bay, a survey was conducted in the Virginia portion of the Chesapeake Bay from 1992–1997 using an otter trawl. This study had three objectives: (1) determine what and how selected abiotic factors affect brief squid presence within the Chesapeake Bay, (2) assess the abundance of brief squid in the Chesapeake Bay relative to other nekton, and (3) document the size distribution of brief squid in the Chesapeake Bay. The abiotic factors of greatest interest were: salinity, water temperature, bottom depth, dissolved oxygen, tidal stage, and water clarity. Since temporal variation in the Chesapeake Bay ecosystem is high, the effects of season and year also were considered.

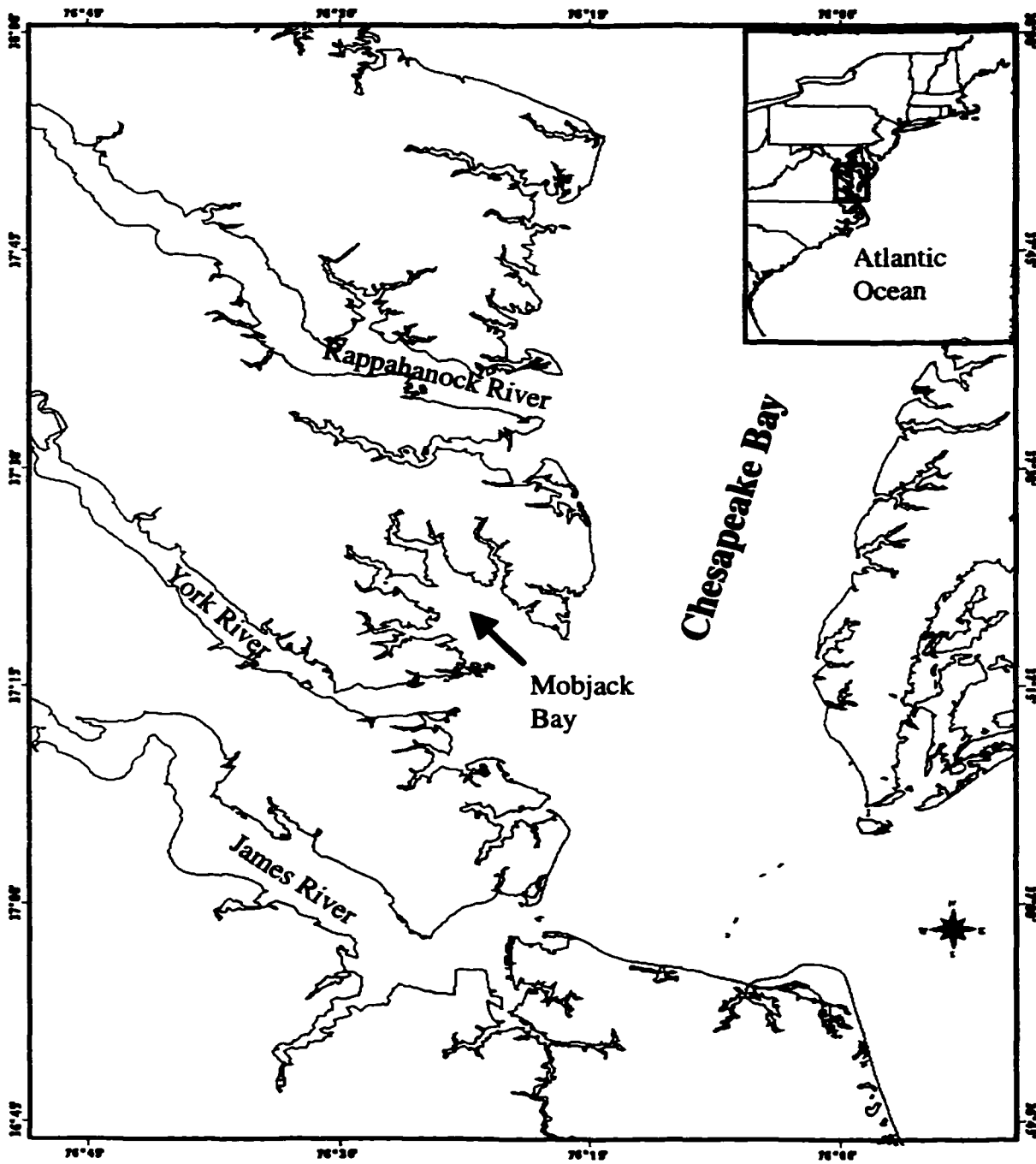
MATERIALS AND METHODS

Sampling Design

Data on *L. brevis* distribution were collected from 1992–1997 during the Virginia Institute of Marine Science (VIMS) Trawl Survey Monitoring Program, which was established to generate annual indices for juvenile marine and estuarine finfish and invertebrates within Virginia waters. During this study, both the mainstem of the lower Chesapeake Bay from the Bay mouth to 37° 40' N and three major Virginia tributaries, the James, York, and Rappahanock Rivers, were sampled (Figure 1). The gear used consisted of a 9.1 m semi-balloon otter trawl with 3.8 cm body mesh, 3.2 cm cod-end mesh, 1.3 cm cod-end liner mesh, a tickler chain, and steel China-V doors (71 cm x 49 cm). Each tow lasted five minutes (bottom time) and was performed at a speed of 9.7 km/h.

A stratified random design with stratification by latitude and water depth was used to sample sites within the Chesapeake Bay mainstem. Three latitudinal strata (36° 55' N – 37° 10' N; 37° 10' N – 37° 25' N; and 37° 25' N – 37° 40' N) and four depth strata (eastern bay shoal areas (3.6–9.1 m); western bay shoal areas (3.6–9.1 m); plain areas (9.1–13 m); and deep areas (> 13 m)) were considered, resulting in a total of 12 strata. Sampling sites were selected randomly within the 12 strata using computerized files of the National Ocean Survey's Chesapeake Bay bathymetric grid system. Sampling was conducted monthly from April through December and in February of each year.

Figure 1. Map of Chesapeake Bay study site. The mainstem of the lower Chesapeake Bay from the Bay mouth to 37° 40' N and three Virginia tributaries, the James, York, and Rappahanock Rivers, were sampled.



Within each of the three latitudinal strata for every month considered during a given year, sampling included four stations within the plain stratum, three stations within the deep stratum, and either three (in May through November) or two (in December, February, March, and April) stations within each of the two shoal strata.

Within the three tributaries, fixed stations located in the center of the river channels at 8 km intervals from the river mouths to the freshwater interfaces were sampled monthly from 1992–1997. In 1996 and 1997, additional stations were sampled using a stratified random design partitioned by region and depth. Each river was divided into four regions, but the number of depth strata (2–5) within each region varied according to the dimensions of the tributaries.

Bottom depth, bottom salinity, bottom water temperature, bottom dissolved oxygen, and Secchi depth (a measure of water clarity) were recorded at all stations immediately following each tow. Bottom depth (± 0.1 m) was measured using an ultrasonic depth sounder; salinity ($\pm 0.1\text{‰}$), water temperature ($\pm 0.1^\circ\text{C}$) and bottom dissolved oxygen (± 0.1 mg/l) were measured using a Hydrolab; and Secchi depth (± 0.1 m) was measured using a Secchi disk. Tidal stage was estimated using predictions published for mariners by the National Oceanic and Atmospheric Administration (NOAA), and latitude and longitude at the beginning and ending of each tow were determined using Loran C conversions or a Global Positioning System (GPS) receiver. Tow distance was defined as the distance between beginning and ending latitude/longitude coordinates. The number and dorsal mantle lengths (DML) of squid and the number and types of vertebrate nekton captured in the trawls were recorded.

Occasionally, squid were dissected to characterize the approximate stage of gonad maturity.

One limitation of the trawl survey data was that squid captured prior to 1997 in the Chesapeake Bay were simply classified as squid and assumed to be *L. brevis*. Examinations of squid captured in 1997 and 1998 revealed that several, larger (> 110 mm DML) squid captured in trawls at the Chesapeake Bay mouth in high salinities were *Loligo pealei*, a loliginid that is typically larger than *L. brevis*, reaching sizes up to 500 mm DML (Vecchione et al. 1989). The number of squid identified in 1997 and 1998 as *L. pealei* was small relative to those identified as *L. brevis*, however, and no squid less than 110 mm has been identified to date as *L. pealei*. Since *L. brevis* rarely grows larger than 110 mm DML (Hixon, 1980), all squid \geq 110 mm DML were considered *L. pealei* and eliminated from the analysis. Conversely, all squid < 110 mm were considered *L. brevis* and included in the analysis. Although this does not guarantee that only *L. brevis* were considered in this study, the number of *L. pealei* in the samples was probably negligible. This assertion is based on: (1) independent, personal trawling experience in the Chesapeake Bay ecosystem, where < 0.1% of squid encountered have been *L. pealei*, (2) identifications of present and past trawl survey specimens, which reveal small numbers of *L. pealei*, and (3) physiology and ecology of *L. pealei* (*L. pealei* avoids euryhaline environments, preferring areas > 32‰, and resides in waters > 40 m (Hixon, 1980), which are rare in the Chesapeake Bay).

Statistical Analysis to Assess the Effects of Selected Factors on Squid Presence

Since a primary objective of this study was to determine what and how selected variables influence squid presence within the Chesapeake Bay, the outcome or dependent variable was simply the presence or absence of squid at each sampling site and the independent variables were the selected factors of interest (e.g., salinity, depth, etc.). Logistic regression using the logit link, a standard method of analyzing dichotomous, discrete outcome variables (Hosmer and Lemeshow, 1989), is the most appropriate method for modeling the presence/absence of brief squid in trawl catches. The specific form of the logistic regression model is as follows:

$$P = \exp(\alpha + \beta_1 X_1 + \beta_2 X_2 \dots \beta_i X_i) / \{1 + \exp(\alpha + \beta_1 X_1 + \beta_2 X_2 \dots \beta_i X_i)\}$$

where P = event probability (i.e. probability of catching at least 1 squid)

α = a constant

X_i = independent variable, i (e.g. temperature, salinity, etc.)

β_i = coefficient of the independent variable, X_i

To make the logistic regression model more interpretable, the dependent variable (P) is expressed as a linear function of the independent variables ($X_1 \dots X_i$) using the logit (L) transformation (Hosmer and Lemeshow, 1989):

$$L = \ln\{P / (1 - P)\} = \alpha + \beta_1 X_1 + \beta_2 X_2 \dots \beta_i X_i$$

Both discrete and scaled continuous independent variables were considered in the logistic regression model. The discrete variables considered in this analysis were: year (1992, 1993, 1994, 1995, 1996, and 1997), season (spring, fall, summer, and winter), and tidal stage (early flood, maximum flood, late flood, slack before ebb, early ebb, maximum ebb, late ebb, and slack before flood). In logistic regression, the coefficients of categories within the discrete variable are expressed in reference to the coefficient of another category, known as the reference level (Hosmer and Lemeshow, 1989; Agresti, 1990). For example, within the discrete variable, season, the coefficients of fall, summer, and winter may be expressed relative to the coefficient of spring. Scaled continuous variables considered in this analysis were: Secchi depth, tow distance, bottom depth, bottom water temperature, bottom salinity, and bottom dissolved oxygen. The coefficients of scaled continuous variables reflect how the event probability changes when the variable increases by one unit. Consequently, the interpretation of a continuous independent variable within a logistic regression model will depend heavily on what units are selected for the variable, and thus selected units should be of biological relevance (Hosmer and Lemeshow, 1989). For example, it may be more biologically informative to determine how catch probabilities vary with every 2°C change in water temperature rather than with every 0.2°C change, when ecological variations may be very slight. Therefore, continuous variables were scaled and coded according to units of reasonable biological relevance and to ensure there was a sufficient sample size in each category level (Table 1).

Logistic regression model construction and refinement were performed following procedures suggested by Hosmer and Lemeshow (1989; Chapter 4). First univariate

Table 1. Factors, factor type, and categories considered initially in logistic regression model construction.

Factors	Factor Type	Categories
Tide	Discrete	1) early ebb 2) max ebb 3) late ebb 4) slack before flood 5) early flood 6) max flood 7) late flood 8) slack before ebb
Secchi Depth	Scaled Continuous	1) 0.0 – 0.4 m 2) 0.5 – 0.9 m 3) 1.0 – 0.4 m 4) 1.5 – 1.9 m 5) 2.0 – 2.4 m 6) 2.5 – 2.9 m 7) 3.0 – 3.4 m 8) 3.5 – 3.9 m 9) ≥ 4.0 m
Tow Distance	Scaled Continuous	1) 50 – 149 m 2) 150 – 249 m 3) 250 – 349 m 4) 350 – 449 m 5) 450 – 549 m 6) 550 – 649 m 7) ≥ 650 m
Depth	Scaled Continuous	1) 0.0 – 1.9 m 2) 2.0 – 3.9 m 3) 4.0 – 5.9 m 4) 6.0 – 7.9 m 5) 8.0 – 9.9 m 6) 10.0 – 11.9 m 7) 12.0 – 13.9 m 8) 14.0 – 15.9 m 9) 16.0 – 17.9 m 10) 18.0 – 19.9 m 11) ≥ 20.0 m
Bottom Water Temperature	Scaled Continuous	1) 0 – 1.9°C 2) 2.0 – 3.9°C 3) 4.0 – 5.9°C 4) 6.0 – 7.9°C 5) 8.0 – 9.9°C 6) 10.0 – 11.9°C 7) 12.0 – 13.9°C 8) 14.0 – 15.9°C 9) 16.0 – 17.9°C 10) 18.0 – 19.9°C 11) 20.0 – 21.9°C 12) 22.0 – 23.9°C 13) 24.0 – 25.9°C 14) 26.0 – 27.9°C 15) ≥ 28.0 °C

Factors	Factor Type	Categories
Bottom Salinity	Scaled Continuous	1) 0 – 1.9‰ 2) 2.0 – 3.9‰ 3) 4.0 – 5.9‰ 4) 6.0 – 7.9‰ 5) 8.0 – 9.9‰ 6) 10.0 – 11.9‰ 7) 12.0 – 13.9‰ 8) 14.0 – 15.9‰ 9) 16.0 – 17.9‰ 10) 18.0 – 19.9‰ 11) 20.0 – 21.9‰ 12) 22.0 – 23.9‰ 13) 24.0 – 25.9‰ 14) 26.0 – 27.9‰ 15) ≥ 28.0‰
Bottom Dissolved Oxygen	Scaled Continuous	1) 0 – 2.9 mg/l 2) 3 – 5.9 mg/l 3) 6 – 8.9 mg/l 4) 9 – 11.9 mg/l 5) 12 – 14.9 mg/l 6) ≥ 15.0 mg/l
Year	Discrete	1) 1992 2) 1993 3) 1994 4) 1995 5) 1996 6) 1997
Season	Discrete	1) winter 2) spring 3) summer 4) fall

logistic regression analyses were performed on each variable. Significance was assessed at $\alpha = 0.25$ using the $-2 \log$ likelihood estimation chi-square, and non-significant variables were eliminated from consideration. This level of significance, rather than the conventional $\alpha = 0.05$ level, was selected to minimize the chance of excluding variables that may be important outcome predictors when considered collectively with other variables in a multivariate analysis (Mickey and Greenland, 1989). At the univariate stage, scaling of discrete variables also was examined; when several categories within a discrete variable had similar coefficients and odds ratios, they were combined to form broader categories (Hosmer and Lemeshow, 1989).

Upon completion of the univariate analyses, all significant variables were included in a multivariate model. Variables that were not significant at the $\alpha = 0.05$ level within the multivariate model were eliminated, and further multivariate logistic regression models were performed. Coefficients were monitored carefully in models generated after variable removal, since wide fluctuations may be indicative of the importance of an eliminated variable that should remain in the model (Hosmer and Lemeshow, 1989). Once all essential variables were determined, the scale of continuous variables was examined. Linearity of scaled continuous variables was examined by dividing values into quartiles (or smaller groupings when higher resolution was necessary) and treating continuous variables as discrete variables in the multivariate model, using the lowest quartile (or group) as the reference level. This procedure revealed that it was sometimes necessary to truncate the range of categories within a variable, increase unit size, and treat some scaled continuous variables as discrete variables when assumptions of linearity were violated. Although this scaling may reduce

resolution within the model, it stabilizes parameter estimates, produces goodness of fit measures of greater reliability, and makes the model more interpretable (Hosmer and Lemeshow, 1989; Agresti, 1990).

Once all relevant variables were determined and expressed in the correct scale, further model refinement involved the consideration of interactions. Because of practical considerations, it is not possible to include all interactions in logistic regression models that have many variables. Only those interactions that make biological sense should be investigated (Hosmer and Lemeshow, 1989). Thus, I restricted my search for interactions to those involving the four abiotic factors of greatest interest: water temperature, salinity, depth, and dissolved oxygen level. Each interaction involving these factors was added separately to the final, main-effects-only multivariate model. A determination as to whether to include the interaction in further models was based on both the significance of the -2 log likelihood estimation of the new model and the p -value of the interaction. Interactions that were significant at $\alpha = 0.05$ and that provided significant improvement over the main effects only model were added to the final model. To decouple the effects of factors involved in significant interactions, logits for all factor combinations were computed and significance assessed at $\alpha = 0.05$ using procedures described in detail on pp. 102–106 in Hosmer and Lemeshow (1989). The fit of the final, most parsimonious model was assessed using Hosmer and Lemeshow, Pearson chi-square, and deviance goodness-of-fit tests, and by using various logistic regression diagnostics (Hosmer and Lemeshow, 1989: pp. 149–170). All tests revealed there was no overdispersion in the model.

Spatial Maps

To help visualize some of the effects of variables in the models, spatial maps of squid catches and selected factors of interest were generated using ArcView GIS software (Environmental Systems Research Institute (ESRI), Inc., Redlands, CA). Since detailed, high-resolution bottom water temperature and bottom salinity maps of the Chesapeake Bay were not available for the entire sampling period, temperature and salinity maps generated in 1993-1994 by Rennie and Nelson (1994) were used to provide the reader with a spatial representation of conditions within the Chesapeake Bay during a typical year. Mean bottom water temperatures and salinities recorded in the present six-year study during winter, spring, summer, and fall were similar to conditions recorded by Rennie and Nelson (1994) in January, April, July, and October, respectively, and were used in this study for illustrative purposes.

RESULTS

The majority of *L. brevis* captured during the survey were collected in the mainstem of the Chesapeake Bay and not the tributaries, and the greatest overall number of squid collected in trawls occurred within the central channel of the lower Bay and along the eastern portion of the Bay (Figure 2). *Lolliguncula brevis* were captured during spring, summer, and fall, but no squid were captured in trawls conducted during winter. Throughout this study, brief squid were collected over a wide range of bottom temperatures (8.1–29.6 °C), bottom salinities (17.9–35.0 ‰), dissolved oxygen levels (1.9–14.6 mg O₂/l), and depths (1.8–29.9 m). In 1993, 1994, 1995, and 1997, *L. brevis* ranked in the upper 10% of nektonic catches in terms of overall number captured, while *L. brevis* ranked in the lower 50% of nektonic catches in 1992 and 1996. In the fall of 1995 and 1997, *L. brevis* ranked second in overall abundance behind bay anchovies *Anchoa mitchilli*. Most of the squid captured during this survey were < 60 mm DML, though some larger squid (> 80 mm DML) were present in the spring and summer (Figure 3). Interestingly, no ontogenetic shift in mantle length was apparent from season to season throughout the study, and the greatest overall number of squid was recorded during the fall (Figure 3).

Since there was a zero percent probability of catching squid in areas sampled during the winter or in areas with salinities below 17.5‰, all sites meeting these criteria were eliminated and not used in logistic regression models. A total of 3,159 sampling

Figure 2. Number of *Lolliguncula brevis* captured in trawls from 1992–1997 in the Chesapeake Bay. All squid displayed in this figure are < 110 mm in dorsal mantle length. Each tow lasted five minutes (bottom time) and was performed at a speed of 9.7 km/h.

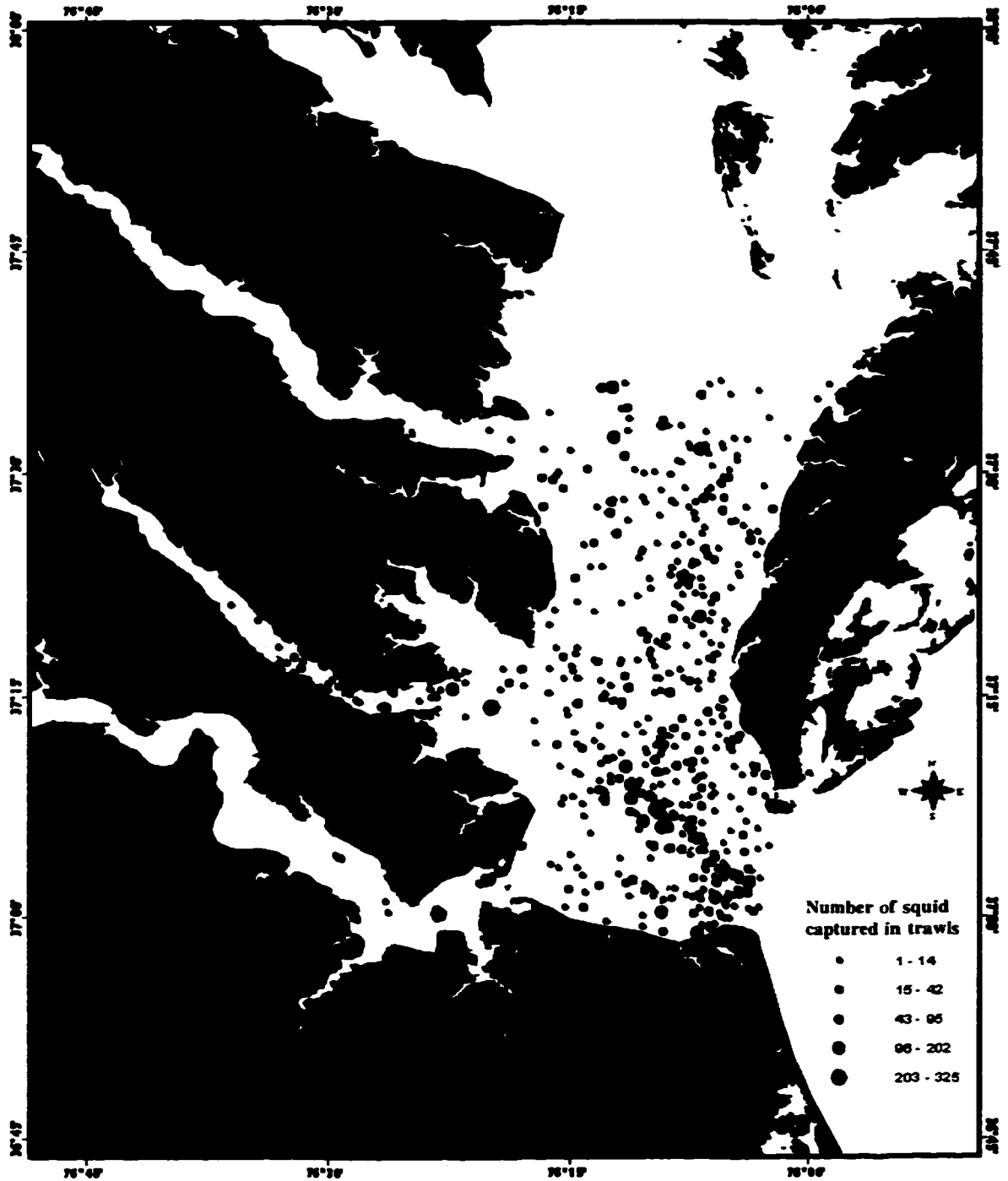
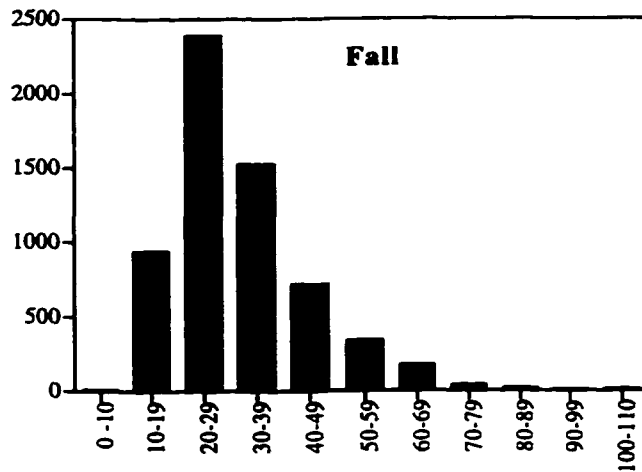
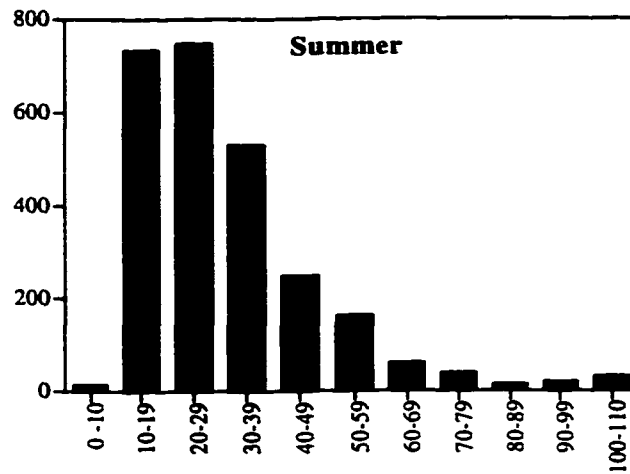
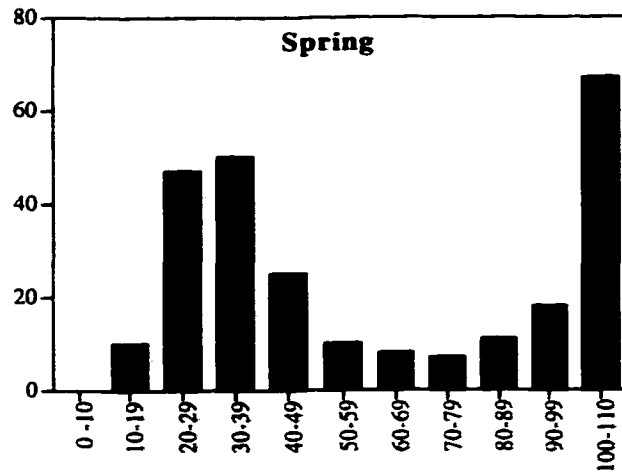


Figure 3. Length/frequency data of *Lolliguncula brevis* (0–110 mm DML) captured in spring, summer, and fall during the VIMS Trawl Surveys from 1992–1997.

Number of Squid Captured



Dorsal Mantle Length (mm)

sites were eliminated, leaving 2,979 sampling sites for consideration within the logistic regression models. Tow distance and Secchi depth did not significantly influence the probability of catching at least one squid in a trawl and were eliminated from the final logistic regression model. The factors and respective categories considered in the final, most parsimonious model are shown in Table 2. The final multivariate logistic regression model was highly significant (-2 log-likelihood chi square = 930.48; G = 726.97; df = 16; $p < 0.001$), and the model adequately fit the data (Hosmer and Lemeshow, Pearson, and deviance tests have p -values > 0.05) (Table 3).

The coefficients (β) of the variables included in the model are most interpretable when expressed in terms of the odds ratio (ψ):

$$\psi = e^{\beta}$$

For scaled continuous independent variables, the odds ratio (ψ) is a measure of how much more likely (or unlikely if the odds ratio is < 1) it is for the outcome (in this case, the presence of at least 1 squid in a trawl) to be present when the variable is increased by one unit. For discrete independent variables (e.g., tide, depth, etc.), the odds ratio is a measure of how much more likely (or unlikely) it is for the outcome to be present relative to the reference level (Hosmer and Lemeshow, 1989; Agresti, 1990).

The probability of catching a squid was significantly less during maximum flood/maximum ebb ($p < 0.001$; $\psi = 0.53$) and late flood through early ebb ($p = 0.004$; $\psi = 0.67$) than during late ebb through early flood (Table 3). The probability of catching a squid increased with depth to a point, after which there was no detectable difference in squid catch probability; there was significantly higher probability of catching a squid at

Table 2. Factors, factor type, and categories used in the final multivariate logistic regression model.

Factor	Factor Type	Categories
Tide	Discrete	1) late ebb – early flood 2) max flood and max ebb 3) late flood – early ebb
Depth	Discrete	1) 0.0 – 4.9 m 2) 5.0 – 9.9 m 3) 10.0 – 14.9 m 4) ≥ 15 m
Temperature	Scaled Continuous	1) $< 5.9^{\circ}\text{C}$ 2) $6.0 - 8.9^{\circ}\text{C}$ 3) $9.0 - 11.9^{\circ}\text{C}$ 4) $12.0 - 14.9^{\circ}\text{C}$ 5) $15.0 - 17.9^{\circ}\text{C}$ 6) $18.0 - 20.9^{\circ}\text{C}$ 7) $21.0 - 23.9^{\circ}\text{C}$ 8) $24.0 - 26.9^{\circ}\text{C}$ 9) $\geq 27.0^{\circ}\text{C}$
Salinity	Scaled Continuous	1) 17.5 – 19.4‰ 2) 19.5 – 21.4‰ 3) 21.5 – 23.4‰ 4) 23.5 – 25.4‰ 5) $\geq 25.5\text{‰}$
Dissolved O ₂	Discrete	1) < 3 mg O ₂ /l 2) ≥ 3 mg O ₂ /l
Year	Discrete	1) 1992 2) 1993 3) 1994 4) 1995 5) 1996 6) 1997
Season	Discrete	1) spring 2) summer 3) fall

Table 3. Multivariate logistic regression of *Lolliguncula brevis* presence/absence in trawls conducted within the Chesapeake Bay. Five discrete factors (tide, depth, dissolved oxygen, year, and season), two scaled continuous factors (water temperature and salinity) and one interaction (water temperature*salinity) were included in the model. For the factor, tide, late ebb through early flood was the reference level and categories 2 and 3 represented max flood/max ebb and late flood through early ebb, respectively. For the factor, depth, 0.0–4.9 m was the reference level and categories 2, 3, and 4 represented depths of 5.0–9.9 m, 10–14.9 m, and ≥ 15 m, respectively. The reference level for the factor, dissolved O₂, was < 3 mg O₂/l (hypoxia) and category 2 represented conditions ≥ 3 mg O₂/l (normoxia). For the factor, year, 1992 was the reference level and the remaining categories (2-6) represented the years 1993–1997. For the factor, season, spring was the reference level and categories 3 and 4 represented the summer and fall, respectively. For the factors, water temperature and salinity, incremental units of 3°C and 2‰, respectively, were used.

Predictor	Coefficient	Z-Value	P-Value	Odds Ratio (ψ)	Lower 95% C.I.	Upper 95% C.I.
Constant	-15.192	-13.03	<0.001			
Tide						
2	-0.633	-4.27	<0.001	0.53	0.40	0.71
3	-0.404	-2.85	0.004	0.67	0.51	0.88
Depth						
2	0.852	3.72	<0.001	2.34	1.50	3.67
3	1.267	5.44	<0.001	3.55	2.25	5.60
4	0.376	1.31	0.192	1.46	0.83	2.56
Water Temperature	0.816	6.60	<0.001	2.26	1.78	2.88
Salinity	1.280	6.79	<0.001	3.60	2.49	5.21
Dissolved O ₂						
2	2.512	4.74	<0.001	12.33	4.36	34.82
Year						
2	1.279	5.57	<0.001	3.59	2.29	5.64
3	1.173	5.16	<0.001	3.23	2.07	5.05
4	1.993	9.58	<0.001	7.34	4.88	11.03
5	0.250	0.86	0.387	1.28	0.73	2.26
6	1.486	7.12	<0.001	4.42	2.94	6.65
Season						
3	0.809	3.41	0.002	2.25	1.41	3.58
4	2.078	10.55	<0.001	7.99	5.43	11.76
Water Temperature*	-0.084	-3.23	0.003	0.92	0.87	0.97
Salinity						

-2 log-likelihood = -930.48, G = 726.97, df = 16, P-Value < 0.001

Goodness-of-Fit Tests

Method	chi-square	df	P-Value
Hosmer-Lemeshow	8.804	8	0.359
Pearson	1456.312	1338	0.279
Deviance	1136.232	1338	0.987

depths of 5.0 to 9.9 m than at depths less than 5.0 m ($p < 0.001$; $\psi = 2.34$) and even higher probability of catching a squid at depths between 10.0 and 14.9 m than at depths less than 5.0 m ($p < 0.001$; $\psi = 3.55$), but no significant difference in catch probability was detected when depths ≥ 15.0 m were compared with depths less than 5.0 m ($p = 0.192$) (Table 3). Within the Chesapeake Bay, the optimal depth range (10–14.9 m) occurs in the central channels (Figure 4), where the highest overall number of squid were collected (Figure 2).

Water temperature ($p < 0.001$; $\psi = 2.26$) and salinity ($p < 0.001$; $\psi = 3.60$) had a strong influence on squid catch probability, although the effects were confounded by a water temperature*salinity interaction ($p = 0.003$; $\psi = 0.92$) (Table 3). Since the odds ratio of the water temperature*salinity interaction was close to 1.00, the interaction only manifests itself at the extremes of one or both of the factors (Hosmer and Lemeshow, 1989). Logit comparisons of all water temperature/salinity combinations revealed that this was indeed the case. Only at low temperatures ($\leq 9^\circ\text{C}$) did the probability of catching at least one squid not increase with increased salinity (Figure 5). Otherwise, the probability of catching at least one squid generally increased with increased salinity and water temperature, and when both salinity and water temperature were high, there was approximately a 50% probability of catching a squid in a trawl (Figure 5). Based on the odds ratios where catch probability increased by a factor of 2.26 with every 3°C rise (between $5\text{--}30^\circ\text{C}$) and increased by a factor of 3.60 with every 2‰ rise (between $17.5\text{--}37.1\text{‰}$), salinity had a larger influence on catch probability than water temperature.

Figure 4. Bathymetry of the Chesapeake Bay. Note that much of the Chesapeake Bay is less than 25 m in depth, and most of the channels of the Bay are 10–15 m (denoted in red).

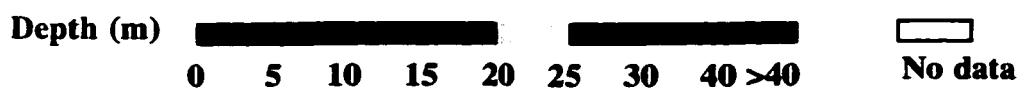
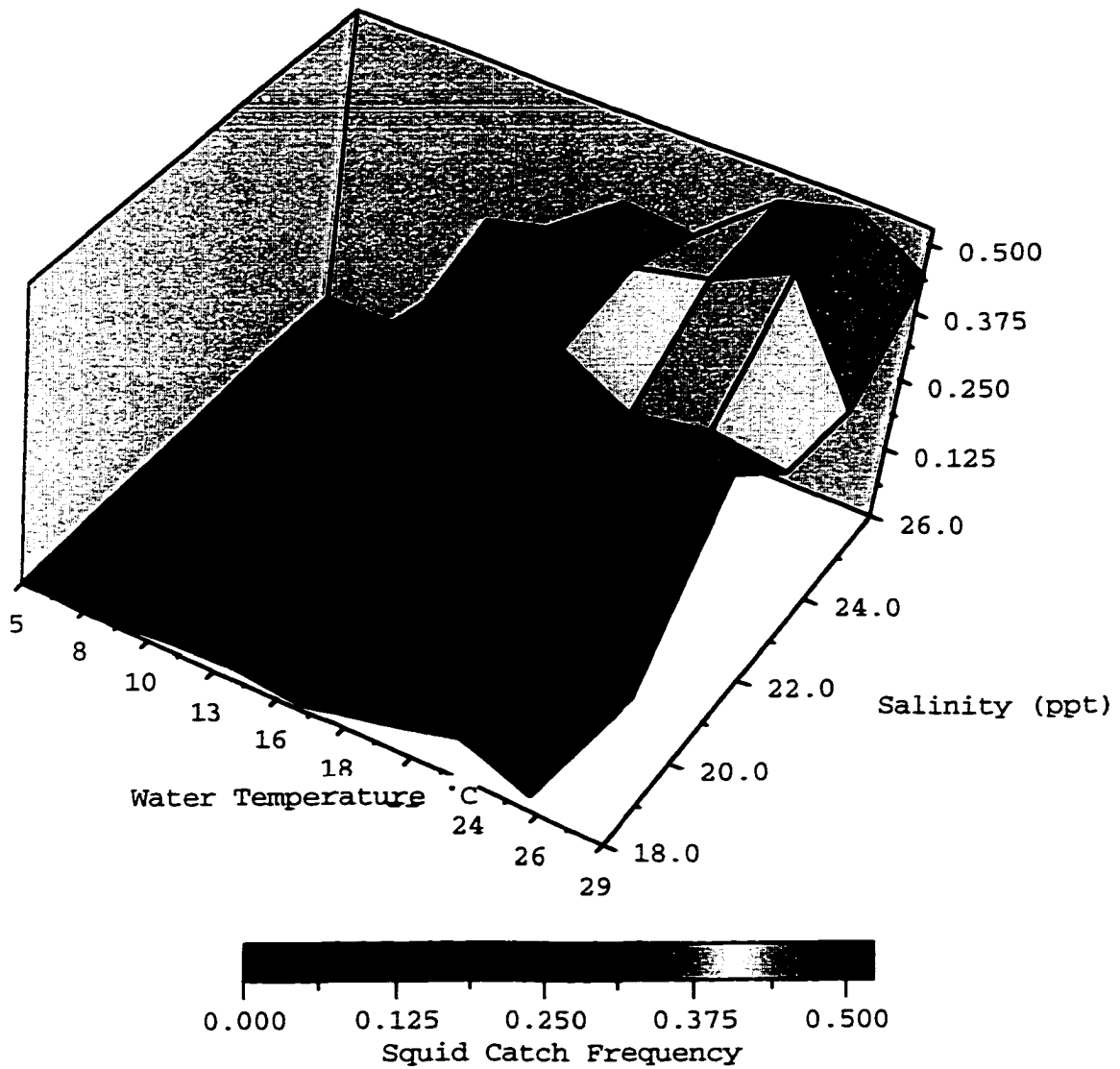


Figure 5. Probability of catching at least one squid in a trawl plotted as a function of water temperature (°C) and salinity (ppt). Generally, catch probabilities increased with increased water temperature and salinity; however, when water temperatures were ≤ 9 °C, catch probability did not increase with increased salinity.



Dissolved oxygen was treated as a dichotomous discrete variable because the only clear difference in catch probability occurred between normoxic and hypoxic sites (i.e., no linear or quadratic relationships between the logit and dissolved oxygen levels were present). Not surprisingly, catch probability increased dramatically ($p < 0.001$; $\psi = 12.33$) when sampling in normoxic as opposed to hypoxic waters.

The probability of catching a squid was lowest in 1992 and 1996 and was highest in 1995, when the probability of catching a squid was 7.34 times greater than in 1992 (Table 3). In 1995, mean monthly bottom salinities for all stations sampled did not decline below 18.1‰ (± 7.4 S.D.) and mean monthly bottom salinities for mainstem Chesapeake Bay stations remained above 22.9‰ (± 3.3 S.D.) (Figure 6). Furthermore, mean monthly bottom water temperatures for all stations sampled were higher from June through October of 1995 than during these months in other years (Figure 7). In 1996, when the probability of catching a squid was low, mean monthly bottom salinities for all stations remained at or below 15.1‰ (± 6.6 S.D.), and mean monthly bottom salinities for Bay mainstem stations remained at or below 20.7‰ (± 4.1) (Figure 6). However, low salinity (< 17.5 ‰) was not a problem in 1992, when catch probability was also low (Figure 6). Hypoxic areas were less prevalent in 1992 than in successive years and bottom water temperatures were not appreciably different (Figure 7). Finally, in 1992 and 1995 when mean bottom salinities for all stations were high during the early part of the year (Figure 6), squid entered the Chesapeake Bay in April, while in other years squid entered the Bay in May.

There were distinct seasonal differences in the probability of catching a squid. No squid were caught within the Chesapeake Bay during the winter, when bottom water

Figure 6. Mean monthly bottom water salinities of sampling sites considered during VIMS Trawl Surveys from 1992–1997. Mean monthly salinities for all stations sampled (Bay and Tributaries), Chesapeake Bay mainstem sampling sites (Bay), and tributary sampling sites (Tributaries) are plotted. The 17.5 ppt line represents the lower physiological limit of brief squid salinity tolerance. Error bars denote ± 1 standard error.

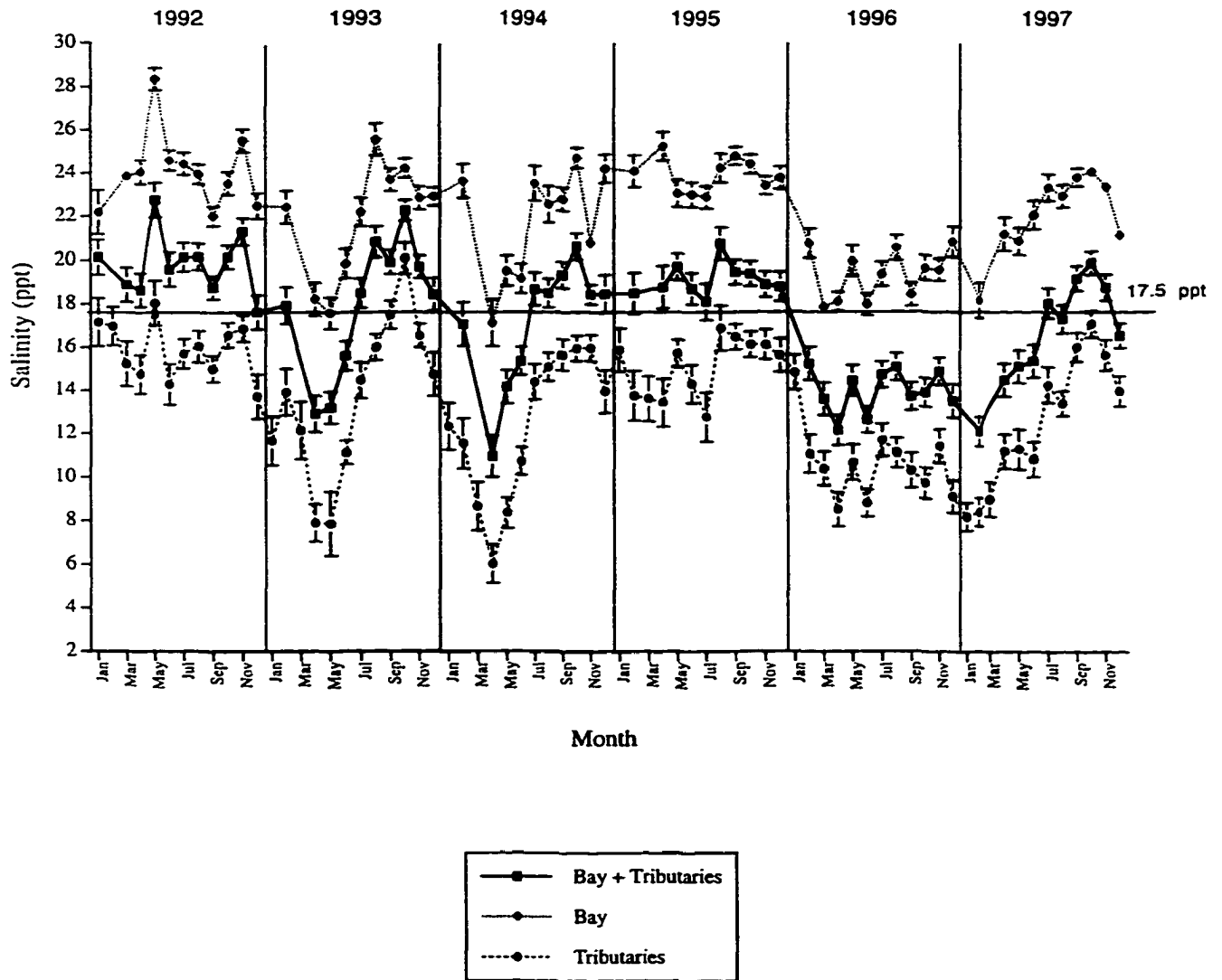
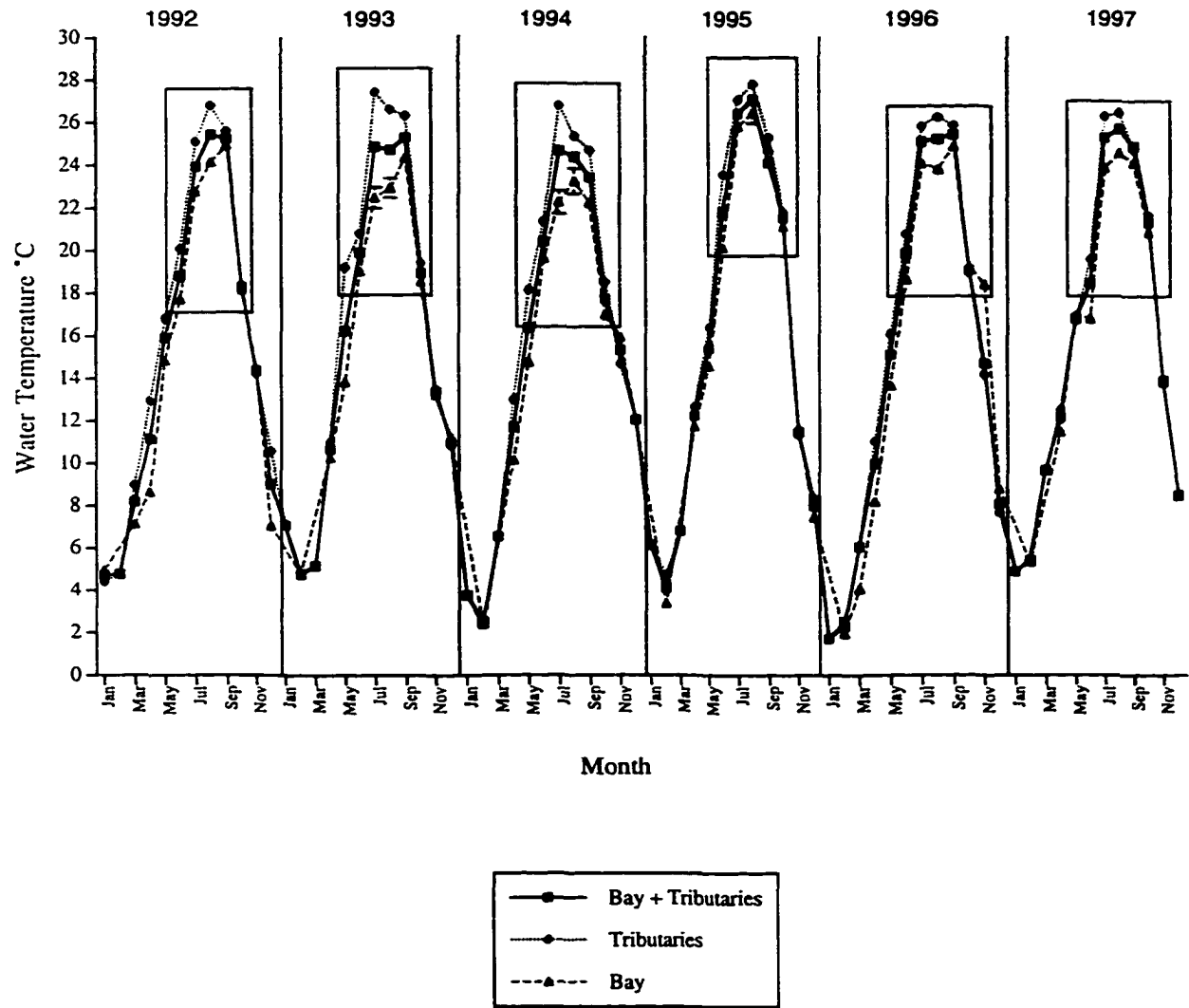


Figure 7. Mean monthly bottom water temperatures of sampling sites considered during VIMS Trawl Surveys from 1992–1997. Mean monthly temperatures for all stations sampled (Bay and Tributaries), Chesapeake Bay mainstem sampling sites (Bay), and tributary sampling sites (Tributaries) are plotted. Boxes highlight conditions from June–October. Since there was little variability in water temperature between sites during a given month, standard error bars denoting ± 1 standard error are not always visible.



temperatures are routinely $< 8^{\circ}\text{C}$ (Figure 8) and bottom salinities are $> 18\text{‰}$ in Mobjack Bay and throughout much of the Bay mainstem (Figure 9). Relative to catch probabilities observed during the summer and fall, the probability of catching a squid was low in the spring as well (Table 3). During a typical spring, bottom salinities are generally above 18‰ only within the mainstem of the Chesapeake Bay and above 21‰ only within the lower portion of the Chesapeake Bay (Figure 9). Within these regions spring bottom water temperatures are typically $< 14^{\circ}\text{C}$ (Figure 8). Although some squid were captured during the spring in areas between 18 and 21‰ , the majority of squid were captured in the lower reaches of the Chesapeake Bay where salinities were $> 21\text{‰}$. Squid catch probability increased by a factor of 2.25 during the summer ($p = 0.002$) and by a factor of 7.99 during the fall ($p < 0.001$) relative to catch probabilities during the spring (Table 3). During the summer, bottom water temperatures in regions of the Chesapeake Bay where squid were captured (see Figure 2) range typically from 20 to 28°C , and salinities $> 18\text{‰}$ occur in much of the lower Chesapeake Bay and portions of the James and York Rivers (Figure 8, 9). During the fall when catch probabilities are the highest, bottom water temperatures are typically more uniform (20 – 22°C) throughout the Chesapeake Bay and regions where salinities are $> 21\text{‰}$ and $> 24\text{‰}$ are more abundant (Figure 9).

During the course of this study, *L. brevis* egg masses were occasionally observed within the trawl mesh. These masses were collected in September and October within sandy bottom habitats along the eastern portion of the Chesapeake Bay mainstem. Individual egg cases were generally < 2.5 cm in length and contained < 30 *L. brevis* paralarvae. Furthermore, mature males, characterized by a well-developed penis, tightly packed spermatophores within the spermatophoric sac, and a yellowish or whitish testis,

Figure 8. Typical bottom water temperatures (°C) within the Chesapeake Bay in winter (January), spring (April), summer (July), and fall (October). (Adapted from Rennie and Nelson, 1994).

winter



spring



summer



fall

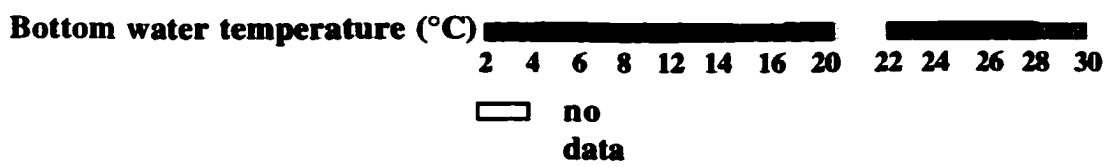
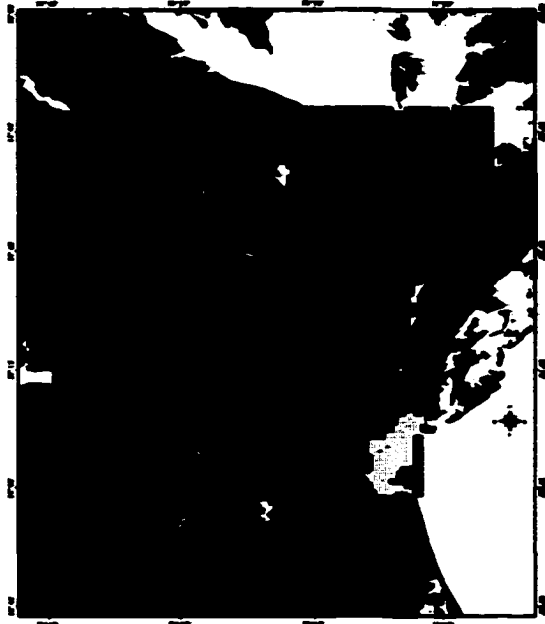


Figure 9. Typical bottom salinities (‰) within the Chesapeake Bay in winter (January), spring (April), summer (July), and fall (October). (Adapted from Rennie and Nelson, 1994).

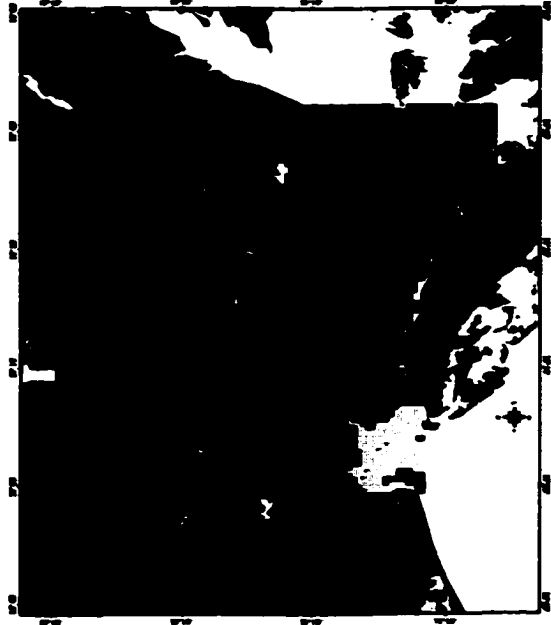
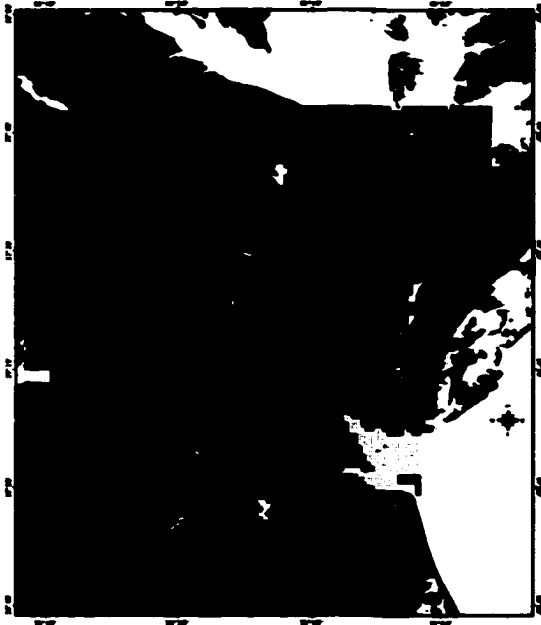
winter

spring



summer

fall



Bottom salinity (‰)



no data

and ripe females, characterized by an internal oviduct filled with mature, amber-colored eggs, were observed in late July–September.

DISCUSSION

Salinity and water temperature play critical roles in *L. brevis* distribution and abundance within the Chesapeake Bay. Estuarine waters of 0.0–35.0‰ and 0.0–30.0°C were sampled during this six-year study, yet *L. brevis* were observed only at sites with salinities between 17.9 and 35.0 ‰ and water temperatures between 8.1 and 29.6°C. The lower salinity limit detected in this study is consistent with the physiological limit, 17.5‰, determined in the laboratory (Hendrix et al. 1981). No laboratory studies designed to examine the temperature limits of *L. brevis* have been conducted. However, Wells et al. (1988) have demonstrated that *L. brevis* respire proficiently at 15°C, even under conditions of progressive hypoxia. In field studies, Dragovich and Kelly (1967) captured *L. brevis* in waters of 18.2–36.2‰ and 12.6–31.6°C along the western coast of Florida, Hixon (1980) collected *L. brevis* in waters of 20–37‰ and 11–31°C in the northwest Gulf of Mexico, and Laughlin and Livingston (1982) captured *L. brevis* in waters of 8.5–35.5‰ and 15–31°C in an estuary in north Florida. In this study, when water temperature was 10–30°C, the probability of catching *L. brevis* increased as salinity increased between 17.5 and 29.6‰. (In waters $\leq 9^\circ\text{C}$, catch probability did not increase significantly with salinity). Moreover, when salinities were $\geq 17.5\text{‰}$, the probability of catching a squid increased as water temperature increased. These findings are consistent with those of Laughlin and Livingston (1982), who found that brief squid are most

prevalent in estuarine waters of Florida that are high in both salinity (25–30‰) and temperature (20–30°C).

Both salinity and water temperature appear to influence seasonal distribution patterns of brief squid. Low water temperature accounted largely for the absence of squid during the winter months. Brief squid left the Chesapeake Bay in the early winter (late December), when mean bottom water temperatures throughout the Bay dropped below 8°C, and began to re-enter the Chesapeake Bay in the spring (April and May), when water temperatures were greater than 10°C. Similar migratory responses of *L. brevis* to low water temperatures have been reported by Hixon (1980) and Laughlin and Livingston (1982). Hixon (1980) determined that *L. brevis* move offshore from Galveston Bay, Texas in December through February, when mean water temperatures are 12.8–13.9°C, and re-enter inshore, bay habitats in March, when water temperatures are above 15°C. Laughlin and Livingston (1982) determined that many *L. brevis* leave Appalachicola estuary, FL in December through April, when water temperatures and salinities are the lowest of the year, and return in May through November. Although salinity did not contribute to the exodus of brief squid from the Chesapeake Bay in late December (salinities were high and well within tolerance limits), salinity did play an important role in determining when and where *L. brevis* re-entered the Chesapeake Bay in the spring. In years when spring bottom salinities were low (1993, 1994, 1996, and 1997), squid re-entered the Chesapeake Bay later in the spring than in years (i.e., 1992 and 1995) when spring bottom salinities were high, even though Bay water temperatures were within tolerance limits. Furthermore, during the spring, squid were found exclusively in the mainstem and the majority of squid were found in the lower reaches of

the Chesapeake Bay, despite warmer bottom water temperatures in the tributaries and western portion of the Bay. This was because salinities in these warmer regions were below 17.5‰—the lower physiological limit of brief squid (Hendrix et al., 1981).

Since the probability of catching a squid increased when salinity and water temperature increased, low spring water temperatures and salinities probably accounted for lower catch probabilities during the spring compared with the summer and fall. During the fall when there was the highest probability of catching a squid, baywide water temperatures are generally lower than those in the summer, but the regions of high salinity (> 21‰ and 24‰) are generally more extensive. Results from the logistic regression model indicated that although both water temperature and salinity significantly affect squid catch probability, salinity has a larger influence. Thus, the benefits provided by the expansion of high salinity areas in the fall outweighed the disadvantages of lower water temperatures and therefore increased squid catch probability. Similarly, Laughlin and Livingston (1982) found that the spatial distribution of brief squid within a Florida estuary is determined mostly by salinity and habitat structure, while water temperature plays a lesser role, influencing distribution primarily during the fall and winter.

Salinity and water temperature also appear to affect inter-annual catch probability. The low catch probability detected for the year, 1996, may be attributed to low baywide salinities. Mean monthly bottom salinities for all stations sampled throughout 1996 were consistently below the physiological 17.5‰ limit, and even mean mainstem Chesapeake Bay station salinities, which generally reach 24‰ during the year, never increased above 20.7‰. Laughlin and Livingston (1982) detected similar declines in squid abundance during years when salinities were low. The highest probability for catching squid

occurred in 1995 and was likely a result of high salinities throughout the year (overall mean monthly salinities never declined below 18.1‰ and mean Chesapeake Bay monthly salinities remained above 22.9‰) and high water temperatures (mean bottom temperatures were higher from June through October of '95 than at any other time throughout the sampling period). The synergistic effects of temperature and salinity fail to explain low catch probabilities in 1992, however. Water temperatures did not significantly diverge from temperatures observed in other years, and mean monthly salinities for all stations were consistently above the 17.5‰ limit throughout the year. Other factors, such as food availability and trophic interactions, may influence squid abundance (Livingston et al., 1974; Livingston and Louck, 1979; Laughlin and Livingston, 1982) and may have been responsible for the observed decline in squid catches.

Squid catches were greatest in the central Chesapeake Bay near the mouth and along eastern portions of the Chesapeake Bay. These regions typically have the highest salinities throughout the year, and thus salinity assuredly played a role in the observed distribution patterns; however, depth played a significant role as well. In general brief squid are thought of as shallow water cephalopods, preferring habitats < 30 m in Galveston Bay, TX (LaRoe, 1967; Hixon, 1980) and along the eastern U.S. Coast (unpublished NMFS Groundfish Survey data: 1963–1997). The bathymetry of the Chesapeake Bay is predominantly < 20 m, and thus the Chesapeake Bay provides optimal depths for squid residence. The data presented in this study suggest that at depths less than 30 m there are further preferences that may help explain regional probability differences within the Chesapeake Bay ecosystem. Based on odds ratios computed in the

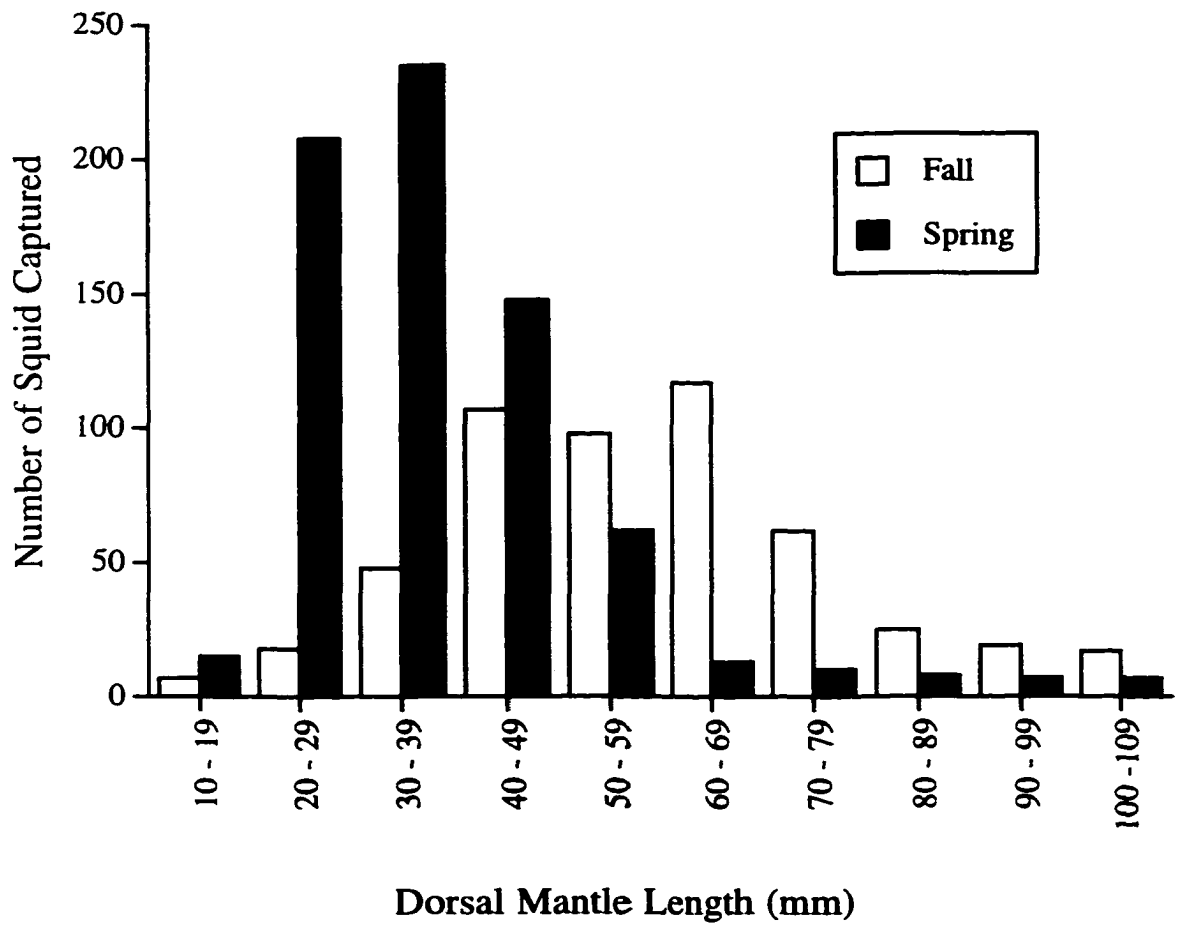
logistic regression model, the probability of catching at least one squid increased as depth increased incrementally from 0–5 m (category 1) to 5–10 m (category 2) to 10–15 m (category 3), the depth range at which the highest probabilities were observed. At depths of 15–40 m, however, there was no significant difference in catch probability relative to depths of 0–5 m. Many of the central channels of the Chesapeake Bay are 10–15 m in depth, and these locations are where the highest overall number of squid were encountered. Thus, when salinities and water temperatures are within tolerance limits, brief squid prefer central channel areas 10–15 m in depth. Laughlin and Livingston (1982) found a similar preference for channels by brief squid in Apalachicola estuary, FL.

Tidal stage and dissolved oxygen level, not surprisingly, had an impact on catch probability of brief squid within the Chesapeake Bay. The probability of catching a squid was greater from late ebb through early flood than at maximum flood/maximum ebb or at late flood through early ebb. This finding suggests that when water volume within the Chesapeake Bay ecosystem is low and currents are not substantial, squid populations are more concentrated and squid are easier to catch by trawl. The low catch probabilities observed at maximum flood or ebb suggest that brief squid are not always most prevalent in high currents as detected by Laughlin and Livingston (1982). Higher catch probability in normoxic waters compared with hypoxic waters was expected; however, the fact that squid were captured in hypoxic waters as low as 1.93 mg O₂/l is of interest and is consistent with the findings of Vecchione and Roper (1991) and Vecchione (1991a, b). Vecchione and Roper (1991) observed *L. brevis* in hypoxic waters (0.7 mg O₂/l) of the western North Atlantic using remotely operated submersibles, and Vecchione (1991b)

documented *L. brevis* in hypoxic waters ($< 3 \text{ mg O}_2/\text{l}$) within coastal and estuarine waters of southwestern Louisiana during trawl surveys. Vecchione (1991a) proposed that brief squid may be in these areas to exploit a food niche or avoid predation.

Brief squid were clearly abundant in the Chesapeake Bay relative to other nekton captured in the VIMS Trawl Survey from 1992–1997, ranking in the upper 10% of nektonic catches in terms of total number of organisms captured in four of the six sampling years. Moreover, during the fall of some years, squid ranked second behind bay anchovies. Length/frequency breakdowns of squid catches revealed that two size classes of *L. brevis* use the Chesapeake Bay: one class $< 60 \text{ mm DML}$, which use the Bay in spring through fall, and a second, less abundant class $> 80 \text{ mm DML}$, which is most prevalent in the spring and summer. Interestingly, no ontogenetic size shift in the smaller size class was visible from season to season in this study (Figure 3). Conversely, a clear ontogenetic shift in *L. brevis* size distribution is apparent when data from NMFS bottom trawl surveys, which are conducted along the continental shelf from Delaware to Florida annually during the spring and fall, are examined. In the NMFS surveys, mean *L. brevis* DML was $32 \text{ mm DML} (\pm 12 \text{ S.D})$ during the spring and $62 \text{ mm DML} (\pm 23 \text{ S.D})$ in the fall (Figure 10). The absence of a distinct intermediate size class in the Chesapeake Bay in the summer or fall suggests that *L. brevis* may leave the Bay once a specific size is reached. Heavy utilization of certain habitats by smaller individuals and subsequent migration of larger individuals is common among cephalopods (Hixon, 1983; Nesis, 1983; Okutani, 1983; Summers, 1983; Nagasawa et al., 1993; Hanlon and Messenger, 1996).

Figure 10. Length/frequency data of *Lolliguncula brevis* collected during NMFS Groundfish Surveys (1992–1997) along the coastline of the U.S. from Delaware to Florida. Data from spring and fall surveys are presented.



Limited field observations suggest that larger brief squid may be using the Chesapeake Bay as spawning grounds at least during late July through early September. This is consistent with the findings of Vecchione (1982), who found paralarvae near the mouth of the Chesapeake Bay during the warmest months of late summer. Within the Gulf of Mexico, spawning occurs to some degree year-round and peak spawning occurs during April–July and September–November (LaRoe, 1967; Hixon, 1980; Jackson et al., 1997). More work on fecundity and paralarval ecology needs to be performed in the Chesapeake Bay to determine if spawning occurs in the spring, summer, and fall and if there are peak spawning events in the spring and late summer. Given that recent statolith studies have revealed that *L. brevis* live approximately 100–200 days in the Gulf of Mexico (Jackson et al., 1997), it is likely that spawning occurs to some degree most of time that brief squid are in the Chesapeake Bay. Early juveniles that either hatch in the Chesapeake Bay or that migrate into the Bay from offshore habitats may remain in the Bay to exploit its rich food supply, namely crustaceans and juvenile finfishes.

The common occurrence of brief squid within the Chesapeake Bay, a euryhaline, highly variable environment which is home to hundreds of species of fishes each year, is intriguing. Squid are generally thought to be hampered by a deficient physiology and are notorious for possessing an inefficient means of propulsion. Consequently, squid are thought to have evolved in environments such as deep-sea or offshore, pelagic habitats where interaction with more efficient nekton is minimized (O’Dor and Webber, 1986). Nonetheless, brief squid are present in an inshore habitat rich with nektonic fauna. Further research examining the physiology and locomotive abilities of brief squid, especially the smaller individuals that appear to be most abundant within the Chesapeake

Bay, may further our evolutionary and ecological understanding of this unique cephalopod.

LITERATURE CITED

- Agresti, A. 1990. *Categorical Data Analysis*. New York: Wiley.
- Alexander, R. M. 1977. Swimming. In *Mechanics and Energetics of Animal Locomotion* (ed. R. M. Alexander and G. Goldspink), pp. 222-248. London: Chapman and Hall.
- Ballantyne, J.S., P. W. Hochachka, and T. P. Mommsen. 1981. Studies on the metabolism of the migratory squid, *Loligo opalescens*: enzymes of tissues and heart mitochondria. *Mar. Biol. Lett.* 2: 75-85.
- Dragovich, A., and J. A. Kelly, Jr. 1967. Occurrence of the squid, *Lolliguncula brevis*, in some coastal waters of western Florida. *Bull. Mar. Sci.* 17: 840-844.
- Finke, E., H. O. Pörtner, P. G. Lee, and D. M. Webber. 1996. Squid (*Lolliguncula brevis*) life in shallow waters: oxygen limitation of metabolism and swimming performance. *J. Exp. Biol.* 199: 911-921.
- Gunter, G. 1950. Seasonal population changes and distributions as related to salinity of certain invertebrates of the Texas Coast, including the commercial shrimp. *Publ. Inst. Mar. Sci. Univ. Tex.* 1: 7-51.
- Haefner, P. A. 1959. Morphometry and biology of *Loligo pealei* (Lesueur 1821) and *Lolliguncula brevis* (Blainville, 1823) in Delaware Bay. Master's Thesis, University of Delaware, DE, 61 p.
- Hanlon, R. T. and J. B. Messenger. 1996. *Cephalopod Behaviour*. Cambridge: Cambridge University Press.
- Hendrix, J. P., Jr., W. H. Hulet, and M. J. Greenberg. 1981. Salinity tolerances and the response to hypoosmotic stress of the bay squid *Lolliguncula brevis*, a euryhaline cephalopod mollusc. *J. Comp. Biochem. Physiol.*, 69A: 641-648.
- Hixon, R. F. 1980. Growth, reproductive biology, distribution and abundance of three species of loliginid squid (Myopsida, Cephalopoda) in the Northwest Gulf of Mexico. Ph.D. dissertation, University of Miami, Miami, Fl, 182 p.

- Hixon, R. F. 1983. *Loligo opalescens*. In *Cephalopod Life Cycles, Vol. 1: Species Accounts* (ed. P.R. Boyle), pp. 95-114. London: Academic Press.
- Hosmer, D. W. and S. Lemeshow. 1989. *Applied Logistic Regression*. New York: John Wiley and Sons.
- Jackson, G. D., J. W. Forsythe, R. F. Hixon, and R. T. Hanlon. 1997. Age, growth, and maturation of *Lolliguncula brevis* (Cephalopoda: Loliginidae) in the northwestern Gulf of Mexico with a comparison of length-frequency versus statolith age analysis. *Can. J. Fish. Aquat. Sci.* 54: 2907-2919.
- Laughlin, R. A., and R. J. Livingston. 1982. Environmental and trophic determinants of the spatial/temporal distribution of the brief squid (*Lolliguncula brevis*) in the Apalachicola Estuary (North Florida, USA). *Bull Mar. Sci.* 32: 489-497
- LaRoe, E. T. 1967. A contribution to the biology of the Loliginidae (Cephalopoda: Myopsida) of the tropical western Atlantic. Master's Thesis, University of Miami, Miami, FL, 162p.
- Livingston, R. J., G. J. Kobylinski, F. G. Lewis, III, and P. F. Sheridan. 1975. Long-term fluctuations of epibenthic fish and invertebrate populations in Apalachicola Bay, Florida. *Fish. Bull.* 74: 311-321.
- Livingston, R. J. and O. L. Loucks. 1979. Productivity, trophic interactions, and food-web relationships in wetlands and associated systems. In *Wetland Functions and Values: The State of our Understanding* (ed. P. E. Greeson, J. R. Clark, and J. E. Clark), pp. 101-119. American Water Resources Association, Minneapolis, Minn.
- Mangum, C. P. 1991. Salt sensitivity of the hemocyanin of eury- and stenohaline squids. *Comp. Biochem. Physiol.* 99A: 159-161.
- Mickey, J., and S. Greenland, S. 1989. A study on the impact of confounder-selection criteria on effect estimation. *Am J. Epid.* 129: 125-137.
- Mommsen, T. P., and P. W. Hochachka. 1981. Respiratory and enzymatic properties of squid heart mitochondria. *Eur. J. Biochem.* 120: 345-350.
- Nagasawa, K., S. Takayanagi, and T. Takami. 1993. Cephalopod tagging and marking in Japan: a review. In *Recent Advances in Cephalopod Fisheries Biology* (ed. T. Okutani, R. K. O'Dor, and T. Kubodera), pp. 313-329. Tokyo: Tokai University Press.
- Nesis, K. N. 1983. *Dosidicus gigas*. In *Cephalopod Life Cycles, Vol. 1: Species Accounts* (ed. P.R. Boyle), pp. 215-231. London: Academic Press.

- O'Dor, R. K. 1982. Respiratory metabolism and swimming performance of the squid, *Loligo opalescens*. *Can. J. Zool.* 39: 580-587.
- O'Dor, R. K. and D. M. Webber. 1986. The constraints on cephalopods: why squid aren't fish. *Can. J. Zool.* 64: 1591-1605.
- O'Dor, R.K. and D. M. Webber. 1991. Invertebrate athletes: tradeoffs between transport efficiency and power density in cephalopod evolution. *J. Exp. Biol.* 160: 93-112.
- Okutani, T. 1983. *Todarodes pacificus*. In *Cephalopod Life Cycles, Vol. 1: Species Accounts* (ed. P.R. Boyle), pp. 201-214. London: Academic Press.
- Pörtner, H. O., D. M. Webber, R. G. Boutilier, and R. K. O'Dor. 1991. Acid-base regulation in exercising squid (*Illex illecebrosus*, *Loligo pealei*) *Am. J. Physiol.* 261: R239-R246.
- Pörtner, H. O., D. M. Webber, R. K. O'Dor, and R.G. Boutilier. 1993. Metabolism and energetics in squid (*Illex illecebrosus*, *Loligo pealei*) during muscular fatigue and recovery. *Am. J. Physiol.*, 265: R157-R165.
- Rennie, S.E., and B. Nelson. 1994. *A CD-Rom Atlas of Data from the Chesapeake Bay Monitoring Program*. Virginia Institute of Marine Science, Gloucester Point, VA, 14 p.
- Summers, W. C. 1983. *Loligo opalescens*. In *Cephalopod Life Cycles, Vol. 1: Species Accounts* (ed. P.R. Boyle), pp. 115-142. London: Academic Press.
- Tokahashi, T. S. 1960. Studies on the utilization of cuttlefish, *Ommastrephes sloani pacificus*—III. The seasonal variation in the gravimetric constitution and chemical composition of the various parts of the body. *Bull. Jpn. Soc. Sci. Fish.* 26: 95-98.
- Vecchione, M. 1982. Larval distribution of a euryhaline squid near its northern range limit. *Bull. Am. Malacol. Union* 81: 36.
- Vecchione, M. 1991a. Dissolved oxygen and the distribution of the euryhaline squid *Lolliguncula brevis*. *Bull. Mar. Sci.* 49: 668-669.
- Vecchione, M. 1991b. Observations on the paralarval ecology of a euryhaline squid *Lolliguncula brevis* (Cephalopoda: Loliginidae). *Fish. Bull.* 89: 515-521.
- Vecchione, M. and C. Roper. 1991. Cephalopods observed from submersibles in the western North Atlantic. *Bull. Mar. Sci.* 49: 433-445.

- Vecchione, M., C. F. Roper, and M. J. Sweeney. 1989. Marine Flora and Fauna of the Eastern United States Mollusca: Cephalopoda. NOAA Technical Report NMFS 73, 23p.
- Vogel, S. 1994. *Life in Moving Fluids*, 2nd ed. Princeton: Princeton University Press.
- Voss, G. L. 1956. A review of the cephalopods of the Gulf of Mexico. *Bull Mar. Sci.* 49: 668-669.
- Webber, D. M. and R. K. O'Dor. 1985. Respiration and swimming performance of short-finned squid (*Illex illecebrosus*). *Scientific Council Studies. Northw. Atl. Fish. Org.* 9: 133-138.
- Wells, M. J. 1994. The evolution of the racing snail. *Mar. Fresh. Behav. Physiol.* 25: 1-12.
- Wells, M. J., R. T. Hanlon, P. G. Lee, and F. P. Dimarco. 1988. Respiratory and cardiac performance in *Lolliguncula brevis* (Cephalopods, Myopsida): the effects of activity, temperature, and hypoxia. *J. Exp. Biol.* 138: 17-36.

CHAPTER 2

RESPIRATORY COSTS OF SWIMMING IN THE NEGATIVELY BUOYANT BRIEF SQUID: AN ANALOGUE TO AERIAL FLIGHT

ABSTRACT

Because of the inherent inefficiency of jet propulsion, squids are considered to be at a competitive disadvantage to fishes, which generally rely on forms of undulatory/oscillatory locomotion. The brief squid, *Lolliguncula brevis*, which uses significant fin motion, swims at low speeds, and lives in inshore, complex, frequently euryhaline environments, differs from cephalopods considered in present squid/fish energetic comparisons and may swim in a very different way. To estimate the swimming costs of this unique cephalopod and determine where it ranks metabolically in relation to other mobile nekton, O₂ consumption rates were measured for *L. brevis* of various sizes (2–9 cm dorsal mantle length (DML)) swimming over a range of speeds (3–30 cm s⁻¹) in swim tunnel respirometers. Angles of attack, fin motion, and position within the flow stream were recorded during trials using video and motion analysis equipment. Many squid demonstrated partial (J-shaped) and full (U-shaped) parabolic patterns of O₂ consumption as a function of swimming speed. O₂ consumption rates at 0.5–1.5 mantle lengths s⁻¹ were significantly less than those at < 0.5 and > 1.5 mantle lengths s⁻¹. The mean body angle of attack and mean number of fin beats s⁻¹ decreased with increased swimming velocity for all size classes examined, and the greatest deviation in horizontal position (implying greater variation in velocity) typically occurred at low speeds. The observed parabolic relation between oxygen consumption and velocity is probably the result of the high cost of generating lift at low speeds, which is achieved by elevating the

angle of attack of the body, increasing fin activity, orienting the funnel more vertically, and accelerating and subsequently coasting/gliding within the tunnel, and the high cost of overcoming drag at high speeds. *Lolliguncula brevis* has lower O_2 consumption than the squids *Illex illecebrosus* and *Loligo opalescens* studied in swim tunnel respirometers. Furthermore, O_2 consumption in *L. brevis* is 1.0–3.5x higher than mullet, striped bass, and flounder when swimming velocities are expressed in $cm\ s^{-1}$, but is actually lower than that of striped bass, flounder, and menhaden at certain speeds when swimming velocities are expressed in body lengths s^{-1} . *Lolliguncula brevis* is thus different from other cephalopods examined previously because its parabolic pattern of oxygen consumption as a function of velocity is similar to aerial flight and its swimming costs are competitive with ecologically equivalent fishes.

INTRODUCTION

Many squids rely on jet propulsion for locomotion, which is inherently less efficient than undulatory/oscillatory locomotion employed by many fishes (Vogel, 1994). Jet propulsion is inefficient because squid fill a cavity of limited volume with water and eject that water through an orifice, thus expelling relatively small volumes of water backwards with each jet thrust. Undulatory swimmers drive significantly larger volumes of water backwards with each sweep of the body, tail, and/or fins, and the mass of water directed backwards is not constrained by internal morphology. Since thrust is a product of the mass (m) per unit time and velocity (v) of water displaced backwards and jet-propelled organisms cannot increase the mass of water due to internal volume limitations, jet locomotors must expel the water at high velocity. This is costly because the energy required for thrust increases with velocity squared ($E = 1/2mv^2$) (O'Dor and Webber, 1991; Vogel, 1994). Not surprisingly, direct comparisons between fish, such as *Salmo*, and certain squid that rely heavily on jet propulsion for locomotion, such as *Illex illecebrosus* and *Loligo opalescens*, show that squid typically have O_2 consumption rates 5–7x higher than fish (O'Dor, 1982; Webber and O'Dor, 1986; O'Dor and Webber, 1986; 1991). As a result, O'Dor and Webber (1986) conclude "squid are not so much competing with fish as trying to stay out of their way".

The assumption that all squids, the most mobile of the cephalopods, are not competitive with fish because of the inefficiency of jet propulsion may be too simplistic.

Squids, like fishes, are diverse and have evolved many behavioral and physiological mechanisms that allow them to compete in a variety of environments. One species, the brief squid *Lolliguncula brevis*, is particularly distinctive from the squids *Loligo opalescens* and *Illex illecebrosus* considered in previous studies. Brief squid have small rounded bodies, large rounded fins, heavily keeled third (III) arms, and may live in shallow, complex, temporally variable environments (Hixon, 1980; Chapter 1). Conversely, *Loligo opalescens* and *Illex illecebrosus* are larger, more elongate, and pelagic (Hixon, 1980, 1983; O'Dor, 1983; Hanlon and Messenger, 1996). Brief squid swim at low speeds, where the costs of jet propulsion are reduced, and they use significant fin movement, which lacks the volume limitations of jet propulsion. Thus, the inherent inefficiencies of jet propulsion may not be as pronounced for *L. brevis*. *Loligo* and *Illex* swim at moderate to high speeds and use their fins primarily for steering and maneuvering (O'Dor, 1988; Hoar et al., 1994). *Lolliguncula brevis* is also the only cephalopod to invade the inshore, euryhaline waters of the Chesapeake Bay, where it is abundant (ranking in the upper 10% of annual nektonic trawl catches (Bartol and Vecchione, 1997)) and competes as a predator with hundreds of species of fishes.

Aside from jet propulsion, squid are distinct from many pelagic nekton because they are often negatively buoyant, and consequently, many may have a parabolic O₂ consumption/speed relationship similar to that of birds. Birds, which are negatively buoyant in air, expend considerable energy both staying aloft at low speeds, when lift forces are minimal, and overcoming drag at high speeds, when drag forces dominate. Oxygen consumption rates are low at intermediate speeds when lift forces are greater than at low speeds as a result of increased flow over the body and wings and when drag

forces are less important than at high speeds. The resulting O₂ consumption versus speed curve is U-shaped (see Tucker, 1968, 1973; Pennycuik, 1968, 1989). A similar relationship may exist in negatively buoyant squid because they also presumably have high lift generation costs at low speeds and substantial drag costs at high velocities. Parabolic O₂ consumption versus velocity relationships have been detected in negatively buoyant mandarin fish, *Synchiropus picturatus* (Blake, 1979). No such relationship has been observed previously in squid, but low speeds (1–10 cm s⁻¹)—speeds frequently used by brief squid and when lift generation costs are highest—have not yet been examined.

L. brevis is morphologically, ecologically, and physiologically unlike many cephalopods, especially those considered in previous comparisons between squids and fishes, and may swim differently. Brief squid's reliance on fin motion and preference for low-speed swimming may minimize the inefficiencies of jet propulsion and therefore reduce the costs of swimming. Moreover, negative buoyancy and costs associated with maintaining vertical position in the water column may influence the relationship between O₂ consumption and speed, such that costs are lower at intermediate speeds than at high or low speeds. Brief squid that swim at these intermediate speeds may be more competitive with fish than is presently thought. Therefore, O₂ consumption rates of *L. brevis* of various sizes (2–9 cm dorsal mantle length (DML)) swimming over a continuum of speeds (1–30 cm s⁻¹) were measured to: 1) characterize the O₂ consumption versus speed relationship and 2) to compare their energetics with other ecologically comparable nekton.

MATERIALS AND METHODS

Experimental Animals

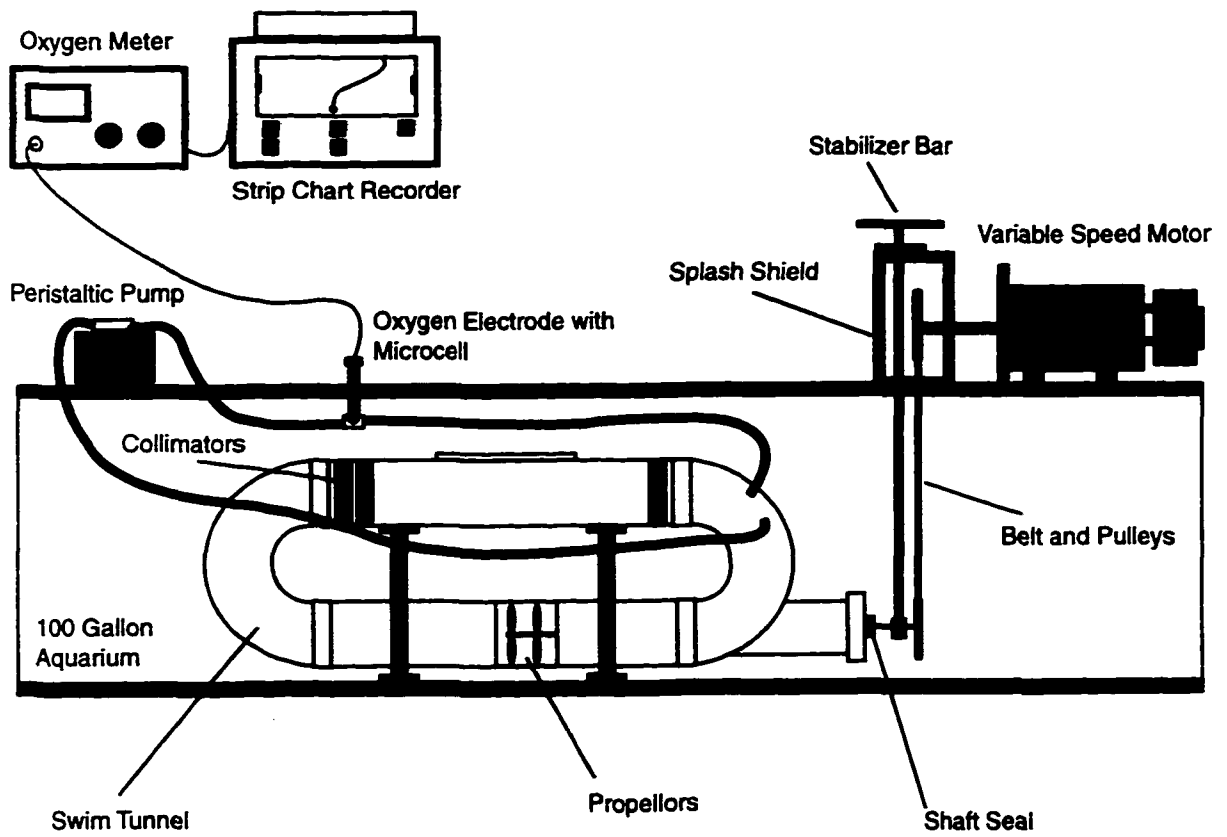
Lolliguncula brevis (2.9–8.8 cm DML, 1.7–52.3 g) were captured by trawl both within embayments along the seaside of Virginia's Eastern Shore and in the York River, VA, a sub-estuary of the Chesapeake Bay. Squid captured along the Eastern Shore of Virginia were transported to the Virginia Institute of Marine Science (VIMS) Eastern Shore Lab located in Wachapreague, VA, while squid captured in the York River were transported to the VIMS main campus located in Gloucester Point, VA. Squid were kept alive in the field using 120-quart coolers equipped with filtration and aeration systems, which were powered by 12 V DC rechargeable batteries. At both Wachapreague and Gloucester Point, squid were kept in flow-through raceway tanks and fed a diet of grass shrimp, *Palaemonetes pugio*. All squid considered in this study were kept in captivity for at least one week prior to experimentation and were not fed 24 hours before trials so that digestion (specific dynamic action) was not reflected in O₂ measurements. Experiments on three squid 2.9–3.9 cm DML, four squid 4.0–4.9 cm DML, four squid 5.0–5.9 cm DML, six squid 6.0–6.9 cm DML, five squid 7.0–7.9 cm DML, and five squid 8.0–8.9 cm DML were performed.

O₂ Consumption Measurements

Two separate swim tunnel respirometers, one with a 15.6 L capacity and the other with a 3.8 L capacity, were used. Within each swim tunnel respirometer, flow velocity was controlled using two propellers attached to a stainless steel shaft in a rotor-stator configuration driven by a 1/4 hp variable speed motor with a belt and pulleys (Figure 1). To keep water temperatures as constant as possible within the respirometer and to facilitate the removal of air bubbles, each of the tunnels was completely submerged in a 100 gallon aquarium filled with aerated seawater. During the experiments water from within the respirometers was pumped to a submerged microcell using a peristaltic pump, and dissolved oxygen was measured using a Strathkelvin 1302 oxygen electrode and Strathkelvin 78 L oxygen meter and recorded on a Kipp and Zonen BD 41 strip chart recorder.

Lolliguncula brevis < 5 cm DML were examined in the 3.8 L respirometer, and *L. brevis* ≥ 5 cm DML were tested in the 15.6 L respirometer. Each squid was placed in the respirometer and allowed to acclimate for 40 minutes. Flow was set at 3 cm s⁻¹ during the initial 10 and final 20 minutes of the acclimation period. During an interim 10-minute period, flow speeds were gradually elevated to 21 cm s⁻¹ to allow the squid to acclimate to higher flow speeds. After the 40-minute adjustment period, the respirometer lid was closed, oxygen measurements were recorded for 15 minutes, and the respirometer was subsequently opened, allowing water from the surrounding water bath to enter the respirometer. This flushing procedure was carried out for 10 minutes to ensure that fresh, oxygenated water was present in the system for the next trial. This procedure was repeated for speeds of 6, 9, 12, 15, 18, 21, 24, 27, and 30 cm s⁻¹ or until the squid could

Figure 1. Schematic diagram of swim tunnel respirometer.



no longer keep pace with flow velocity. During each trial swimming behavior was recorded using a Sony Hi-8 video camera. After the final trial each squid was measured (DML) and weighed, and blanks were run to correct for bacterial oxygen consumption, electrode drift, and/or endogenous oxygen consumption of the electrode. Mean water temperature and salinity (\pm SD) for this study were $24.5 \pm 2.0^\circ\text{C}$ and $29.2 \pm 5.6\text{‰}$, respectively.

Video Analysis

Portions of the video footage were analyzed on a Peak Motion Measurement and Biomechanics System (Peak Performance Technologies, Englewood, CO) to account for some of the variability in swimming behavior. For all squid tested, two representative minutes of footage at each speed were examined. Mantle angle ($^\circ$), arm angle ($^\circ$), and distance from the eye to the respirometer floor (cm) were recorded every second within the two-minute video sequence. Change in position along the axis parallel to flow and the number of fin beats s^{-1} also were recorded. For all squid, mean overall body angle of attack (which was simply the mean of the mantle and arm angles), mean distance from bottom, mean number of fin beats s^{-1} , and mean horizontal change during the two-minute video sequence were computed. Using an acoustic doppler velocimeter (Son-Tek, Inc., San Diego, CA) bottom flow profiles were recorded in each swim tunnel for the range of speeds considered in this study. These measurements were used in conjunction with measurements of mean height above the bottom and mean horizontal change to calculate actual swimming velocities.

Statistical Procedures

Polynomial regression analysis was performed both on data pooled by size class (size classes: 2.9–3.9, 4.0–4.9, 5.0–5.9, 6.0–6.9, 7.0–7.9, and 8.0–8.9 cm DML) and on data collected from individual squid. Regression analysis involved fitting data initially to a linear regression and subsequently fitting the data to higher degree polynomial regressions when additional terms significantly improved the accuracy of the prediction of dependent values (pp. 361-365, Zar 1984; pp. 671-683, Sokal and Rohlf, 1981). Unfortunately, regression analyses performed on pooled data did little to characterize the nature of patterns clearly apparent in scatter plots of individual squid. This was because high variability among individuals masked underlying relationships. Furthermore, when the data were analyzed separately for each squid, limited data points precluded the consistent detection of significant linear or curvilinear relationships. Therefore, an additional procedure was employed to determine if a significant parabolic relationship was present, i.e., are consumption rates at intermediate speeds less than those at low and high speeds? For each squid tested, data were divided into three speed ranges, < 0.5 mantle lengths s^{-1} , $0.5-1.5$ mantle lengths s^{-1} , and > 1.5 mantle lengths s^{-1} , and mean consumption rates were calculated for each speed range. Friedman's test, which ranks the three mean consumption rates for each squid tested (blocks), was used to determine if there was an overall significant difference in consumption rate at the three speed ranges. When a significant difference was detected, a Tukey-type multiple comparison analysis applicable to ranked data in a randomized block design was used (pp. 230-231, Zar 1984).

Mean wet weights and mean weight-specific oxygen consumption values were calculated for the six size classes. To characterize the metabolic scaling relationship in brief squid, a power-law regression of mean weight-specific oxygen consumption on mean wet weight was performed. The power-law function was defined as: $R = aM^b$, where R was weight-specific oxygen consumption, a was the mass coefficient, M was wet weight, and b was the mass exponent.

RESULTS

Swimming Behavior

In the swim tunnel respirometers brief squid were capable of both arms-first swimming, where the arms extended in front in a streamlined, conical arrangement while the mantle and fins trailed behind, and tail-first swimming, where the mantle and fins were forward while the arms formed a sharp trailing edge. Upon initial placement within either respirometer, most squid oriented arms-first in the direction of flow during the acclimation period. However, during exposure to higher speeds, brief squid frequently shifted to tail-first swimming, which allowed them to keep pace more effectively at high swimming velocities. The majority of data reported here were collected during tail-first swimming periods because tail-first swimming appeared to be the preferred mode of swimming throughout the speed range tested. However, many specimens would not swim exclusively in either a tail-first or arms-first mode at low speeds ($< 6 \text{ cm s}^{-1}$), and thus low speed consumption rates often reflected both modes of swimming.

Most squid tested were capable of detecting areas of low flow within the tunnel respirometer and consistently swam at speeds lower than that of the target velocity. Moreover, several behaviors were employed by some to aid swimming and presumably reduce swimming costs. A number of squid remained on the tunnel floor either in a horizontal orientation, with the body and appendages aligned parallel to flow, or in an inverted V-posture, with the tips of the mantle and arms touching the tunnel floor and the

head projected upwards. Since these squid were in contact with the bottom, they were not actually swimming. Other squid frequently pushed off the bottom and/or downstream collimator with their arms during trials to assist locomotion. Some squid even swam with their body and fin pressed against the respirometer side wall to exploit low flows near the wall and to help maintain horizontal and vertical position. These behaviors were most prevalent during low and high speed trials when squid had the most difficulty matching free stream flow.

Speed trials where the above behaviors were used > 30% of the time were eliminated. For eight squid, this resulted in no measurements at speeds < 0.5 mantle lengths s^{-1} and, in one case, speeds > 1.5 mantle lengths s^{-1} . Since one objective of this study was to characterize the nature of the O_2 consumption versus speed relationship over the entire range of sustained swimming velocities, these squid, which ranged in size from 4.7–8.2 cm DML, were eliminated. When all speed trials were considered for the eight squid with questionable performance, even those trials where squid remained on the bottom, pushed off with their arms, and pressed against the side of the respirometer, linear relationships between speed and O_2 consumption frequently were observed (Table 1).

O_2 Consumption

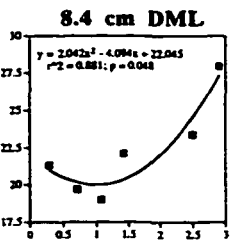
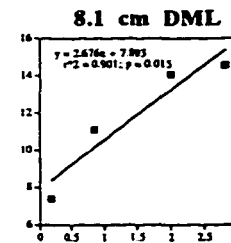
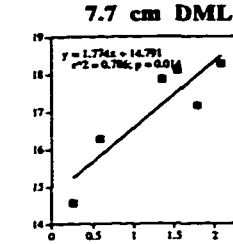
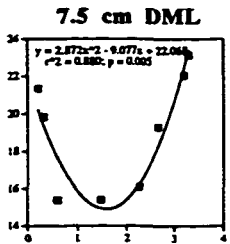
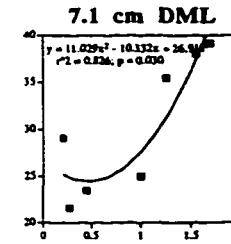
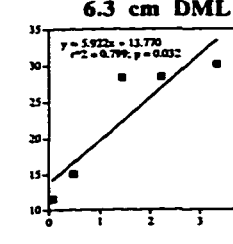
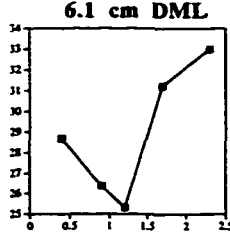
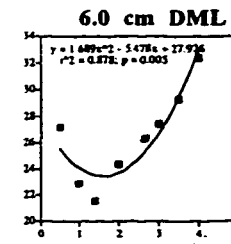
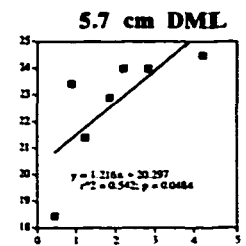
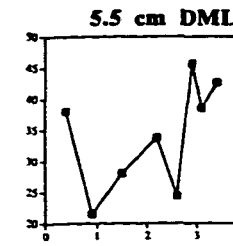
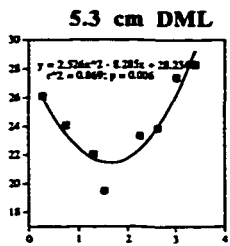
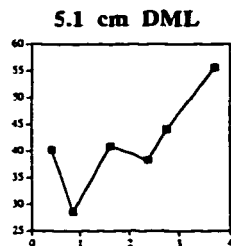
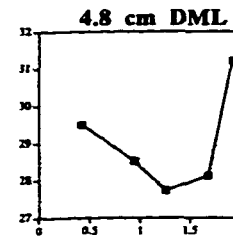
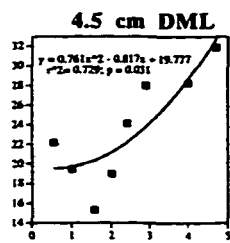
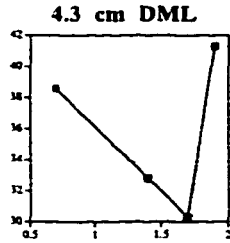
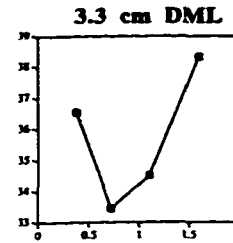
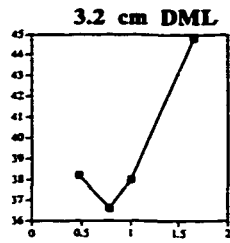
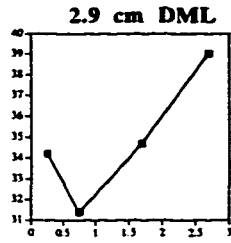
Partial (J-shaped) or full (U-shaped) parabolic patterns of O_2 consumption as a function of speed were observed for squid with measurements at all three speed ranges (< 0.5 mantle lengths s^{-1} , 0.5 – 1.5 mantle lengths s^{-1} , > 1.5 mantle lengths s^{-1}) (Figure 2). Friedman's test revealed a significant difference in O_2 consumption rates between the

Table 1. Linear regression results of O₂ consumption on swimming speed for eight *Lolliguncula brevis* (4.7–8.2 cm DML) that were uncooperative at low and sometimes high speeds during respirometry trials. Asterisks signify significance at $\alpha = 0.05$

Dorsal Mantle Length (cm)	Mass (g)	P-Value	r ²
4.7	8.4	0.157	0.264
6.0	15.3	*0.034	0.820
6.2	13.2	0.638	0.131
6.3	15.8	*0.042	0.824
7.2	28.2	*0.017	0.786
7.5	31.4	*0.015	0.724
8.2	42.5	*0.002	0.866
8.2	44.3	*0.030	0.901

Figure 2. O₂ consumption rates ($\mu\text{moles O}_2 \text{ h}^{-1} \text{ g}^{-1}$) of *Lolliguncula brevis* (2.9–8.4 cm DML) plotted as a function of swimming velocity (mantle lengths s^{-1}). Linear or polynomial regression equations, r^2 values, and p-values are included in plots when a significant relationship was detected. As a result of limited data, linear or curvilinear relationships were not detected in some squid, and in these cases, data points were simply connected with lines. Note that many of the consumption curves are J- or U-shaped.

Micromoles O₂ h⁻¹ g⁻¹



Swimming Velocity (mantle lengths s⁻¹)

three speed ranges ($df = 2$, $chi-square = 19.63$, $P < 0.0001$). Subsequent Tukey-type multiple comparison tests indicated that O_2 consumption rates at low and high speeds were significantly greater than those at intermediate speeds, and there was no significant difference between O_2 consumption rates at low and high speeds.

Despite high variation among individuals, mean O_2 consumption rates at the intermediate speed range (0.5–1.5 mantle lengths s^{-1}) were less than those in the low (< 0.5 mantle lengths s^{-1}) and high (> 1.5 mantle lengths s^{-1}) speed ranges for most sizes (Table 2), which is consistent with the results of the Friedman and Tukey-type multiple comparison tests. Furthermore, the mean range of O_2 consumption values generally decreased with increased size, and *L. brevis* had a limited factorial aerobic scope for swimming (i.e., mean maximum O_2 consumption divided by mean minimum O_2 consumption) (Table 2). The mass-specific scaling coefficient, b , for brief squid was -0.24 and the scaling relationship between mass-specific metabolism and size was: $y = 48.28x^{-0.24}$ ($P = 0.0001$; $r^2 = 0.889$), where $y =$ oxygen consumption ($\mu\text{mol } O_2 \text{ h}^{-1} \text{ g}^{-1}$) and $x =$ mass (g).

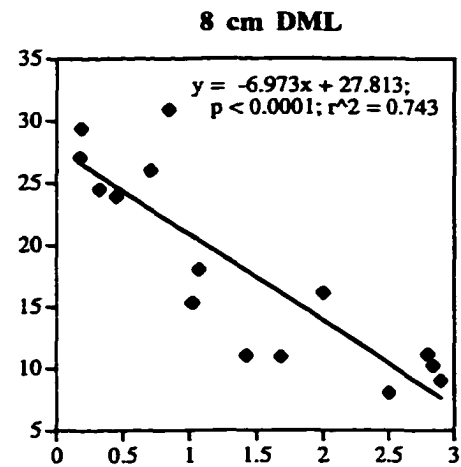
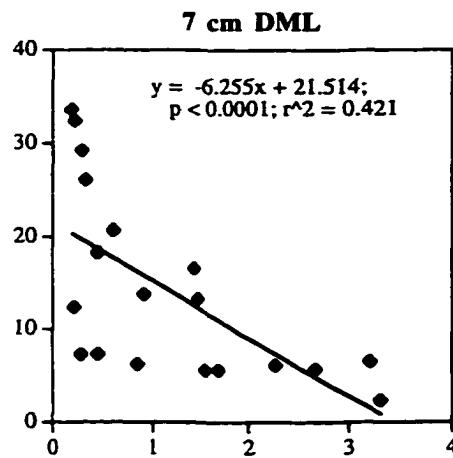
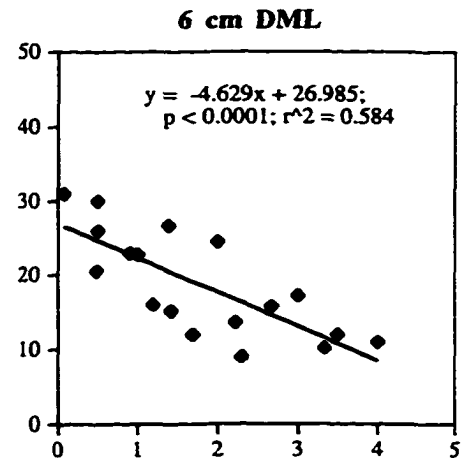
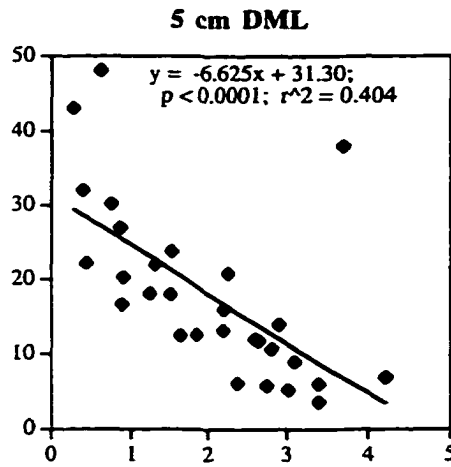
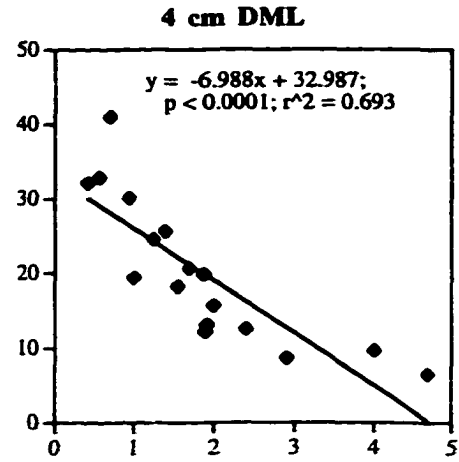
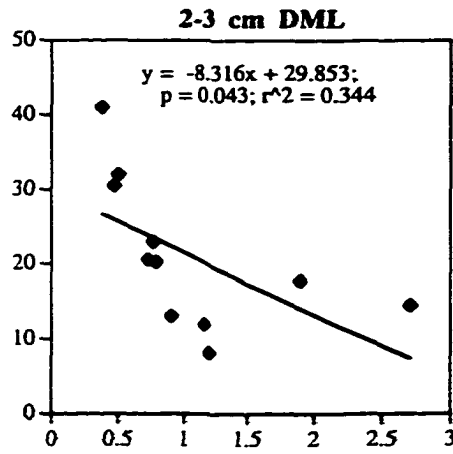
For all size classes, there was a clear decline in mean angle of attack and number of fin beats s^{-1} with increased swimming velocity (Figures 3, 4). Generally, the greatest standard deviation in horizontal position occurred at speeds < 1.0 mantle lengths s^{-1} (Figure 5).

Table 2. Mean wet weights, O₂ consumption values, and aerobic swimming capacities for *Lolliguncula brevis* of various size classes. Factorial aerobic scope is the mean maximum O₂ consumption divided by the mean minimum O₂ consumption during swimming.

Size Class (DML (cm))	Mean Mass (g)	Mean O ₂ Consumption ($\mu\text{mol O}_2 \text{h}^{-1} \text{g}^{-1}$) Velocities <0.5 DML s ⁻¹	Mean O ₂ Consumption ($\mu\text{mol O}_2 \text{h}^{-1} \text{g}^{-1}$) Velocities 0.5 – 1.5 DML s ⁻¹	Mean O ₂ Consumption ($\mu\text{mol O}_2 \text{h}^{-1} \text{g}^{-1}$) Velocities > 1.5 DML s ⁻¹	Mean Range of O ₂ Consumption ($\mu\text{mol O}_2 \text{h}^{-1} \text{g}^{-1}$)	Factorial Aerobic Scope
2.9 – 3.9	2.31 ± 0.59 (SD)	35.78 ± 2.30 (SD)	33.74 ± 2.14 (SD)	38.95 ± 0.59 (SD)	33.80 ± 2.62 (SD) – 39.27 ± 5.11 (SD)	1.16
4.0 – 4.9	7.50 ± 2.21 (SD)	30.09 ± 8.21 (SD)	27.13 ± 5.57 (SD)	28.21 ± 7.45 (SD)	25.67 ± 5.92 (SD) – 33.58 ± 6.84 (SD)	1.31
5.0 – 5.9	12.25 ± 3.59 (SD)	30.71 ± 10.27 (SD)	24.17 ± 3.02 (SD)	32.78 ± 10.93 (SD)	22.00 ± 4.58 (SD) – 38.54 ± 14.69 (SD)	1.75
6.0 – 6.9	14.76 ± 1.38 (SD)	24.91 ± 8.62 (SD)	23.51 ± 2.71 (SD)	29.19 ± 2.85 (SD)	19.45 ± 7.14 (SD) – 31.84 ± 1.51 (SD)	1.64
7.0 – 7.9	27.70 ± 2.98 (SD)	22.21 ± 3.99 (SD)	21.62 ± 7.17 (SD)	26.29 ± 9.83 (SD)	16.63 ± 2.59 (SD) – 27.19 ± 10.51 (SD)	1.63
8.0 – 8.9	41.10 ± 10.11 (SD)	14.41 ± 9.81 (SD)	17.97 ± 4.76 (SD)	20.00 ± 6.82 (SD)	13.20 ± 8.18 (SD) – 21.27 ± 9.48 (SD)	1.61

Figure 3. Linear regressions of mean body angle of attack ($^{\circ}$) on swimming speed (mantle length s^{-1}) for six size classes of *Lolliguncula brevis* (2.9–3.9, 4.0–4.9, 5.0–5.9, 6.0–6.9, 7.0–7.9, and 8.0–8.9 cm DML). Regression equations, p-values and r^2 values are included for each size class. Angles of attack consistently decreased with increased swimming velocity, regardless of overall size.

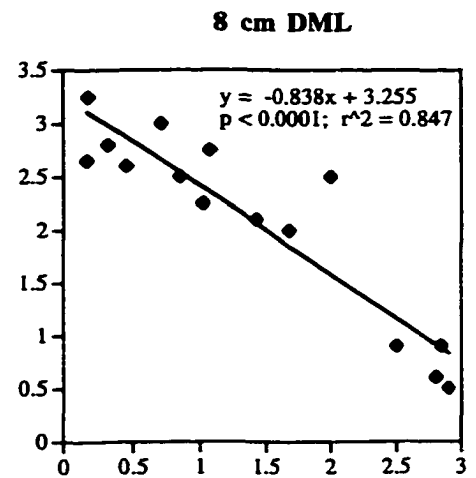
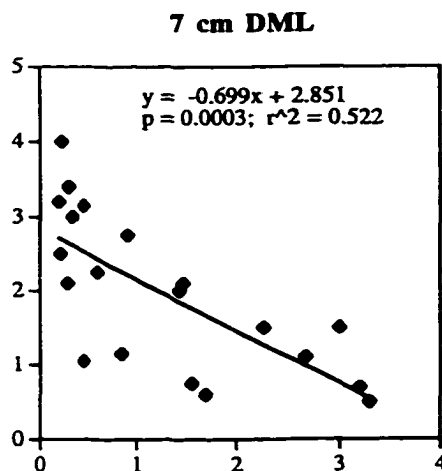
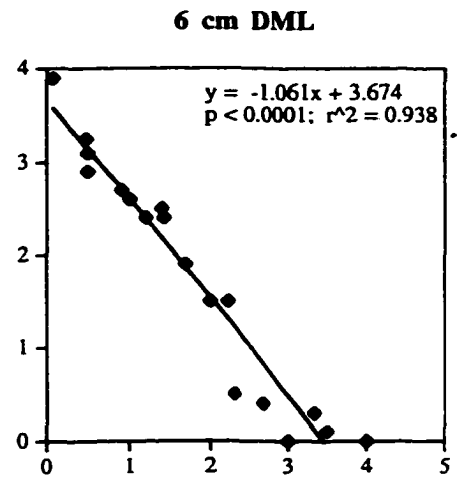
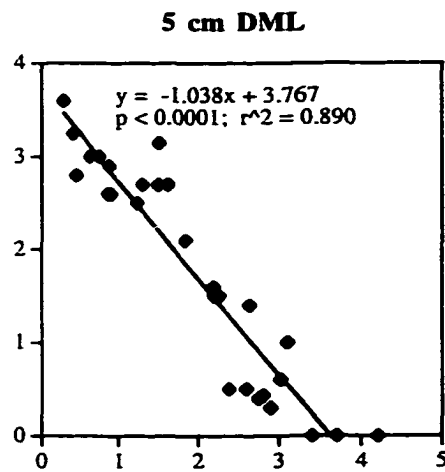
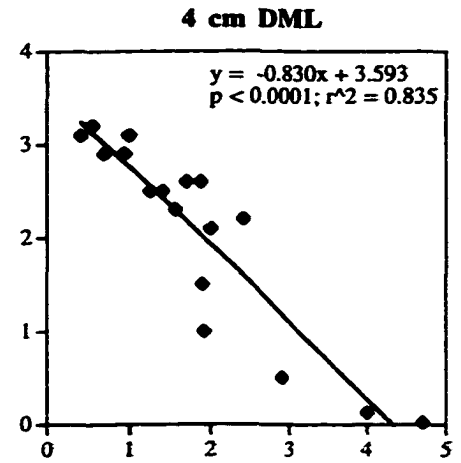
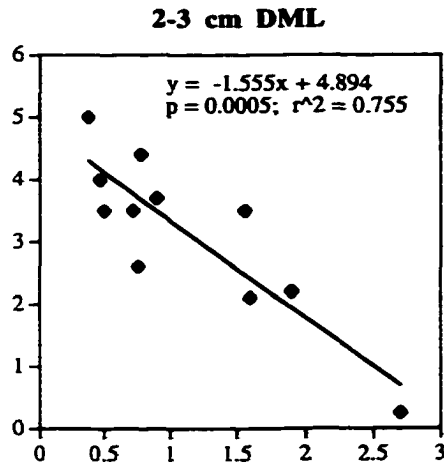
Mean Angle of Attack (°)



Swimming Speed (mantle lengths s⁻¹)

Figure 4. Linear regressions of mean number of fin beats s^{-1} on swimming speed (mantle length s^{-1}) for six size classes of *Lolliguncula brevis* (2.9–3.9, 4.0–4.9, 5.0–5.9, 6.0–6.9, 7.0–7.9, and 8.0–8.9 cm DML). Regression equations, p-values and r^2 values are included for each size class. The frequency of fin beats consistently decreased with increased swimming velocity, irrespective of overall size.

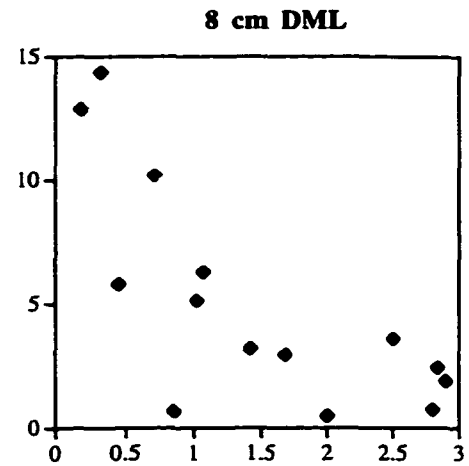
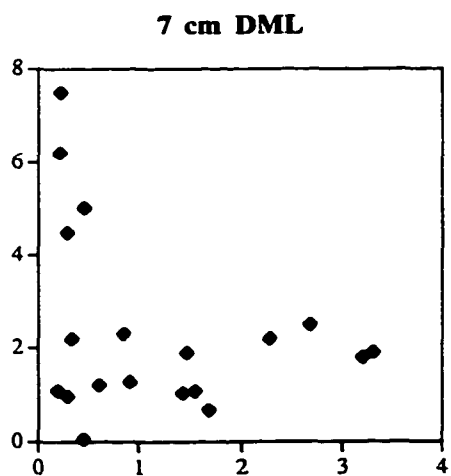
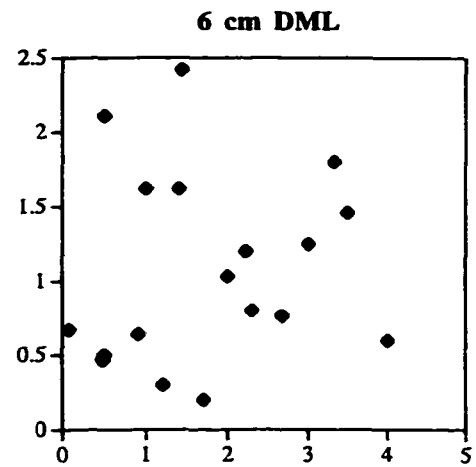
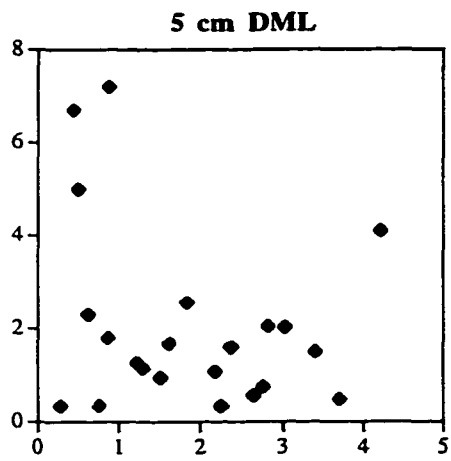
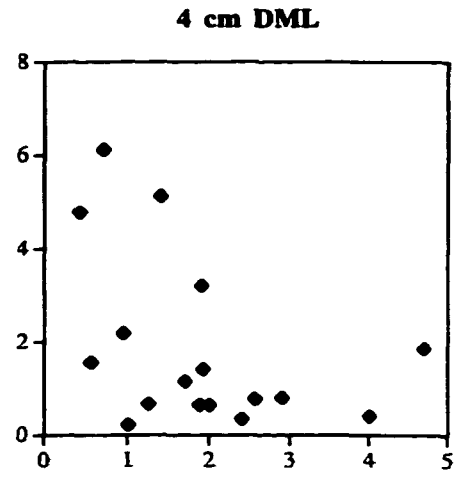
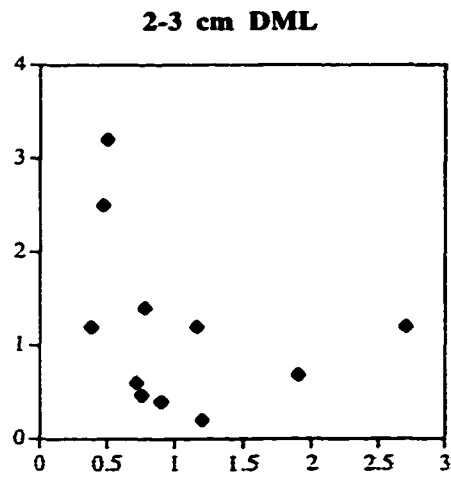
Fin Beats s^{-1}



Swimming Speed (mantle length s^{-1})

Figure 5. Mean standard deviation along the axis parallel to free stream flow (x -coordinate deviation) plotted as a function of swimming speed (mantle lengths s^{-1}). Data from six size classes (2.9 - 3.9, 4.0 - 4.9, 5.0 - 5.9, 6.0 - 6.9, 7.0 - 7.9, and 8.0 - 8.9 cm DML) are depicted. Generally, greatest deviation was observed at low speeds (< 1.0 mantle lengths s^{-1}).

Standard Deviation of X Coordinate (cm)



Swimming speed (mantle lengths s⁻¹)

DISCUSSION

The results of this study indicate that a partial (J-shaped) or full (U-shaped) parabolic pattern of O₂ consumption as a function of swimming velocity exists in *Lolliguncula brevis* and that O₂ consumption rates at intermediate speeds are less than those at low and high speeds. Parabolic relationships between power or O₂ consumption and velocity have been observed in aircraft (Bramwell, 1976), birds (Pennycuik, 1968; Tucker, 1973; Greenwalt, 1975; Rayner, 1979), and bees (Ellington et al., 1990). Both aircraft and flying organisms require considerable power to fly slowly and fast but fly more economically at intermediate speeds. Thus, the relationship between power or O₂ consumption and speed is often characterized as U-shaped, though there has been some recent debate over whether the relationship in birds is actually L- or J-shaped in form (see Dial et al., 1997; Alexander, 1997). Parabolic relationships have been detected in the aquatic realm as well for slow-swimming negatively buoyant fish, such as the mandarin fish *Synchiropus picturatus* (Blake, 1979). However, O₂ consumption increases exponentially with swimming speed for most fish, and parabolic relationships are rare (for a review of fish swimming respiration see Beamish, 1978). High metabolic/power costs at low speeds are absent in most pelagic swimmers because they are neutrally buoyant or close to it, and thus generation of lift at low speeds—a considerable energetic expense for negatively buoyant organisms—is not a significant issue.

Lift generation at low speeds is energetically expensive for negatively buoyant birds, bees, fish, and squid in part because of induced, skin friction, and pressure drag. To boost lift at low speeds organisms, such as negatively buoyant fish and birds, frequently increase the angle of attack of biofoils (a generic device that creates forces via circulatory mechanisms), which induces downward flow that alters the pressure distribution so that the lift vector increases but also tilts the resultant vector backwards (Dickinson, 1996). The rearward component of the resultant force vector is a product of induced drag caused by tip forces shed off the fins or wings that are of finite length, skin friction drag from viscous shear acting on the surface of the organism, and pressure drag due to flow separation from the surface of the animal (Vogel, 1994; Dickinson, 1996). The power required to overcome the additive effect of these drag forces is high initially at low speeds, but falls dramatically with speed as lift forces increase exponentially and a smaller angle of attack is required to generate the required lift (Blake, 1983; Vogel, 1994). It is noteworthy that squid that remained on the bottom or that consistently pushed off the bottom generally did not have high costs at low speeds like free swimming squid. These organisms had linear rather than parabolic consumption curves, suggesting that the large overall locomotive costs observed at low speeds in squid swimming off the bottom are due to low-speed lift generation.

The fins and third (III) arms with heavy keels, which resemble traditional human-made lift-generating airfoils, as well as the mantle, head, and remaining arms were positioned at high angles of attack and used by *L. brevis* to increase lift. Both the fins and third (III) arms were extended laterally during low speeds while the body of the squid was positioned at high angles of attack, which forces water to move faster over their

upper surfaces, increases the pressure differential above and below the biofoil, and consequently increases lift. Although the mantle, head, and remaining arms (i.e., the body) do not resemble traditional airfoils/biofoils, they too generate lift when positioned at high angles of attack. Body lift plays a critical role in lift generation in ski jumpers (Ward-Smith and Clements, 1982), honeybees (Nachtigall and Hanauer-Thieser, 1992), birds (Tobalske and Dial, 1996), and negatively buoyant fish (He and Wardle, 1986; Heine, 1992; Webb, 1993). There is an upper limit to the angle of attack of the fins, arms, and body, however, before flow separation occurs above the organism and lift drops in a process called stall. For most human-made wings this limit is generally 15–20° (Kundu, 1990; Vogel, 1994), but higher limits may be reached by organisms, especially those that swim using unsteady mechanisms to delay stall (Vogel, 1994; Dickinson, 1996). In this study, higher angles of attack were used, and there is evidence that *L. brevis* may employ unsteady mechanisms for lift generation (see Chapter 3).

To maintain vertical position in the respirometer, *L. brevis* also relied heavily on fin motion, which consisted of dorsoventral flapping coupled with a wave passing along the length of the fin, and directed jet thrust more vertically. Lift-based fin propulsion has been reported in the vampire squid *Vampyroteuthis infernalis* (Seibel et al., 1998), while drag-based propulsion has been described in the squids *Loligo opalescens* and *Illex illecebrosus* and in cuttlefish (O’Dor, 1988; Hoar et al., 1994). Elements of both forms of fin propulsion are probably used in *Lolliguncula brevis*. At low speeds, metachronal waves were observed on the fins regularly, which provides drag-based thrust, while at other times a single wave of varying angle of attack was present, which provides lift-based propulsion (Webb, 1973; Lauder and Jayne, 1996). Both forms of propulsion may

provide vertical thrust. Drag-based fin activity provides upward directed thrust when the mantle is positioned at high angles of attack, while lift-based fin activity, where flow strikes the fin flapping up and down at varying angles of attack, produces a resultant force that is tilted both forwards (forward thrust) and upwards (lift) (Vogel, 1994). Since lift generation is a critical issue at low speeds, birds and insects frequently manipulate angles of attack, flapping planes, and wing beat frequencies during lift-based low speed flying to maximize lift and not necessarily the lift to drag ratio (Ellington, 1984; Dickinson, 1996; Dickinson and Götz, 1996). Although overcoming additional drag during lift maximizing behavior and flapping wings at high frequencies is energetically costly, staying aloft is more important for birds/insects at low speeds than saving energy. This also appears to be the case in brief squid. Furthermore, the funnel of squid is often directed at high angles of attack at low speeds (see Chapter 3), which provides vertical thrust and aids the squid in maintaining altitude. However, directing the jet more vertically also increases swimming costs since high velocity jets are required to swim horizontally.

High standard deviation in position along the axis parallel to flow observed at low speeds suggests that brief squid had difficulty matching low-speed flow velocities. At intermediate and high speeds, brief squid generally held position within the tunnel respirometer from one jet cycle to the next. However, at low speeds, they frequently jetted forward for several jet cycles, often using considerable fin motion and gaining altitude, drifted backwards in the tunnel for a cycle or two with fins and arms projected outwards while gradually losing altitude, and jetted forward again for several cycles. This behavior, which incorporates components of both “burst-and-glide” and “climb-and-

glide” swimming, may be used as a mechanism to conserve energy (Weihs, 1973, 1974; O’Dor, 1988). However, given that this behavior was rarely observed at intermediate and high speeds, the animals may simply have been accelerating forward to increase lift and gliding back when they reached the forward limit of the tunnel.

For negatively buoyant swimmers, metabolic costs are high both at low speeds and high speeds, and are lowest at intermediate speeds. Drag forces scale approximately with the square of velocity just like lift, and thus as speed increases the power required to overcome drag acting on appendages (profile power) and the body (parasite power) increases exponentially (Blake, 1983). Exponential increases in O_2 consumption with speed have been widely reported in fish (Brett, 1965; Webb, 1973; Blake, 1983; Dewar and Graham, 1994) and squid (O’Dor, 1982; Webber and O’Dor, 1985, 1986). In this study, exponential increases in O_2 consumption were not always apparent, even at speeds > 0.5 mantle lengths s^{-1} . Anaerobic metabolism, which may begin as early as 1.5–2.0 mantle length s^{-1} and account for 14.4 and 21.9% of the energy required for swimming at 2.5 and 3.5 mantle lengths s^{-1} , respectively (Finke et al., 1996), may be responsible for the lack of exponential relationships. Nonetheless, sizable lift generation costs at low speeds and considerable drag costs at high speeds allowed for the development of O_2 consumption minima at speeds between 0.5–1.5 mantle lengths s^{-1} .

Given that costs were lower at speeds between 0.5 and 1.5 mantle lengths s^{-1} than at speeds < 0.5 mantle lengths s^{-1} , brief squid should spend more time swimming at this intermediate speed than hovering. In flow-through tanks in the lab, many brief squid tended to congregate near tank intakes in areas of low/moderate flow or swam

continuously, which is consistent with the prediction above. However, squid also were frequently observed away from intakes hovering arms-first with their arms oriented in front of the body at low angles of attack (often in a conical arrangement), while their mantles were positioned near the tank floor at high angles of attack. During this posture fin flapping often was employed. This behavior is of interest because several squid that did not show parabolic oxygen consumption curves swam near the bottom in a similar manner at low speeds. Blake (1979) determined that negatively buoyant fish reduce induced power costs from 30–60% by positioning themselves near the bottom and exploiting ground effects. Thus, brief squid positioned near the bottom in this arms-first posture may reduce lift generation costs during hovering or while swimming slowly, thereby lowering overall low-speed metabolic costs. A preference for arms-first swimming upon initial placement in the tunnel respirometers, when speeds were set at 3 cm s^{-1} , may reflect this energy-saving strategy.

The relationship between organism mass (M) and metabolic rate (R), is frequently described by a power law function $R = aM^b$, where a is the mass coefficient and b the mass exponent (Schmidt-Nielsen, 1997). This relationship is not well understood in most cephalopods and the scaling data that are available are quite variable. The mass specific exponent (i.e., b when metabolic rates are expressed per unit mass) for *L. brevis* in this study was -0.24, which is within the range of that measured in other aquatic invertebrates and algae (mass specific b ranges from -0.53 to 0.28 (Patterson, 1992)). This mass specific exponent is also consistent with that reported by O'Dor and Webber (1986) for *Illex illecebrosus* ($b = -0.25$ to -0.27) and by Seibel et al. (1997) for *Vampyroteuthis infernalis* ($b = -0.30$), *Japatella diaphana* ($b = -0.27$), and *Histioteuthis heteropsis* ($b =$

-0.20). However, less concordance has been found in other metabolic studies on cephalopods. Manginnis and Wells (1969) determined that mass specific b was -0.17 for *Octopus cyanea*; Johansen et al. (1982) reported a mass specific b between -0.30 and -0.01 for *Sepia officinalis*; Macy (1960) found b to be between -0.56 and 0.28 for *Loligo pealei*; and Segawa and Hanlon (1988) determined a mass specific b of -0.10 for *Octopus maya*, -0.09 for *Lolliguncula brevis*, and -0.15 for *Loligo forbesi*. The wide range of mass specific exponents among the various cephalopods is likely a product of inter- and intra-species behavioral variation during experimentation, which was frequently reported in the above studies.

The O_2 consumption rates recorded in this study are in reasonable agreement with those reported for *L. brevis* previously. Segawa and Hanlon (1988) placed *Lolliguncula brevis* in 2–4 L bottles for 0.3–1.3 h, and determined that oxygen consumption rates of brief squid hovering in the middle or near/on the bottom of bottles ranges from $24.4 \mu\text{mol h}^{-1}\text{g}^{-1}$ for 39.98 g squid to $28.4 \mu\text{mol h}^{-1}\text{g}^{-1}$ for 2.00 g squid. Wells et al. (1988) measured oxygen uptake of *L. brevis* hovering in 2 L jars over a wide range of temperatures, and reported that mean O_2 consumption rates of brief squid (mean size = 9.21–10.78 g) vary from $24.3 \mu\text{mol h}^{-1}\text{g}^{-1}$ at 20°C to $34.1 \mu\text{mol h}^{-1}\text{g}^{-1}$ at $27\text{--}30^\circ\text{C}$ ($Q_{10} = 1.47$).

Wells et al. (1988) and Finke et al. (1996) provided limited data on O_2 consumption of *L. brevis* during swimming. Wells et al. (1988) measured oxygen extraction by five *L. brevis* at two swimming speeds, 9.5 cm s^{-1} and 16 cm s^{-1} . Unfortunately, only extraction percentages were presented and without knowledge of the tunnel dimensions and trial duration, swimming O_2 consumption rates could not be calculated in $\mu\text{mol O}_2 \text{ h}^{-1}\text{g}^{-1}$ for comparison purposes. Finke et al. (1996) measured O_2

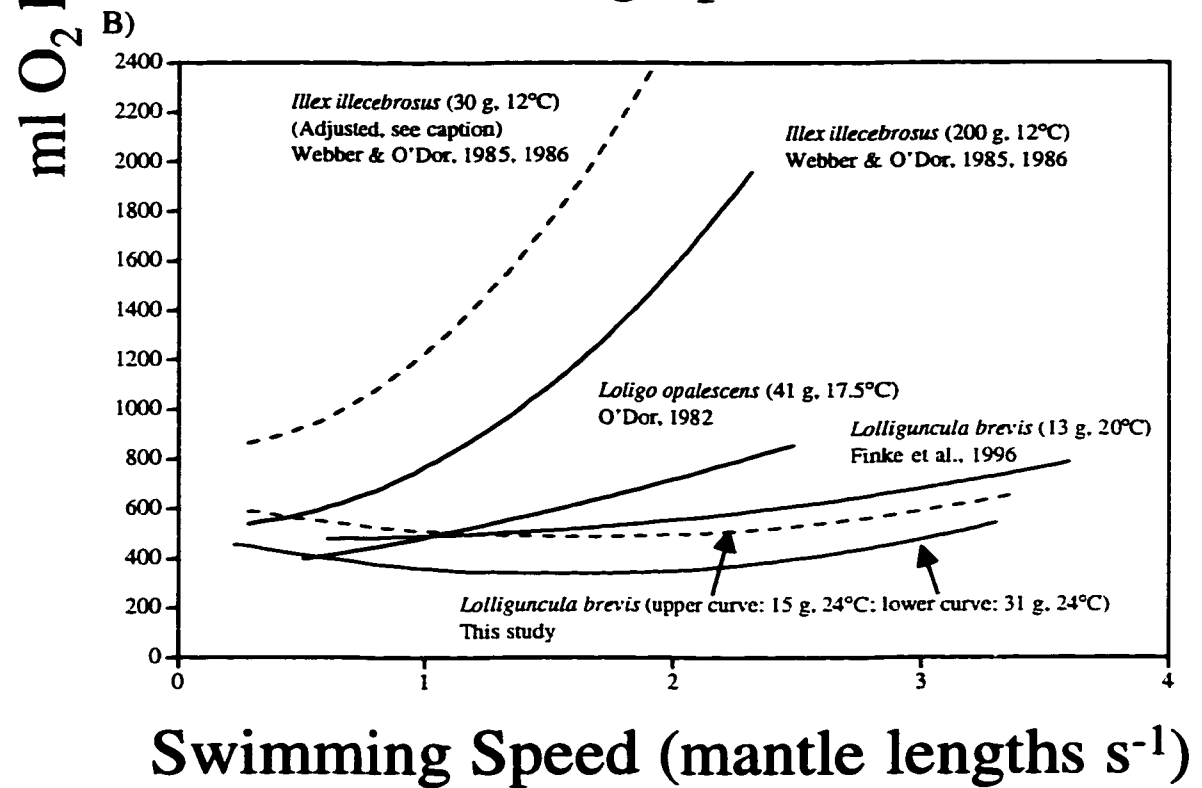
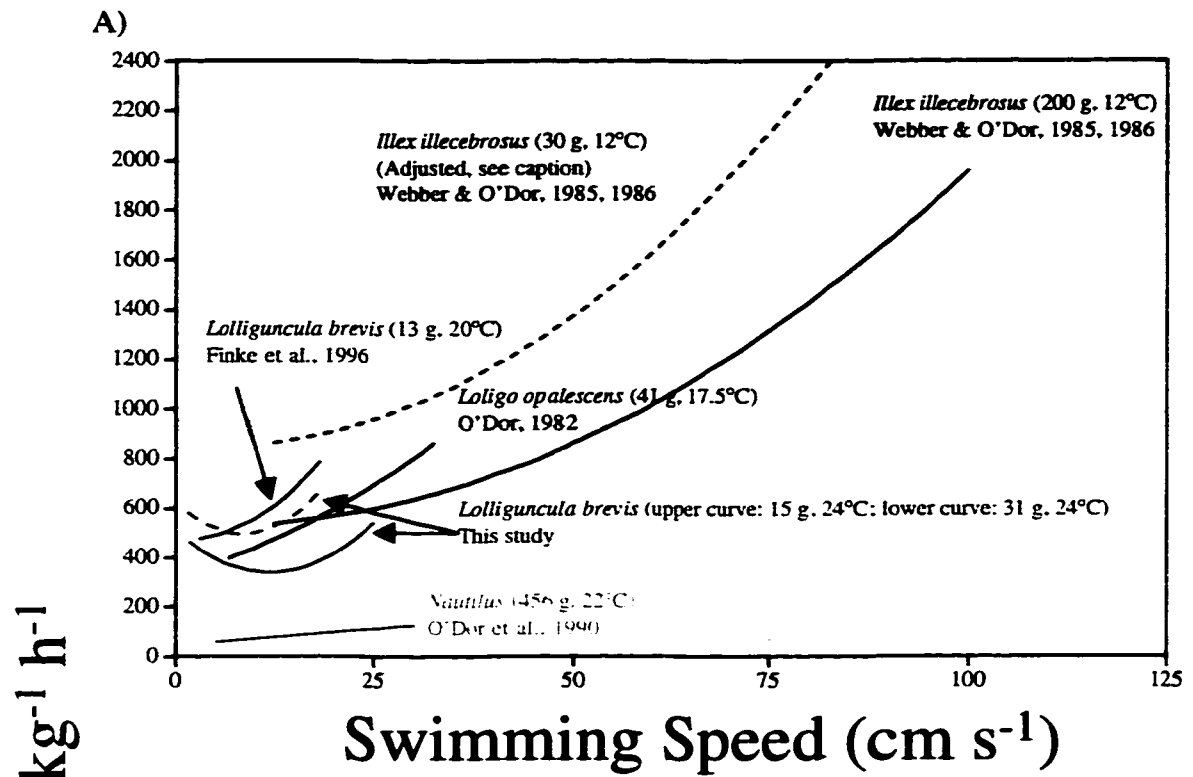
consumption rates of four *L. brevis* (11.9–15.1 g) during swimming that increased from 21 $\mu\text{mol O}_2 \text{ h}^{-1} \text{ g}^{-1}$ at 0.5 mantle lengths s^{-1} to 36 $\mu\text{mol O}_2 \text{ h}^{-1} \text{ g}^{-1}$ at 2.9 mantle lengths s^{-1} . These values, which were measured at 20–22°C, are similar to those recorded in the present study for squid of similar size at 24°C (see Table 1). No parabolic relationship was detected by Finke et al. (1996), but no speeds lower than 0.5 mantle lengths s^{-1} —speeds at which lift generation is especially costly—were considered. Interestingly, Finke et al. (1996) discovered that the pressure of mantle contractions actually falls in some brief squid from 0.5 to 1.1 mantle lengths s^{-1} and attributed this to a reduction in lift requirements.

In the present study, squid 4.5–8.4 cm DML were capable of sustained speeds as high as 21–27 cm s^{-1} for 15 minutes, which is similar to the upper limit (22.3 cm s^{-1}) measured by Finke et al. (1996) for *L. brevis* (11.9–14.1 g), but anaerobic metabolism may be used at much lower speeds. Finke et al. (1996) determined that anaerobic metabolism contributes to energy production in *L. brevis* beginning at speeds of 1.5–2.0 mantle lengths s^{-1} by measuring α -glycerophosphate, succinate, and octopine accumulation in the mantle tissue. This finding coupled with the small factorial scope of aerobic metabolism recorded in this study (1.16–1.75) suggest that brief squid are adapted for low speed swimming. Based on data in Finke et al. (1996), O_2 consumption rates measured above 1.5–2 mantle lengths s^{-1} in the present study may not reflect the total metabolic costs for swimming, but consumption rates at speeds of 0.5–1.5 mantle lengths s^{-1} , when costs are lowest, and at speeds < 0.5 mantle lengths s^{-1} , when costs are high, probably are qualitatively representative.

In the present study *L. brevis* rarely swam faster than 24 cm s^{-1} for sustained periods, whereas *Nautilus*, *Loligo opalescens*, and *Illex illecebrosus* swim up to 30, 40, and 100 cm s^{-1} , respectively, for sustained periods (O'Dor, 1982; Webber and O'Dor, 1985, 1986; O'Dor et al., 1990) (Figure 6A). When velocities are converted to mantle lengths s^{-1} , however, *L. brevis* is more competitive, swimming above 3 mantle lengths s^{-1} while other squids swim at speeds < 2.5 mantle lengths s^{-1} (Figure 6B). Oxygen consumption rates during swimming for a typical *L. brevis* (31 g, 24°C) recorded in this study are less than those of *I. illecebrosus* (30 g (adjusted), 200 g (unadjusted), 12°C) recorded by Webber and O'Dor (1985, 1986) and *Loligo opalescens* (41 g, 18°C) measured by O'Dor (1982).

Loligo opalescens and *Illex illecebrosus* are negatively buoyant yet parabolic metabolic relationships have not been reported. This is surprising because O'Dor (1988) determined that 66–92% of the total force required for *Illex* to swim at 10 cm s^{-1} is associated with maintenance of vertical position and counteracting negative buoyancy. Speeds $< 10 \text{ cm s}^{-1}$ were not considered for either *L. opalescens* or *I. Illecebrosus* (O'Dor, 1982; Webber and O'Dor, 1985, 1986). However, suggesting that parabolic relationships were undetected simply because low speeds (where lift generation costs are most problematic) were not tested is not entirely satisfying, at least for *Illex*. This is because when the speeds considered for *Illex* are converted to mantle lengths s^{-1} , speeds of 0.25 mantle lengths s^{-1} , which are similar to speeds considered in the present study, were actually investigated. Conversely, the lowest speed considered for *Loligo* was > 0.5 mantle lengths s^{-1} , which may be too high to detect high low-speed O_2 consumption. The

Figure 6. O₂ consumption rates (ml O₂ kg⁻¹ h⁻¹) of various cephalopods plotted against swimming speed. Swimming speeds are expressed in (A) cm s⁻¹ and (B) mantle lengths s⁻¹. Since *Illex illecebrosus* was considerably larger than *L. brevis*, its mass was adjusted to 30 g using the metabolic scaling equation: $R = aM^b$, where R is metabolic rate (ml O₂ kg⁻¹ h⁻¹), M is organism mass in kg, *a* is the mass coefficient and *b* the mass exponent (-0.25) (O'Dor and Webber, 1986). The mass of each organism and the temperature of water within respirometers are included in parenthesis. Sources of the data are listed in the figure.

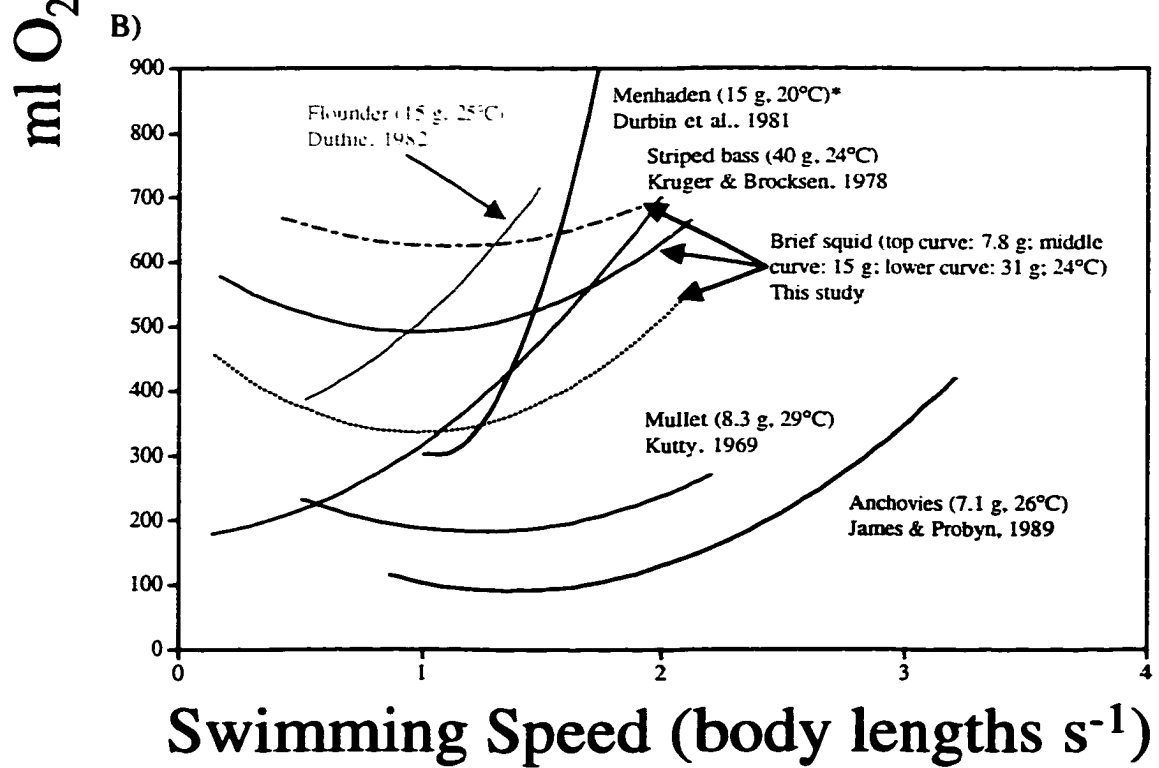
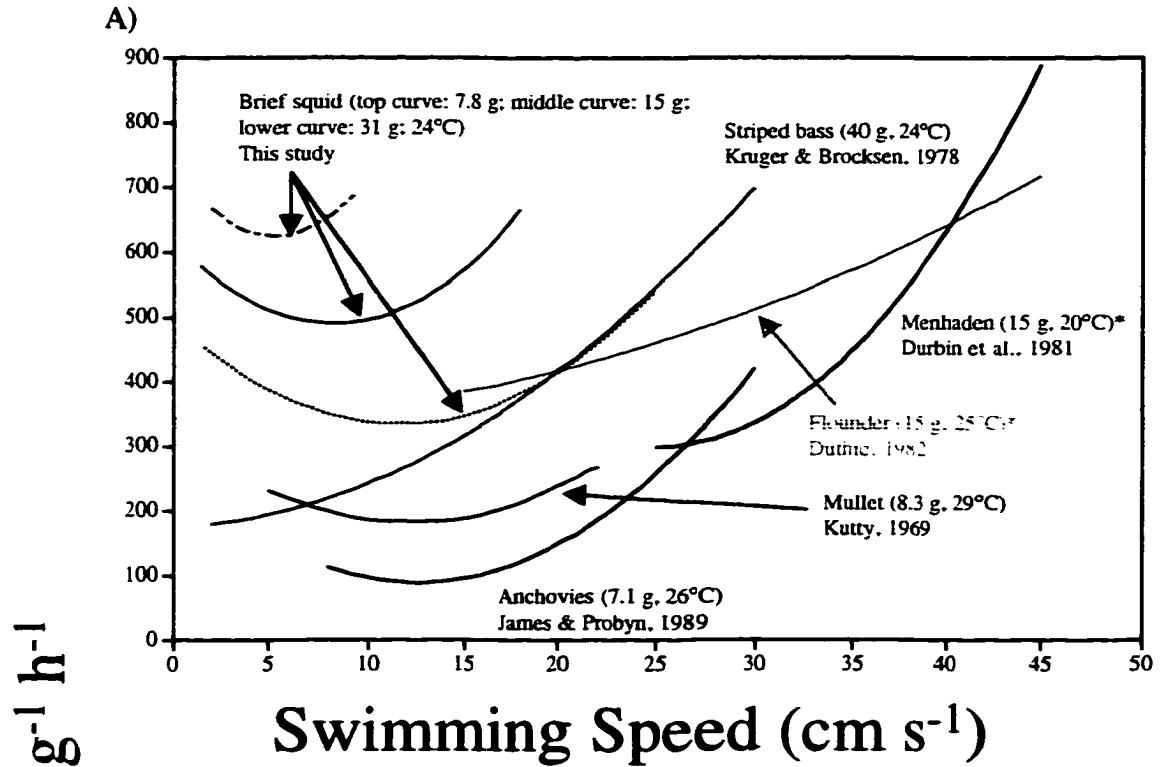


absence of a parabolic relationship in *Illex* may be attributed to the fact that oxygen curves were fit to pooled data. When high variation is present, as was the case in the present study, patterns visible in individual squid may become masked when data are considered collectively.

Presently, squid are thought to consume 5–7x more oxygen per unit mass per unit time than fish during swimming (O’Dor, 1982; Webber and O’Dor, 1985, 1986; O’Dor and Webber, 1986), but comparisons between *Lolliguncula brevis* and ecologically comparable fishes reveal that the O₂ consumption differences are less dramatic. In Figure 7, brief squid O₂ consumption rates are compared with those of anchovies, mullet, flounder, menhaden, and striped bass. When swimming velocities are expressed in cm s⁻¹ and comparisons are made between organisms of similar mass, brief squid have O₂ consumption rates 6–8x higher than those of anchovies, 2.7–3.5x higher than those of mullet, 1–2.5x higher than those of striped bass, and 1.4–1.7x higher than those of flounder (Figure 7A). When swimming velocities are expressed in body lengths s⁻¹ and comparisons are made between organisms of similar mass, brief squid actually have lower O₂ consumption rates at certain speeds than those of striped bass, flounder, and menhaden (Figure 7B). These comparisons suggest that brief squid are not as ill-equipped to compete with fish as once thought, but rather may be quite competitive with certain fish found in similar habitats.

O’Dor and Webber (1991) and Wells (1994) suggest that in environments where food density is low, jet-propelled cephalopods must maximize speed and power density to compete effectively. In environments such as the Chesapeake Bay and inshore,

Figure 7. O₂ consumption rates (ml O₂ kg⁻¹ h⁻¹) of *Lolliguncula brevis* and various fishes plotted against swimming speed. Swimming speeds are expressed in (A) cm s⁻¹ and (B) body lengths s⁻¹. Squid mantle lengths (ML) were converted to body lengths (BL) using the equation BL = 1.6 ML derived from morphological measurements of *L. brevis*. The mass of menhaden and flounder (denoted with asterisks (*)) were adjusted to 15 g using the equation: $R = aM^b$, where R is metabolic rate (ml O₂ kg⁻¹ h⁻¹), M is organism mass in kg, a is the mass coefficient, and b is the mass exponent (-0.25). Sources of the data are listed in the figure.



complex ecosystems where prey are abundant, the requirements may differ. *Lolliguncula brevis* swims slowly, uses considerable fin activity, and is competitive metabolically with ecologically comparable fish, despite the inherent inefficiencies of jet propulsion. Fin flapping used by *L. brevis* helps to lower metabolic costs because large volumes of water are driven backwards with each fin movement, allowing for a more economical generation of thrust than with the jet alone. Since the energy required for jet propulsion increases exponentially with swimming velocity, simply swimming at low speeds also may minimize the inefficiencies of jet propulsion and lower cost. As a result of negative buoyancy, there is a lower limit to swimming speed before energetic efficiency is compromised. Based on the results of this study, this limit is approximately 0.5 mantle lengths s^{-1} . Many mid and deepwater cephalopods have eliminated the problems associated with negative buoyancy by incorporating ammoniacal tissue throughout much of their bodies and reducing muscle density (Wells, 1994, Hanlon and Messenger, 1996). These organisms frequently rely less on the jet and more on fin motion for propulsion, and consequently their metabolic rates are low (Seibel et al., 1997). *Lolliguncula brevis* likely has not reduced muscle and incorporated ammoniacal tissue to achieve neutral buoyancy because sudden, powerful jet thrusts directed in various orientations via its maneuverable funnel are highly advantageous in highly populated environments, both for avoiding predators and ambushing prey.

SUMMARY

The results of this study suggest that a parabolic pattern between O_2 consumption and swimming velocity exists in *L. brevis* and that O_2 consumption rates at certain intermediate speeds are less than those at low and high speeds. Since negative buoyancy is not a significant issue for most swimmers, parabolic patterns are rarely seen in the aquatic realm, but the observed parabolic pattern is analogous to aquatic flight. Moreover, comparisons between brief squid and ecologically comparable fishes suggest that brief squid are more metabolically competitive with fishes than previously thought, especially at the minima of O_2 consumption curves. Enhanced efficiency may in part be a product of emphasis on low swimming velocities and fin motion. However, focused research on swimming mechanics is necessary to better characterize swimming behavior and to document mechanisms for enhancing efficiency in this unique cephalopod.

LITERATURE CITED

- Alexander, R. M. 1997. The U, J and L of bird flight. *Nature* 390: 13.
- Bartol, I. K. and M. Vecchione. 1997. Distribution of the euryhaline squid *Lolliguncula brevis* in the Chesapeake Bay: relationships between movement patterns and physical gradients. *ICES Ann. Sci. Con. CM 1997/IS*: 12, 7p.
- Beamish, F. W. H. 1978. Swimming capacity. In *Fish Physiology, Vol. VII: Locomotion* (ed. W.S. Hoar and D. J. Randall), pp. 101 - 172. Academic Press: New York.
- Blake, R. W. 1979. The energetics of hovering in the mandarin fish (*Synchiropus picturatus*). *J. Exp. Biol.* 82: 25-33.
- Blake, R. W. 1983. *Fish Locomotion*. Cambridge: Cambridge University Press.
- Bramwell, A. R. S. 1976. *Helicopter Dynamics*. London: Edward Arnold.
- Brett, J. R. 1965. The relation of size to rate of oxygen consumption and sustained swimming speed of sockeye salmon (*Oncorhynchus nerka*). *J. Fish Res. Board Can.* 23: 1491-1501.
- Dewar, H. and J. B. Graham. 1994. Studies of tropical tuna swimming performance in a large water tunnel. *J. Exp. Biol.* 192: 13-31.
- Dial, K. P., A. A. Biewener, B. W. Tobalske, and D. R. Warrick. 1997. Mechanical power output of bird flight. *Nature* 390: 67-70.
- Dickinson, M. H. 1996. Unsteady mechanisms of force generation in aquatic and aerial locomotion. *Amer. Zool.* 36: 537-554.
- Dickinson, M. H. and K. G. Götz. 1996. The wake dynamics and flight forces of the fruit fly, *Drasophila melanogaster*. *J. Exp. Biol.* 199: 2085-2104.
- Durbin, A. G., E. G. Durbin, P. G. Verity, T. J. Smayde. 1981. Voluntary swimming speeds and respiration rates of a filter-feeding planktivore, the Atlantic menhaden *Brevoortia tyrannus* (Pisces: Clupeidae). *Fish Bull. U.S.* 78: 877-886.

- Duthie, G. G. 1982. The respiratory metabolism of temperature-adapted flatfish at rest and during swimming activity and the use of anaerobic metabolism at moderate swimming speeds. *J. Exp. Biol.* 97: 359-373.
- Ellington, C. P. 1984. The aerodynamics of hovering insect flight. *Phil. Trans. Roy. Soc. Lond.* B305: 1-181.
- Ellington, C. P., K. I. Mackin, and T. M. Casey. 1990. Oxygen consumption of bumblebees in forward flight. *Nature* 347: 472-473
- Finke, E. H., H. O. Pörtner, P. G. Lee, and D. M. Webber. 1996. Squid (*Lolliguncula brevis*) life in shallow waters: oxygen limitation of metabolism and swimming performance. *J. Exp. Biol.* 199: 911-921.
- Greenwalt, C. H. 1975. The flight of birds. *Trans. Am. Phil. Soc.* 65: 1-67.
- Hanlon, R.T. and J. B. Messenger. 1996. *Cephalopod Behaviour*. Cambridge: Cambridge University Press.
- He, P. and Wardle, C. S. 1986. Tilting behavior of the Atlantic mackerel, *Scomber scombrus*, at low swimming speeds. *J. Fish Biol.* 29: 223-232.
- Heine, C. 1992. Mechanics of flapping fin locomotion in the cownose ray, *Rhinoptera bonasus* (Elasmobranchii: Myliobatidae). Ph. D. dissertation, Duke University, Durnham, NC, 286 p.
- Hixon, R. F. 1980. Growth, reproductive biology, distribution and abundance of three species of loliginid squid (Myopsids, Cephalopoda) in the northwest Gulf of Mexico. Ph.D. dissertation, University of Miami, Miami, FL, 182 p..
- Hixon, R. F. 1983. *Loligo opalescens*. In *Cephalopod Life Cycles. Vol. I: SpeciesAccounts* (ed. P. R. Boyle), pp 95-114. New York: Academic Press.
- Hoar, J. A., E. Sim, D. M. Webber, and R. K. Webber, and R. K. O'Dor. 1994. The role of fins in the competition between squid and fish. In *Mechanics and Physiology of Animal Swimming* (ed. L. Maddock, Q. Bone, and J. M. V. Rayner), pp. 27-33. Cambridge: Cambridge University Press.
- James, A. G. and T. Probyn. 1989. The relationship between respiration rate, swimming speed and feeding behaviour in the cape anchovy *Engraulis capensis* Gilchrist. *J. Exp. Mar. Biol. Ecol.* 131: 81-100.
- Johansen, K., O. Brix, and G. Lykkeboe. 1982. Blood gas transport in the cephalopod *Sepia officinalis*. *J. Exp. Biol.* 99: 331-338.

- Kruger, R. L. and R. W. Brocksen. 1978. Respiratory metabolism of striped bass, *Morone saxatilis* (Walbaum) in relation to temperature. *J. Exp. Mar. Biol. Ecol.* 31: 55-66.
- Kundu, P. K. 1977. *Fluid Mechanics*. San Diego: Academic Press, Inc.
- Kutty, M. N. 1969. Oxygen consumption in the mullet *Liza macrolepis* with special reference to swimming velocity. *Mar. Biol.* 4: 239-242.
- Lauder, B. G. and B. C. Jayne. 1996. Pectoral fin locomotion in fishes: testing drag-based models using three-dimensional kinematics. *Am Zool.* 36: 567-581.
- Macy, W. K. 1980. The ecology of the common squid *Loligo pealei* Lesueur, 1821 in Rhode Island waters. Ph. D. Dissertation, University of Rhode Island, RI, 190 p.
- Manginnis, L. A. and M. J. Wells. 1969. The oxygen consumption of *Octopus cyanea*. *J. Exp. Biol.* 51: 607-613.
- Nachtigall, W., and U. Hanauer-Thieser. 1992. Flight of the honeybee. V. Drag and lift coefficients of the bee's body: implications for flight dynamics. *J. Comp. Physiol.* B162: 267-77.
- O'Dor, R. K. 1982. Respiratory metabolism and swimming performance of the squid, *Loligo opalescens*. *Can. J. Fish. Aquat. Sci.*, 39: 580-587.
- O'Dor, R. K. 1983. *Illex illecebrosus*. In *Cephalopod Life Cycles. Vol. I: Species Accounts* (ed. P. R. Boyle), pp 95-114. New York: Academic Press.
- O'Dor, R. K. 1988. Forces acting on swimming squid. *J. Exp. Biol.* 137: 421-442.
- O'Dor, R. K. and D. M. Webber. 1986. The constraints on cephalopods: why squid aren't fish. *Can. J. Zool.* 64: 1591-1605.
- O'Dor, R. K. and D. M. Webber. 1991. Invertebrate athletes: trade-offs between transport efficiency and power density in cephalopod evolution. *J. Exp. Biol.* 160: 93-112.
- O'Dor, R. K., J. Wells, and M. J. Wells. 1990. Speed, jet pressure, and oxygen consumption relationships in free-swimming *Nautilus*. *J. Exp. Biol.* 154: 383-396.
- Patterson, M. R. 1992. A mass transfer explanation of metabolic scaling relations in some aquatic invertebrates and algae. *Science* 255: 1421-1423.

- Pennycuick, C. J. 1968. Power requirements for horizontal flight in the pigeon *Columba livia*. *J. Exp. Biol.* 49: 527-555.
- Pennycuick, C. J. 1989. *Bird Flight Performance*. Oxford: University Press.
- Rayner, J. M. V. 1979. A new approach to animal flight mechanics. *J. Exp. Biol.* 80: 17-54.
- Segawa, S. and R. Hanlon. 1988. Oxygen consumption and ammonia excretion rates in *Octopus maya*, *Loligo forbesi*, and *Lolliguncula brevis* (Mollusca: Cephalopoda). *Mar. Behav. Physiol.* 13: 389-400.
- Seibel, B. A., E. V. Thuesen, J. J. Childress. 1998. Flight of the vampire: ontogenetic gait-transition in *Vampyroteuthis infernalis* (Cephalopoda: Vampyromorpha). *J. Exp. Biol.* 201: 2413-2424.
- Seibel, B. A., E. V. Thuesen, J. J. Childress, and L. A. Gorodezky. 1997. Decline in pelagic cephalopod metabolism with habitat depth reflects differences in locomotory efficiency. *Biol. Bull.* 192: 262-278.
- Schmidt-Nielsen, K. 1997. *Animal Physiology: Adaptation and Environment*. Cambridge: Cambridge University Press.
- Sokal, R. R. and F. J. Rohlf. 1981. *Biometry*, 2nd ed. New York: W.H. Freeman and Company.
- Tobalske, B. W. and K. P. Dial. 1996. Flight kinematics of black-billed magpies and pigeons over a wide range of speeds. *J. Exp. Biol.* 199: 263-280.
- Tucker, V. A. 1968. Respiratory exchange and evaporative water loss in the flying budgerigar. *J. Exp. Biol.* 48: 67-87.
- Tucker, V. A. 1973. Bird metabolism during flight: evaluation of a theory. *J. Exp. Biol.* 58: 689-709.
- Vogel, S. 1994. *Life in Moving Fluids*, 2nd ed. Princeton: Princeton University Press.
- Ward-Smith, A. J., and D. Clements. 1982. Experimental determinations of the aerodynamic characteristics of ski-jumpers. *Aeronaut. J.* 86: 384-91.
- Webb, P. W. 1973. Kinematics of pectoral fin propulsion in *Cymatogaster aggregata*. *J. Exp. Biol.* 59: 697-710.

- Webb, P. W. 1993. Is tilting behaviour at low swimming speeds unique to negatively buoyant fish? Observations on steelhead trout, *Oncorhynchus mykiss*, and bluegill, *Lepomis macrochirus*. *J. Fish Biol.* 43: 687-694.
- Webber, D, M. and R. K. O'Dor. 1985. Respiration and swimming performance of short-finned squid (*Illex illecebrosus*). *Scientific Council Studies. Northw. Atl. Fish. Org.*, 9: 133-138.
- Webber, D, M. and R. K. O'Dor. 1986. Monitoring the metabolic rate and activity of free-swimming squid with telemetered jet pressure. *J. Exp. Biol.* 126: 205-224.
- Weihs, D. 1973. Mechanically efficient swimming techniques for fish with negative buoyancy. *J. Mar. Res.* 31: 194-209.
- Weihs, D. 1974. Energetic advantages of burst swimming of fish. *J. Theor. Biol.* 48: 215-229.
- Wells, M. J. 1994. The evolution of a racing snail. *Mar. Fresh. Behav. Physiol.* 25: 1-12.
- Wells, M. J., R. T. Hanlon, P. G. Lee, and F. P. Dimarco. 1988. Respiratory and cardiac performance in *Lolliguncula brevis* (Cephalopoda, Myopsida): the effects of activity, temperature, and hypoxia. *J. Exp. Biol.* 138: 17-36.
- Zar, J. H. 1984. *Biostatistical Analysis*, 2nd ed. Englewood Cliffs: Prentice Hall.

CHAPTER 3

SWIMMING MECHANICS AND BEHAVIOR OF BRIEF SQUID

ABSTRACT

Although squids are among the most versatile swimmers and rely on a unique locomotive system, involving a jet, fins, and arms, many aspects of squid locomotion remain unexplored, including how swimming mechanics and behavior change with size, how slow-swimming squids locomote, and what role unsteady phenomena, swimming orientation, fin activity, arm motion, and other behaviors play in locomotion over a range of speeds. Brief squid, *Lolliguncula brevis*, ranging in size from 1.8–8.9 cm dorsal mantle length (DML) were placed in flumes, videotaped, and analyzed using motion analysis equipment. Flow visualization and force measurement experiments using live squid and/or models were performed to investigate particular aspects of swimming, such as characteristics of the jet wake and magnitude of drag and lift forces. Using kinematic data collected from video, and force measurements recorded from models, estimates of drag, lift, acceleration reaction, jet thrust, and fin thrust were calculated during various swimming cycles.

Power-speed curves over the sustained speed range ($0\text{--}23\text{ cm s}^{-1}$) were parabolic in shape, with high costs at both low and high speeds because of power requirements for lift generation and for overcoming drag, respectively. At low speeds, negatively buoyant brief squid generated lift using three mechanisms: (1) positioning the mantle and arms at high angles of attack, often with the trailing body section (i.e. the arms during tail-first swimming or mantle during arms-first swimming) at a higher angle of attack than the

leading body section, (2) directing high speed jets downward using the funnel positioned at a high angle of attack ($> 50^\circ$), and (3) and relying on fin activity, which was responsible for as much as 78.6% of the total vertically directed thrust. Fin action, which could not be characterized exclusively as drag- or lift-based propulsion, was used over 50–95% of the sustained speed range and was important in horizontal movement as well, providing as much as 55.1% of total horizontal thrust at low speeds.

Generally, no dramatic shifts in swimming behavior were present within a given swimming orientation; behavioral changes tended to be gradual with speed and the greatest behavioral disparities were apparent when comparing size classes or swimming orientations. To swim at higher velocities in the tail-first swimming mode, small squid (< 3.0 cm DML) increased contraction frequency and kept mantle volume relatively constant to maximize the benefits of toroidal induction, whereas squid belonging to larger classes (≥ 3.0 cm DML) increased mantle volume and kept contraction rates relatively constant while maintaining 30% thrust augmentation from a pulsed jet. Based on aerobic efficiency curves, brief squid 3–5 cm DML were most efficient and large squid were most inefficient. Squid frequently swam both arms-first and tail-first in swim tunnels. Arms-first swimming, which allowed for greater observance of forward surroundings, increased readiness for prey strikes and predator defense, and reduced fin wake interactions with the body, was preferred for low-speed swimming. Tail-first swimming, which allowed for more efficient jetting and greater use of arms for pitch and lift control, was favored at high speeds.

The acceleration reaction, which was greatly influenced by angles of attack, was an important instantaneous force during the jet cycle, frequently exceeding drag and lift

forces by an order of magnitude, although relative contributions of the acceleration reaction averaged over a cycle were much less. Acceleration reaction forces over the body and fins probably play important roles in thrust production, and unsteady flows over various appendages have the potential to augment thrust substantially. These results suggest that slow-swimming squid rely on complex interactions of the mantle, fins, arms, and funnel, swim in various orientations, and probably benefit from unsteady phenomena.

INTRODUCTION

Resistive and propulsive forces associated with jet propulsion have been investigated in scallops (Trueman, 1975; Vogel, 1985; Dadswell and Weihs, 1990. Millward and Whyte, 1992, Cheng and Demont, 1996; Cheng et al., 1996), jellyfish (Daniel, 1983, 1985; DeMont and Gosline, 1988), salps (Madin, 1990), and frogfishes (Fish, 1987). The best known jettors are cephalopods, including the chambered *Nautilus*, octopuses, cuttlefishes, and squids. Much of the hydrodynamic work on cephalopods has been performed on *Nautilus* and centers around the effect of the shell on surrounding flow, locomotion, and mode of life (Raup, 1967; Chamberlain and Westerman, 1976; Chamberlain, 1976; 1980, 1981, 1990, Holland, 1987, O'Dor et al., 1990). Although there are a number of papers examining swimming energetics of squid (O'Dor, 1982; Webber and O'Dor, 1985, 1986, O'Dor and Webber, 1986a, 1991, O'Dor et al., 1994; Finke et al. 1996, Chapter 2), only Johnson et al. (1972) and O'Dor (1988) focus on the hydrodynamics and mechanics of squid locomotion. Johnson et al. (1972) outlined a theoretical approach to squid swimming, but it has limited applicability since it is based on one contraction of the mantle musculature and incorporates a number of oversimplifications and assumptions. O'Dor (1988) provided a more in-depth and informative examination of the forces acting on adult squid *Loligo opalescens* and *Illex illecebrosus* using video analysis and records of mantle cavity pressure. The limited research on squid swimming mechanics is surprising given the versatility of squid as

swimmers. Squid may hover in one spot, change direction rapidly with apparent ease, stop and reverse direction, and ascend and descend almost vertically (Hoar et al., 1994). Squid are capable of such impressive maneuvers because of complex interactions between three systems: (1) the jet, which may be directed using a funnel maneuverable within a hemisphere below the body, (2) the fins, which may undulate and/or flap independently or synchronously, and (3) the arms, which may be positioned at different angles of attack, moved vertically and laterally, and extended and retracted to maximize and minimize surface area.

O'Dor (1988) provided important information on the swimming behavior and forces acting on two moderately large squid species, which swam at moderate to high speeds and relied on fins for thrust only at low speeds. Hoar et al. (1996) provided an overview of fin diversity and potential contribution of fins to swimming in squids. However, several important areas of locomotion in squids remain unexplored. For instance, little is known about how swimming mechanics change with size in squids. With the exception of some general observations on *Illex illecebrosus* hatchlings in aquariums (O'Dor et al. 1985), all hydrodynamics work on squids has focused on adults of similar size. Squid are capable of swimming in two orientations: (1) tail-first, where the posterior closed end of the mantle and fins are located at the leading edge and the arms trail behind and (2) arms-first, where the arms are at the leading edge and the fins and mantle trail behind. However, very little is known about arm-first swimming, which is frequently observed in the field and in captivity (Hanlon et al., 1983; Vecchione and Roper, 1991; Chapter 2) and is the primary swimming mode used for prey capture (Hanlon and Messenger, 1996; Kier and van Leeuwen, 1997). Although the effects of

unsteady flow play integral roles in force and lift generation in other aquatic organisms (Daniel, 1983, 1984, 1988; Dickinson, 1996; Westneat, 1996), unsteady flow effects on squid, which swim in a pulsatile fashion, have received little attention. In addition, little is known about the swimming mechanics of slow-moving squids, which maneuver in complex, inshore environments and appear to use considerable fin motion. Finally, the role of the arms in locomotion and the interaction of the funnel, fins, and arms while swimming is not fully understood.

The brief squid *Lolliguncula brevis* differs in ecology and physiology from the squids *Loligo opalescens* and *Illex illecebrosus* considered in past hydrodynamic studies and is an excellent candidate with which to investigate the issues described above. The brief squid is the only cephalopod known typically to inhabit low-salinity estuaries (Vecchione, 1991; Chapter 1). Using physiological mechanisms we do not yet fully understand, it is capable of tolerating salinities as low as 17.5‰ under laboratory conditions (Hendrix et al., 1981; Mangum, 1991). Brief squid have short rounded bodies, large rounded fins, third arms with heavy keels, and often reside in shallow, complex, temporally variable environments (Hixon, 1980; Chapter 1). Conversely, *Loligo opalescens* and *Illex illecebrosus* are larger, more elongate, and reside in deeper, more open regions (Hixon, 1980, 1983; O'Dor, 1983; Hanlon and Messenger, 1996). While *Illex illecebrosus* and *Loligo opalescens* frequently swim at moderate to high speeds (50–85 cm s⁻¹) (O'Dor, 1982, 1988; Webber and O'Dor, 1986) and use their fins primarily for maneuvering and steering (O'Dor, 1988; Hoar et al., 1994), *L. brevis* appears to swim at lower speeds (< 30 cm s⁻¹), uses considerable fin activity, and swims in either arms-first or tail-first orientations readily (Finke et al., 1996; Chapter 2). Moreover, there is

also metabolic evidence suggesting that brief squid have high swimming costs at low speeds because of negative buoyancy and have parabolic oxygen consumption/speed relationships (Chapter 2), which to date have not been detected in *Illex* and *Loligo*.

To provide insight into how size, swimming orientation, unsteady phenomena, fin activity, arm motion, and other behaviors affect swimming mechanics for slow-swimming squids, brief squid *Lolliguncula brevis* ranging in size from 1.8–8.9 cm DML swimming in flumes were videotaped and the footage was analyzed using motion analysis equipment. Subsequent hydrodynamic calculations were based on these data. Flow visualization and force measurement experiments using live squid and/or models also were performed to investigate particular aspects of swimming, such as the characteristics of the jet wake and magnitude of lift and drag forces. Because brief squid appear to possess a unique parabolic relationship between oxygen consumption and speed and appear to swim over a more restricted speed range than other squids examined to date, particular emphasis was placed on the effects of speed on swimming mechanics.

MATERIALS AND METHODS

Experimental Animals

From May through November 1996–1998, brief squid *Lolliguncula brevis* (Blainville) were captured by trawl within embayments along the seaside of Virginia's Eastern Shore and within the Chesapeake Bay near Kiptopeke, VA. Squid captured along the Eastern Shore of Virginia were transported to the Virginia Institute of Marine Science (VIMS) Eastern Shore Lab in Wachapreague, VA, while squid captured in the Chesapeake Bay were transported to the VIMS main campus in Gloucester Point, VA. Squid were kept alive in the field using 120-quart coolers equipped with filtration and aeration systems, which were powered by 12-volt, sealed, rechargeable batteries. At Wachapreague and Gloucester Point, squid were kept in flow-through raceway tanks for at least one week prior to experimentation and fed a diet of grass shrimp, *Palaemonetes pugio*. A total of 32 squid ranging from 1.8–8.9 cm dorsal mantle length (DML) were examined for this study.

Flow Tunnels

Three flumes were used for live animal work; flume selection depended on capture location and squid size. Squid < 3.0 cm DML were examined in a portable, 16 L Vogel/LaBarbera-type flume (Vogel and LaBarbera, 1978) with a 10 x 10 x 75 cm working section. Flow velocity was controlled in the tunnel with two propellers in a

rotor-stator configuration powered by a 1/4 hp variable speed motor. Experiments on larger squid captured at Wachapreague and Gloucester Point, VA were conducted in a 5-m long, gravity-fed, recirculating flume with a 35 x 50 x 100 cm working section (see Orth et al., 1994 for a description) and a 3-m long Vogel/LaBarbera-type flume with a 15 x 20 x 100 cm working section (see Patterson, 1984), respectively. To calibrate velocity settings and to determine boundary layer thickness in each of the three flumes, flow velocities were measured from the flume floor to the water surface (in 1.0 cm increments) over a range of motor/valve settings using an acoustic doppler velocimeter (ADV) (SonTek, Inc., San Diego, CA).

Critical and Transition Swimming Speeds

Lolliguncula brevis (n = 32) were allowed to acclimate to the flumes at flow velocities of 6–9 cm s⁻¹ until they were capable of swimming steadily against flow, which generally occurred within 15 minutes. After the acclimation period, squid were exposed to a flow velocity of 3 cm s⁻¹ for 15 minutes. Speed was subsequently increased by 3 cm s⁻¹ every 15 minutes until the squid could no longer keep pace with free stream flow. Critical swimming speed (U_c) was calculated using the equation (Brett, 1964):

$$U_c = U_1 + [(T_f/T_i)U_i] \quad (1)$$

where U₁ is the last speed at which the squid swam for the entire 15-minute period, T_f is the time the squid swam at the final test speed, T_i is the time interval at each speed (15 minutes), and U_i is the velocity increment (3 cm s⁻¹).

During the critical swimming trials, many squid swam in two different orientations: tail-first and arms-first. The transition speed (U_t) above which these squid swam exclusively in the tail-first orientation was recorded.

Swimming Kinematics

During the 15-minute swimming periods, squid were frequently videotaped using either a Sony Hi-8 or Kodak Ektapro high-speed video camera. The long axis of the camera was positioned perpendicular to the side of the flume, which provided a lateral view of the swimming squid. A mirror also was placed within the camera field above the flume at a 45° angle to provide aerial views and simultaneous aerial/lateral footage of the swimming squid. Reference scales were placed on the walls and floor of the flumes for measurement calibration, but various landmarks on the squid, such as eye diameter, often were more useful calibration aids since the focal distance between the squid and camera lens varied among trials. Squid were illuminated in the flumes using both fiber optic and 1000-watt halogen lights. After each experiment, the squid were over-anesthetized in an isotonic solution of magnesium chloride (7.5% $\text{MgCl}_2 \cdot 6\text{H}_2\text{O}$) and seawater (Messenger et al. 1985), and wet mass out-of-water (± 0.1 g), mass in-water (determined using a submerged spring scale)(± 0.1 g), dorsal mantle length (± 0.1 cm), and eye diameter (± 0.1 cm) were recorded. The organisms then were transferred to 10% buffered formalin. Preserved specimens were used later for wetted surface area and aspect ratio calculations. For many of the squid considered in this study, volume of the mantle tissue (without the fins) and internal viscera were measured after over-anesthesia by determining the volume of water displaced by the tissues in graduated cylinders (± 0.1 ml). However, for some of

the squid, this step was performed after preservation. For these squid, corrections based on volume measurements performed both before and after preservation were necessary to account for minor shrinkage.

Video footage of three squid within each of four size classes (1.0–2.9 cm dorsal mantle length (DML), 3.0–4.9 cm DML, 5.0–6.9 cm DML, and 7.0–8.9 cm DML) was analyzed using a Sony EVO-9700 editing deck and a Peak video and computer motion measurement system (Peak Performance Technologies Inc., Englewood, CO). For the Hi-8 footage, 30 frames per second (fps) were analyzed. For the high-speed footage, where as many as 1000 fps were recorded, 32 fps were analyzed. All of the frames in the high-speed footage were not analyzed because the features of interest could be followed easily at 30–32 fps. For all 12 squid, 2.0–2.5 seconds of footage (3–6 jet cycles) were examined at each swimming speed. At speeds where squid swam in both tail-first and arms-first orientations, footage of swimming in both modes was analyzed. The criteria for selecting video footage were as follows: (1) squid had to be at least 5 cm above the flume floor and away from the flume sides (5 cm was the vertical distance above which boundary-layer effects within the tunnels were minimal based on ADV measurements and where speeds most closely matched calibration settings); (2) the squid had to swim perpendicular to the major axis of the camera, which was determined from aerial views provided by the mirror; and (3) the squid had to begin and end at the same horizontal position after a period of 2.0–2.5 seconds to ensure the squid was swimming at a net velocity that matched free stream flow.

The following parameters were measured on a frame-by-frame basis using the Peak motion system: mantle, arm, and funnel angles of attack relative to free-stream

flow; mantle diameter (measured at a point 60% of the mantle length from the tail); fin beat frequency (# beats s^{-1}); fin amplitude (measured at a location where chord length was greatest); speed of the trailing edge of the fin; distance above the flume bottom; swimming velocity relative to free stream flow (calculated from eye coordinates); and acceleration. Furthermore, the time required for expansion and contraction of the mantle and duration of the upward and downward strokes of the fins were calculated. All of the above parameters were measured from lateral close-up views, although one parameter, mantle diameter, also was measured in footage with simultaneous lateral and aerial views to determine if mantle expansion and contraction were uniform laterally and dorsally. To smooth out video jitter and human error during digitization, all raw coordinates were transformed using a fourth-order Butterworth filter (Hamming, 1983).

Flow Visualization

The velocity of water expelled from the funnel during mantle contraction was calculated by seeding the flume water with brine shrimp eggs (Argent Chemical Laboratories, Redmond, WA), videotaping the trajectory of particles ejected from the funnel using a Kodak high-speed video camera (500–1000 fps), and calculating particle velocities using the Peak motion system. A total of 10 squid ranging from 3.0 to 7.8 cm DML were examined between speeds of 3.0–30.0 $cm s^{-1}$ swimming in tail-first and arms-first orientations. Froude propulsion efficiency was determined at each speed using the equation (Vogel, 1994):

$$\text{Froude propulsion efficiency (FPE)} = 2U / (U_j + U) \quad (2)$$

where U is the free stream swimming velocity and U_j is the velocity of water expelled from the funnel determined from the particle trajectories.

Flow visualization studies of broad-scale characteristics of the jet wake also were performed. Two squid (6.20 ± 0.15 (SD) cm DML) were anesthetized in an isotonic solution of MgCl_2 (7.5% $\text{MgCl}_2 \cdot 6\text{H}_2\text{O}$) and seawater (Messenger et al. 1985). A 1.5 mm diameter hole was subsequently bored into the lateral mantle wall using a hypodermic needle, and 3.0 m of Tygon tubing (1.5 mm outer diameter) was threaded through the hole. A small bead of silicone placed at one end of the tubing prevented dislodgment from the mantle wall. After surgery each squid was placed in a 100-gallon aquarium filled with aerated seawater and allowed to recover. After recovery dye was pumped slowly into the mantle cavity using a peristaltic pump, and plumes of dye were subsequently expelled from the squid during jetting. Footage of the dye released from the funnel was recorded using Hi-8 video. When the jet efflux rolled up into a series of vortex rings, often called toroidal vortices, ring spacing, ring radius, jet core radius, and swimming speed were measured using the Peak motion analysis system.

Since squid swim at various angles of attack relative to free-stream flow, it was of interest to determine at which angles flow separation occurs. Therefore, a Plaster of Paris cast of the body (mantle, fins, head) and third (III) pair of arms was constructed from a 6.5 cm DML *L. brevis*. A conical, less detailed cast of the remaining arm assemblage also was made. Aquasil Smart Wetting™ Impression material (Dentsply International Inc., Milford, DE) was poured into the molds and allowed to dry. The final model consisted of a main body attached via imbedded wire to the third arm pair and the conical

section, which represented the remaining arms. The arms were connected using embedded wire to allow for independent manipulation from the main body.

The model was attached ventrally to a support stand and placed in a recirculating water tunnel, which had a 31 x 40 x 240 cm working section, located at the NASA Langley Research Center (LaRC), Hampton, VA. The model was oriented both tail-first and arms-first, and the mantle and arms were positioned independently at various angles of attack ($0\text{--}50^\circ$) relative to free stream flow. At the anterior-most stagnation point, dye was injected into the water using a NASA dye injection system and flow patterns were videotaped using Hi-8 video.

Force Measurements

The model was attached to a force beam containing strain gauges positioned to measure forces parallel (drag) and perpendicular (lift) to free stream flow. Signals from the strain gauges were amplified using an Omega DMD-465WB strain gauge amplifier, and flow velocity, which was measured simultaneously with force measurements, was recorded using the serial output from the Son-Tek ADV. The models were oriented tail-first and arms-first in the direction of free stream flow, and the arms and mantle were positioned at various attack angle combinations that were representative of behavior videotaped previously. Generally, angles of attack varied from $0\text{--}50^\circ$ and the angle of attack of the leading body section, whether it was the mantle or arms, rarely exceeded the angle of attack of the trailing body section. To reduce the number of arm/mantle combinations, the arms and mantle were positioned in 10° increments. Drag and lift measurements were performed in the water tunnel at NASA LaRC at 4 flow velocities (6,

12, 18, and 24 cm s⁻¹) for each combination of orientation (arms-first or tail-first), arm angle (0–50°), and mantle angle (0–50°).

Acceleration reaction measurements were performed using the same model placed in the Gloucester Point flume, which was capable of generating higher acceleration rates than the NASA LaRC tunnel. For these experiments, the model again was oriented tail-first and arms-first relative to free stream flow, and the arms and mantle were positioned at various representative angle combinations (the arms and mantle were positioned in 10° increments). Forces parallel to free stream flow and velocities measurements were recorded using a force beam and the Son-Tek ADV, respectively, as flow speed was elevated rapidly from 0 to approximately 45 cm s⁻¹. Four separate trials were performed for each orientation and mantle/arm angle combination.

Data acquisition for all force measurements was accomplished using LabVIEW software (National Instruments), a 16-bit analog-to-digital converter (National Instruments), and an Apple Macintosh G3 microcomputer. Using a LabVIEW Virtual Instrument (VI) developed by the author, force and velocity measurements were recorded simultaneously to a file at a scan rate of 250 readings s⁻¹ for a duration of 10 s for each combination of parameters (i.e. orientation, mantle angle, arm angle, and trial/speed). For acceleration reaction measurements, acceleration rates 2 s after flow was increased from rest, which was the approximate time required for flume velocity to reach 45 cm s⁻¹, were computed from velocity measurements.

Within the LabVIEW VI, drag, lift, and added mass coefficients were calculated continuously during the experiments using two equations. The equation used for drag or lift coefficient calculations was as follows:

$$C_{D \text{ or } L} = 2F / (D_w S_w U^2) \quad (3)$$

where $C_{D \text{ or } L}$ is the drag or lift coefficient, F is the force parallel to free stream flow (for drag calculations) or perpendicular to free stream flow (for lift calculations), D_w is the density of freshwater (998 kg m^{-3}), S_w is the wetted surface area of the model, and U is the free stream velocity. The wetted surface area of the models was determined by covering the model with aluminum foil and subsequently cutting the foil, laying it flat on a piece of paper, tracing the outline of the foil, and calculating the area within the tracing ($\pm 0.1 \text{ cm}^2$). Mean drag and lift coefficients were calculated for each mantle/arm angle combination at each swimming orientation.

Since the model was stationary and the fluid around the model was accelerating during acceleration reaction trials, the following equation was used to calculate the added mass coefficient (Denny, 1993):

$$C_a = [(F_1 - F_2 / (D_w V a) - 1] \quad (4)$$

where C_a is the added mass coefficient, F_1 is the instantaneous force acting parallel to free stream flow recorded 2 s after flow was accelerated from rest, F_2 is the force acting parallel to free stream flow under steady-state flow conditions at the velocity recorded 2 s after flow was accelerated from rest, D_w is the density of freshwater (998 kg m^{-3}), V is the volume of the model, and a is the acceleration of the water relative to the model. F_2 was calculated by inserting C_D computed above for the appropriate mantle/arm angle

combination into the steady-state drag equation (drag = $0.5C_D D_w S_w U^2$), where U = flow velocity 2 s after acceleration from rest. Mean added mass coefficients were calculated for each mantle/arm angle combination at each of the two swimming orientations.

Hydrodynamics

Using the coefficients computed from force measurements described above, instantaneous drag, lift, and acceleration reaction forces were calculated on a frame-by-frame basis for 3 squid. The 3 squid, which were 1.8, 4.4, and 7.6 cm DML, were selected because (1) they were representative of the size range considered in this study, (2) they were particularly cooperative, and (3) they swam in both orientations (tail-first and arms-first) for many speeds $\leq 12 \text{ cm s}^{-1}$. For each digitized frame, drag and lift were calculated using the following steady-state equations:

$$\text{Drag (D)} = 0.5C_D D_w S_w U^2 \quad (5)$$

$$\text{Lift (L)} = 0.5C_L D_w S_w U^2 \quad (6)$$

Drag and lift coefficients measured from the models were used for these equations. Since coefficients derived from the models were measured at 10° intervals, mantle and arm angles recorded in the video frames were rounded to the nearest 10° and assigned appropriate coefficients. A seawater density of 1023 kg m^{-3} was used for D_w . For wetted surface areas (S_w) calculations, the head and arms of each squid were treated as a right cone with height equal to the distance from the head to the tip of the third (III) arm pair

and radius equal to the mean of the dorsal and lateral head radii. The surface area of the cone was simply πrs , where r was the mean radius and s was the hypotenuse of the mean radius and height. For wetted surface area calculations of the remainder of the body, the mantle and fins were cut, placed flat on a sheet of paper, traced, and areas within tracings were calculated ($\pm 0.1 \text{ cm}^2$). In addition to calculating drag and lift values for each digitized frame, mean drag and mean lift values for each video sequence were calculated.

Since the squid were accelerating within the flume, the following equation was used to compute the acceleration reaction (Denny, 1993):

$$\text{acceleration reaction (AR)} = ma + C_a D_w V a \quad (7)$$

The only new term introduced here is m , which is the mass of the squid (kg). As was the case for drag and lift measurements, mantle and arm angles were rounded to the nearest 10° for simplicity, and the appropriate added mass coefficients were used in frame calculations. In addition to the instantaneous acceleration reaction computed for each digitized frame, an overall mean acceleration reaction for each video sequence was calculated.

During the contraction phase of the jet cycle, water is forcibly ejected from the mantle cavity through the funnel to generate thrust. Jet thrust (T_j) may be calculated using the equation (Daniel, 1983; O'Dor, 1988):

$$T_j = U_j D_w (V_w/t) \quad (8)$$

where U_j is the velocity of water expelled from the funnel, D_w is the density of seawater (1023 kg m^{-3}), and V_w is the volume of water expelled over time (t). U_j was determined using flow visualization studies described above. U_j was considered constant throughout the contraction phase of the jet cycle. O'Dor (1988) determined that changes in jet velocity during the jet cycle are negligible, contributing only 0.5–1.0% of the total jet thrust over the speed range. Thus, an assumption of a constant U_j should not lead to significant errors in thrust calculations. To determine the volume of expelled water (V_w), mantle outlines (of the three squids) visible in frames of lateral video footage were divided up into a series of cylinders and a cone, which represented the posterior tip of the mantle, using the Peak motion system. Division of the mantle into a series of cylinders and a cone was accomplished by sectioning the mantle of the three squids into a series of equally spaced segments over several jet cycles. Distance between adjacent segments was considered the height of a given cylinder or cone; heights varied from 0.20 to 0.60 cm depending on the size of the squid. The radius of each cylinder was simply 1/2 of the mean of the two segments forming the cylinder; the radius of the cone was 1/2 the segment forming the cone base. (Given that differences in mantle diameter viewed aurally and laterally were negligible, uniform circumferential expansion of the mantle was assumed). A linear regression of the volumetric sum of the cylinders and cone (computed in each video frame throughout several jet cycles) on mantle diameter (measured at point 60% of the mantle length from the tail in each video frame throughout the jet cycles) was performed. This regression equation allowed for prediction of external volume from mantle diameter. For each frame of video, subtracting the volume

of the mantle tissue (without fins) and internal viscera from the external volume value determined the volume of water within the mantle. The volume of expelled water per time (V_w/t) was simply the difference in internal mantle water volume between frames divided by the frame rate.

Since the funnel was oriented at various angles relative to flow throughout the jet cycle, jet thrust was divided into horizontal and vertical components using the equations:

$$T_{j(h)} = T \cos (\text{funnel angle}) \quad (9)$$

$$T_{j(v)} = T \sin (\text{funnel angle}) \quad (10)$$

Throughout the jet cycle the vertical force components should equal the buoyant weight of the squid if altitude is maintained. Based on weight measurements made in air and water, the water/air weight ratio was $0.034 (\pm 0.012 \text{ S.D.})$ for *L. brevis*, which is remarkably similar to a water/air weight ratio of 0.033 measured for *Loligo opalescens* (O'Dor, 1988). Given this ratio, buoyant weight (B) = $0.034 m g$, where m is the mass of the squid (kg) and g is the acceleration of gravity (9.81 m s^{-2}). Although squid did not begin and end video sequences at the same altitude as was the case for horizontal position, vertical altitude did not differ dramatically at the beginning and end of video sequences (see Table 4). Therefore, the following equation is a reasonable predictor of the balance of vertical forces at the end of the video sequence:

$$B = T_{j(v)} + T_{f(v)} + L \quad (11)$$

B is buoyant weight, $T_{j(v)}$ is mean vertical jet thrust, $T_{f(v)}$ is mean vertical fin thrust, and L is mean lift over the video sequence. In squid it is very difficult to separate fin thrust generation from that of the jet because squid are constantly refilling and ejecting water from the mantle cavity. However, given that B, $T_{j(v)}$, and L were known, mean vertical fin thrust ($T_{f(v)}$) over the video sequence was estimated using equation (11).

Horizontal thrust forces should be equal to the horizontal resistive forces if there is no acceleration or deceleration. Therefore, at the end of the each video sequence when there was no net velocity change:

$$T_{j(h)} + T_{f(h)} = F_r + D + AR \quad (12)$$

where $T_{j(h)}$ is mean horizontal jet thrust, $T_{f(h)}$ is mean horizontal fin thrust, F_r is the mean refilling force, D is mean drag, and AR is the mean acceleration reaction over the video sequence. The refilling force (F_r) = $D_w(V_v/t)U_i$, where D_w is the density of seawater, V_v/t is the amount of water entering the mantle over time (t), and U_i is intake water velocity (intake water velocity was assumed to be equal to the swimming velocity of the squid). Mean horizontal fin thrust ($T_{f(h)}$) over video sequences was calculated using equation (12) and the above parameters.

RESULTS

Critical and Transition Swimming Speeds

Mean critical swimming speeds (U_c) for squid in the 1.0–2.9 cm DML, 3.0–4.9 cm DML, 5.0–6.9 cm DML, and 7.0–8.9 cm DML size class were 15.3 ± 5.3 (SD) cm s^{-1} , 22.8 ± 5.6 (SD) cm s^{-1} , 20.5 ± 3.5 (SD) cm s^{-1} , and 22.2 ± 5.3 (SD) cm s^{-1} , respectively; however, certain squid were capable of sustaining much higher swimming velocities (Table 1). The majority of squid swam in an arms-first orientation upon initial placement into swim tunnels. Many squid continued to swim in an arms-first orientation or alternated between arms-first and tail-first swimming at low speeds before switching exclusively to tail-first swimming at some higher speed. Mean transition speeds (U_t), i.e., speeds above which squid swam exclusively in a tail-first orientation, for those squid that swam in both orientations belonging to the 1.0–2.9 cm DML, 3.0–4.9 cm DML, 5.0–6.9 cm DML, and 7.0–8.9 cm DML size classes were 9.0 ± 0.0 (SD) cm s^{-1} , 10.5 ± 1.8 (SD) cm s^{-1} , 12.6 ± 2.5 (SD) cm s^{-1} , and 15.3 ± 2.7 (SD) cm s^{-1} , respectively (Table 1).

Kinematic Measurements

During tail-first swimming, angles of attack of the mantle, arms, and funnel decreased with increased speed for squid in all four size classes (linear regressions $P < 0.05$; Figure 1, 2). Over the speed range considered in this study, angles of attack during tail-first swimming differed significantly according to body section (i.e. mantle, arms,

Table 1. Mean critical swimming speeds (U_c), U_c ranges, mean transition speeds (U_t), and U_t ranges for four size classes of *Lolliguncula brevis*. The critical swimming speed is the maximum velocity squid can sustain for 15 minutes, whereas the transition speed is the speed above which squid swim exclusively in a tail-first orientation. The number of squid considered in critical speed (n_c) and transition speed (n_t) calculations also are listed. All error terms represent ± 1 standard deviation.

Size Class (cm DML)	n_c	U_c mean (cm s^{-1})	U_c range (cm s^{-1})	n_t	U_t mean (cm s^{-1})	U_t range (cm s^{-1})
1.0 – 2.9	8	15.3 + 5.3	11.9 – 24.1	2	9.0 + 0.0	9.0
3.0 – 4.9	10	22.8 + 5.6	14.8 – 32.4	7	10.5 + 1.8	8.0 – 12.0
5.0 – 6.9	8	20.5 + 3.5	15.0 – 25.5	5	12.6 + 2.5	9.0 – 15.0
7.0 – 8.9	6	22.2 + 5.3	18.1 – 33.7	4	15.3 + 2.7	12.0 – 18.0

Figure 1. Mantle, arm, and funnel angles of attack for *Lolliguncula brevis* swimming at various speeds. Squid swimming in a tail-first orientation are displayed in graphs A, C, E, and G, whereas squid swimming in an arms-first orientation are shown in graphs B, D, F, and H. Data from four size classes are included in the figure. Size class 1 (1.0–2.9 cm DML) is depicted in A and B, size class 2 (3.0–4.9 cm DML) is depicted in C and D, size class 3 (5.0–6.9 cm DML) is depicted in E and F, and size class 4 (7.0–8.9 cm DML) is depicted in G and H. When a significant linear relationship between angle of attack and speed was detected, regression lines were plotted in graphs and regression equations, r^2 values, and p-values were included to the right of graphs. When significant relationships were not detected, data points were simply connected with lines and no regression information was included. All error bars represent ± 1 standard error.

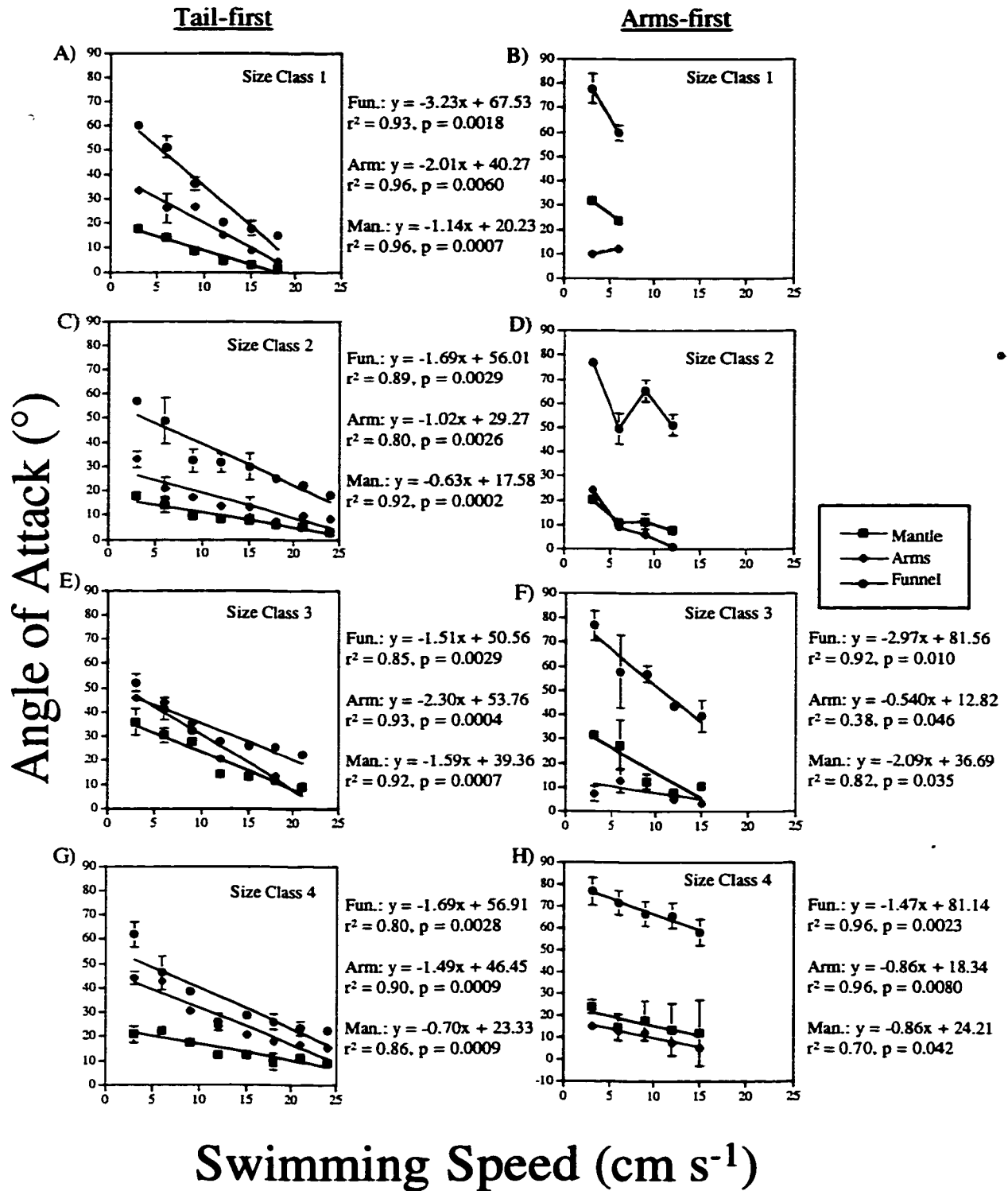
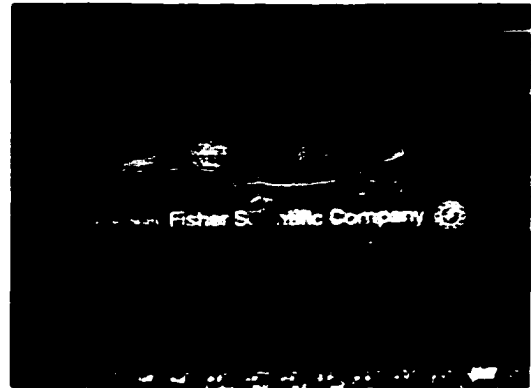


Figure 2. Video frames of a 4.4 cm DML *Lolliguncula brevis* swimming tail-first at 3 and 24 cm s⁻¹ (upper frames) and arms-first at 3 and 12 cm s⁻¹ (lower frames). Mantle and arm angles of attack decreased with increased swimming speed for both swimming orientations. Angle of attack differences were less pronounced for arms-first swimming because a more restricted velocity range was considered (*L. brevis* only swam arms-first at low to intermediate speeds). Note that the trailing body section, whether the arms during tail-first swimming or mantle during arms-first swimming, was often positioned at higher angles of attack than the leading body section.

Tail-first

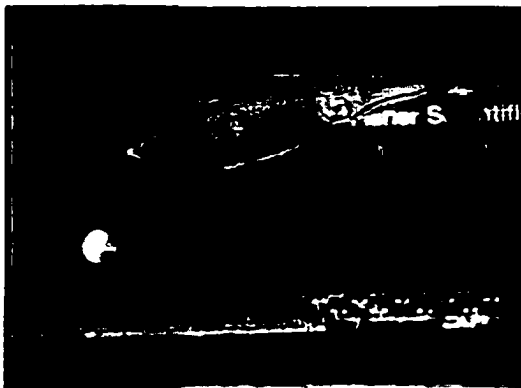


3 cm s⁻¹



24 cm s⁻¹

Arms-first



3 cm s⁻¹



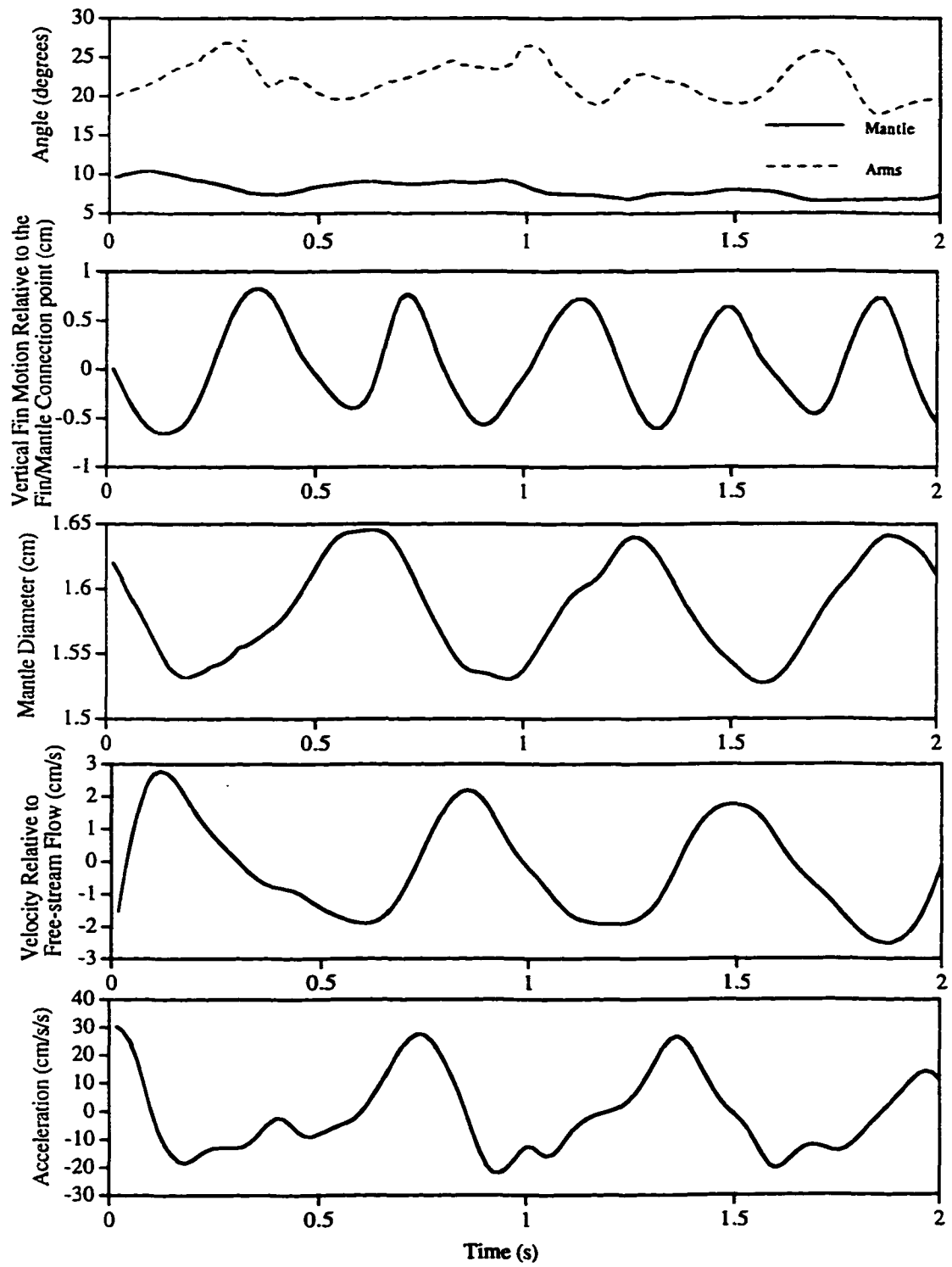
12 cm s⁻¹

funnel) and size class (1-4) (2-factor ANOVA: (body section) $df = 2, 74, F = 14.99, P < 0.0001$; (size class) $df = 3, 75, F = 6.59, P = 0.0005$). Subsequent *a posteriori* Student-Newman-Keuls (SNK) tests revealed that the funnel was oriented at the greatest angle of attack, the arms were positioned at a higher angle of attack than the mantle (see Figure 2), and squid belonging to size class 2 (3.0–4.9 cm DML) had the lowest overall angles of attack. Moreover, in the tail-first swimming mode, angles of attack of the arms often increased briefly during mantle expansion (refilling) (Figure 3).

Because of limited data, significant declines in angles of attack with speed during arms-first swimming were not always detected for all size classes. However, a clear declining trend in angle of attack of most of the body sections with increased speed was apparent in size classes 1 and 2 (1.0–2.9 and 3.0–4.9 cm DML, respectively), while significant declines in angles of attack with increased speed were detected for size classes 3 and 4 (5.0–6.9 and 7.0–8.9 cm DML) (Figure 1). Angles of attack during arms-first swimming differed according to body part but not according to size class (2-factor ANOVA (body part) $df = 2, 33, F = 124.85, P < 0.0001$; (size class) $df = 3, 33, F = 2.03, P = 0.1294$). SNK tests revealed that during arms-first swimming, funnel angles were greatest over the speed range, and mantle angles of attack were greater than arm angles of attack (Figure 2).

To assess whether there were significant differences in angles of attack between tail-first and arms-first swimming modes, a 2-factor (body section and orientation) ANOVA was performed on data pooled by size class. (Only those speeds at which both tail-first and arms-first swimming were employed were considered). A significant interaction between body section and orientation was detected (2-factor ANOVA: (body

Figure 3. Arm and mantle angles of attack, vertical fin motion (relative to the point at which the fin connects to the mantle), mantle diameter, changes in linear velocity (relative to free stream flow), and acceleration for a 4.4 cm DML *Lolliguncula brevis* swimming tail-first at 6 cm s^{-1} against a current in a flume. A total of 60 frames were analyzed to generate the traces.



section*orientation) $df = 2, 78$; $F = 31.602$; $P < 0.0001$). Subsequent SNK tests performed to decouple the interaction revealed that there was no significant difference between mantle angles of attack during arms-first and tail-first swimming, but that the angle of attack of the funnel was greater during arms-first swimming and the angle of attack of the arms was greater during tail-first swimming.

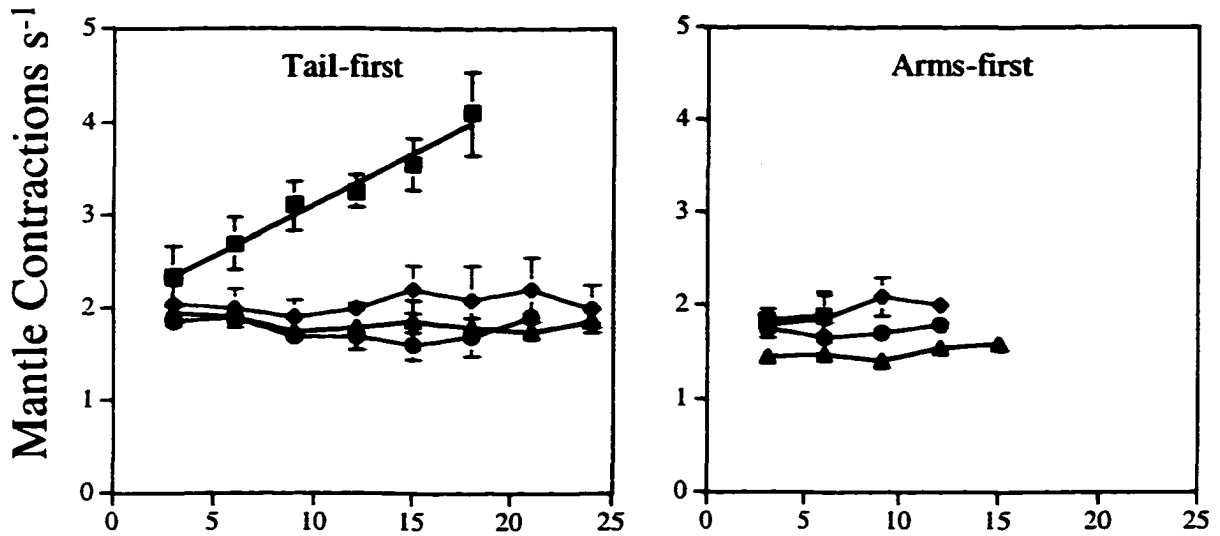
Mantle contraction rates for squid swimming in the tail-first swimming mode belonging to size class 1 (1.0–2.9 cm DML) increased from 2.4 ± 0.6 (SD) contractions s^{-1} at 3 cm s^{-1} to 4.1 ± 0.9 (SD) contractions s^{-1} at 18 cm s^{-1} (Figure 4). However, contraction rates for squid belonging to larger size classes did not increase significantly with swimming speed (range: 1.6 ± 0.2 (SD) – 2.2 ± 0.5 (SD) contractions s^{-1}) (Figure 4). Not surprisingly, mean mantle contraction rates over the speed range differed according to size class (1-factor (size class) ANOVA: $df = 3, 25$; $F = 12.726$; $P < 0.0001$); contraction rates in size class 1 were greater than those in the other size classes, and no significant differences were detected among size classes 2-4.

While swimming arms-first, no clear increase in mantle contraction rate with speed was apparent (Figure 4). Based on a 1-factor (size class) ANOVA ($df = 3, 10$; $F = 21.381$; $P < 0.0001$) performed over the speed range and subsequent *a posteriori* SNK tests, contraction rates for squid in size class 4 (7.0–8.9 cm DML) were lowest, and squid in size class 3 (5.0–6.9 cm DML) had lower contraction rates than squid in size class 2 (3.0–4.9 cm DML).

When data were pooled by size class, mantle contraction frequency was found to be greater during tail-first swimming than arms-first swimming (1-factor ANOVA (orientation): $df = 1, 26$; $F = 6.536$; $P < 0.0168$). (Again only speeds where both

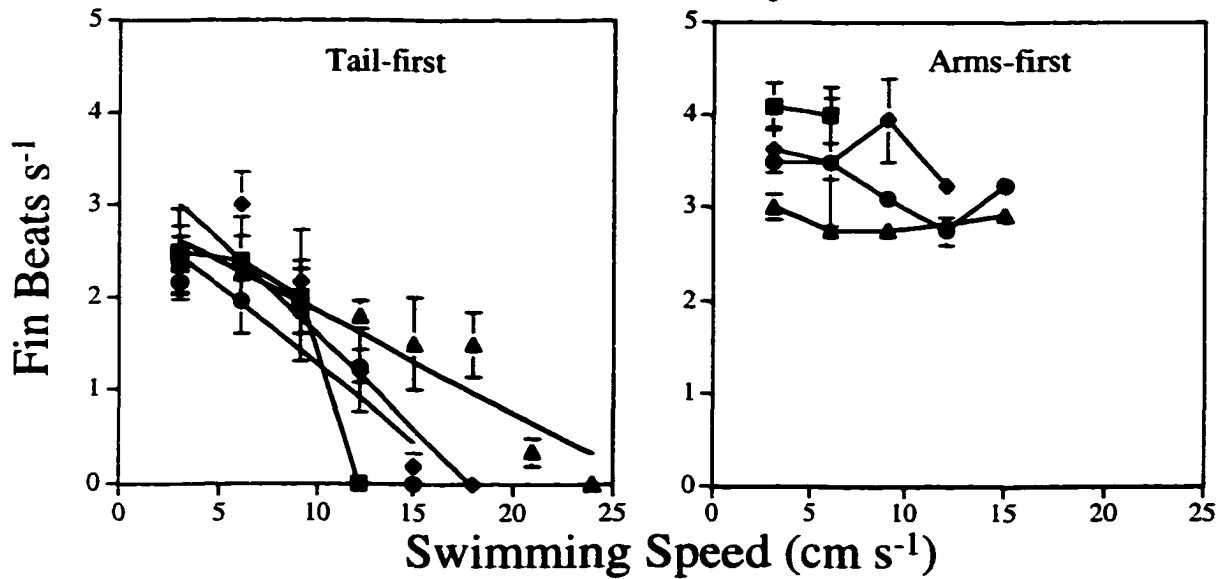
Figure 4. Number of mantle contractions s^{-1} and fin beats s^{-1} for *Lolliguncula brevis* swimming against a steady current in a flume over a range of speeds in both tail-first and arms-first orientations. Data from four size classes are depicted; size class 1 represents squid 1.0–2.9 cm DML, size class 2 represents squid 3.0–4.9 cm DML, size class 3 represents squid 5.0–6.9 cm DML, and size class 4 represents squid 7.0–8.9 cm DML. When significant linear relationships were detected, regression lines were plotted in graphs, and regression equations, r^2 values, and p-values were included underneath graphs. All error bars represent ± 1 standard error.

Mantle Activity



Size class 1: $y = 0.11x + 2.03$, $r^2 = 0.98$, $p = 0.0002$

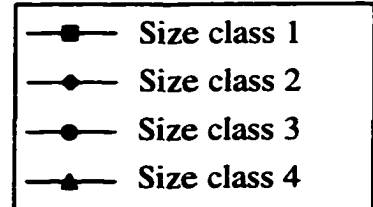
Fin Activity



Size class 2: $y = -0.20x + 3.62$, $r^2 = 0.86$, $p = 0.006$

Size class 3: $y = -0.17x + 2.96$, $r^2 = 0.83$, $p = 0.007$

Size class 4: $y = -0.11x + 2.94$, $r^2 = 0.88$, $p = 0.0006$



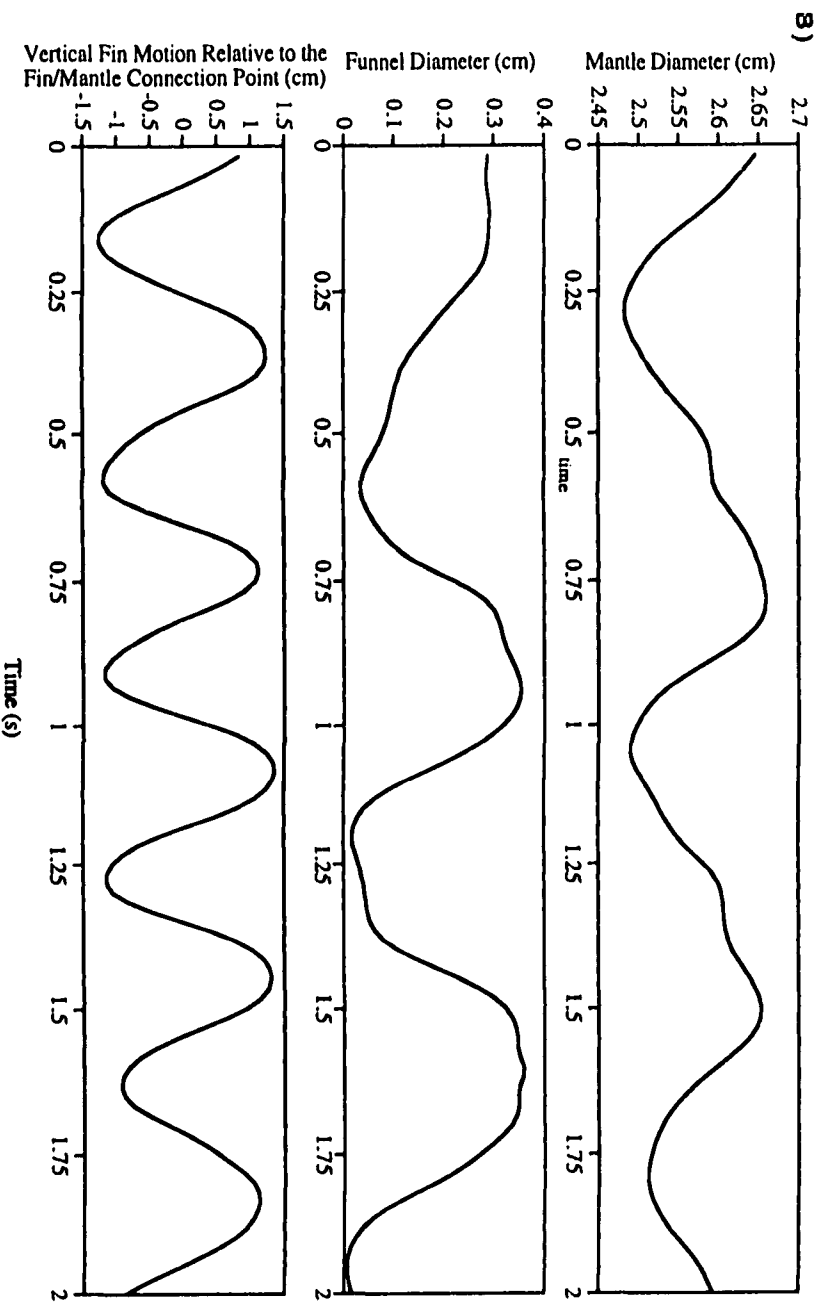
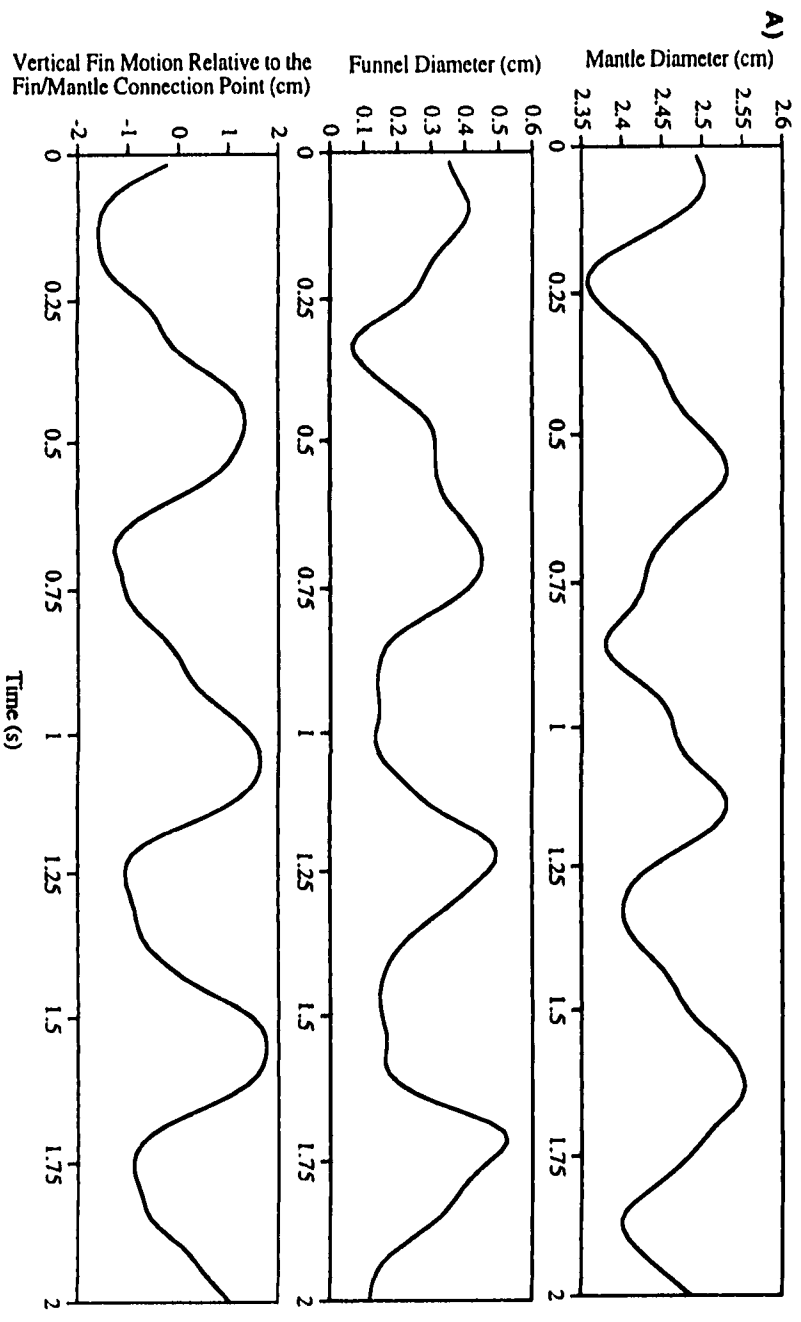
swimming orientations were used were considered). During mantle contractions, funnel diameter frequently increased during the initial portion of the contraction but then decreased gradually throughout the remainder of the contraction and even into mantle refilling (expansion) (Figure 5).

For squid in size classes 2–4 swimming tail-first, fin activity decreased significantly with swimming velocity until a velocity was reached at which the fins simply remained wrapped around the mantle (Figure 4). Although a significant linear decline in fin beat rates with speed was not detected for squid in size class 1, a clear decreasing trend in fin use with speed was apparent (Figure 4). No significant difference in the overall number of fin beats s^{-1} over the speed range was detected between the size classes (1-factor (size class) ANOVA: $df = 3, 19$; $F = 0.072$; $P = 0.9744$).

Squids used fin motion for all speeds where arms-first swimming was employed, and no linear decrease in fin use with speed was detected (Figure 4). During arms-first swimming, squid belonging to the two smaller size classes (1.0–2.9 cm DML and 3.0–4.9 cm DML) had greater fin beat rates than squid belonging to the large size class (7.0–8.9 cm DML) over the speed range considered (1-factor ANOVA (size class): $df = 3, 11$; $F = 12.36$; $P = 0.0008$).

When data were pooled by size class fin beat rates were higher during arms-first swimming than during tail-first swimming (1-factor ANOVA (orientation) ANOVA: $df = 1, 26$; $F = 46.39$; $P < 0.0001$) (Figure 4). At low speeds ($\leq 6 \text{ cm s}^{-1}$) during tail-first swimming and at all speeds during arms-first swimming, fin downstrokes often occurred during mantle contraction and refilling (Figure 3, 5B), whereas at higher speeds when fin

Figure 5. Mantle diameter, funnel diameter, and vertical fin motion (relative to the point at which the fin connects to the mantle) of *Lolliguncula brevis* (7.3 cm DML) swimming A) tail-first and B) arms-first at 9 cm s^{-1} against a steady flow in a flume. A total of 60 frames were analyzed to generate the traces.



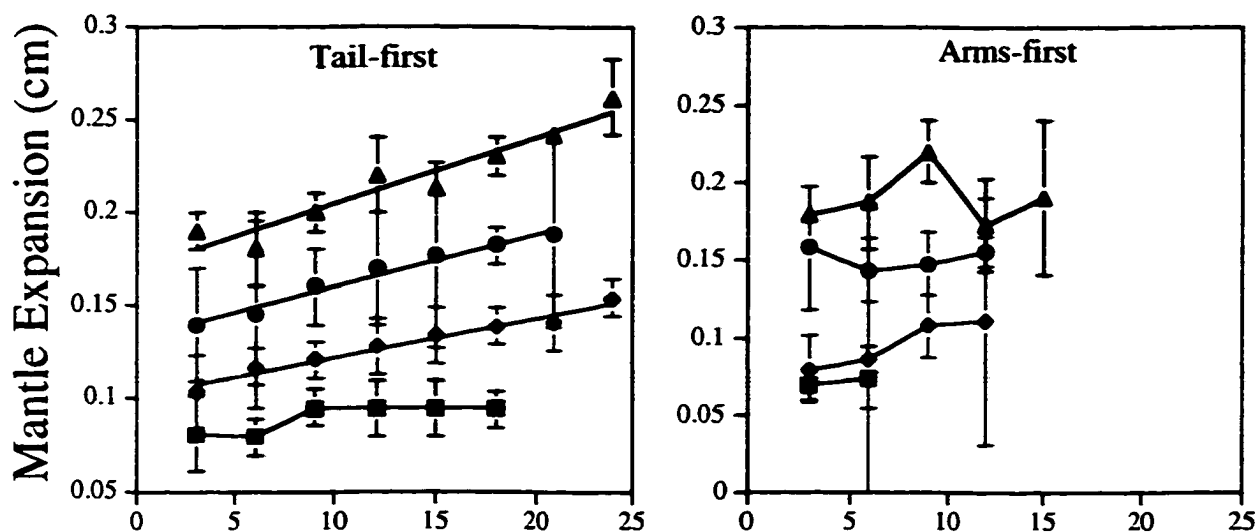
activity was less, fin downstrokes frequently occurred during mantle contractions (Figure 5A).

Although contraction rates during tail-first swimming did not increase significantly with speed for squid in size classes 2–4, mantle expansion did increase with speed (linear regressions $P < 0.05$; Figure 6). However, no clear increase in mantle expansion with speed was detected for squid in size class 1—the size class where mantle contraction did increase with swimming speed. Mantle expansion of squid swimming in an arm-first orientation did not increase significantly with speed (Figure 6). During tail-first swimming vertical fin motion (absolute vertical distance between maximum upstroke and maximum downstroke) decreased with increased swimming velocity (linear regressions: $P < 0.05$), but no detectable decrease in fin amplitude was found for arm-first swimming (Figure 6).

The time required for mantle expansion during tail-first swimming was greater than that required to contract the mantle for squid in size classes 2, 3, and 4 over the range of speeds considered (paired t-test: $P < 0.05$) (Table 2). When data from all of the size classes were pooled this difference was highly significant ($P = 0.0002$). When swimming in an arms-first orientation, only squid belonging to size class 2 had greater mantle expansion than contraction times; but mantle expansion times were significantly greater than contraction times when data from all of the size classes were pooled ($P = 0.0064$) (Table 2). Mantle expansion time decreased with increased swimming speed only for squid belonging to size class 1 while swimming tail-first (linear regression: $P = 0.0080$; $R^2 = 0.857$) (Table 2). Mantle contraction time decreased with increased swimming speed for squid belonging to size classes 1 and 2 while swimming tail-first

Figure 6. Mantle expansion and vertical fin motion (absolute vertical distance between maximum upstroke and downstroke) of *Lolliguncula brevis* swimming over a range of speeds in both tail-first and arms-first orientations. Data from four size classes are depicted; size class 1 represents squid 1.0–2.9 cm DML, size class 2 represents squid 3.0–4.9 cm DML, size class 3 represents squid 5.0–6.9 cm DML, and size class 4 represents squid 7.0–8.9 cm DML. When significant linear relationships were detected, regression lines were plotted in graphs, and regression equations, r^2 values, and p-values were included underneath graphs. All error bars represent ± 1 standard error.

Mantle

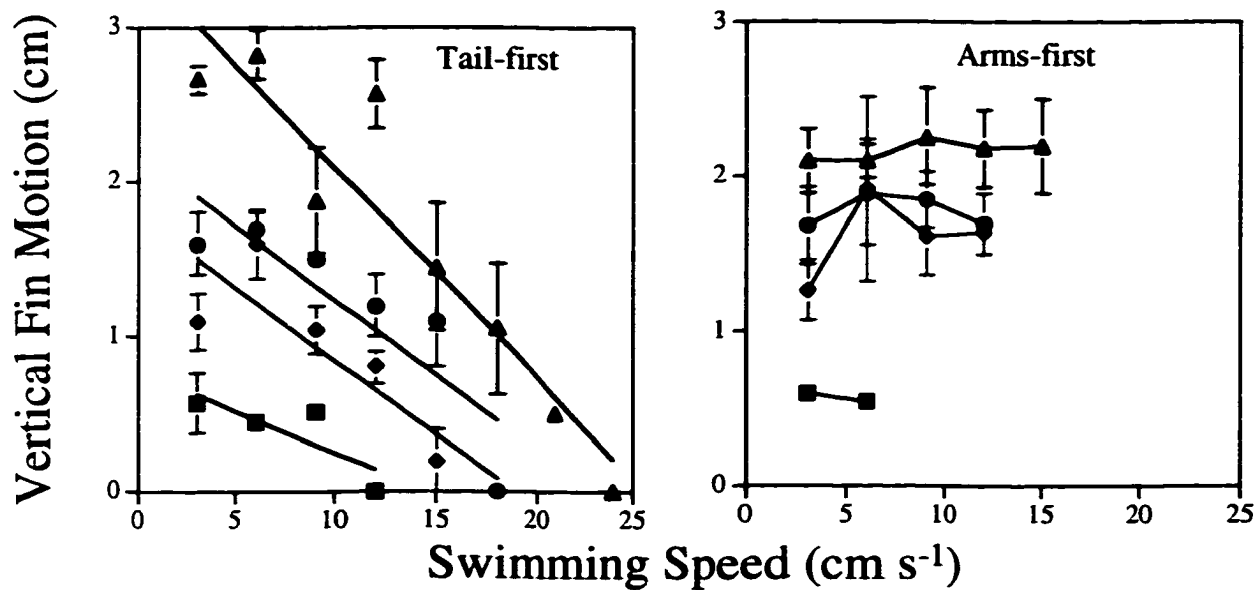


Size class 2: $y = 0.002x + 0.10$, $r^2 = 0.97$, $p < 0.0001$

Size class 3: $y = 0.003x + 0.14$, $r^2 = 0.97$, $p < 0.0001$

Size class 4: $y = 0.004x + 0.17$, $r^2 = 0.92$, $p = 0.0002$

Fins



Size class 1: $y = -0.055x + 0.79$, $r^2 = 0.67$, $p = 0.043$

Size class 2: $y = -0.095x + 1.78$, $r^2 = 0.79$, $p = 0.018$

Size class 3: $y = -0.096x + 2.19$, $r^2 = 0.75$, $p = 0.026$

Size class 4: $y = -0.13x + 3.43$, $r^2 = 0.88$, $p = 0.0005$

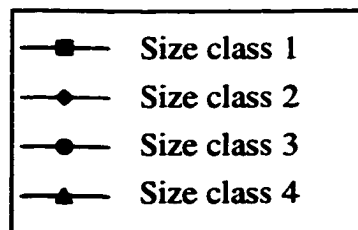


Table 2. Summary of results of paired t-tests and linear regressions performed on kinematic data collected from *Lolliguncula brevis* swimming in tail-first and arms-first orientations over a range of speeds. The four size classes considered are as follows: 1.0–2.9 cm DML (size class 1), 3.0–4.9 cm DML (size class 2), 4.0–6.9 cm DML (size class 3), and 7.0–8.9 cm DML (size class 4). No statistical analyses were performed on squid in size class 1 swimming in an arms-first orientation because of limited data. Asterisks (*) denote significance at $\alpha = 0.05$.

Size Class	Orien- tation (T = Tail- first; A = Arms- first)	Paired Comparison of mantle expansion and contraction times (s) (E = expansion time; C = contraction time)	Paired Comparison of upward and downward fin stroke times (s)	Regression of mantle expansion and contraction times (s) on swimming speed (cm/s) (E = expansion time; C = contraction time; m =slope)	Regression of upward and downward fin stroke times (s) on swimming speed (cm/s) (U = upward stroke time; D = downward stroke time)	Regression of trailing fin wave speed (s) on swimming speed (cm/s)	Regression of mean max. positive (+) and negative (-) speed deviations (cm/s) on swimming speed (cm/s) (m =slope)	Regression of mean max. acceleration (+) and deceleration (-) on swimming speed (cm/s) (m =slope)
1	T	P=0.2856	P=0.0694	E: P=0.0080*; R ² =0.857; m=-0.006 C: P=0.0034* R ² =0.907; m=-0.004	U: P=0.6667 D: P=0.4065	P=0.3111	(+): P=0.0824 (-): P=0.0133* R ² =0.818; m=-0.148	(+): P<0.0001* R ² =0.985; m=3.285 (-): P=0.0003* R ² =0.974; m=-4.446
1	A	NA	NA	NA	NA	NA	NA	NA
2	T	P=0.0095*; E > C	P=0.4274	E: P=0.2783 C: P=0.0391*; R ² =0.535; m=-.0004	U: P=0.2339 D: P=0.6143	P=0.2833	(+): P=0.0087* R ² =0.709; m=0.168 (-): P=0.0088* R ² =0.708; m=-0.165	(+): P=0.0008* R ² =0.868; m=3.223 (-): P=0.7374
2	A	P=0.0463*; E > C	P=0.3910	E: P=0.8236 C: P=0.7418	U: P=0.8790 D: P=0.9418	P=0.1048	(+): P=0.3808 (-): P=0.9200	(+): P=0.3660 (-): P=0.5479
3	T	P=0.0245*; E > C	P=0.3280	E: P=0.1126 C: P=0.3157	U: P=0.4556 D: P=0.2134	P=0.3155	(+): P=0.0311* R ² =0.612; m=0.193 (-): P=0.0439* R ² =0.563; m=-0.152	(+): P<0.0007* R ² =0.824; m=2.834 (-): P=0.0397* R ² =0.555; m=-2.111

Size Class	Orien- tation (T = Tail- first; A = Arms- first)	Paired Comparison of mantle expansion and contraction times (s) (E = expansion time; C = contraction time)	Paired Comparison of upward and downward fin stroke times (s)	Regression of mantle expansion and contraction times (s) on swimming speed (cm/s) (E = expansion time; C = contraction time; m =slope)	Regression of upward and downward fin stoke times (s) on swimming speed (cm/s) (U = upward stroke time; D = downward stroke time)	Regression of trailing fin wave speed (s) on swimming speed (cm/s)	Regression of mean max. positive (+) and negative (-) speed deviations (cm/s) on swimming speed (cm/s) (m =slope)	Regression of mean max. acceleration (+) and deceleration (-) on swimming speed (cm/s) (m =slope)
3	A	P=0.0663	P=0.3325	E: P=0.8863 C: P=0.7324	U: P=0.4568 D: P=0.1838	P=0.6143	(+): P=0.5447 (-): P=0.1156	(+): P=0.2894 (-): P=0.2252
4	T	P=0.0119*; E>C	P=0.3933	E: P=0.3362 C: P=0.4155	U: P=0.7115 D: P=0.7594	P=0.1554	(+): P=0.2391 (-): P=0.0897	(+): P=0.0293* R ² =0.575; m=.745 (-): P=0.9235
4	A	P=0.0814	P=0.2038	E: P=0.1888 C: P=0.3437	U: P=0.2116 D: P=0.2557	P=0.7694	(+): P=0.1097 (-): P=0.0659	(+): P=0.7270 (-): P=0.4159
Pool d	T	P=0.0002*; E>C	P=0.8596	E: P=0.8580 C: P=0.4726	U: P=0.3347 D: P=0.8263	P=0.0151; R ² =0.461; m=0.461	(+): P=0.0004* R ² =0.823; m=0.0183 (-): P=0.0039* R ² =0.675; m=-0.145	(+): P<0.0001* R ² =0.904; m=3.297 (-): P=0.0005* R ² =0.785; m=-2.586
Pool d	A	P=0.0064*; E>C	P=0.3517	E: P=0.9473 C: P=0.8285	U: P=0.8240 D: P=0.1931	P=0.3601	(+): P=0.6989 (-): P=0.0869	(+): P=0.1449 (-): P=0.0975

(linear regression: $P = 0.0034$, $R^2 = 0.907$ (size class 1); $P = 0.0391$; $R^2 = 0.535$ (size class 2)) (Table 2).

No significant differences between upward and downward fin stroke times were detected, and there was no increase or decrease in upward or downward fin stroke time with increased speed for squid swimming in either tail-first or arms-first orientations (Table 2). Furthermore, no increase or decrease in trailing fin wave speed with increased swimming velocity was detected when size classes were examined separately; however, when the size classes were pooled, a linear increase in trailing fin wave speed with increased swimming velocity was detected for squid swimming tail-first ($P = 0.0151$; $R^2 = 0.461$) (Table 2). Mean trailing fin wave speeds ranged from 4.2–12.3 cm s^{-1} . At swimming speeds $< 9 \text{ cm s}^{-1}$ trailing fin wave speeds generally exceeded swimming speeds, whereas at speeds $\geq 9\text{--}12 \text{ cm s}^{-1}$ trailing fin wave speeds were generally less than swimming speed.

When tail-first swimming data from the four size classes were pooled, mean maximum positive and negative (converted to absolute values) deviation in velocity and acceleration were found to increase with swimming speed ($P < 0.0039$; $R^2 > 0.675$) (Table 2). Although linear relationships were not always detected when velocity and acceleration deviations were regressed against swimming speed and examined separately by size class, P -values < 0.10 were frequently observed (Table 2). No linear relationships between mean maximum velocity deviation and speed and mean maximum acceleration deviation and speed were detected for squid swimming in the arms-first orientation ($P > 0.05$).

Flow Visualization

Based on measurements collected from particles expelled by squid swimming in flumes, the lowest Froude propulsion efficiencies (FPE) for both tail-first and arms-first swimming were detected at 3 cm s^{-1} (FPE = 0.177 (tail-first) and 0.151 (arms-first)) (Table 3). Peak efficiencies were 0.472 for tail-first swimming at 9 cm s^{-1} and 0.411 for arms-first swimming at 12 cm s^{-1} (Table 3)

When dye was injected into the mantle of squid (6.2 ± 0.15 (SD) cm DML), the squid appeared agitated and frequently jetted abruptly and erratically across the aquarium or into the aquarium walls. During these episodes, the jet wake was generally very turbulent, and it was difficult to extract any meaningful data. However, on several occasions, the squid swam steadily across the aquarium at 8.6 ± 2.5 (SD) cm s^{-1} , and the formation of toroidal vortices was observed (Figure 7). The mean ring spacing to ring radii ratio (a/b) was 7.39 ± 2.34 (SD) and the mean ring radii to jet core radius ratio (b/e) was 1.75 ± 0.38 (SD).

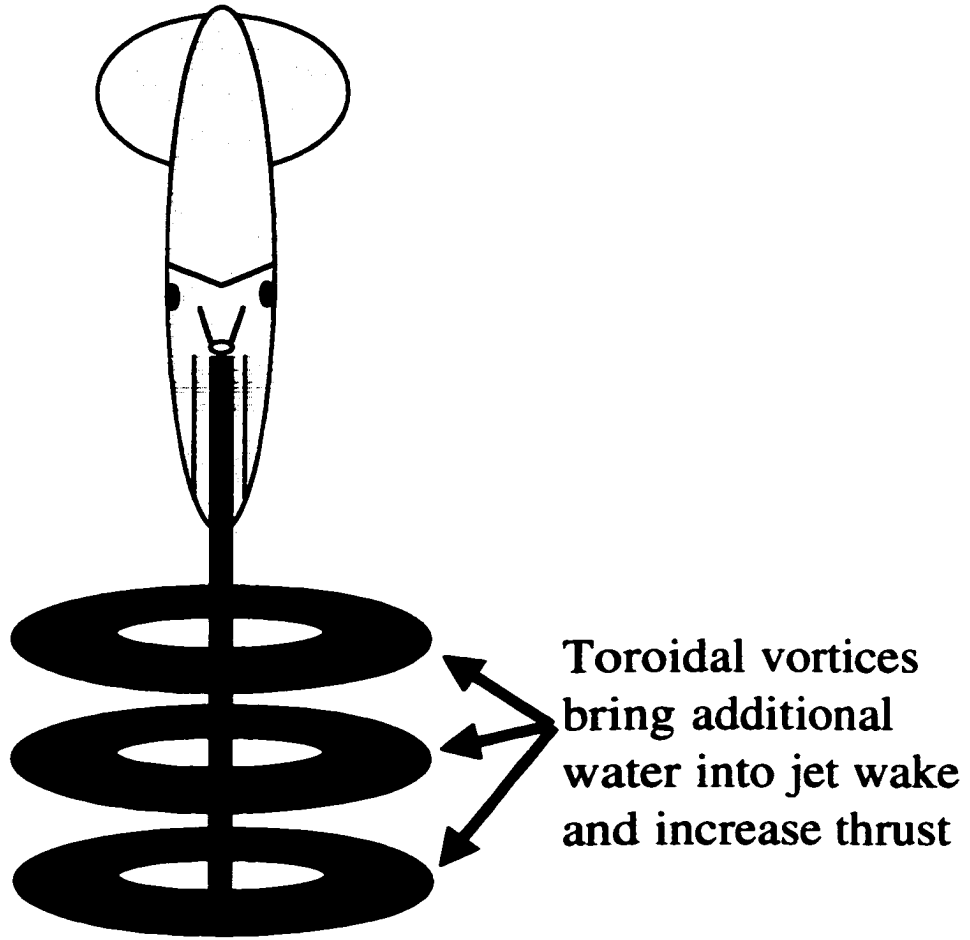
Flow separation and the subsequent migration of flow along the body in a counter-free stream flow direction was observed when the mantle and arms of models were both positioned at $>35^\circ$ relative to flow, irrespective of whether the models were positioned tail- or arms-first. Separation also was observed when the leading body section, i.e., the mantle when in the tail-first swimming mode or the arms when in the arms-first swimming mode, was at 0° and the trailing body section was positioned at $>35^\circ$. However, when the leading body section was at $10\text{--}20^\circ$ separation did not occur until the trailing section was $\geq 45^\circ$. During tail-first swimming, no squid positioned the mantle at a higher angle of attack than the arms, but during arms-first swimming, angles

Table 3. Froude propulsion efficiencies (FPE) for *Lolliguncula brevis* swimming in both tail-first (T) and arms-first (A) orientations. Since the majority of squid did not swim $> 12 \text{ cm s}^{-1}$ in the arms-first mode, Froude propulsion efficiencies were only calculated for speeds 3–12 cm s^{-1} . For tail-first swimming Froude propulsion efficiencies were calculated for speeds 3–27 cm s^{-1} .

		Swimming Velocity (cm/s)								
		3	6	9	12	15	18	21	24	27
FPE		0.177(T)	0.287(T)	0.472(T)	0.441(T)	0.409(T)	0.378 (T)	0.400(T)	0.421(T)	0.431(T)
		0.151(A)	0.231(A)	0.389(A)	0.411 (A)					

Figure 7. A) Hypothetical and B) actual toroidal vortex formation in brief squid.

A)



B)

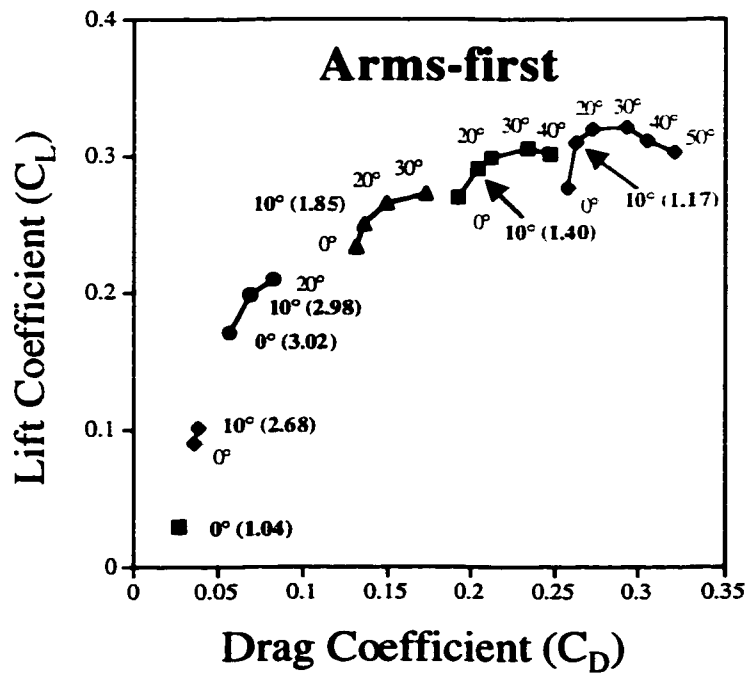
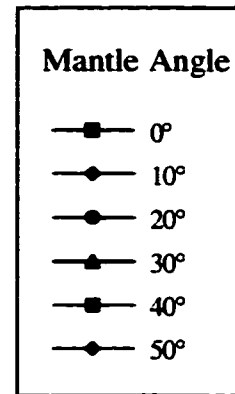
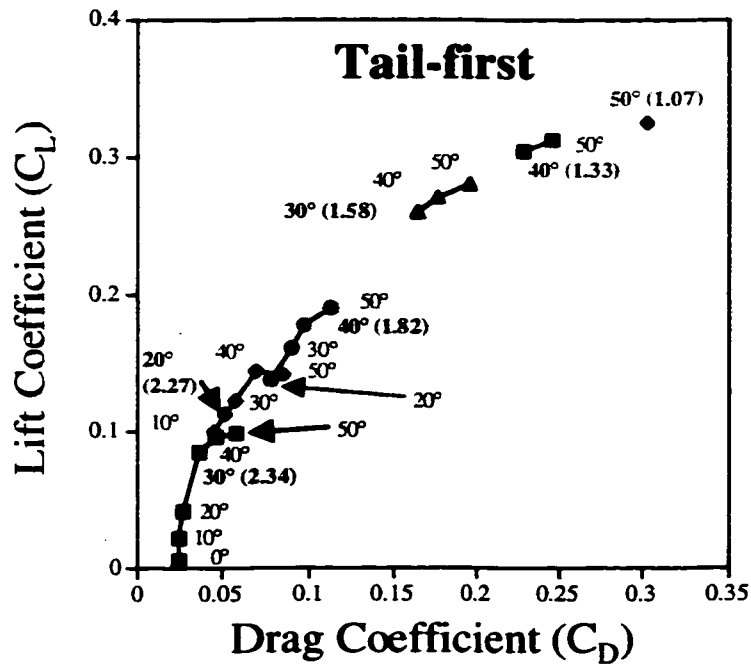


of attack of the arms occasionally were observed at higher angles than the mantle. In flow visualization experiments using models oriented arms-first, separation occurred whenever the arms were at angles of attack 10° greater than that of the mantle.

Force Measurements

A polar diagram of drag and lift coefficients calculated from squid models positioned at various angles of attack in both tail-first and arms-first orientations in a water tunnel is depicted in Figure 8. The symbols, which are displayed in the legend, represent the various mantle angles of attack, while the degree designations on the actual figures represent arm angles of attack. (Only mantle/arm angle combinations observed in video footage of swimming squid were included in the figures). For the mantle/arm angle combinations considered, the highest lift to drag ratios for tail-first swimming were detected at mantle/arm angle combinations of $0^\circ/30^\circ$ (2.34) and $10^\circ/20^\circ$ (2.27) (Figure 8). The highest lift to drag ratios for arms-first swimming were detected at mantle/arm angles of $20^\circ/0^\circ$ (3.02) and $20^\circ/10^\circ$ (2.98). Based on video footage of tail-first swimming mean mantle/arm angle combinations over all size classes for low (3 cm s^{-1}), intermediate (12 cm s^{-1}), and high (21 cm s^{-1}) speeds were $20.9^\circ/33.4^\circ$, $10.1^\circ/17.8^\circ$, and $8.7^\circ/10.7^\circ$, respectively. Lift-to-drag ratios were therefore 1.78 for low speeds, 2.27 for intermediate speeds, and 2.26 for high speeds. Based on video footage of arms-first swimming, mean mantle/arm angle combinations for low (3 cm s^{-1}) and intermediate (12 cm s^{-1}) speeds were $24.2^\circ/18.8^\circ$ and $8.8^\circ/6.3^\circ$, respectively (squid did not swim arms-first at high speeds). Lift-to-drag ratios for low and intermediate speeds were 2.18 and 2.68, respectively.

Figure 8. Polar diagrams of drag (C_D) and lift coefficients (C_L) calculated from squid models oriented tail-first and arms-first and at various angles of attack. The various symbols, which are described in the legend, represent angles of attack of the mantle. Degree markings within the figures represent angles of attack of the arms. Only mantle/arm angle combinations observed during swimming trials of brief squid are represented. At each mantle angle, the arm angle providing the highest lift/drag ratio is denoted in bold and the ratio is provided next to the angle.



Added mass coefficients calculated from force measurements collected from squid models are plotted in Figure 9. Added mass coefficients increased exponentially as the angle of attack of the mantle and arms increased, regardless of whether the models were positioned in tail-first or arms-first orientations.

Hydrodynamics

Resistive and propulsive forces acting on three squid (1.8 cm DML, 4.4 cm DML, and 7.6 cm DML) swimming tail-first and arms-first over a range of speeds are displayed in Table 4. For all three squid, buoyant weight was greater than lift and vertical jet thrust for swimming velocities $\leq 12\text{--}15\text{ cm s}^{-1}$ (see negative values in vertical force balance column of Table 4 and balance of forces in Figure 10). Fin thrust was not calculated directly, but the force imbalance between buoyant weight, lift, and vertical jet thrust may serve as a good approximation of vertical fin thrust, especially since there was little net change in height from the beginning to end of the video sequences (vertical change $< 0.9\text{ cm}$, Table 4). Based on the vertical force imbalance, the potential contribution of the fins to upward directed forces was substantial at low speeds ($3\text{--}6\text{ cm s}^{-1}$), ranging from 28.4–78.6%, but then declined as speed increased. Fin activity ceased at 12, 15, and 18 cm s^{-1} for 1.8, 4.4, and 7.6 cm DML squid, respectively, and fin use predictions were in reasonable agreement with these velocities. For example, only 3.4% of the upward directed force by the 1.8 cm DML squid was unaccounted for at 12 cm s^{-1} , when no fin activity was employed.

The acceleration reaction was clearly the dominant instantaneous horizontal force (Figure 10 and 11). Although the mean acceleration reaction over a video sequence was

Figure 9. Added mass coefficients (C_A) calculated from squid models oriented tail-first and arms-first and at various angles of attack. Mantle angles ($^\circ$) are plotted on the x-axis and arm angles are denoted using symbols. Only mantle/arm angle combinations observed during swimming trials of *L. brevis* are represented. Polynomial regressions were performed when > 4 data points were available and these results are displayed under the figure legends.

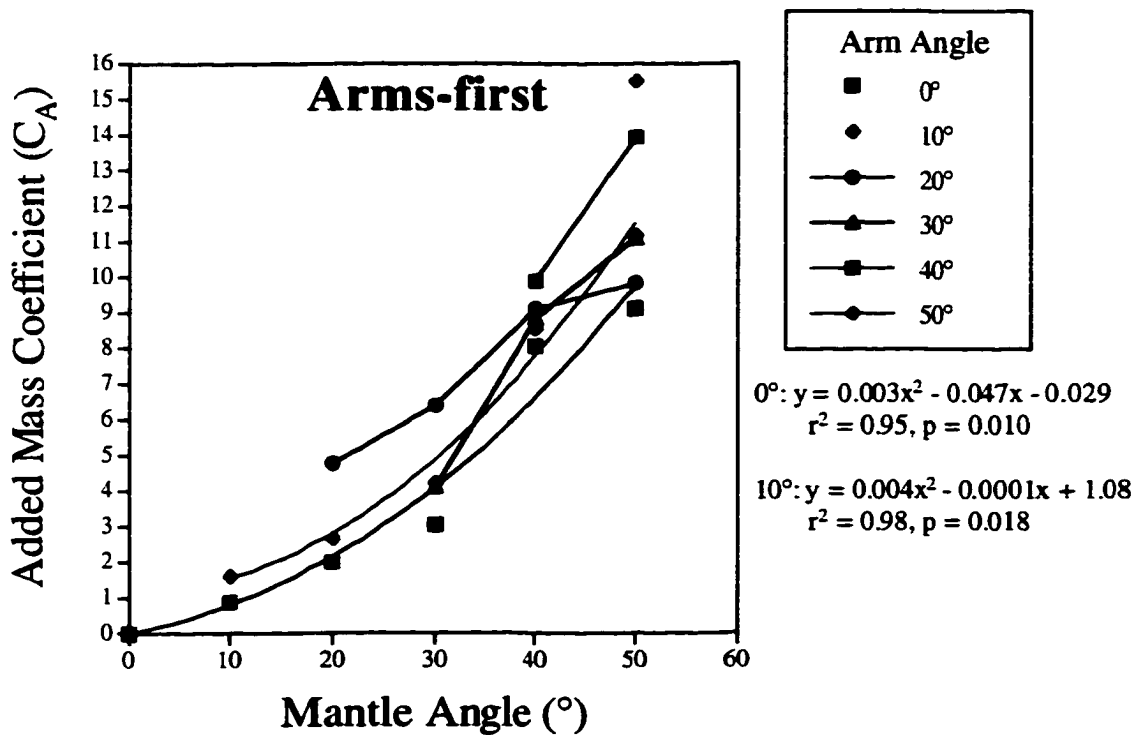
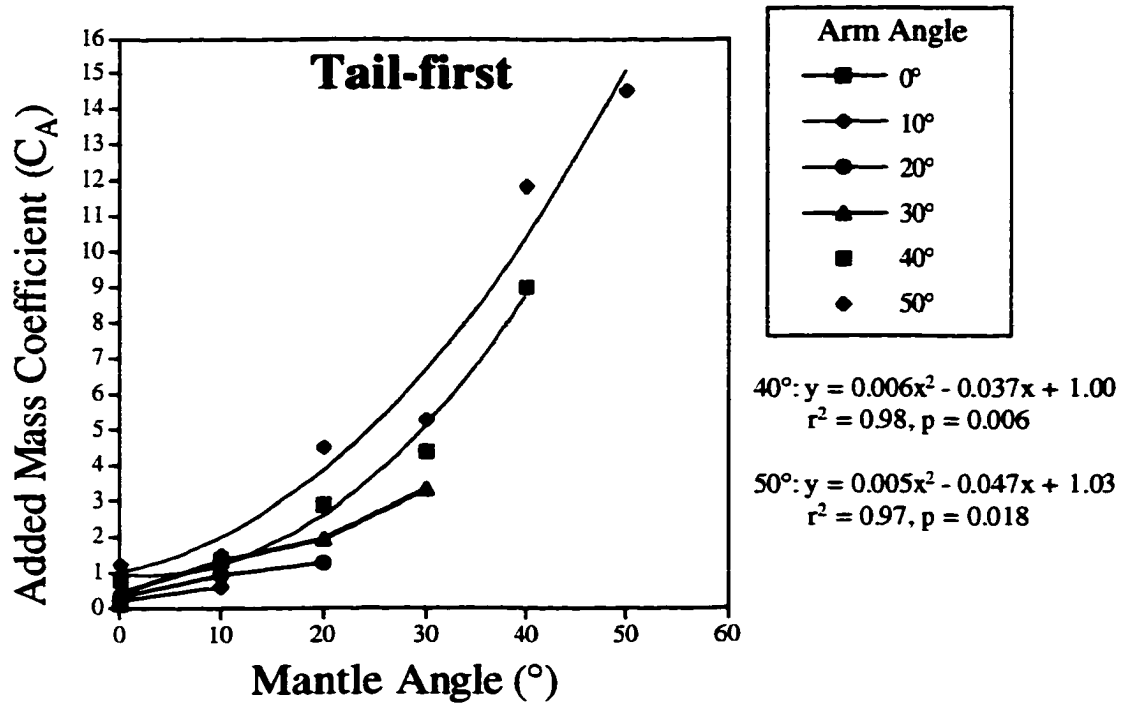


Table 4. Mean resistive and propulsive forces computed for *Lolliguncula brevis* (1.8 cm DML, 4.4 cm DML, and 7.6 cm DML) swimming in both tail-first (T) and arms-first (A) orientations over a range of speeds in a flume. In the vertical direction lift, vertical jet thrust, and vertical fin thrust must equal buoyant weight (B) at constant elevation. There was some minor net change in elevation over video sequences, which is depicted in the change of height column. In the horizontal direction drag and the refilling force should equal horizontal jet thrust and horizontal fin thrust, and the acceleration reaction should equal zero over a jet cycle. Since vertical and horizontal fin thrust were not calculated directly, negative vertical and positive horizontal force imbalances were considered potential fin thrust. Lines in the potential % fin contribution columns indicate where observed fin activity ceased. In the vertical direction, negative values represent forces acting towards the flume floor (e.g., buoyant weight), and in the horizontal direction, negative values represent forces acting counter to the direction of free stream flow (e.g., jet thrust).

Squid (cm DML)	Swimming vel. (cm/s) & orientation (T=Tail-first A=Arms-first)	Change of height (cm)	Lift (N)	Vertical jet thrust (N)	Vertical force balance (N)	Potential % contribution of fins to upward directed forces	Drag (N)	Refilling force (N)	Horizontal jet thrust (N)	Horizontal force balance (N) w/o acc. reaction	Potential % contribution of fins to horiz. thrust	Acc. reaction (N) over video sequence	% of drag associated with angle of attack
1.8	3 T	+0.408	0.0000267	0.0000393	-0.000154	70.1	0.0000128	0.00000504	-0.0000110	+0.0000068	38.2	+0.0000314	65.5
1.8	3 A	+0.104	0.0000281	0.0000411	-0.000151	68.5	0.0000121	0.00000673	-0.0000100	+0.0000088	48.9	-0.0000114	62.3
1.8	6 T	+0.0920	0.000124	0.0000339	-0.0000625	28.4	0.0000648	0.0000157	-0.0000521	+0.0000284	35.3	+0.0000264	72.8
1.8	6 A	+0.0311	0.000114	0.0000351	-0.0000708	32.2	0.0000653	0.0000132	-0.0000514	+0.0000271	34.5	+0.0000778	65.1
1.8	9 T	-0.0841	0.000134	0.0000373	-0.0000486	<u>22.9</u>	0.0000953	0.0000158	-0.0000795	+0.0000316	<u>28.4</u>	+0.000113	60.4
1.8	12 T	+0.312	0.000159	0.0000531	-0.0000757	3.4	0.000100	0.0000400	-0.000131	+0.0000093	6.6	+0.0000178	25.9
1.8	15 T	-0.915	0.000163	0.0000739	+0.0000166	-	0.000126	0.0000522	-0.000166	-0.0000102	-	-0.0000829	22.6
1.8	18 T	-0.274	0.000215	0.0000944	+0.0000884	-	0.000197	0.0000735	-0.000281	-0.00000105	-	-0.0000511	25.7
4.4	3 T	+0.034	0.000237	0.000331	-0.00221	78.6	0.000132	0.0000267	-0.000103	+0.000056	35.3	-0.000218	77.0
4.4	3 A	+0.627	0.000341	0.000366	-0.00212	75.0	0.000149	0.0000878	-0.000127	+0.000115	46.3	+0.000448	77.9
4.4	6 T	-0.312	0.000565	0.000395	-0.00184	65.7	0.000260	0.0000848	-0.000234	+0.000118	32.0	-0.00018	53.4
4.4	6 A	+0.0430	0.000576	0.000442	-0.00178	63.6	0.000245	0.0000835	-0.000206	+0.000120	36.8	-0.000758	36.2
4.4	9 T	-0.0337	0.00124	0.000460	-0.00112	39.3	0.000571	0.000131	-0.000515	+0.000180	25.6	+0.00024	52.2
4.4	9 A	+0.0540	0.00131	0.000529	-0.000962	34.3	0.000561	0.000154	-0.000500	+0.000215	30.1	-0.00159	38.2
4.4	12 T	-0.0900	0.00220	0.000500	-0.000104	3.7	0.000909	0.000227	-0.000956	+0.000174	14.9	-0.00211	46.6
4.4	12 A	+0.0825	0.00248	0.000515	+0.000194	<u>0</u>	0.000827	0.000212	-0.000781	+0.000258	<u>24.7</u>	+0.00186	36.5
4.4	15 T	+0.325	0.00237	0.000434	+0.0000215	0	0.00119	0.000287	-0.00136	+0.000113	7.6	-0.0000768	36.2
4.4	18 T	-0.188	0.00230	0.000697	+0.000863	0	0.00211	0.000327	-0.00242	+0.000017	0.7	+0.000191	41.7
4.4	21 T	+0.027	0.00299	0.000691	+0.000878	0	0.00244	0.000444	-0.00313	-0.000246	-	-0.00622	47.8
4.4	24 T	+0.866	0.00304	0.00110	+0.00414	0	0.00283	0.000463	-0.00331	-0.0000171	-	+0.000199	36.1

Squid (cm DML)	Swimming vel. (cm/s) & orientation (T=Tail-first A=Arms-first)	Change of height (cm)	Lift (N)	Vertical jet thrust (N)	Vertical force balance (N)	Potential % contribution of fins to upward directed forces	Drag (N)	Refilling force (N)	Horizontal jet thrust (N)	Horizontal force balance (N) w/o acc. reaction	Potential % contribution of fins to horiz. thrust	Acc. reaction (N) over video sequence	% of drag associated with angle of attack
7.6	3 T	-0.0893	0.000876	0.00220	-0.00789	71.9	0.000772	0.000178	-0.000461	+0.000491	51.5	-0.000232	90.2
7.6	6 T	+0.107	0.00214	0.00243	-0.00640	58.3	0.00103	0.000281	-0.000638	+0.000673	51.3	-0.000235	91.3
7.6	6 A	+0.196	0.00263	0.00265	-0.00569	51.8	0.00100	0.000300	-0.000385	+0.000717	55.1	+0.00932	63.7
7.6	9 T	-0.0780	0.00337	0.00277	-0.00483	44.0	0.00197	0.000627	-0.00158	+0.000817	25.7	+0.00333	56.8
7.6	9 A	+0.0322	0.00314	0.00261	-0.00522	47.5	0.00173	0.000722	-0.00165	+0.000773	41.1	+0.0098	61.3
7.6	12 T	+0.0174	0.00520	0.00313	-0.00264	27.5	0.00274	0.00906	-0.00242	+0.000125	34.0	-0.0000174	58.4
7.6	12 A	-0.0645	0.00507	0.00345	-0.00245	22.4	0.00281	0.000951	-0.00199	+0.000166	43.2	+0.00718	52.2
7.6	15 T	+0.787	0.00752	0.00266	-0.000789	7.2	0.00393	0.00107	-0.00332	+0.000171	13.2	-0.00046	51.9
7.6	18 T	+0.572	0.00847	0.00432	+0.00432	-	0.00434	0.00122	-0.00510	+0.000460	8.3	-	37.3
7.6	21 T	+0.328	0.01075	0.00512	+0.00512	-	0.00717	0.00059	-0.0122	+0.000874	6.7	-	38.3
7.6	24 T	+0.173	0.01223	0.00603	+0.00603	-	0.00946	0.00081	-0.0158	+0.000176	1.0	-	38.9

Figure 10. Vertical and horizontal forces acting on a 4.4 cm *Lolliguncula brevis* swimming tail-first at 6 cm s^{-1} . In the vertical forces graph, negative values represent forces acting towards the flume floor (e.g., buoyant weight), whereas in the horizontal forces graph negative values represent forces acting counter to the direction of free-stream flow (e.g., horizontal jet thrust). Since there was some net vertical change over the 2 s video sequence, height of *L. brevis* above the flume floor is displayed next to the vertical forces graph. There was no net horizontal change over the video sequence. Fin thrust contributions are not included in the figure.

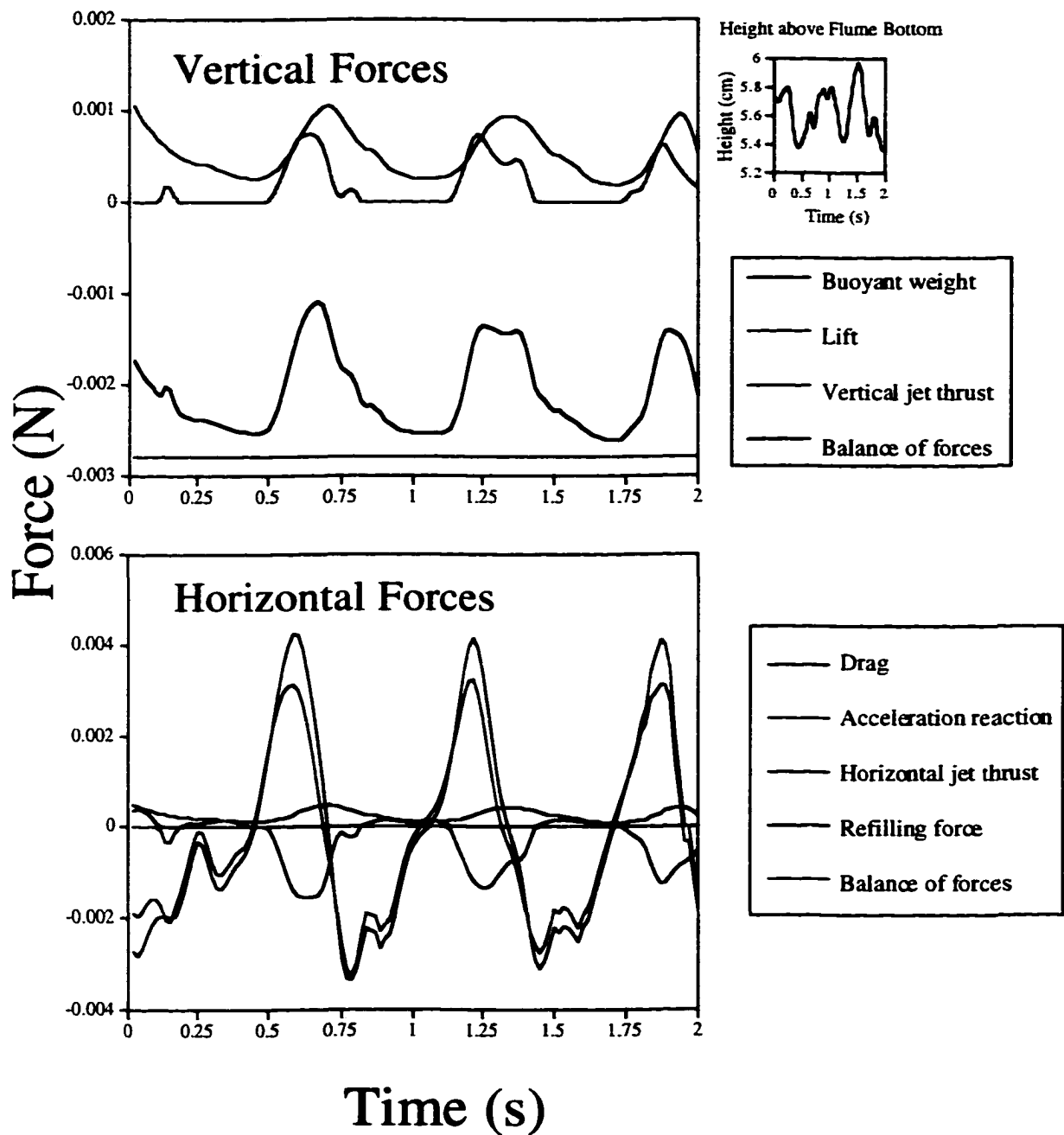
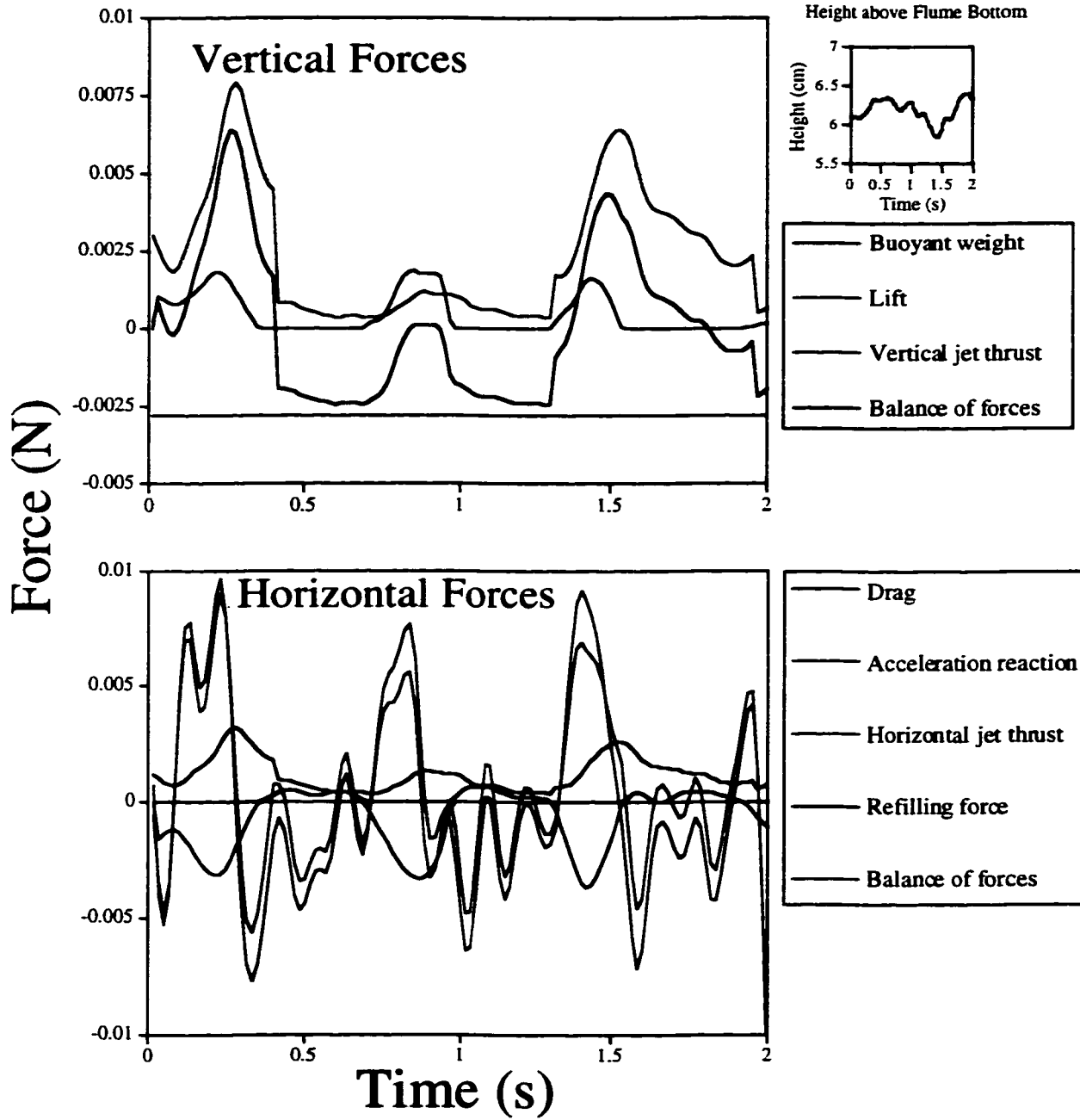


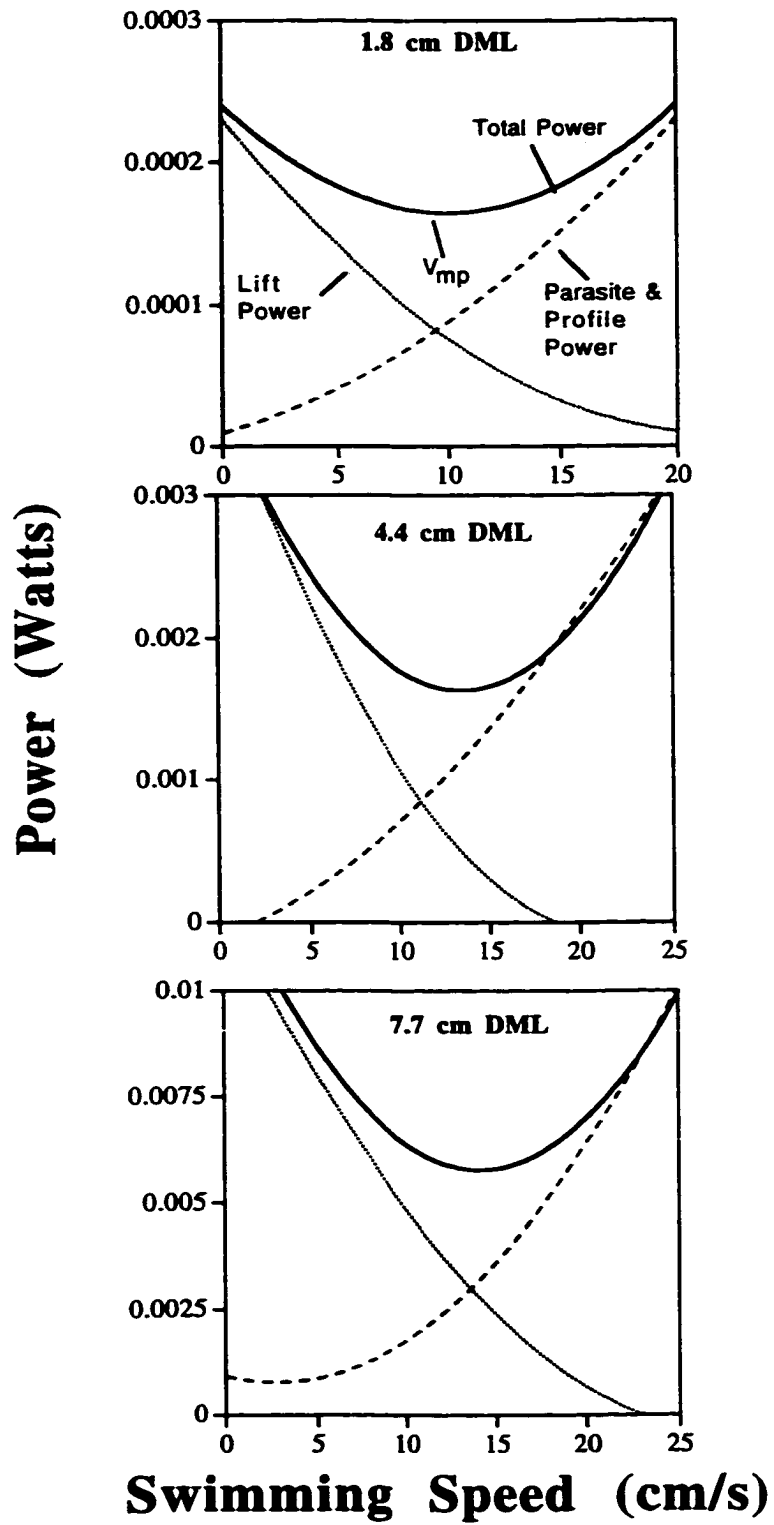
Figure 11. Vertical and horizontal forces acting on a 4.4 cm *Lolliguncula brevis* swimming tail-first at 15 cm s⁻¹. In the vertical forces graph, negative values represent forces acting towards the flume floor (e.g., buoyant weight), whereas in the horizontal forces graph negative values represent forces acting counter to the direction of free-stream flow (e.g, horizontal jet thrust). Since there was some net vertical change over the 2 s video sequence, height of *L. brevis* above the flume floor is displayed next to the vertical forces graph. There was no net horizontal change over the video sequence. Fin thrust contributions are not included in the figure.



low relative to the range of instantaneous acceleration reaction values within a series of jet cycles, mean values were nonetheless high and variable relative to the other forces (Table 4). The high variability is attributed to its sensitivity to velocity changes. Since the acceleration reaction should theoretically balance out over several jet cycles (Daniel, 1983), the horizontal force balance was calculated assuming the mean acceleration reaction was zero for the video sequence. (If actual acceleration reaction forces were included in force balance equations, they would dominate the force balance and obscure fin thrust calculations). Based on the horizontal force balance equation, fins appeared to contribute significantly to horizontal thrust, especially at low speeds (3–6 cm s⁻¹) when potential contribution of the fins to horizontal thrust ranged from 32.0–55.1% (Table 4). Although horizontal force balance equations frequently predicted fin activity for speeds when actual fin motion had ceased, thrust predictions were low ($\leq 8.3\%$) (Table 4). A significant proportion of the drag in the horizontal direction was a product of positioning the mantle and arms at angles of attack $> 0^\circ$, especially at low speeds (3–6 cm s⁻¹) when 62–91% of the drag was associated with angles of attack (Table 4).

The power required to generate vertical thrust to counteract negative buoyancy (lift power), power required to overcome horizontal resistive forces (parasite + profile power), and total power (sum of lift, parasite, and profile power) for the three squid considered in the hydrodynamic phase of this project are plotted over a range of speeds in Figure 12. A parabolic relationship between total power and speed was detected for all three squid. The speed where the rate of energy expenditure was least (V_{mp}), was approximately 10, 12, and 14 cm s⁻¹ for squid 1.8, 4.4, and 7.7 cm DML, respectively.

Figure 12. Lift (...), parasite/profile(----), and total power (—) requirements for three size classes of *Lolliguncula brevis* (1.8, 4.4, and 7.7 cm DML) swimming over a range of speeds. Lift power is the power required to maintain vertical position, parasite/profile power is the power required to overcome drag on the body, fins, and arms, and total power is the sum of lift and parasite/profile power. V_{mp} is the speed where the rate of energy expenditure is the least (Tucker, 1968).



DISCUSSION

Data from this study indicate that brief squid *Lolliguncula brevis* typically swims at low sustained swimming speeds ($U_c < 22 \text{ cm s}^{-1}$) relative to other squids measured in swim tunnels, such as *Loligo opalescens* and *Illex illecebrosus*, which swim for sustained periods at speeds as high as 50 and 85 cm s^{-1} , respectively (Webber and O'Dor, 1986; O'Dor, 1988; O'Dor and Webber, 1991). High costs associated with maintaining vertical position at low speeds and overcoming drag at high speeds within *L. brevis*' sustained speed range (0 - 22 cm s^{-1}) produced parabolic relationships between total power and swimming velocity. The observed parabolic power-speed relationships are similar in shape to *L. brevis* oxygen consumption curves plotted as a function of speed (see Chapter 2) and to power relationships recorded in birds (Pennycuik, 1968; Tucker, 1973; Greenwalt, 1975; Rayner, 1979), bees (Ellington et al., 1990), and mandarin reef fish, *Synchropus picturaus* (Blake, 1979). Like birds, bees, and mandarin reef fish, brief squid are negatively buoyant. Therefore, to maintain vertical position at low speeds in flumes, they expended considerable power flapping fins, directing high velocity water jets downward, and overcoming added profile and induced drag brought on by positioning the body and appendages at high angles of attack for lift maximization. As brief squid swam at greater speeds, however, the power required to maintain altitude declined parabolically as velocity over the fins, mantle, and arms increased and lift consequently elevated parabolically (lift scales approximately with $(\text{velocity})^2$). Overall power requirements

declined with speed until the power required to overcome drag on the body (parasite power) and fins (profile power) dominated and increased parabolically (drag also scales approximately with (velocity)²). Therefore, an intermediate speed (V_{mp}) existed where the rate of power expenditure was lowest. Over the size range considered in this study, V_{mp} was 10–15 cm s⁻¹ (1.8–5.6 mantle lengths s⁻¹) and peak Froude propulsion efficiency, which is a measure of jet efficiency, occurred at 9–12 cm s⁻¹ (1.6–2.4 mantle lengths s⁻¹). The V_{mp} range predicted from power estimates is higher than that predicted from oxygen consumption data, which tended to fall within the 0.5–1.5 mantle lengths s⁻¹ range (Chapter 2). The discrepancy may be related to the fact that unsteady mechanisms were not factored into quasi steady-state power estimates. Some potential unsteady mechanisms affecting power estimates will be discussed later in the paper.

At the low end of *L. brevis*' swimming range (< 6 cm s⁻¹), generating lift to counteract negative buoyancy is obviously an important hydrodynamic consideration. One important mechanism used by brief squid for lift generation at low speeds was elevation of mantle and arm angles of attack, which induce downward flow, enhance the pressure differential above and below the body, and increase lift (Vogel, 1994; Dickinson, 1996). Although the mantle and arms of squid do not resemble traditional human-made airfoils, lift may be generated when the mantle with attached fins and arms are positioned at high attack angles (see polar diagrams). Lift enhancement by increasing body angles of attack at low speeds also has been observed in negatively buoyant fish (He and Wardle, 1986; Webb, 1993), and body lift plays critical roles in lift generation in ski jumpers (Ward-Smith and Clements, 1982), honeybees (Nachtigall and Hanauer-Thieser, 1992), birds (Tobalske and Dial, 1996), and rays (Heine, 1992).

The trailing body section (i.e., the arms or mantle depending on swimming orientation) was frequently positioned at higher angles of attack than the leading body section. Flow visualization and lift measurement studies using squid models indicate that positioning the trailing body section at higher angles of attack than the leading body section delays flow separation (when coupled with appropriate leading body section angles) and elevates lift production during both tail-first and arms-first swimming. This is analogous to control surfaces on aircraft wings, such as ailerons, which are located on the trailing edge of the wing and positioned at higher angles of attack than the main wing to elevate lift (Kundu, 1990). Just as pilots make fine lift adjustments with ailerons, squid in the tail-first swimming mode frequently adjusted angles of attack of the arms (trailing body section) throughout the jet cycle, especially during refilling to generate extra lift when the jet was no longer producing any downward directed thrust. At low speeds the mantle and arms were positioned at high angles of attack that maximized lift but that had relatively low lift-to-drag ratios. Thus, low-speed lift generation took precedence over low-speed drag reduction. In fact, 62–91% of the drag at speeds of 3–6 cm s^{-1} was associated with elevating the angle of attack of the mantle and arms. This finding is consistent with O'Dor's (1988) hydrodynamic study on *Loligo opalescens*, where maintenance of vertical position required 66–92% of the total force at 10 cm s^{-1} , which was the lowest speed examined.

In addition to increasing the angle of attack of the mantle and arms, lift was generated by directing high velocity jets of water downward and by relying on fin activity. At 3–6 cm s^{-1} the funnel was positioned at very high angles of attack (frequently $> 50^\circ$) while swimming both tail- and arms-first, and consequently more jet thrust was

directed vertically than horizontally. This may explain the observed low Froude propulsion efficiencies at 3–6 cm s⁻¹ and the need to employ a high velocity jet to swim horizontally. The fins were very active at low speeds, and vertical force imbalances indicated that fins contribute 28.4–78.6% of the vertical thrust at 3–6 cm s⁻¹.

O'Dor (1988) estimated that the fins of *Loligo* and *Illex* contribute 38 and 25%, respectively, to overall horizontal thrust at the lowest speed considered in his swimming analyses (10 cm s⁻¹), but that fins play no role in thrust production at higher speeds (20–140 cm s⁻¹) since at these speeds, fin trailing wave speeds are less than swimming velocity. Moreover, Webber and O'Dor (1986), O'Dor (1988), and O'Dor and Webber (1991) assumed the fins of *Loligo* and *Illex* play only minor roles in lift generation and are used primarily for control and steering. For *Lolliguncula brevis*, which swims at lower sustained swimming speeds than *Loligo* and *Illex*, the fins appear to be important mechanisms both for vertical and horizontal thrust production over a broad range of sustained swimming speeds, which is significant since fin activity is more economical than the jet (Hoar et al., 1994; Vogel, 1994). In this study, fins were used over 50–95% of the sustained speed range, and could account for potentially as much as 78.6% of the total vertically directed force and 55.1% of the horizontal thrust. As mentioned above, there is probably some error in fin thrust contribution estimates. However, predictions of fin cessation using the force equation often were within a speed increment (3 cm s⁻¹) of actual observations, and even when fin activity was predicted at higher speeds than those observed in the video, predicted thrust was low ($\leq 8.3\%$). Furthermore, predicted tail-first fin thrust frequently decreased with speed and predicted arms-first fin thrust generally remained high, which is consistent with kinematic data on fin activity and

amplitude. Therefore, in the absence of direct fin thrust measurements, the force balance equations provide reasonable estimates of fin thrust.

Direct fin thrust measurements, like wing thrust measurements, are complex and require high-resolution flow visualization of wake structure (Rayner 1979; Blake, 1983a, b; Ellington 1984, Spedding et al. 1984, Dickinson and Götz, 1996), precise force measurements of the oscillating appendage (Dickinson and Götz, 1996; Lehmann and Dickinson, 1997), and/or three-dimensional kinematic footage (Lauder and Jayne, 1996; Westneat, 1996). These procedures were beyond the scope and resources of this project. Even theoretical models that require only lateral views of the fins, such as Daniel's (1988) model for fin propulsion in clearnose skates, could not be applied here because of the difficulty of separating out the effects of the fins and jet on swimming thrust. Furthermore, observations of this species shows no situations where (1) the mantle is not contracting or expanding, (2) the fins are active, and (3) there is no net change in horizontal position that could be used to estimate fin thrust, in contrast to situations observed by O'Dor (1988).

Fin activity in *Lolliguncula brevis* cannot be characterized as strictly drag- or lift-based propulsion. In conventional drag-based propulsion, the fins move along an anteroposterior axis in a "rowing" motion with the fins perpendicular to the direction of motion during the power stroke and parallel to the direction of motion during the recovery stroke. In lift-based fin propulsion, the fins move approximately parallel to a dorsoventral axis and the angle of attack of the fins is adjusted during the fin beat cycle so that positive thrust is achieved during both the upstroke and downstroke (Vogel, 1994; Lauder and Jayne, 1996; Westneat, 1996). In lateral video footage, brief squid fins

flapped in a dorsoventral axis while a travelling wave moved in an anteroposterior direction. The presence of both a fin wave and fin flap is typical of loliginids but not of ommastrephids, which use only a dorsoventral flap, or cuttlefish, which employ only an anteroposterior fin wave (Hoar et al., 1994). Interestingly, the shape of the travelling wave changed with swimming speed. At low speeds a pronounced sideways S-shaped wave was frequently present, which is more characteristic of drag-based propulsion. At higher speeds, the travelling wave more closely resembled an inverted V where the distal portion of the wave made an obtuse angle with the anteroposterior plane, which is characteristic of lift-based propulsion (Lauder and Jayne, 1996). Furthermore, at low speeds, wave progression was slightly greater than swimming speed, but at intermediate and high speeds, wave progression was less than swimming speed (even with an increase in fin wave speed with swimming velocity). Drag-based propulsion is most effective at low speeds when the fin or fin wave move backwards faster than the animal's forward progression (Westneat, 1996), while lift-based propulsion is most effective at higher speeds and when local Re of the fin are > 1000 (Blake, 1983a; Webb and Weihs, 1986; Seibel et al., 1998). Local Re computed for the fins of squid in the four size classes considered in this study are very close to the $Re = 1000$ transition, with local Re at low speeds often ≤ 1000 and local Re at intermediate/high speeds often > 1000 (Table 5). Based on shape changes of the trailing fin wave with speed, variation in travelling wave speed relative to swimming speed, and local fin Re near 1000, it is likely that squid fin movement involves both drag- and lift-based propulsive mechanisms, which also has been observed in largemouth bass pectoral fin activity (Lauder and Jayne, 1996). Since drag and lift are both products of the same circulatory mechanisms, obscuring the line

Table 5. Local Reynolds numbers calculated for fins of four size classes of *Lolliguncula brevis* swimming over a range of speeds. Chord length of the fin was used as the length parameter in Reynolds number calculations. Lines denote when fin activity ceased.

Swimming Velocity (cm s ⁻¹)	1.0 – 2.9 cm DML	3.0 – 4.9 cm DML	5.0 – 6.9 cm DML	7.0 – 8.9 cm DML
3	260	480	790	1,000
6	520	960	1,600	2,000
9	780	1,400	2,400	3,000
12	<u>1,000</u>	1,900	3,100	4,100
15	1,300	<u>2,400</u>	3,900	5,100
18	1,600	2,900	<u>4,800</u>	6,100
21	1,800	3,400	5,500	<u>7,100</u>
24	2,100	3,800	6,300	8,200
27	2,300	4,300	7,100	9,200
30	2,600	4,800	7,900	10,200

between drag and lift based mechanisms is not uncommon, especially when angles of attack are high in unsteady flows (Dickinson, 1996).

One caveat in suggesting that lift-based mechanisms occur in *Lolliguncula brevis* fin movement is that at higher speeds when lift-based propulsive mechanisms were presumably operating, fin activity and amplitude decreased and eventually ceased in the tail-first swimming mode. Reduction and termination of fin activity at higher speeds is surprising given that lift-based propulsion may still provide thrust at high speeds, even when fin wave speeds are less than swimming speed, and that fin propulsion is more efficient than the jet since it provides continuous thrust and lift throughout the fin cycle and interacts with larger volumes of water (Hoar et al., 1994; Vogel, 1994). O'Dor and Webber (1991), who assumed that only drag-based fin propulsion is operating in squid, suggested fin motion ceases when, because of limitations in shortening speeds of obliquely striated muscle in the fin muscular hydrostat, undulatory waves cannot move backwards faster than the animal moves forward. If this is true, why then is fin flapping/undulation used at all at speeds when swimming speed exceeds travelling wave speeds? O'Dor (1988) found that fin waves of *Loligo opalescens* frequently travel at speeds below swimming velocities, but suggested that thrust is still possible since finning occurs during refilling when the squid slows down. Although fin activity was sometimes observed in *L. brevis* during refilling at high speeds (when fin wave speed was less than swimming speed), fin activity was more frequently observed during mantle contractions. As mentioned above, fin activity is probably a composite of drag and lift-based propulsion and conventional rules for either mechanism probably do not apply. Termination and reduction of fin activity may very well be related to the morphology and

physiology of the fin muscular hydrostat (Kier, 1988; Kier, 1989), but because both drag- and lift-based mechanisms probably underlie fin activity and squid are capable of making behavioral adjustments throughout the jet cycle, fin activity does not simply cease when swimming speeds exceed fin wave speeds.

O'Dor (1988) reported four distinct gaits in *L. opalescens* during tail-first swimming that were related to the use of collagen springs in the mantle. In this study, some similar behavioral transitions were detected in *L. brevis* during tail-first swimming, but overall behavioral changes tended to be more gradual over the sustained speed range considered, with behavioral differences most apparent when comparing size classes. For example, O'Dor (1988) found that the amplitude of mantle expansion for *L. opalescens* was initially low at low speeds (10 cm s^{-1}), but then increased significantly and remained constant over a broad range of speeds between 20 cm s^{-1} and 40 cm s^{-1} , only to increase again at critical speeds of 50 cm s^{-1} and burst speeds of 140 cm s^{-1} . For brief squid, mantle expansion generally increased consistently with speed during tail-first swimming and did not remain constant over a broad range of speeds. One notable exception was squid in the 1.0–2.9 cm DML size class, which did not vary the amplitude of mantle expansion significantly over the entire range of swimming speeds.

During tail-first swimming, angles of attack and fin amplitude decreased linearly with speed for all size classes of brief squid, and the number of mantle contractions s^{-1} either remained constant (size classes $\geq 3 \text{ cm DML}$) or increased steadily with speed (size class $< 3 \text{ cm DML}$). O'Dor (1988) found that mantle contraction frequency of adult *L. opalescens* remains relatively constant with speed, and Webber and O'Dor (1986) found that contraction frequency of *Illex illecebrosus* increases from 28 to 48 cm s^{-1} , but that

above 48 cm s^{-1} , contraction frequency increases less or remains constant with elevated swimming speed. O'Dor (1988) reported that the fins beat twice with each mantle contraction at 10 cm s^{-1} , once during refilling over a broad range of speeds between 20 and 40 cm s^{-1} , and none at both sustained and burst speeds $> 50 \text{ cm s}^{-1}$. In this study, fin activity during tail-first swimming generally decreased linearly with swimming speeds until sub-critical speeds, at which the fins simply wrapped around the mantle. The exception again was squid within the 1.0–2.9 cm DML size class, which abruptly shifted from 2 fin beats s^{-1} at 9 cm s^{-1} to none at 12 cm s^{-1} . As mentioned above, fin flapping did sometimes coincide with refilling at intermediate speeds when fin activity was low, but fin flapping was more frequently coupled with mantle contraction at intermediate speeds. Moreover, at low speeds when fin activity was high, fin flapping was often coupled with both refilling and contraction. Finally, mantle refilling times were greater than mantle contraction times as was suggested by O'Dor (1988), but for most of the size classes, refilling did not occur progressively faster over a range of speeds. The exception was squid in the small size class (1.0–2.9 cm DML), which refilled and contracted their mantles progressively faster with swimming speed during tail-first swimming.

To swim at higher velocities, small squid ($< 3.0 \text{ cm DML}$) swimming tail-first increased contraction frequency and kept mantle expansion relatively constant, whereas squid belonging to larger classes ($\geq 3.0 \text{ cm DML}$) increased mantle expansion and kept contraction rates relatively constant. The dichotomy in swimming approaches was probably not a result of differences in relative speed ranges. Although a broader range of relative swimming speeds was considered for squid $< 3 \text{ cm DML}$ (1.25–6.37 mantle lengths s^{-1}) than squid $> 5 \text{ cm DML}$ (0.41–3.33 mantle lengths s^{-1}), squid 3.0–4.9 cm

DML were examined over a similar speed range (0.82–6.21 mantle lengths s^{-1}) to that of smaller squid, yet did not increase mantle contraction frequency with speed.

Furthermore, even within a speed range of 0–3 mantle lengths s^{-1} , mantle contraction frequency for squid < 3 cm DML increased with speed and amplitude was relatively constant.

The observed behavioral differences in swimming approaches among size classes do not appear to be related to the mantle musculature. Squid mantle tissue functions as a constant volume system with a 3-dimensional array of tightly bundled muscles commonly called a muscular-hydrostat (Kier and Smith, 1985; Smith and Kier, 1989). When circular muscles shorten during mantle contraction, they increase in diameter, causing the mantle wall to thicken. Obliquely oriented collagen fibers traversing the thickness of the mantle wall are strained and store energy at times in the jet cycle when, because of the geometry of the locomotor apparatus, the circular muscles cannot do useful hydrodynamic work (Gosline and Shadwick, 1983; Pabst, 1996). Elastic energy stored in the collagen fibers power much of the refilling phase of the jet cycle, although contraction of radially oriented muscle fibers, which extend from the inner to outer surface of the mantle, also play a role in refilling (Gosline and Shadwick, 1983; Gosline et al., 1983; Kier, 1988). The elastic spring system within the mantle is non-resonant, depending simply on the degree of loading by the circular muscles, and the system does not have to be driven at or near its natural frequency as is the case with hydromedusan jellyfish (DeMont and Gosline, 1988; Pabst, 1996). Therefore, constant rates of mantle contraction observed in larger squid are probably not products of a resonant elastic spring system. There are ontogenetic differences in the arrangement, mechanical properties, and

physiological properties of the mantle musculature of squid, especially mantle connective tissue (Thompson, 1997, 1998), but these differences contribute to reduced mantle expansion and increased muscle shortening with age (size). Therefore, these differences do not help explain the observed dichotomy in swimming strategies.

The differences in contraction rates and swimming strategies may relate to hydrodynamics. Weihs (1977) and Siekman (1963) discovered that jets pulsed at certain frequencies generate a series of toroidal vortex rings that bring additional water from surrounding areas into the jet wake. Since jet thrust is the product of the mass (per unit time) and velocity of water expelled backwards, additional water (mass) entrained by the toroidal vortices may elevate thrust by as much as 60% when compared with a steady jet (Weihs, 1977). In evaluating the benefits of toroidal induction in medusae, Daniel (1983) made the assumption that vortex rings were thin relative to the jet core and that ring to jet core radius ratios (b/e) were ~ 5.37 . Given this assumption and a calculated ring spacing to ring radii ratio (a/b) of 10, Daniel (1983) concluded that there was no thrust augmentation. Flow visualization of torus formation in the jet wake of brief squid revealed that each torus does not simply form a thin disk as is the case with medusae, but rather each torus typically rolls into a spherical vortex, which also has been reported for salps (Madin, 1990). Based on measurements recorded for brief squid, the relationship between a/b and F_p/F_s (ratio of thrust from pulsed jet to thrust from a steady jet) most closely resembles curve 2 in Figure 1c of Weihs (1977), suggesting that brief squid (6.2 ± 0.15 (SD) cm DML) with a/b ratios of 7.39 ± 3.34 (SD) experience a 30% thrust augmentation from a pulsed jet. Curve 2 is rather flat over a broad range of a/b ratios, and thus 30% thrust augmentation may be maintained even if spacing between rings

increases with speed. Thus, increasing mantle contraction rate (to keep ring spacing low) with speed is not critical for intermediate/large squid to maintain thrust augmentation, allowing for the selection of more cost-effective mechanisms for increasing thrust with speed, such as increasing expelled water volume. Elevating expelled water volume is advantageous because energy expenditure is proportional to $1/2 \text{ mass} * (\text{velocity})^2$, and thus it is more energetically efficient to increase the mass (volume) of water expelled backwards than the velocity (rate) of mantle contraction or velocity of expelled water. Even though ring spacing will increase with speed when contraction frequencies are kept constant, resulting in the elevation of a/b ratios, the rate of increase in a/b will be mitigated somewhat by larger spherical vortices and ring radii, which result from expelling large volumes of water.

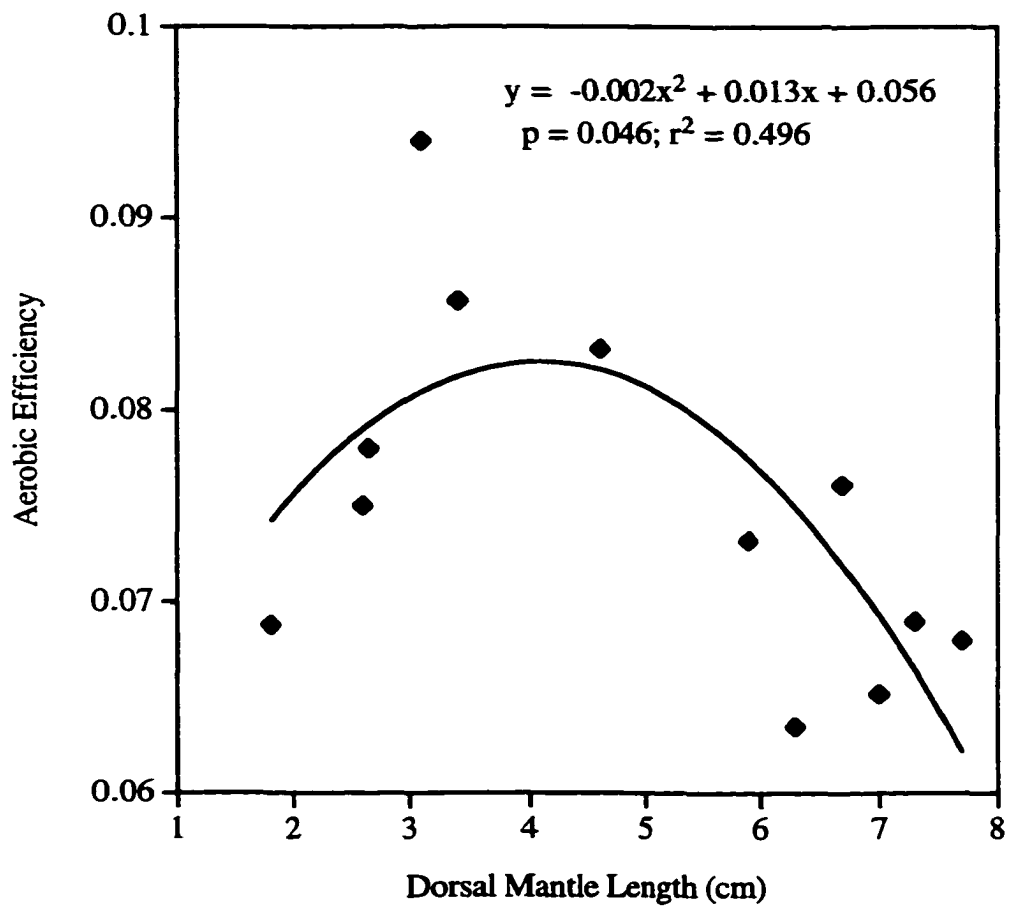
No visualization of toroidal vortices was performed on small squid (squid < 3.0 cm DML). However, smaller squid with large relative mantle orifices and high contraction frequencies have considerably lower a/b ratios, placing them on a steeper portion of curve 2, where thrust augmentation is much greater. To stay within a high thrust augmentation range (50–60%), smaller squid may increase contraction rates with speed to keep a/b low. Increasing contraction rates rather than mantle volume has a more direct effect on a/b (Madin, 1990), which is more critical on the steep portion of the curve than the flat portion where larger squid fall. The disadvantage of increasing frequency rather than water volume is higher energetic requirements, but thrust augmentation may outweigh added energetic costs.

A useful measure of swimming performance is aerobic efficiency (η_a), which is power output, i.e., the power required to move an animal forward through the water and

maintain altitude, divided by aerobically supplied power input, i.e., active metabolic rate, which is the potential power available to perform work (Fish 1993, 1996). Using the hydrodynamic measurements of this study to calculate power output and oxygen consumption data from Chapter 2 to calculate power input, squid falling within the 3–5 cm DML range were the most efficient (Figure 13). This suggests that maximizing thrust augmentation for small squid (< 3 cm DML) does not necessarily lead to greater swimming performance, but rather a compromise between maximizing thrust augmentation and minimizing overall energetic costs is most advantageous for *Lolliguncula brevis*. Within the Chesapeake Bay where competition between fish and squid is particularly fierce, *L. brevis* often leave the Bay when they are > 6 cm DML and only return to spawn (Chapter 1). This may be because larger squid (> 6 cm DML), which have the lowest aerobic efficiency and a more restricted relative speed range (0.4–3.0 mantle lengths s^{-1}), are less competitive with fish. This is consistent with O’Dor and Webber’s (1986b) suggestion that smaller jet-propelled squid are most competitive with undulatory fishes.

Greater preference for arms-first swimming at low speeds in swim tunnels followed by a transition to exclusive tail-first swimming at intermediate and high speeds suggests that there may be velocity-specific advantages associated with each swimming mode. Tail-first swimming is probably more preferable at high speeds because the funnel does not need to bend to generate the necessary horizontal thrust. In arms-first swimming, the funnel must curve approximately 180° to direct thrust rearwards in a horizontal path, and lateral video views of the funnel indicate that some funnel

Figure 13. Aerobic efficiency (η_a), which is the power required to move an animal through the water (i.e., total power required to overcome drag, acceleration reaction, and generate lift) divided by aerobically supplied power input (i.e., active metabolic rate), versus mantle length for *Lolliguncula brevis*. Power required to overcome drag, acceleration reaction, and generate lift was computed using force data and kinematic measurements from this study. Active metabolic rates were calculated using oxygen consumption values and/or scaling relationships in Chapter 2. Oxygen consumption values of brief squid swimming at 1.5 mantle lengths s^{-1} were used in calculations.



constriction is concomitant with significant curvature. This constriction in the funnel significantly lowers expelled water volume flux (J) since J is proportional to the fourth power of funnel radius (r) ($J = (\pi r^4 / 8 \mu) (\Delta p / l)$), where μ is dynamic viscosity of water and $(\Delta p / l)$ is the pressure gradient (Denny, 1993). Therefore, water must be expelled at high velocity to produce thrust comparable to that generated by a non-constricted funnel, leading to lower Froude propulsion efficiencies for arms-first swimming, as was observed in this study. Since $E = 1/2 m v^2$ and energy requirements scale with the square of expelled water velocity, swimming arms-first at high speeds is energetically costly. In *L. brevis* funnel constriction during arms-first swimming is presumably most deleterious during the early portion of mantle contraction when the funnel expands to maximal diameter. During the remainder of the contraction cycle, *L. brevis* purposely restricts funnel diameter probably to keep expelled jet velocity constant and maximize power output from a given volume change (at the expense of high energetic costs). O'Dor (1988) detected similar dynamic control of the funnel in *Loligo opalescens* and suggested that squid may regulate funnel orifice diameter in relation to acceleration to optimize thrust and power, while minimizing accompanying energetic costs as much as possible. During high-speed, tail-first cruising the fins may be used for forward attitude control, steering, and lift generation, while the trailing arms, especially the third arms with heavy keels that are often spread out to act as high aspect ratio airfoils, may serve to stabilize the body, adjust pitch, and make lift adjustments (as was observed during mantle refilling). During arms-first swimming the arms, which are located at the leading edge, collapse into a conical arrangement and play less of a role in stabilization and lift adjustment.

There are benefits to arms-first swimming as well, especially at low speeds. Arms-first swimming allows for greater observance of forward surroundings than tail-first swimming, since the eyes are located more anteriorly and the arms may be moved if necessary for clearer forward views. Because prey strikes occur in an arms-first orientation (Hanlon and Messenger, 1996; Kier and van Leeuwen, 1997), arms-first swimming enables swift prey attacks whenever opportunities arise, while tail-first swimming requires rotation to arms-first swimming prior to attack. Arms-first swimming is also beneficial for deimatic posturing during sudden encounters with predators (Hanlon and Messenger, 1996). While swimming arms-first, the fins are located near the trailing edge, which reduces interaction between the fin wake and the body, and this consequently enhances fin propulsion and efficiency (Lighthill and Blake, 1990; Daniel et al., 1992).

As mentioned earlier, maximizing fin propulsion and efficiency is advantageous since, unlike jet propulsion, fin locomotion provides continuous lift and thrust throughout the fin cycle and affects relatively large volumes of water with each fin stroke. Optimal fin placement, high fin thrust efficiency, and volume flux limitations associated with funnel bending and jetting all contributed to greater reliance on fin propulsion and less on jetting during arms-first swimming. In fact, neither fin-beat frequency nor fin amplitude decreased appreciably with speed during arms-first swimming as was observed in tail-first swimming, despite the fact that swimming speeds exceeded fin wave speeds at higher velocities. (This is further evidence that drag-based propulsion is not necessarily the only mechanism underlying fin motion in *L. brevis*). The degree of funnel bending and volume flux limitations during arms-first swimming were reduced by positioning the

funnel at high angles of attack (funnel angles of attack were 15° greater during arms-first swimming compared with tail-first swimming) and relying on the jet more for vertical than horizontal thrust. Since less dynamic lift from flow over the body was required when the funnel was positioned at high angles of attack during arms-first swimming, composite mantle/arm angles of attack were lowered (6° relative to tail-first swimming) and lift-to drag ratios increased as profile drag and induced drag were reduced by the change of angle of attack. Most of the adjustment in angle of attack was achieved by lowering arm attack angles and not mantle attack angles.

No consistent increase in mantle contraction frequency, mantle diameter, fin activity, fin amplitude, fin speed, or fin downstroke time with increased speed was observed during arms-first swimming. Where then does extra thrust come from to power locomotion at higher speeds? Unlike tail-first swimming no one dominant mechanism was responsible for thrust elevation. An examination of the three squid considered in the force balance equations revealed that jet thrust did increase with speed but that the mechanism(s) responsible for this increase varied among squid and with speed. Jet thrust elevation was achieved due to one or more of the following: (1) higher mantle contraction frequency, (2) greater mantle expansion, (3) lower funnel angles of attack. High variability in the mechanism(s) selected to achieve greater jet thrust coupled with limited arms-first data (a more restricted size range was considered during arms-first swimming than tail-first swimming) made it difficult to detect consistent behavioral mechanisms for jet thrust enhancement. Furthermore, even though fin speed, frequency, and amplitude did not increase with speed, some additional horizontal thrust may be provided by keeping fin frequency and amplitude high, lowering the angle of attack of the mantle to

which the fins are attached, and positioning the fins at various angles of attack to maximize lift-based propulsion.

Since squid rely on a pulsating jet for propulsion, they swim in an unsteady fashion, constantly accelerating and decelerating as they move through the water, and experience a force known as the acceleration reaction, which resists changes in the animal's velocity (Batchelor, 1967; Webb, 1979; Daniel, 1983, 1984, 1985; Vogel, 1994). In his work with jetting medusae, Daniel (1983, 1984) found that the acceleration reaction is an important *instantaneous* force, often far outweighing drag at a given point in the jet cycle, but that the relative contribution of the acceleration reaction *averaged* over a jet cycle is much less. When starting from rest, the relative importance of the acceleration reaction in resisting movement averaged over a jet cycle is about 50%, but after several jet cycles the acceleration reaction contributes < 5% of resistance. This is because the acceleration reaction resists both acceleration and deceleration and consequently changes direction during the cycle. During steady swimming mean acceleration and deceleration should balance out over a cycle or else the organism would increase or decrease velocity, respectively. Therefore, the net acceleration reaction over the cycle should approach zero. As was the case with Daniel's (1983, 1984) work with swimming medusae, the acceleration reaction of *L. brevis* was the most important instantaneous force during the jet cycle and relative contributions of the acceleration reaction averaged over a cycle were much less than instantaneous contributions. Because increasing angles of attack of both the mantle and the arms elevated added mass coefficients substantially, the instantaneous contribution of the acceleration reaction was even greater relative to instantaneous drag (and lift) in the present study than reported by

Daniel (1983, 1984), where medusae swam in a horizontal orientation. Furthermore, the net acceleration reaction did not approach zero over several jet cycles as predicted by Daniel (1983, 1984), especially as speed and the range of accelerations and decelerations increased. This is not surprising given that measurement errors are often magnified when taking the second derivative of positional changes to compute acceleration.

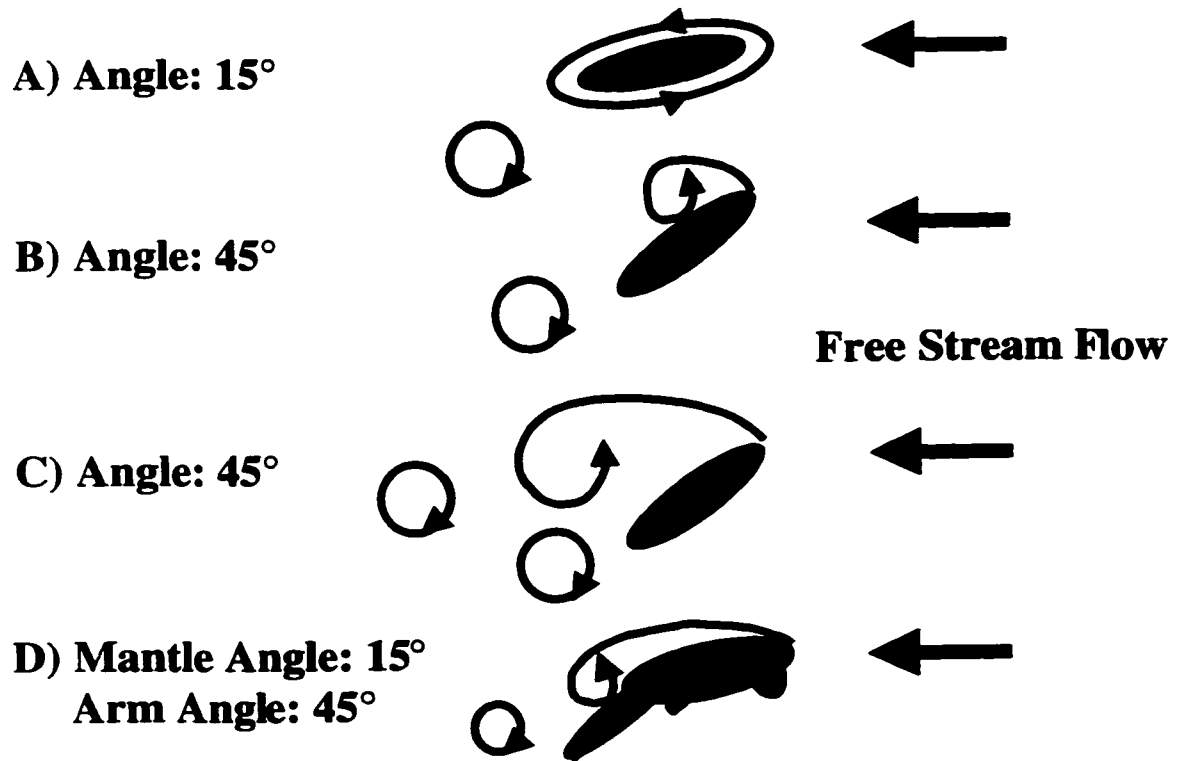
Unsteady aspects of flow likely impact other aspects of thrust and lift production in *L. brevis*. As discussed above, jets pulsed at certain frequencies have advantages over continuous, steady jets. Using 3-D kinematic data, bio- and hydro-mechanical modeling, and/or electromyography, Daniel (1988) Lauder and Jayne (1996), and Westneat (1996) offered evidence that the acceleration reaction provides propulsive thrust during fin motion in fishes both during dorsoventral flapping and anteroposterior rowing. Dickinson and Götz (1996), using sensitive force measurement and flow visualization equipment, demonstrated that unsteady movements in insect wings dramatically elevate lift and thrust. Given that flow around squid fins is unsteady as a result of pulsatile swimming and fin velocity changes during upstrokes and downstrokes, unsteady flow effects assuredly affect fin vertical and horizontal thrust, though the effects were not examined directly in this study.

Until now, the role of the arms in squid swimming has been largely ignored. As discussed above, orienting the arms at different angles of attack during tail- and arms-first swimming affects drag and lift. Unsteady aspects of flow over the arms may also enhance lift. When a *biofoil*—a generic biological device that creates forces via circulatory mechanisms—is oriented at low angles of attack to oncoming flow, circulation forms and remains bound around the biofoil (Figure 14). However, at high

Figure 14. Diagram of vortex formation around biofoils at various angles of attack.

A) At low angles of attack circulation remains bound to a biofoil. B) At higher angles of attack circulation no longer remains bound, but rather an attached vortex forms above the biofoil. This attached vortex affects the pressure distribution around the biofoil such that significantly greater lift may be generated relative to that provided by bound circulation. C) After a short period of time, the attached vortex is shed and stall occurs in steady flow systems. D) In squid, flow likely remains bound to the mantle, which seldom is positioned at high angles of attack, and an attached vortex may form above the arms, which are positioned at high angles of attack. Unsteady flow around squid produced by either jetting or arm oscillation may stabilize the attached vortex and possibly prevent or delay shedding.

Attached Vortex Formation



angles of attack, circulation does not remain bound, but rather forms an attached vortex on the leading edge of the biofoil (see Figure 14). Because of the effects of this vortex on the pressure distribution around the biofoil, significantly greater lift is generated relative to that provided by bound circulation (Dickinson and Götz, 1993). As Dickinson (1996) points out this benefit is short-lived in steady situations because stall soon ensues as the attached vortex is shed from the biofoil. However, in unsteady situations when translation distances and times are short between speed changes (e.g., pulsed jet propulsion), attached vortices may be retained by velocity changes and stall may be delayed and/or eliminated. Attached vortices may form and be retained above the arms in *L. brevis*. When in the tail-first swimming mode, the mantle is positioned at angles of attack below which stall occurs, allowing flow to follow along the mantle. When flow approaches the arms, which are positioned at higher angles of attack, an attached vortex may form and provide beneficial lift augmentation (Figure 14). As the squid decelerates during the refilling phase of the jet cycle, the attached vortex may stay on the body and either remain there or be replaced by a new leading edge bubble during the next acceleration. Unsteady jetting may not be the only mechanism to retain attached vortices. Significant arm oscillation was observed in *L. brevis* throughout the jet cycle, and these movements may help generate, stabilize, and retain attached vortices, as oscillating wings in insects do to provide thrust and lift enhancement (Dickinson and Götz, 1993). If attached vortices are used in squid locomotion, lift and thrust forces will increase, which will affect present power estimates calculated using quasi steady-state equations and possibly alter the V_{mp} range.

The data presented above provide an overview of swimming behaviors and mechanics of a slow-swimming squid, *Lolliguncula brevis*, over a range of sizes, speeds, and at various swimming orientations. Based on the results of this study, *L. brevis* clearly uses complex interactions between the mantle, fins, arms, and funnel during locomotion. Given that the interactive behaviors occur under unsteady flow, it is of great interest to determine next what impact these behaviors have on the surrounding fluid medium. A powerful tool in the quest to understand wake structure in unsteady flow is particle image velocimetry (PIV), which is just beginning to be used to examine biological aquatic locomotion (Stamhuis and Videler, 1995; Muller et al., 1997). When wake features around fins, arms, the mantle, and funnel are understood, we may then begin to form explicit links between kinematics, force production, and fluid mechanics, which will be critical in understanding squid locomotion.

LITERATURE CITED

- Batchelor, G. K. 1967. *An Introduction to Fluid Dynamics*. London: Cambridge University Press.
- Blake, R. W. 1979. The energetics of hovering in the mandarin fish (*Synchiropus picturatus*). *J. Exp. Biol.* 82: 25-33.
- Blake, R. W. 1983a. *Fish locomotion*. London: Cambridge University Press.
- Blake, R. W. 1983b. Median and paired fin propulsion. In *Fish Biomechanics* (ed. P. W. Webb and D. Weihs), pp. 214-247. New York: Praeger Publishers.
- Brett, J. R. 1964. The respiratory metabolism and swimming performance of young sockeye salmon. *J. Fish. Res. Bd. Can.* 21: 1183-1226.
- Chamberlain, J. A., Jr. 1976. Flow patterns and drag coefficients of cephalopod shells. *Palaeontology (Lond.)* 19: 539-563.
- Chamberlain, J. A., Jr. 1980. The role of body extension in cephalopod locomotion. *Palaeontology (Lond.)* 23: 445-461.
- Chamberlain, J. A., Jr. 1981. Hydromechanical design of fossil cephalopods. *Syst. Assoc. Spec.*, 18: 289-336.
- Chamberlain, J. A., Jr. 1990. Jet propulsion of *Nautilus*: a surviving example of early Paleozoic cephalopod locomotor design. *Can. J. Zool.* 68: 806-814.
- Chamberlain, J.A. and G.E. Westerman. 1976. Hydrodynamic properties of cephalopod shell ornament. *Paleobiology(Lond.)* 2: 316-331.
- Cheng, J-Y., I. G. Davison, and M. E. DeMont. 1996. Dynamics and energetics of scallop locomotion. *J. Exp. Biol.* 199: 1931-1946.
- Cheng, J-Y., and M. E. DeMont. 1966. Hydrodynamics of scallop locomotion: unsteady forces on clapping shells. *J. Fluid Mech.* 317: 73-90.

- Dadswell, M. J. and D. Weihs. 1990. Size-related hydrodynamic characteristics of the giant scallop *Placopecten magellanicus* (Bivalvia: Pectinidae). *Can J. Zool.* 68: 778-785.
- Daniel, T. L. 1983. Mechanics and energetics of medusan jet propulsion. *Can. J. Zool.* 61: 1406-1420.
- Daniel, T. L. 1984. Unsteady aspects of aquatic locomotion. *Amer. Zool.* 24: 121-134
- Daniel, T. L. 1985. Cost of locomotion: Unsteady medusan swimming. *J. Exp. Biol.*, 119: 149-164.
- Daniel, T. L. 1988. Forward flapping flight from flexible fins. *Can. J. Zool.* 66: 630-638.
- Daniel, T., C. Jordan, and D. Grunbaum. 1992. Hydromechanics of swimming. In *Advances in Comparative and Environmental Physiology*, vol 11 (ed. R. M. Alexander), pp. 17-49. Berlin: Springer-Verlag.
- DeMont, M. E. and J. M. Gosline. 1988. Mechanics of jet propulsion in the hydromedusan jellyfish *Polyorchis penicillatus*. II. Energetics of the jet cycle. *J. Exp. Biol.* 134: 333-345.
- Denny, M. W. 1993. *Air and Water: The Biology and Physics of Life's Media*. Princeton: Princeton University Press.
- Dickinson, M. H. 1996. Unsteady mechanisms of force generation in aquatic and aerial locomotion. *Amer. Zool.* 36: 537-554.
- Dickinson, M. H. and K. G. Götz. 1996. The wake dynamics and flight forces of the fruit fly *Drosophila melanogaster*. *J. Exp. Biol.* 199: 2085-2104.
- Ellington, C. P. 1984. The aerodynamics of insect flight. (I-IV). *Phil. Trans. R. Soc. Lond. B.* 305: 1-181.
- Ellington, C. P., K. I. Mackin, and T. M. Casey. 1990. Oxygen consumption of bumblebees in forward flight. *Nature* 347: 472-473.
- Finke, E. H., H. O. Pörtner, P. G. Lee, and D. M. Webber. 1996. Squid (*Lolliguncula brevis*) life in shallow waters: oxygen limitation of metabolism and swimming performance. *J. Exp. Biol.* 199: 911-921.
- Fish, F. E. 1987. Kinematics and power output of jet propulsion by the frogfish genus *Anternnarius* (Lophiiformes: Anternnariidae). *Copeia* 1987: 1046-1048.

- Fish, F. E. 1993. Power output and propulsive efficiency of swimming bottlenose dolphins (*Tursiops truncatus*). *J. Exp. Biol.* 185: 179-193.
- Fish, F. E. 1996. Transitions from drag-based to lift-based propulsion in mammalian swimming. *Amer. Zool.* 36: 628-641.
- Greenwalt, C. H. 1975. The flight of birds. *Trans. Am. Phil. Soc.* 65: 1-67.
- Gosline, J. M. and R. E. Shadwick. 1983. The role of elastic energy storage mechanisms in swimming: an analysis of mantle elasticity in escape jetting in the squid, *Loligo opalescens*. *Can. J. Zool.* 61: 1421-1431.
- Gosline, J.M., J. D. Steeves, A. D. Harman, and M. E. DeMont. 1983. Patterns of circular and radial mantle activity in respiration and jetting in the squid *Loligo opalescens*. *J. Exp. Biol.* 104: 97-109.
- Hamming, R. W. 1983. *Digital Filters*. Englewood Cliffs: Prentice-Hall.
- Hanlon, R. T., R. F. Hixon, and W. H. Hulet. 1983. Survival, growth, and behavior of the loliginid squids *Loligo plei*, *Loligo pealei*, and *Lolliguncula brevis* (Mollusca: Cephalopoda) in closed sea water systems. *Biol. Bull.* 165: 637-685.
- Hanlon, R. T. and J. B. Messenger. 1996. *Cephalopod Behaviour*. Cambridge: Cambridge University Press.
- He, P. and Wardle, C. S. 1986. Tilting behavior of the Atlantic mackerel, *Scomber scombrus*, at low swimming speeds. *J. Fish Biol.* 29: 223-232.
- Heine, C. 1992. Mechanics of flapping fin locomotion in the cownose ray, *Rhinoptera bonasus* (Elasmobranchii: Myliobatidae). Ph. D. dissertation, Duke University, Durham, NC, 286 p.
- Hendrix, J. P., Jr., W. H. Hulet, and M. J. Greenberg. 1981. Salinity tolerances and the responses to hypoosmotic stress of the bay squid *Lolliguncula brevis*, a euryhaline cephalopod mollusc. *J. Comp. Biochem. Physiol.* 69A: 641-648.
- Hixon, R. F. 1980. Growth, reproductive biology, distribution and abundance of three species of loliginid squid (Myopsida, Cephalopoda) in the northwest Gulf of Mexico. Coral Gables: Ph.D. dissertation, University of Miami, Miami, FL, 182 p.
- Hixon, R. F. 1983. *Loligo opalescens*. In *Cephalopod Life Cycles, Vol I: Species Accounts* (ed. P.R. Boyle), pp. 95-114. London: Academic Press.

- Hoar, J. A., E. Sim, D. M. Webber, and R. K. O'Dor. 1994. The role of fins in the competition between squid and fish. In *Mechanics and Physiology of Animal Swimming* (ed. L. Maddock, Q. Bone, and J. M. V. Rayner), pp. 27-33. Cambridge: Cambridge University Press.
- Holland, C. H. 1987. The nautiloid cephalopods: a strange success. *J. Geol. Soc. (Lond.)* 144: 1-15.
- Johnson, W., P. D. Soden, and E. R. Trueman. 1972. A study in jet propulsion: an analysis of the motion of the squid, *Loligo vulgaris*. *J. Exp. Biol.* 56: 155-165.
- Kier, W. M. 1988. The arrangement and function of molluscan muscle. In *The Mollusca, Form and Function*, vol. 11 (ed. Trueman, E. R., and M. R. Clarke), pp. 211-252. New York: Academic Press.
- Kier, W. M. and K. K. Smith. 1985. Tongues, tentacles and trunks: the biomechanics of movement in muscular hydrostats. *Zool. J. Linn. Soc.* 83: 307-324.
- Kier, W. M. 1989. The fin musculature of cuttlefish and squid (Mollusca, Cephalopoda): morphology and mechanics. *J. Zool. Lond.* 217: 23-38.
- Kier, W. M. and J. L. van Leeuwen. 1997. A kinematic analysis of tentacle extension in the squid *Loligo pealei*. *J. Exp. Biol.* 200: 41-53.
- Kundu, P. K. 1990. *Fluid Mechanics*. San Diego: Academic Press.
- Lauder, G. V. and B. C. Jayne. 1996. Pectoral fin locomotion in fishes: testing drag-based models using three-dimensional kinematics. *Amer. Zool.* 36: 567-581.
- Lehmann, F-O. and M. H. Dickinson. 1997. The changes in power requirements and muscle efficiency during elevated force production in the fruit fly, *Drosophila melanogaster*. *J. Exp. Biol.* 200: 1133-1134.
- Lighthill, M. J. and R. W. Blake. 1990. Biofluidynamics of balistiform and gymnotiform locomotion. Part 1. Biological background, and analysis by elongated body theory. *J. Fluid Mech.* 212: 183-207.
- Madin, L. P. 1990. Aspects of jet propulsion in salps. *Can. J. Zool.* 68: 765-777.
- Mangum, C. P. 1991. Salt sensitivity of the hemocyanin of eury- and stenohaline squids. *Comp. Biochem. Physiol.* 19A: 159-161.
- Messenger, J. B., M. Nixon, and K. P. Ryan. 1985. Magnesium chloride as an anaesthetic for cephalopods. *Comp. Biochem. Physiol.* 82C: 203-205.

- Millward, A. and M. A. Whyte. 1992. The hydrodynamic characteristics of six scallops of the Super Family Pectinacea, Class Bivalvia. *J. Zool. (Lond.)* 227: 547-566.
- Müller, U. K., B. L. E. van den Heuvel, E. J. Stamhuis, and J. J. Videler. 1997. Fish footprints: morphology and energetics of the wake behind a continuously swimming mullet (*Chelon Labrosus* Risso). *J. Exp. Biol.* 200: 2893-2906.
- Nachtigall, W., and U. Hanauer-Thieser. 1992. Flight of the honeybee. V. Drag and lift coefficients of the bee's body: implications for flight dynamics. *J. Comp. Physiol. B* 162: 267-77.
- O'Dor, R. K. 1982. Respiratory metabolism and swimming performance of the squid, *Loligo opalescens*. *Can. J. Fish. Aquat. Sci.* 39: 580-587.
- O'Dor, R. K. 1983. *Illex illecebrosus*. In *Cephalopod Life Cycles. Vol. 1: Species Accounts* (ed. P. R. Boyle), pp. 95-114. New York: Academic Press.
- O'Dor, R. K. 1988. Forces acting on swimming squid. *J. Exp. Biol.* 137: 421-42.
- O'Dor, R. K., N. Balch, E. A. Foy, and P. L. Helm. 1985. The locomotion and energetics of hatchling squid, *Illex illecebrosus*. *Am. Malacol. Bull.* 4: 55-60.
- O'Dor, R. K., J. A. Hoar, D. M. Webber, F. G. Carey, S. Tanaka, H. R. Martins, and F. M. Porteiro. 1994. Squid (*Loligo forbesi*) performance and metabolic rates in nature. *Mar. Fresh. Behav. Physiol.* 25: 163-177.
- O'Dor, R. K. and D. M. Webber. 1986a. Monitoring the metabolic rate and activity of free-swimming squid with telemetered jet pressure. *J. Exp. Biol.* 126: 205-224.
- O'Dor, R. K. and D. M. Webber. 1986b. The constraints on cephalopods: why squid aren't fish. *Can. J. Zool.* 64: 1591-1605.
- O'Dor, R. K. and D. M. Webber. 1991. Invertebrate athletes: tradeoffs between transport efficiency and power density in cephalopod evolution. *J. Exp. Biol.* 160: 93-112.
- O'Dor, R. K., J. Wells, and M. J. Wells. 1990. Speed, jet pressure and oxygen consumption relationships in free-swimming *Nautilus*. *J. Exp. Biol.* 154: 383-396.
- Orth, R. J., M. W. Luckenbach, and K. A. Moore. 1994. Seed dispersal in a marine macrophyte: implications for colonization and restoration. *Ecology* 75: 1927-1939.

- Pabst, D. A. 1996. Springs in swimming animals. *Amer. Zool.* 36: 723-735.
- Patterson, M. R. 1984. Patterns of whole colony prey capture in the octocoral, *Alcyonium siderium*. *Biol. Bull.* 167: 613-629.
- Pennycuick, C. J. 1968. Power requirements for horizontal flight in the pigeon *Columba livia*. *J. Exp. Biol.* 49: 527-555.
- Raup, D. M. 1967. Geometric analysis of shell coiling: coiling in ammonoids. *J. Paleontol.* 41: 43-65.
- Rayner, J. M. V. 1979. A new approach to animal flight mechanics. *J. Exp. Biol.* 80: 17-54.
- Seibel, B. A., E. V. Thuesen, J. J. Childress. 1998. Flight of the vampire: ontogenetic gait-transition in *Vampyroteuthis infernalis* (Cephalopoda: Vampyromorpha). *J. Exp. Biol.* 201: 2413-2424.
- Siekman, J. 1963. On the pulsating jet from the end of a tube, with application to the propulsion of certain aquatic animals. *J. Fluid Mech.* 15: 399-418.
- Spedding, G.R., J.M.V. Rayner, and C.J. Pennycuick. 1984. Momentum and energy in the wake of a pigeon (*Columba livia*) in slow flight. *J. Exp. Biol.* 111: 81-102.
- Stamhuis, E. J. and J. J. Videler. 1995. Quantitative flow analysis around aquatic animals using laser sheet particle image velocimetry. *J. Exp. Biol.* 198: 283-294.
- Smith, K. K. and W. M. Kier. 1989. Trunks, tongues and tentacles: moving with skeletons of muscle. *Am. Sci.* 77: 28-35.
- Thompson, J. T. 1997. Changes in squid mantle kinematics during ontogeny: consequences for mantle connective tissue architecture. *Amer. Zool.* 37: 79A.
- Thompson, J. T. 1998. Ontogenetic changes in mantle kinematics in the squid, *Sepioteuthis lessoniana*. *Amer. Zool.* 38: 20A.
- Tobalske, B. W. and K. P. Dial. 1996. Flight kinematics of black-billed magpies and pigeons over a wide range of speeds. *J. Exp. Biol.* 199: 263-280
- Trueman, E. R. 1975. *The Locomotion of Soft-bodied Animals*. London: Edward Arnold.

- Tucker, V. A. 1973. Bird metabolism during flight: evaluation of a theory. *J. Exp. Biol.* 58: 689-709.
- Vecchione, M. 1991. Dissolved oxygen and the distribution of euryhaline squid *Lolliguncula brevis*. *Bull. Mar. Sci.* 49: 668-669.
- Vecchione, M. and C. F. E. Roper. 1991. Cephalopods observed from submersibles in the Western North Atlantic. *Bull. Mar. Sci.* 49: 433-445.
- Vogel, S. 1985. Flow-assisted shell reopening in swimming scallops. *Biol Bull.* 169: 624-630
- Vogel, S. 1994. *Life in Moving Fluids*. 2nd ed. Princeton: Princeton University Press.
- Ward-Smith, A. J., and D. Clements. 1982. Experimental determinations of the aerodynamic characteristics of ski-jumpers. *Aeronaut. J.* 86: 384-91.
- Webb, P. W. 1979. Mechanics of escape responses in crayfish (*Orconectes virilis*). *J. Exp. Biol.* 79: 245-263.
- Webb, P. W. 1993. Is tilting behaviour at low swimming speeds unique to negatively buoyant fish? Observations on steelhead trout, *Oncorhynchus mykiss*, and bluegill, *Lepomis macrochirus*. *J. Fish Biol.* 43: 687-694.
- Webber, D. M. and R. K. O'Dor. 1985. Respiration and swimming performance of short-finned squid (*Illex illecebrosus*). *Scientific Council Studies Northw. Atl. Fish. Org.* 9: 133-138.
- Webber, D. M. and R. K. O'Dor. 1986. Monitoring the metabolic rate and activity of free-swimming squid with telemetered jet pressure. *J. Exp. Biol.* 126: 205-224.
- Webb, P. W. and D. Weihs. 1986. Functional locomotor morphology of early life history stages of fishes. *Trans. Am. Fish. Soc.* 115: 115-127.
- Weihs, D. 1977. Periodic jet propulsion of aquatic creatures. *Fortschr. Zool.* 24: 171-175.
- Westneat, M. W. 1996. Functional morphology of aquatic flight in fishes: kinematics, electromyography, and mechanical modeling of labriform locomotion. *Amer. Zool.* 36: 582-598.

CHAPTER 4

ROLE OF AEROBIC AND ANAEROBIC CIRCULAR MANTLE MUSCLE FIBERS IN SWIMMING SQUID: ELECTROMYOGRAPHY

ABSTRACT

Circular muscle in the mantle of squids and cuttlefishes consists of distinct zones of aerobic and anaerobic muscle fibers that are thought to have functional roles analogous to red and white muscle in fishes. To test predictions of the functional role of the circular muscle zones during swimming, electromyograms (EMGs) in conjunction with video footage were recorded from brief squid *Lolliguncula brevis* (5.0–6.8 cm dorsal mantle length) swimming in a flume at speeds of 3–27 cm s⁻¹. In one set of experiments, in which EMGs were recorded simultaneously from both the central anaerobic and peripheral aerobic circular mantle muscle, electrical activity was detected during each mantle contraction at all swimming speeds, and the amplitude and frequency of responses increased with speed. In another set of experiments, in which EMGs were recorded from electrodes placed in the central anaerobic circular muscle fibers alone, electrical activity was not detected during mantle contraction until speeds of ~15 cm s⁻¹, when EMG activity was sporadic. At speeds >15 cm s⁻¹, the frequency of central circular muscle activity subsequently increased with swimming speed until maximum speeds of 21–27 cm s⁻¹, when muscular activity coincided with the majority of mantle contractions. These results indicate that peripheral aerobic circular muscle is used for low, intermediate, and probably high speeds, whereas central anaerobic circular muscle is recruited at intermediate speeds and used progressively more with speed for powerful, unsteady jetting. Periodic anaerobic circular mantle activity at intermediate speeds and subcritical

speeds boosts power production and presumably extends net use of anaerobic resources.

The discovery of functional “gears” in squids, which is yet another instance of convergent evolution in fishes and cephalopods, is significant because it suggests that there is specialization and efficient use of locomotive muscle in squids.

INTRODUCTION

Fishes have three myotomal muscle types, i.e., red, pink, and white fibers, that are structurally, metabolically, and functionally distinct. The red muscle is characterized by a high myoglobin content, extensive capillary beds, a high density of mitochondria, and high levels of oxidative enzymes (Bone, 1966, 1978). It operates aerobically, fatigues slowly, has low rates of activation and relaxation, and low shortening velocities (Johnston et al., 1977). White muscle is characterized by a high myofibrillar density, a low content of mitochondria, poor blood supply, and high levels of glycolytic enzymes (Flitney and Johnston, 1979). It operates anaerobically, fatigues rapidly, has high rates of activation and relaxation, and high shortening velocities (Curtin and Woledge, 1988). Pink muscle is intermediate in structure, metabolism, and contractile properties relative to red and white muscle (Johnston et al., 1977; Coughlin et al., 1996). Generally, red muscle is recruited for the lowest, steady, undulatory swimming speeds (Rome et al., 1984); pink muscle is recruited at intermediate swimming speeds (Johnston et al., 1977); both red and pink muscle are recruited at maximum steady swimming speeds (Coughlin et al. 1996); and white muscle is recruited at higher swimming speeds when swimming becomes unsteady (Rome et al., 1984; Jayne and Lauder, 1996).

Squids and cuttlefishes have muscle types in the mantle musculature similar to red and white muscle. The mantle musculature of cephalopods functions as a constant volume system with a 3-dimensional array of tightly bundled muscles commonly called a

muscular-hydrostat (Kier and Smith, 1985; Smith and Kier, 1989). During jet propulsion circular muscles within the mantle contract, which consequently decreases mantle diameter and forces intramantle water out of the funnel. Since mantle length changes during contraction are negligible and the mantle musculature is constant in volume, circular muscle contraction results in concomitant mantle wall thickening. Obliquely oriented collagen fibers traversing the thickness of the mantle wall are strained and store energy. This energy together with contraction of radially oriented muscle fibers, which extend from the inner to outer surface of the mantle, power mantle refilling (Gosline and Shadwick, 1983; Gosline et al., 1983, Kier, 1988). The circular muscle responsible for mantle contraction within this system consists of three anatomically and metabolically distinct muscle layers when viewed in cross section: an inner, outer, and middle layer (Bone et al., 1981; Mommsen et al., 1981). The inner and outer (peripheral) layers are thin, rich in mitochondria, have high succinic dehydrogenase (SDH) activity, a high ratio of oxidative to glycolytic enzyme activity, and heavy vascularization. The middle (central) layer is thick, has sparse vascular beds, low mitochondria density, low SDH activity, and a high ratio of glycolytic to oxidative enzyme activity. Because of these structural and biochemical differences, Bone et al. (1981) and Mommsen et al. (1981) suggested that the inner and outer layers are analogous to aerobic red muscle in fish and are used for slow, steady swimming and rhythmic, respiratory contractions, while the central layer is analogous to anaerobic white muscle and is used during burst swimming, escape, and capture events.

Although peripheral and central circular muscle have several structural and biochemical similarities to red and white muscle in fishes, the functional roles of the

circular muscle types during swimming in squids and cuttlefishes remain unresolved. Bone et al. (1994) found large amplitude electromyographic activity in the mantle of cuttlefish *Sepia officinalis* during escape jetting and concluded that both the central anaerobic and peripheral aerobic circular muscle were active. However, since electrodes were not inserted exclusively in either muscle layer, the functional roles of the circular muscle types are still uncertain. Metabolic end product accumulations within mantle musculature of squids during routine behavior, exercise, and after exercise have been the focus of numerous studies (Hochachka et al., 1975; Grieshaber and Gade, 1976; Storey and Storey, 1978, Fields and Quinn, 1981; Pörtner et al., 1991, 1993; Finke et al., 1996), but in these studies, no distinctions were made between end products found within the various circular muscle layers. Based on mantle pressure measurements, O'Dor (1988) concluded that both circular muscle fiber types of must be active in *Illex illecebrosus* at subcritical swimming speeds to generate the necessary swimming power. Furthermore, Finke et al. (1996) suggested that *Lolliguncula brevis*, which tend to oscillate between high and low muscular activity at increased swimming velocities, rely on both circular muscle fiber types at high speeds. However, once again, direct documentation of the functional roles of the two circular mantle muscle types is lacking.

In this study electromyography (EMG) in conjunction with video recordings were used to determine the role of the peripheral aerobic and central anaerobic circular muscle layers in brief squid *Lolliguncula brevis* swimming over a range of speeds (3–27 cm s⁻¹). Two experiments were conducted. In one experiment EMG activity was recorded from electrodes embedded in both peripheral and central circular muscle layers. In another experiment EMG activity was recorded from electrodes embedded exclusively in the

central circular muscle layer. It was not possible to embed electrodes solely in peripheral circular muscle because the muscle layer was too thin (~100 μm) for reliable placement. However, by comparing results from the two experiments, it was possible to postulate the functional roles of the circular muscle zones.

MATERIALS AND METHODS

Experimental Animals

In August–October 1998, brief squid *Lolliguncula brevis* (Blainville) were captured by trawl within embayments along the seaside of Virginia's Eastern Shore and within the York River, VA. Squid captured along the Eastern Shore of Virginia were transported to the Virginia Institute of Marine Science (VIMS) Eastern Shore Lab located in Wachapreague, VA, while squid captured in the York River were transported to the VIMS main campus located in Gloucester Point, VA. Squid were kept alive in the field using 120-quart coolers equipped with filtration and aeration systems, which were powered by 12-V, sealed, gel-cell batteries. At Wachapreague and Gloucester Point, squid were kept in flow-through raceway tanks for at least one week prior to experimentation and fed a diet of grass shrimp *Palaemonetes pugio*. Experiments on 12 squid (3.5–7.8 cm dorsal mantle length (DML)) were performed, but results from only 5 squid (5.0–6.8 cm DML) are reported here. Some squid were eliminated from consideration because of one or more of the following: (1) there was some uncertainty as to the location of the electrodes in the muscle, (2) there was an excess of ambient electrical noise, (3) the squid were not cooperative in swim tunnels.

Electromyogram (EMG) Recordings

Disposable, paired hook-wire electrodes (150 μm gauge insulated nickel alloy) (Nicolet Biomedical, Madison, WI) were used for EMG recordings. The hook portions of the manufactured electrode wires were too large for recording EMGs from the peripheral and central circular muscle layers, which were approximately 0.1 mm and 1.0 mm thick, respectively. Therefore, the hook portions of the electrodes were modified so that they were 1.0 mm in total length with 0.5 mm of insulation removed at the tip. The squid were anesthetized (~2 minutes) in an isotonic solution of MgCl_2 (7.5% $\text{MgCl}_2 \cdot 6\text{H}_2\text{O}$) and seawater (Messenger et al. 1985), and a pair of electrodes was inserted obliquely using a hypodermic needle into the lateral mantle wall at a point 60% of the mantle length from posterior. One pair of electrodes was inserted during each recording session, and electrode spacing within the muscle was approximately 2–6 mm. The electrode pair was embedded in either the central circular muscle layer or both the central circular muscle layer and the peripheral circular muscle layer adjacent to the skin (it was not possible to embed electrodes exclusively in the peripheral layer of circular muscle because it was too thin (~0.1 mm)). During electrode placement no attempt was made to avoid radial muscles, which extend from the inner to outer mantle surface and partition the circular muscle into 0.1 mm sections. Electrical activity of radial muscles did not obscure electrical activity from the circular muscle layers, however, since radial muscles are active during mantle expansion, while circular muscles are active during mantle contraction (Gosline and Shadwick, 1983; Gosline et al., 1983). To help ensure reliable placement of electrodes, many practice insertions were performed on preserved squid prior to the experiments, and depth references were marked on hypodermic needles used

for implantation. Sufficient slack in the electrode wires was provided so that anchoring electrodes at other locations along the body was not necessary to prevent dislodgment.

After successful implantation, squid were placed in a 20 x 10 x 10 cm holding section within a 16 L Vogel/LaBarbera-type flume (Vogel and LaBarbera, 1978) filled with aerated seawater (24‰, 22°C) and allowed to recover from surgery at low flow velocity (1 cm s⁻¹). Flow velocity in the tunnel was controlled using two propellers arranged in a rotor-stator configuration and a 1/4 hp variable speed motor, which was shielded using aluminum sheeting to reduce radiated EMF noise. A ground electrode was attached to a downstream collimator within the flume. The ground electrode together with the embedded bipolar hook-wire electrodes, which were attached to insulated Nicolet micrograbbers, were plugged into a two-channel differential amplifier using Nicolet DIN 42 802 connectors. The differential amplifier was part of a Nicolet Compass II Portabook system, which is designed to record electromyograms and somatosensory, auditory, and visual evoked potentials from human patients. The Nicolet Compass II Portabook was used to record, amplify, and filter electromyograms collected at various frequencies. For this study, EMGs were collected in the free-run mode using a band pass filter of 0.20–10 kHz, and all EMG traces were recorded on the hard drive.

After the squid became active in the holding section, flow velocity within the flume was increased to 6 cm s⁻¹ and the animal was allowed to acclimate to flow, which generally occurred within 15 minutes. After the acclimation period, squid were exposed to a flow velocity of 3 cm s⁻¹ for 10 minutes. Speed was subsequently increased by 3 cm s⁻¹ every 10 minutes until the squid could no longer keep pace with free stream flow. During each of the 10 minute speed increments EMGs were collected. Because of

limitations of the Nicolet Compass II Portabook, it was not possible to record EMG signals on a channel of a video recorder or precisely timelock video and EMG recordings. Therefore, to provide a synchronized record of EMG responses and swimming behavior, the computer screen of the Nicolet Compass Portabook was positioned below the holding section of the flume, and both Nicolet display output and swimming behavior of the squid were videotaped simultaneously from a lateral perspective using a Sony Hi-8 video camera. After squid were exhausted and could no longer maintain free-stream velocity, they were removed from the flume and over-anesthetized in an isotonic solution of MgCl_2 (7.5% $\text{MgCl}_2 \cdot 6\text{H}_2\text{O}$) and seawater. The squid were then transferred to 10% buffered formalin for later dissection to determine precise electrode location. Some cooperative squid were not euthanized after the initial recording session. Instead, these squid were returned to the raceway tanks after cutting the electrode wires, while leaving the embedded section undisturbed within the mantle so that it could be examined later to determine placement. After several hours these squid were retrieved, electrodes were imbedded in a different circular muscle layer, and EMGs were recorded during another swimming session. Following the completion of the second swimming session, these animals were over-anesthetized, fixed, and dissected as described above to determine electrode placement.

Kinematic Analysis

Video footage of trials where squid were cooperative at all swimming speeds, ambient electrical noise was low, and electrode placement was unambiguous was analyzed using a Sony EVO-9700 editing deck and a Peak video and computer motion

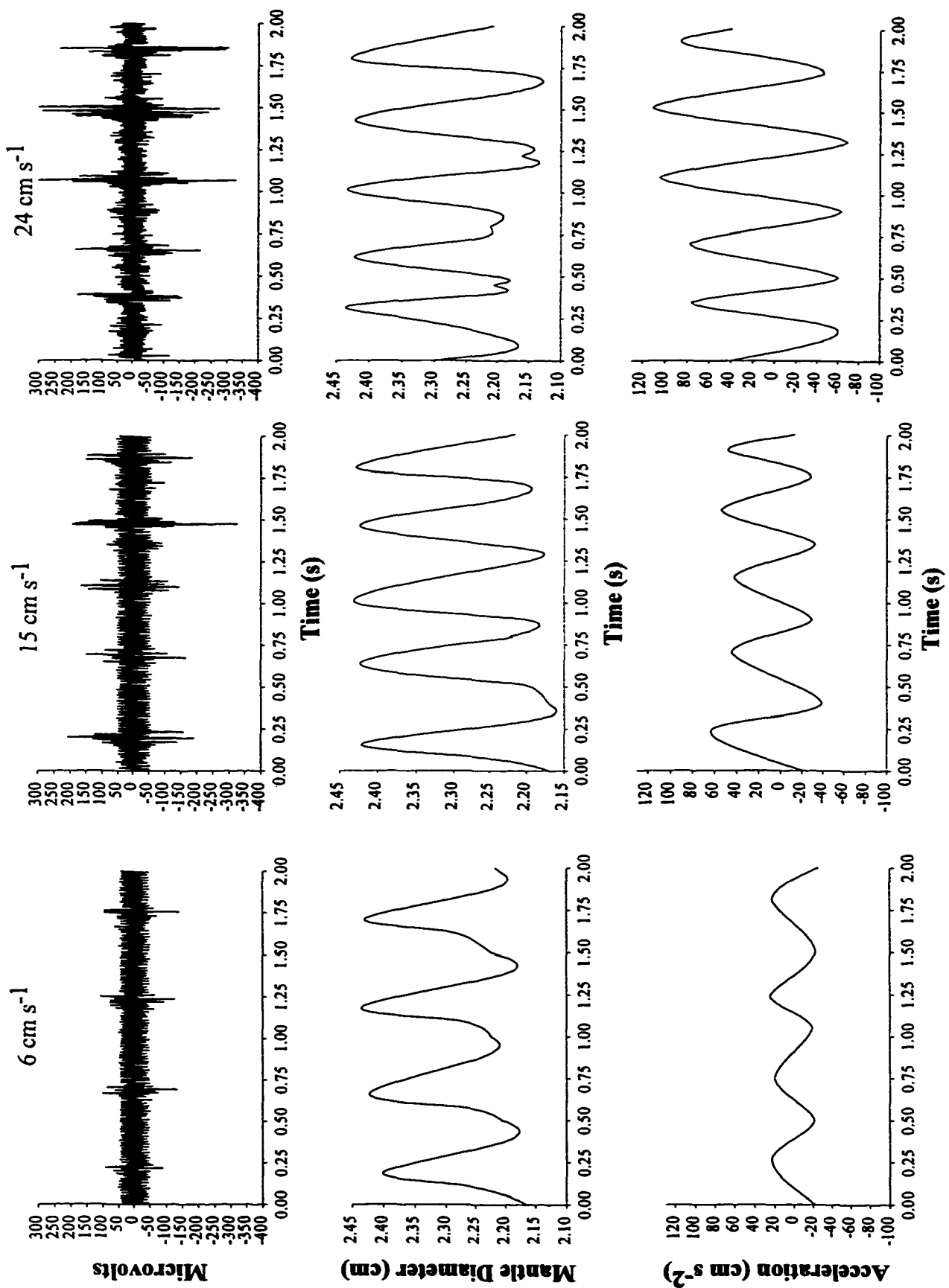
measurement system (Peak Performance Technologies, Englewood, CO). At each speed several video sequences with clear mantle profiles and representative EMG recordings were selected. Mantle diameter at the location of electrode placement, swimming velocity, and acceleration of the squid were measured for each frame of video (30 frames s^{-1}) within the sequence, and frames where EMG responses began and ended were marked using the event feature in the Peak Motion Measurement System. Mantle diameter, velocity, and acceleration data were smoothed using a fourth-order Butterworth filter to account for video jitter and digitization error. Peak video data and Nicolet EMG data were imported into Microsoft Excel and aligned using event markers from the Peak file and timebase frequencies from both files. Synchronization of the data was only reliable to within 33.3 ms since the video camera records at 30 frames s^{-1} . Since the objective of this study was simply to determine the presence or absence of EMG activity within the circular muscle layers during mantle contractions, more precise analysis of the timing of EMG activity was unnecessary.

RESULTS

The five squid (5.0 – 6.8 cm DML) considered in this study matched free-stream flow well at speeds $< 21 \text{ cm s}^{-1}$, but at higher speeds had some difficulty matching flow velocity and eventually collapsed against the downstream weir. Prior to collapse, the squid accelerated and decelerated erratically and contraction frequencies were more irregular than those observed at lower velocities. At low (3–9 cm s^{-1}) and intermediate (12–18 cm s^{-1}) swimming velocities, squid relied on both fin and jet propulsion, while at high subcritical speeds (21–27 cm s^{-1}), squid relied exclusively on jet propulsion and wrapped their fins against the mantle. The electrodes did not appear to impede swimming in the five squid considered; however, some squid, which were excluded from this analysis, were visibly agitated after surgery, swam inconsistently at most swimming speeds, and frequently swam forcibly into the flume sides.

The amplitude and frequency of electrical activity varied from animal to animal, but the basic patterns of activity presented in this paper are representative of all of the squid considered. Figure 1 shows EMG recordings from electrodes inserted into the central and peripheral circular muscle layers, mantle diameter, and the acceleration of a squid (5.5 cm DML) swimming over several speeds. Significant EMG activity was present at low (6 cm s^{-1}), intermediate (15 cm s^{-1}), and high speeds (24 cm s^{-1}), and EMG activity was correlated with mantle contraction. The amplitude of EMG activity increased with speed and, as was typical of other squid examined, mantle contraction

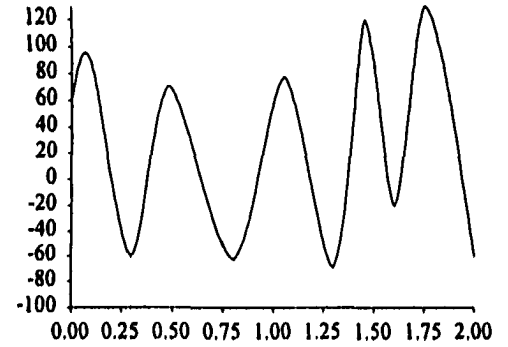
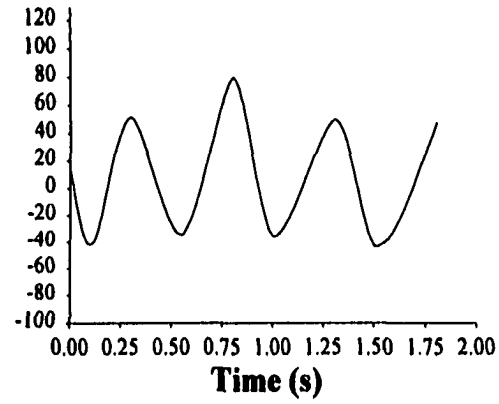
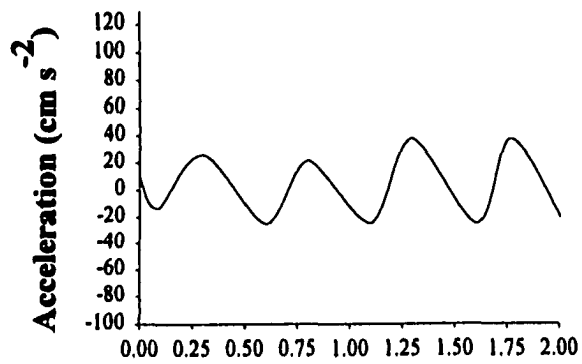
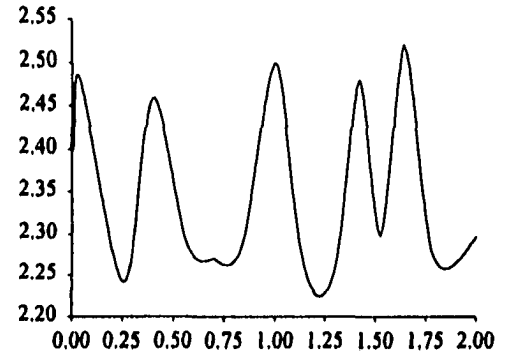
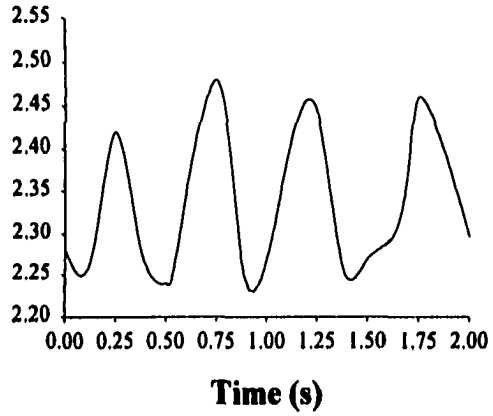
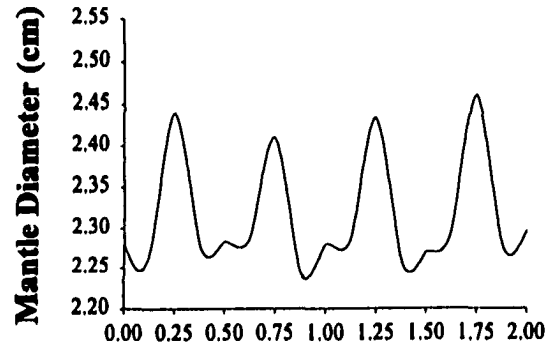
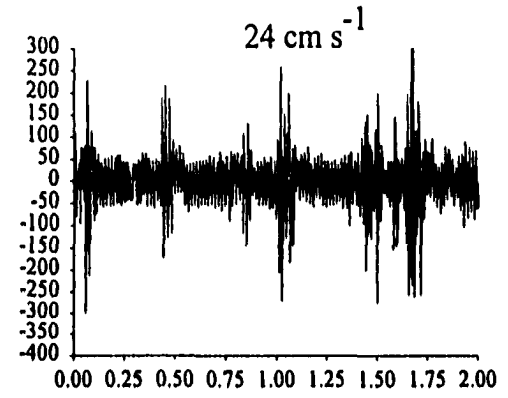
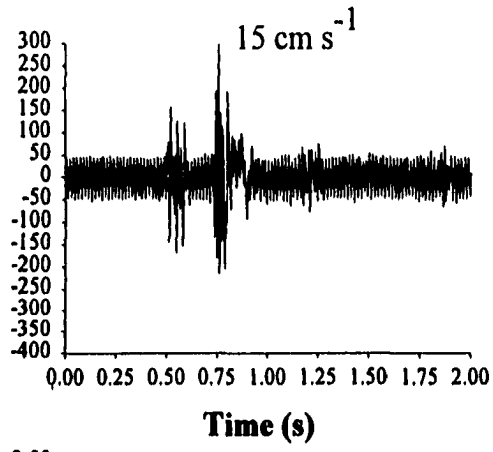
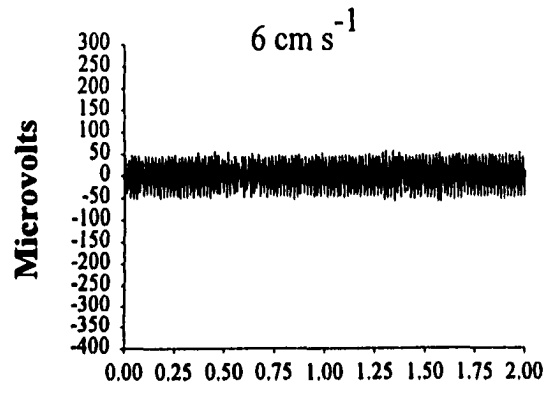
Figure 1. EMG recordings from electrodes embedded in both peripheral aerobic circular muscle and central anaerobic circular muscle of a brief squid (5.5 cm DML) while swimming at 6, 15, and 24 cm s⁻¹. Mantle diameter and acceleration are plotted underneath each EMG recording. Note that EMG activity occurred during each mantle contraction, and at high speeds, EMG activity during mantle expansion was sometimes present.



frequency was greater at the highest speed tested (24 cm s^{-1}) than at low speeds (6 cm s^{-1}). Moreover, maximum accelerations throughout the jet cycle were closely coupled with high magnitude EMG bursts recorded during mantle contraction. At high speeds (24 cm s^{-1}) lower amplitude electrical activity sometimes occurred during mantle expansion.

Figure 2 shows EMG recordings from electrodes embedded in only central circular muscle of another squid (5.7 cm DML). The bandpass filter, sensitivity, timebase, etc. are identical to those used for recordings from both central and peripheral layers. No EMG activity was detected during mantle expansion and contraction at 6 cm s^{-1} . At an intermediate speed of 15 cm s^{-1} , occasional EMG activity was detected. (The mean central circular muscle recruitment speed for all squid considered was 15.3 ± 3.7 (SD) cm s^{-1}). Most of the large amplitude electrical activity occurred during the contraction phase of the jet cycle, but sometimes smaller amplitude activity occurred during mantle expansion (Figure 2). Furthermore, the large amplitude EMGs were coupled with large mantle diameter changes and high acceleration peaks (Figure 2). Generally, the frequency of EMG bursts increased with speed until maximum speeds of $21\text{--}27 \text{ cm s}^{-1}$, when muscular activity coincided with the majority of mantle contractions. Again large amplitude signals were correlated with mantle contraction, while less frequent low amplitude signals were correlated with mantle expansion. Contraction amplitude and frequency were more irregular at 24 cm s^{-1} than at lower velocities, and high amplitude EMG peaks were strongly coupled with high accelerations.

Figure 2. EMG recordings from electrodes embedded in central anaerobic circular muscle of a brief squid (5.7 cm DML) while swimming at 6, 15, and 24 cm s⁻¹. Mantle diameter and acceleration are plotted underneath each EMG recording. Note that there were no obvious EMG waveforms at 6 cm s⁻¹, occasional EMG waveforms at 15 cm s⁻¹, and frequent EMG waveforms at high speeds (24 cm s⁻¹). At high speeds, high amplitude electrical activity occurred during each mantle contraction and lower amplitude electrical activity sometimes occurred during mantle expansion. Furthermore, mantle contractions were more erratic at 24 cm s⁻¹ relative to those observed at 6 cm s⁻¹.



DISCUSSION

Based on these recordings, it seems probable that the peripheral aerobic and the central anaerobic circular muscle fibers have distinct functional roles during swimming. Electrodes implanted in both peripheral and central circular muscle fibers recorded EMG activity with each mantle contraction at all swimming speeds (0–27 cm s⁻¹). However, electrodes implanted exclusively in central (anaerobic) muscle did not record EMG activity during mantle contraction until speeds of ~15 cm s⁻¹, when activity was sporadic. At speeds above 15 cm s⁻¹, the frequency of electrical activity increased with swimming speed until maximum speeds of 21–27 cm s⁻¹, when muscular activity coincided with the majority of mantle contractions and with high accelerations. These results indicate that peripheral aerobic circular muscle is used for slow, intermediate, and probably high speeds, whereas central anaerobic muscle is recruited at intermediate speeds and used progressively more with increasing speed for powerful, unsteady jetting typical of higher speed swimming.

The observed periodic detection of central anaerobic circular muscle activity at intermediate speeds is interesting given that anaerobic muscle is often only associated with burst swimming in fishes (Rome et al., 1984; Jayne and Lauder, 1996) and escape jets in cephalopods (Bone et al., 1981; Mommsen et al., 1981; Bone et al., 1994). Finke et al. (1996) determined that anaerobic end products, such as α -glycerophosphate, succinate, and octopine, begin to accumulate in *Lolliguncula brevis* at speeds of 1.5–2

mantle length s^{-1} , suggesting that anaerobic metabolism may occur in the mantle at low intermediate speeds. Moreover, intramantle pressure records of a 5.0 cm DML squid revealed that at speeds of 15 cm s^{-1} , high mantle pressures comparable to those recorded at speeds of 21 cm s^{-1} were periodically recorded by Finke et al. (1996). Anaerobic end product accumulation and the occasional detection of high intramantle pressures at intermediate speeds is consistent with the observed activity of anaerobic circular muscle at intermediate speeds in this study. Periodic anaerobic circular mantle activity at intermediate speeds boosted power production, which helped squid keep pace with free-stream flow in the tunnels. Periodic anaerobic activity was probably not energetically deleterious since anaerobic metabolic changes can be rapidly reversed in squid (Pörtner et al., 1993). At higher speeds, central anaerobic circular muscle activity was more frequent, but there was still some oscillation between aerobic and anaerobic muscular activity. Finke et al. (1996) suggest that oscillating between aerobic and anaerobic circular muscle recruitment rather than simply relying exclusively on anaerobic muscle at a critical speed allows for an extended net use of anaerobic resources before fatigue sets in.

Despite shielding the variable speed motor used to propel water in the swim tunnel, a high level of background noise ($\pm 40 \mu\text{V}$) was still present. Some of the 60 Hz interference from the motor and other electrical equipment may have been reduced using a 60 Hz notch filter (Loeb and Gans, 1986), but unfortunately one was not available for this study. Nonetheless, EMG activity was recorded from the peripheral muscle zones in spite of the electrical noise, and thus EMG activity from the central zone should have been visible if those fibers were active.

Although electrical noise probably did not mask circular muscle activity, which was the focus of this study, it interfered with detection of EMG activity from the smaller radial muscles. Dissections revealed that electrodes crossed radial muscle bands, which are active during mantle expansion and hyperinflation (i.e., a sharp increase in mantle diameter just prior to contraction) (Gosline et al. 1983, Bone et al. 1994). However, no radial EMG activity was detected at low speeds. This is not surprising given that Wilson (1960) and Ward (1972), who were the first to record electrical activity in the squid mantle musculature, were unable to detect radial muscle activity, and Gosline et al. (1983) and Bone et al. (1994) only were able to detect consistent radial muscle activity in squid and cuttlefish when using a 60 Hz notch filter and a Faraday cage, respectively. Radial muscle activity at low speeds detected by Gosline et al. (1983) and Bone et al. (1994), who examined squid and cuttlefish in dissecting pans and small aquariums and consequently did not have to contend with a motor driven swim tunnel, was often $< 40 \mu\text{V}$. Therefore, low speed radial muscle activity presumably was hidden by the electrical noise.

During escape jets, Gosline et al. (1983) recorded radial muscle activity during refilling and hyperinflation without a 60 Hz notch filter. At high speeds, EMG activity frequently was observed in the present study during mantle expansion. Since circular muscle is not active during mantle expansion (Gosline et al., 1983), radial muscles—the only other muscle into which electrodes were imbedded—were probably responsible for the EMG activity observed during mantle refilling. The detection of radial muscle activity at high speeds when anaerobic circular muscle was active suggests that significant radial muscle activity is used to expand the mantle during vigorous jetting.

Elastic energy stored within the connective tissue of the mantle also likely plays an important role during mantle expansion (Gosline and Shadwick, 1983; Gosline et al., 1983; Pabst, 1996).

Using electromyography, Kier et al. (1989) demonstrated that anaerobic and aerobic zones of muscle in cuttlefish *Sepia officinalis* fins have distinct functional roles, with aerobic fibers responsible for gentle fin movements and anaerobic muscles responsible for vigorous fin movements and support for that movement. The results of the present study indicate that peripheral aerobic circular muscle and central anaerobic circular muscle in brief squid *Lolliguncula brevis* also have distinct functional roles that are analogous to red and white myotomal fibers in fishes. Contrary to the situation in many fishes, however, the anaerobic muscle of squids appears to be used at subcritical speeds. The discovery of functional “gears” in squids, which is yet another instance of convergent evolution in fishes and cephalopods, is significant because it suggests that there is specialization and efficient use of locomotive muscle in squids.

LITERATURE CITED

- Bone, Q. 1966. On the function of the two types of myotomal muscle fibers in elasmobranch fish. *J. Mar. Biol. Assoc. U.K.* 46: 321-349.
- Bone, Q. 1978. Locomotor muscle. In *Fish Physiology*, vol. 7 (ed. W. S. Hoar and D. J. Randall), pp. 361-424. New York: Academic Press.
- Bone, Q., A. Pulsford, and A.D. Chub. 1981. Squid mantle muscle. *J. Mar. Biol.* 61: 327-342.
- Bone, Q., E. R. Brown, and G. Travers. 1994. On the respiratory flow in the cuttlefish *Sepia officinalis*. *J. Exp. Biol.* 194: 153-165.
- Coughlin, D. J., G. Zhang, and L. C. Rome. 1996. Contraction dynamics and power production of pink muscle of scup (*Stenotomus chrysops*). *J. Exp. Biol.* 199: 2703-2712
- Curtin, N. A. and R. C. Woledge. 1988. Power output and force-velocity relationships of live fibers from white myotomal muscle of the dogfish, *Scyliorhinus canicula*. *J. Exp. Biol.* 140: 187-197.
- Flitney, F. W. and I. A. Johnston. 1979. Mechanical properties of isolated fish red and white muscle fibers. *J. Physiol.* 295: 49-50.
- Fields, J. H. A. and J. F. Quinn. 1981. Some theoretical considerations on cytosolic redox balance during anaerobiosis in marine invertebrates. *J. Theor. Biol.* 88: 35-45.
- Finke, E., H. O. Pörtner, P. G. Lee, and D. M. Webber. 1996. Squid (*Lolliguncula brevis*) life in shallow waters: oxygen limitation of metabolism and swimming performance. *J. Exp. Biol.* 199: 911-921.
- Gosline, J. M. and R. E. Shadwick. 1983. The role of elastic energy storage mechanisms in swimming: an analysis of mantle elasticity in escape jetting in the squid, *Loligo opalescens*. *Can. J. Zool.* 61: 1421-1431.
- Gosline, J. M., J. D. Steeves, A. D. Harman, and E. DeMont. 1983. Patterns of circular and radial mantle muscle activity in respiration and jetting of the squid *Loligo opalescens*. *J. Exp. Biol.* 104: 97-109.

- Grieshaber, M. E. and G. Gade. 1976. The biological role of octopine in the squid, *Loligo vulgaris* (Lamarck). *J. Comp. Physiol.* 108:225-232.
- Hochachka, P. W., T. W. Moon, T. Mustafa, and K. B. Storey. 1975. Metabolic sources of power for mantle muscle of a fast swimming squid. *Comp. Biochem. Physiol.* 52B: 151-158.
- Jayne, B. C. and G. V. Lauder. 1996. New data on axial locomotion in fishes: how speed affects diversity of kinematics and motor patterns. *Am Zool.* 36: 642-655.
- Johnston, I. A., W. Davison, and G. Goldspink. 1977. Energy metabolism of carp swimming muscles. *J. Comp. Physiol.* 114: 203-216.
- Kier, W. M. 1988. The arrangement and function of molluscan muscle. In *The Mollusca, Form and Function*, vol. 11 (ed. Trueman, E. R., and M. R. Clarke), pp. 211-252. New York: Academic Press.
- Kier, W. M. and K. K. Smith. 1985. Tongues, tentacles and trunks: the biomechanics of movement in muscular hydrostats. *Zool. J. Linn. Soc.* 83: 307-324.
- Kier, W. M., K. K. Smith, and J. A. Miyan. 1989. Electromyography of the fin musculature of the cuttlefish *Sepia officinalis*. *J. Exp. Biol.* 143: 17-31.
- Loeb, G. E. and C. Gans. 1986. *Electromyography for Experimentalists*. Chicago: University of Chicago Press.
- Messenger, J. B., M. Nixon, and K. P. Ryan. 1985. Magnesium chloride as an anaesthetic for cephalopods. *Comp. Biochem. Physiol.* 82C: 203-205.
- Mommsen, T. P., J. Ballantyne, D. MacDonald, J. Gosline, and P. W. Hochachka. 1981. Analogues of red and white muscle in squid mantle. *Proc. Natl. Acad. Sci.* 78: 3274-3278.
- O'Dor, R. K. 1988. Limitations on locomotor performance in squid. *J. Appl. Physiol.* 64: 128-134.
- Pabst, D. A. 1996. Springs in swimming animals. *Amer. Zool.* 36: 723-735.
- Pörtner, H. O., D. M. Webber, R. G. Boutilier, and R. K. O'Dor. 1991. Acid-base regulation in exercising squid (*Illex illecebrosus*, *Loligo pealei*). *Am. J. Physiol.* 261: R239-R246.
- Pörtner, H. O., D. M. Webber, R. K. O'Dor, and R. G. Boutilier. 1993. Metabolism and energetics in squid (*Illex illecebrosus*, *Loligo pealei*) during muscular fatigue and recovery. *Am J. Physiol.* 265: R157-R165.

- Rome, L. C., P. T. Loughna, and G. Goldspink. 1984. Muscle fiber recruitment as a function of swim speed and muscle temperature in carp. *Am. J. Physiol.* 247: R272-R270.
- Smith, K. K. and W. M. Kier. 1989. Trunks, tongues and tentacles: moving with skeletons of muscle. *Am. Sci.* 77: 28-35.
- Storey, K. B. and J. M. Storey. 1978. Energy metabolism in the mantle muscle of the squid, *Loligo pealeii*. 123: 169-175.
- Vogel, S. and M. LaBarbera. 1978. Simple flow tanks for research and teaching. *BioScience* 10: 638-643.
- Ward, D. V. 1972. Locomotory function of the squid mantle. *J. Zool., Lond.* 167: 487-499.
- Wilson, D. M. 1960. Nervous control of movement in cephalopods. *J. Exp. Biol.* 37: 57-72.

SUMMARY AND CONCLUSIONS

Squids are thought to have physiological and locomotive deficiencies that put them at a competitive disadvantage to fishes, their potential competitors and predators, and exclude them from inshore, highly variable environments that are rich in nektonic fauna. However, the brief squid, *Lolliguncula brevis*, may be a notable exception. This small species swims at low speeds and uses considerable fin activity, which both may help it compensate for the inherent inefficiencies of jet propulsion, and is known to live occasionally in shallow, euryhaline environments. This study was conducted in part to determine how extensively *Lolliguncula brevis* uses the Chesapeake Bay, which is a diverse, highly variable estuary densely populated with fishes but devoid of other cephalopods, and to determine how *L. brevis* distribution changes with selected abiotic factors for which squid typically have limited tolerance. A major objective of this study was to assess locomotion in *Lolliguncula brevis*, which is thought to be inherently inefficient. Aspects of locomotion were examined from mechanical, physiological, and behavioral perspectives.

Lolliguncula brevis is an important component of the Chesapeake Bay ecosystem when salinities and water temperatures are within its tolerance limits, and unlike other cephalopods, *L. brevis* may be well-equipped for inshore, euryhaline existence. Within the Chesapeake Bay, *L. brevis* was collected over a wide range of bottom temperatures (8.1–29.6°C), bottom salinities (17.9–35.0‰), dissolved oxygen levels (1.9–14.6 mg O₂/l), and depths (1.8–29.9 m), but was not found in Bay waters during winter. *Lolliguncula brevis*, especially juveniles < 60 mm dorsal mantle length (DML), were abundant, frequently ranking in the upper 10% of overall annual nektonic catches and

during the fall of certain years ranking second behind only anchovies. The probability of capturing a brief squid in the Chesapeake Bay increased at higher salinities and water temperatures, and these variables had a profound influence on both monthly and annual variability in distribution. Salinity appeared to have the largest influence on squid distribution, with squid being completely absent from the Chesapeake Bay when salinity was $< 17.9\text{‰}$ and most abundant in the fall when salinity was highest (despite declines in water temperature). Furthermore, squid were most prevalent at depths between 10–15 m within the Chesapeake Bay.

Lolliguncula brevis is different from other cephalopods examined previously because its pattern of O_2 consumption as a function of velocity is similar to aerial flight. In addition, its swimming costs are competitive with ecologically equivalent fishes. Many brief squid tested demonstrated partial (J-shaped) and full (U-shaped) parabolic patterns of O_2 consumption as a function of speed, and O_2 consumption rates at 0.5–1.5 mantle lengths s^{-1} were significantly less than those at < 0.5 and > 1.5 mantle lengths s^{-1} . These patterns of O_2 consumption are unlike those of most nekton but similar to those of birds and insects. The observed parabolic relation between O_2 consumption and velocity is probably the result of the high cost of generating lift at low speeds, which was achieved by elevating angles of attack of the body and funnel, increasing fin activity, and accelerating and subsequently coasting/gliding within the tunnel, and the high costs of overcoming drag at high speeds. *Lolliguncula brevis* has lower O_2 consumption than the squids *Illex illecebrosus* and *Loligo opalescens* studied in swim tunnel respirometers. Moreover, when compared with ecologically equivalent fish, such as mullet, striped bass, and flounder, O_2 consumption in *L. brevis* is 1–3x higher, which is substantially less than

that reported in previous squid/fish comparisons, where O₂ consumption of *Illex* and *Loligo* were 5–7x higher than fish.

Analysis of swimming mechanics and behavior of *Lolliguncula brevis* revealed that *L. brevis* swims at relatively low speeds, swims at various orientations, and uses complex behavioral interactions of the mantle, fins, arms, and funnel, which may boost efficiency or help counteract some of the inherent deficiencies associated with jet propulsion and negative buoyancy. A parabolic relationship between power (calculated from hydrodynamic estimates of drag, lift, and thrust) and speed was detected, with high costs at both low and high speeds because of power requirements for lift generation and overcoming drag, respectively. This finding compliments the detection of U and J-shaped patterns of O₂ consumption as a function of speed presented in Chapter 2. At low speeds, squid elevated body angles of attack to increase lift as observed in the respiratory study, but a closer examination of swimming behavior revealed that the trailing body section (i.e., the arms during tail-first swimming or mantle during arms-first swimming) was positioned at a higher angle of attack than the leading body section. This behavior postponed flow separation and elevated lift forces. Low-speed lift also was generated by directing high velocity jets downward at a high angle of attack (60–90°) and by relying on fin activity, which was responsible for as much as 65–80% of the total vertical thrust. Fin action, which could not be characterized exclusively as drag- or lift-based, was important in horizontal swimming as well, providing as much as 55% of total horizontal thrust at low speeds.

No dramatic gait shifts were present; behavioral changes tended to be gradual with speed, with the most abrupt changes being apparent when comparing size classes or

swimming orientations. To swim at higher velocities, small squid (< 3.0 cm DML) swimming tail-first increased contraction frequency and kept mantle volume relatively constant to maximize the benefits of toroidal induction, whereas squid belonging to larger classes (≥ 3.0 cm DML) increased mantle volume and kept contraction rates relatively constant while benefiting from 30% thrust augmentation from a pulsed jet. Based on aerobic efficiency curves, brief squid 3–5 cm DML were most efficient and large squid (> 6.0 cm DML) were most inefficient, which may explain why brief squid > 6.0 cm DML leave the highly competitive Chesapeake Bay and only return to spawn. Squid swam both arms-first and tail-first in swim tunnels. However, arms-first swimming, which allows greater observance of forward surroundings and reduces fin wake interactions with the body, was preferred for low-speed swimming, while tail-first swimming, which allows for more efficient jetting and greater use of the arms for lift and stabilization, was favored at high speeds. The acceleration reaction was an important instantaneous force during the jet cycle, frequently exceeding drag and lift forces by an order of magnitude, although relative contributions of the acceleration reaction averaged over a cycle were much less. Given that the interactive behaviors observed in this study occur under unsteady flow conditions, unsteady phenomena, such as attached vortex formation, may play important roles in squid locomotion.

The two types of circular muscle fibers had distinct functional roles, indicating that there is specialization and efficient use of locomotive muscle in squids, as is the case with fishes. Aerobic circular muscle was active at low, intermediate, and probably high speeds. Anaerobic muscle was recruited at intermediate speeds and used progressively more with increasing speed for powerful, unsteady jetting typical of higher speed

swimming. Periodic anaerobic circular mantle activity at intermediate speeds and subcritical speeds boosts power production and presumably extends net use of anaerobic resources.

The presumption that squids are inescapably constrained by a second-rate propulsive system and physiological deficiencies, which exclude them from inshore, highly variable habitats populated with dense assemblages of fishes, is not applicable to brief squid *Lolliguncula brevis*. *Lolliguncula brevis* has adapted well to the shallow waters of the Chesapeake Bay, where physical conditions are highly variable throughout the year and where hundreds of species of fishes reside. Unlike other squids examined previously, swimming costs of *L. brevis* are reasonably competitive with those of ecologically equivalent fishes, especially at intermediate speeds where O₂ consumption and power costs are lowest and at intermediate sizes where aerobic efficiency is highest. Although there are inherent deficiencies associated with jet propulsion and negative buoyancy, *L. brevis* appears to compensate for these shortcomings by (1) employing complex interactions of the mantle, fins, arms, and funnel, (2) swimming in various orientations, and (3) using functionally distinct circular muscle fibers. Because of the unique body plan of squid where mechanisms of propulsion, attitude control, and/or lift generation are located posteriorly (i.e., fins) and anteriorly (i.e., arms) and a rotating funnel is located at the mid-ventral region, squid are highly maneuverable and may accelerate rapidly in many directions. Maneuverability and rapid acceleration are seldom considered in squid/fish comparisons, but should be since these characteristics are beneficial for predator avoidance and prey capture. Furthermore, given that squid swim

in unsteady flows, exploitation of beneficial unsteady phenomena over fins, arms, and the mantle is likely to be important and should be the subject of future study.

VITA**IAN KURT BARTOL**

Born September 13, 1970 in Winfield, Illinois. Graduated as Valedictorian from Fair Haven Union High School in Fair Haven, VT in 1988. Earned a Bachelor of Science in Biology (with distinction) from the University of Michigan, Ann Arbor in 1992.

Received a Master of Arts in Marine Science at the College of William and Mary, School of Marine Science in 1995. Entered the doctoral program at the College of William and Mary, School of Marine Science in 1995.